Drug delivery in pancreatic cancer

Quantitative studies of gemcitabine and sonoporation in patients and cell line models

Tormod Karlsen Bjånes

Thesis for the degree of Philosophiae Doctor (PhD)
University of Bergen, Norway
2020

UNIVERSITY OF BERGEN

Drug delivery in pancreatic cancer

Quantitative studies of gemcitabine and sonoporation in patients and cell line models

Tormod Karlsen Bjånes

Thesis for the degree of Philosophiae Doctor (PhD)
at the University of Bergen

Date of defense: 06.03.2020

Year: 2020

Title: Drug delivery in pancreatic cancer

Name: Tormod Karlsen Bjånes

Print: Skipnes Kommunikasjon / University of Bergen

Table of Contents

Acknowledgements

A few years into the project, a disturbing message appeared on my computer (Figure 0A). Luckily, this was far from the truth. On the contrary, several people deserve my thanks for their participation in the project, and even more for their general importance in my life.

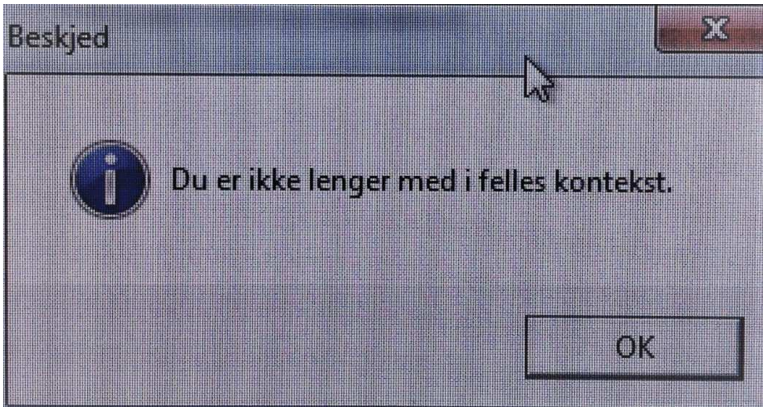

Figure 0A. ***Screenshot of a disturbing message from my computer: "You are no longer part of a common context"*** **(Bergen, July 8th 2016).**

Family, (an alien cat,) and good friends

First and foremost, I want to express gratitude to my dear wife Kristine and our kids Vegard and Emile, who have shown such patience and support throughout the project (despite my complete lack of interest in The Cat). You provide me with love and a meaning in life that endless hours in the lab and in front of a computer cannot replace. It may therefore seem contradictory that I have spent so much time working on the project. However, since I am also cursed (/blessed) with a personality that tends to put me in situations where deeply focused work over time is perceived as required, such dualities in life have become a normality. I thank my parents Solrun and Reidar, my sister Ranveig and my brothers Dagfinn and Øystein, for allowing me the honour of sharing excellent genes, and for your continuous/distant support

throughout the years. Thanks also to Eli[1] and Geir and the rest of Kristine's family for all your friendliness and hospitality.

I also want to thank my friends for all the good times we share together, and for staying around as an extended safety-net in life.

Wisdom, and a self-citation

In many aspects, the project has been an ambivalent journey balancing on edges between frustration and excitement, demotivation and motivation, pessimism and optimism, solitude (Figure 0B) and fellowship.

Figure 0B. ***Floor map adding to the loneliness that can be experienced while passing through the basement level of the laboratory building at Haukeland***

I have continuously tried to convince (or fool?) myself that a huge pile of work is nothing else than a collection of numerous tiny tasks. By solving them one-by-one, the work will eventually be done.

> *"A huge pile of work is nothing else than a collection of numerous tiny tasks"*
>
> Bjånes, T. Journal of Self-deception and Cognitive Diversions 2019; 1(1):1.

My colleagues are also my friends

I want to thank my friends and colleagues at Haukeland University hospital and the University of Bergen for contributing to a vibrant professional and social environment. You have all contributed to this thesis, either directly or indirectly, by being around, asking questions, eating lunch together, or simply by avoiding to disturb me. I also acknowledge that my lack of participation in the routine work has put extra workloads on many of you. Thanks to each and every one of you at Section of Clinical Pharmacology and RELIS Vest! Special thanks to Charlotte for

[1] Although I cannot promise that I will comply with all your hairdressing advices

collaboration in drug-committee-related topics, to Trond for being so inspirational, to Jon for staying in the game despite my discontinuity, and Silje for joining the team. I also want to thank Tina Kamceva for invaluable efforts in LC-MS/MS method development, collaboration in writing papers and for input to this thesis.

Bettina and Jan, and a second self-citation

My main supervisor Bettina Riedel and co-supervisor Jan Schjøtt have been indispensable throughout the project. I thank you for all the practical and financial arrangements that you have helped establish. I thank you for supporting me, pushing me (and yourselves) and for believing in me. Your ability of diving into details (Bettina □ / Jan □) and of zooming out from them (Bettina □ / Jan □), have sometimes been frustrating, but most of all educational. Throughout the project you have been exposed to my wordiness in writing, my interpositions and parentheses (among other things) that may have challenged the fluency in reading (despite the opposite being my intention[2]), but you have continuously provided specific advice and support and, as a consequence, have helped me overcome my wordiness in writing and the use of interpositions (and, to some extent, parentheses). In addition, you have advised me to avoid unnecessary repetitions that would otherwise have been repeated, unless you have repeatedly advised me not to do so (over and over again).

> *"In addition, you have advised me to avoid unnecessary repetitions"*
>
> Bjånes, T. Journal of Perpetual Motion Machines 2019;1(2):3-∞.

Emmet and his group

I want to thank my co-supervisor Emmet McCormack for opening your lab and welcoming me into your research environment. Thanks also to Zina and all the others. The last couple of years with experimental work in cell lines has been an important part of the project. I am grateful for the experience that I have acquired,

[2] Which has usually been to make it easier to read, perhaps with a currently ongoing exception

especially during all the hours spent together with Elisa Thodesen Murvold and Spiros Kotopoulis. I appreciate your friendliness and lightness of mind that has boosted my motivation.

Other co-authors, collaborators and supporters

I want to thank Bjørn Tore Gjertsen for the initiatives that got the project started, Georg Dimcevski for welcoming me into the clinical trial, Wenche Hauge Eilifsen for assistance in blood sampling and PBMC isolation protocols, Asbjørn Svardal and Torunn Eide for their contributions in development of the LC-MS/MS-methods, Philip Webber for technical assistance during Tina's absence, Endre Stigen for sharing experience with cell cultures, and Lars Herfindal and Steinar Hustad for valuable discussions during and after my midway evaluation. Also special thanks to Lars Petter Jordheim for hospitality during my visit in Lyon, and for fruitful collaboration on paper IV. Andreas Westin deserve my gratitude for his previous kind words[3], which might be equally valid the other way. Apart from that, I deeply respect your continuous dedication for the Norwegian Association of Clinical Pharmacology.

Finally, I want to thank Anne Grete Thue for facilitating my research project, and your contributions to the continuous development of our department. Western Norway Regional Health Authority, Department of Medical Biochemistry and Pharmacology and Raagholtstiftelsen, also deserve thanks for supporting the project financially.

Concluding remarks

Last, but not least, as well as first and foremost[4].

[3] Andreas Westin's Doctoral thesis 2018, page 5 (http://hdl.handle.net/11250/2571266)
[4] If you are indifferent to the remaining contents of this thesis, I suggest reading the Acknowledgements over and over again. Further reading also in: Bjånes, T. Journal of Perpetual Motion Machines 2019;1(2):3-∞.

Scientific environment

- Section of Clinical Pharmacology, Department of Medical Biochemistry and Pharmacology, Haukeland University hospital. https://helse-bergen.no/avdelinger/laboratorieklinikken/medisinsk-biokjemi-og-farmakologi.
- The Bergen Pharmacy and Pharmacology Research Group, Department of Clinical Science, University of Bergen. https://www.uib.no/en/rg/pharm
- SonoCURE, University of Bergen and Haukeland University Hospital. https://sonocure.w.uib.no/aboutsonocure/

Section of Clinical Pharmacology at the Department of Medical Biochemistry and Pharmacology at Haukeland University hospital provides an extensive laboratory service within therapeutic drug monitoring (TDM) and drugs-of-abuse testing, in addition to providing decision support in complex drug-regimes, drug interactions and adverse reactions. *Associate Professor / Head senior consultant Bettina Riedel* is the section leader.

The Bergen Pharmacy and Pharmacology Research Group consists of personnel from Section of Clinical Pharmacology who are also employed at the University of Bergen or otherwise engaged in collaborative activities within research related to drugs. *Professor Svein Haavik* is the group leader.

SonoCURE is a research group umbrella connecting researchers with different projects within *sonoporation* and pancreatic cancer in *in vitro* and preclinical models. *Professor Emmet McCormack* and *Associate Professor Spiros Kotopoulis* are the group leaders.

A brief story about the project

The project started early in 2011, when we became engaged in the planning of a phase 1 clinical trial in pancreatic cancer (PDAC) patients. An interdisciplinary team of gastroenterologists, oncologists and ultrasound physicists at Haukeland University hospital and the University of Bergen wanted to explore the potential of ultrasound and microbubbles (*sonoporation*[5]) to improve the efficacy of gemcitabine treatment in PDAC, based on an assumption that chemotherapeutic drug delivery to the tumours could be increased.

Section of Clinical Pharmacology was contacted to provide advice in pharmacokinetic assessments of gemcitabine. This included the study protocol and the application to the Norwegian Medical Agency, in addition to development of analytical methods to quantify gemcitabine and its main metabolites in patients and subsequently in *in vitro* experimental PDAC-models.

Via funding and in collaboration with Professor Asbjørn Svardal at the University of Bergen (UiB), we were able to initiate method development on a UiB-based LC-MS/MS-platform. We developed two analytical methods: one for extracellular gemcitabine and inactive metabolite, and one for the main intracellular active metabolite, and both were published in 2015 [1, 2] (Paper I and II).

In 2016, the final results from the phase 1 clinical trial were published [3], and we turned our focus to *in vitro* PDAC models in order to study basal aspects of gemcitabine uptake and metabolism, with (Paper V) or without (Paper IV) sonoporation.

From January 2017, I became a PhD-candidate with grant from Helse Vest for a 50 % position over three years. I worked with an *in vitro* PDAC model system in which a wide range of ultrasound intensities, microbubble brands and microbubble concentrations were applied in order to optimize membrane permeabilization without destroying the cells. This comprehensive optimization process[6] led to the

[5] A method to increase the permeability of biological barriers. See more details in section 1.3
[6] To be published separately, not included as part of the current PhD-project

selection of a subset of sonoporation parameters that were combined with gemcitabine in further *in vitro* experiments (Paper V).

Early in the project period, there were concerns about the relevance of spending more research efforts on gemcitabine, since new and more effective drug regimens emerged. However, the work was justified for several reasons that continued throughout the period, such as: 1) Gemcitabine monotherapy is still being used in many countries, and not only in patients experiencing toxicity of the combined drug-regimens, and 2) Combined treatment with gemcitabine and nab-paclitaxel became one of two first-choice regimens.

The focus within this thesis is on drug delivery in PDAC, with special emphasis on quantification of gemcitabine uptake and metabolism, with or without sonoporation using ultrasound at diagnostic intensities.

List of publications included in the thesis

I. **Bjånes T**, Kamčeva T, Eide T, Riedel B, Schjøtt J, Svardal A. *Preanalytical Stability of Gemcitabine and its Metabolite 2', 2'-Difluoro-2'-Deoxyuridine in Whole Blood-Assessed by Liquid Chromatography Tandem Mass Spectrometry*. J Pharm Sci 2015; 104(12): 4427-32. doi: 10.1002/jps.24638.

II. Kamčeva T, **Bjånes T**, Svardal A, Riedel B, Schjøtt J, Eide T. *Liquid chromatography/tandem mass spectrometry method for simultaneous quantification of eight endogenous nucleotides and the intracellular gemcitabine metabolite dFdCTP in human peripheral blood mononuclear cells*. J Chromatogr B Analyt Technol Biomed Life Sci 2015; 1001: 212-20. doi: 10.1016/j.jchromb.2015.07.041.

III. Dimcevski G, Kotopoulis S, **Bjånes TK**, Hoem D, Schjøtt J, Gjertsen BT, Biermann M, Molven A, Sørbye H, McCormack E, Postema M, Gilja OH. *A human clinical trial using ultrasound and microbubbles to enhance gemcitabine treatment of inoperable pancreatic cancer*. J Control Release 2016; 243; 172-181. doi: 10.1016/j.jconrel.2016.10.007.

IV. **Bjånes TK**, Jordheim LP, Schjøtt J, Kamceva T, Cros-Perrial E, Langer A, de Garibay GR, Kotopoulis S, McCormack E* and Riedel B*. *Intracellular cytidine deaminase regulates gemcitabine metabolism in pancreatic cancer cell lines*. Submitted to Drug Metabolism and Disposition September 13th 2019 (Manuscript ID: DMD/2019/089334, ongoing minor revision).

V. **Bjånes TK****, Kotopoulis S**, Murvold ET, Kamceva T, Bjørn Tore Gjertsen, Schjøtt J, Riedel B* and McCormack E*. *Ultrasound and microbubble-assisted gemcitabine delivery to pancreatic cancer cells*. Manuscript in preparation.

*Shared last authorship; **Shared first authorship

List of abbreviations

AUC: Area under the curve

BRCA2: Breast cancer gene 2

CDA: Cytidine deaminase

CDKN2A: Cyclin dependent kinase inhibitor 2A

CT: Computed tomography

C_{max}: Maximum drug concentration during a dosing interval

dCK: Deoxycytidine kinase

DCTD: Deoxycytidylate deaminase (or *Deoxycytidine monophosphate deaminase*)

dCTP: 2'-deoxycytidine-5'-triphosphate

ΔΔCT: delta-delta cycle threshold

dFdC: 2',2'-difluoro-2'-deoxycytidine (gemcitabine)

dFdCMP: 2',2'-difluoro-2'-deoxycytidine-5'-monophosphate

dFdCDP: 2',2'-difluoro-2'-deoxycytidine-5'-diphosphate (active metabolite)

dFdCTP: 2',2'-difluoro-2'-deoxycytidine-5'-triphosphate (active metabolite)

dFdU: 2',2'-difluoro-2'-deoxyuridine (inactive deaminated metabolite)

dFdUMP: 2',2'-difluoro-2'-deoxyuridine-5'-monophosphate

DNA: Deoxyribonucleic acid

FOLFIRINOX: Combined regimen of folinic acid, 5-FU, irinotecan and oxaliplatin

GEMM: Genetically engineered mouse model

hCNT: Human concentrative nucleoside transporters

hENT: Human equilibrative nucleoside transporters

IC_{50}: 50 % inhibitory concentration

KRAS: Kirsten rat sarcoma oncogene

LC-MS/MS: Liquid chromatography tandem mass spectrometry

LLOQ: Lower limit of quantification

MB: Microbubbles

MRI: Magnetic resonance imaging

PALB2: Partner and localizer of BRCA2

PD: Pharmacodynamic

PDAC: Pancreatic ductal adenocarcinoma (i.e. “pancreatic cancer” in most setting)

PDX: Patient-derived xenograft

PET: Positron emission tomography

PK: Pharmacokinetic

QC: Quality control

RR: Ribonucleotide reductase

SD: Standard deviation

SMAD4: Suppressor of Mothers Against Decapentaplegic 4

THU: Tetrahydrouridine

T_{max}: Time to C_{max}

TS: Thymidylate synthetase

TP53: Tumor protein 53

US: Ultrasound

Abstract

Background

Pancreatic ductal adenocarcinoma (PDAC) has a dismal prognosis due to late stage diagnosis and unresponsiveness to chemotherapies. A dense *desmoplastic* tumour stroma is considered to represent a *barrier* against drug delivery. Gemcitabine, until recently the first choice chemotherapeutic in metastatic PDAC, improves median overall survival by only 1 – 2 months. Poor drug delivery to PDAC cells may contribute to the limited efficacy. Recently, ultrasound combined with microbubbles has been introduced as a method to increase the permeability of biological barriers, through a process called *sonoporation*.

Overall objective

The overall objective of the project was to evaluate quantitative aspects of gemcitabine delivery and metabolism combined with sonoporation in PDAC patients and in *in vitro* models.

Methods

In paper I, we described the development of a liquid chromatography tandem mass spectrometric (LC-MS/MS) method for quantification of extracellular gemcitabine and inactive metabolite (dFdU), and we studied the stability of the analytes in blood samples. In paper II, a LC-MS/MS method for intracellular active gemcitabine metabolite (dFdCTP) was developed. Paper III was a clinical phase 1 trial in ten PDAC patients who were treated with gemcitabine combined with ultrasound and microbubbles. In this study, safety was a primary and survival a secondary outcome measure. Systemic pharmacokinetics (PK) of gemcitabine was also assessed. Papers IV and V were *in vitro* studies in PDAC cell line models, in which gemcitabine uptake was quantified following exposure to therapeutically relevant gemcitabine concentrations, with and without sonoporation and pharmacological modulation of drug transport and metabolism.

Results

The validated concentration ranges of gemcitabine, dFdU (Paper I) and dFdCTP (Paper II) were 0.125 – 40 µg/mL, 1.25 – 80 µg/mL and 0.05 – 28.1 µM, respectively, with coefficients of variation (CV) of 11.5, 5.2 and 11.4 % at their lower limits of quantification. Stabilities of gemcitabine and dFdU (Paper I) were demonstrated for at least four hours in whole blood samples kept on ice, when the cytidine deaminase (CDA) inhibitor tetrahydrouridine (THU) was added. In the clinical trial (Paper III), no additional toxicity of sonoporation to that of gemcitabine was noted, and gemcitabine PK was not different from patients treated with gemcitabine alone. The study patients tended to survive longer and received a higher number of treatment cycles, compared to a historical control group. In paper IV, we showed that intracellular CDA could inactivate gemcitabine extensively and hereby regulate intracellular dFdCTP accumulation. In paper V, we demonstrated that sonoporation contributed to only a minor extent of gemcitabine uptake compared to physiological membrane transporters.

Conclusions

Quantitative assessments of gemcitabine and its main extra- and intracellular metabolites in different matrices enabled elucidation of drug distribution, uptake and metabolism in PDAC. Our data support further clinical studies of sonoporation combined with chemotherapies, but underscores the importance of taking physiological mechanisms of drug transport and metabolism into account.

Future studies in more complex PDAC models are required to investigate tumour tissue drug distribution and cellular uptake, and to elucidate other mechanisms involved in sonoporation.

Thesis

1. Introduction

The following three main sections cover background topics related to the current research field, focused on pancreatic cancer and chemotherapeutic drug-delivery by sonoporation, with special emphasis on the nucleoside analogue gemcitabine and quantitative aspects of cellular uptake and metabolism.

1.1. PANCREATIC CANCER

1.1.1. Burden of disease

Pancreatic ductal adenocarcinoma (PDAC) is the seventh most common form of all cancers worldwide [4]. In Norway, more than 800 new patients were diagnosed in 2017 [5, 6]. PDAC was the fourth leading cause of cancer deaths in Europe in 2018, with approximately 95.000 cases [4]. The mortality-to-incidence ratio is above 0.9 [6, 7], and the overall five-year survival rate is as low as 5-8 % [5, 6, 8]. This poor prognosis is highly attributable to the fact that a majority of patients develop symptoms at late stage, with incurable disease at the time of diagnosis [8, 9]. Incidences of PDAC is increasing in conjunction with increasing age of the population in developed countries. Within 2040, the number of PDAC patients is projected to increase by 30 % in the European Union and 40 % in the United States of America [4, 7].

The severity of this disease and its increasing incidence represent a highly unmet medical need that challenges the healthcare providers and research communities to develop new and improved diagnostic and therapeutic strategies.

1.1.2. Diagnosis

1.1.2.1. Clinical signs and radiological examinations

Typical symptoms preceding a diagnosis of PDAC include jaundice, poor appetite, loss of weight, and pain [5]. The purpose of diagnostic evaluations is to reveal whether a tumour is present, determine the stage of disease according to the TNM-classification of malignant tumours [5, 10], and whether it can be treated surgically. The main radiologic modalities applied include computed tomography (CT), ultrasound (US), magnetic resonance imaging (MRI) and positron-emission tomography (PET) [11, 12].

Recent studies suggest that endoscopic ultrasound (EUS) and contrast enhanced ultrasound (CEUS), in the hands of skilled clinicians, equal the diagnostic accuracy of CT imaging [13], and may even be superior modalities for detection of small lesions [14]. Furthermore, researchers at our institution have recently proposed funding [15] of a development project in which EUS and CEUS will also be employed in the early response-evaluations of PDAC patients undergoing treatment.

1.1.2.2. Histology and molecular biology

In inoperable patients, ultrasound-guided fine-needle aspirations from tumours are performed prior to commencement of palliative chemotherapy [5]. In resected tumour specimen, the whole tumour and its excised surroundings are examined. Histological examinations are needed in order to verify the PDAC diagnosis, the tumour resection margins and lymph node invasion, and to rule out differential diagnoses such as neuroendocrine tumours [16].

There are no unique diagnostic molecular markers for PDAC, but several mutations are prevalent (e.g. activation of *Kirsten rat sarcoma* (KRAS) and inactivation of *Tumour protein 53* (TP53), *Cyclin dependent kinase inhibitor 2A* (CDKN2A) and *Suppressor of mothers against decapentaplegic 4* (SMAD4)) and provide prognostic information [9, 16]. As they do not convincingly provide guidance into selection of patients for specific personalized treatment strategies, the application of such markers is limited. However, several promising markers are being explored in a research setting, of which approaches encompassing multiple genes and proteins that delineate unique signatures [17, 18] of the cancer cells and their microenvironment, dominate. For example, tumours with a high mutational burden and infiltrated with lymphocytes, may be candidates for immunotherapeutic treatment [16]. Moreover, expression of the *equilibrative nucleoside transporter 1* (hENT1), *deoxycytidine kinase* (dCK) and *cytidine deaminase* (CDA) in tumour tissue may predict the outcome of treatment with gemcitabine (see details

in section 1.2). It has also been suggested that the amount and characteristics of circulating tumour cells [19] and nucleic acids [20] in blood, and the pattern of mutations of KRAS and TP53 in pancreatic juice [21], may be useful prognostic biomarkers.

1.1.2.3. Early detection to improve prognosis

Lifestyle factors such as cigarette smoking, alcohol overuse, overweight and poor blood-glucose control represent potentially modifiable risk factors of developing PDAC [4, 22]. Heritable risk factors, such as mutations in *Breast cancer gene 2* (BRCA2), *Partner and localizer of BRCA2* (PALB2) and other genes, and/or multiple relatives diagnosed with PDAC [22], account for less than 10 % of new cases [4]. For patients with heritable risk, systematic screening strategies may be justified in order to detect the disease at an early stage where curative treatment may still be an option. However, up to date no firm evidence exists that such screening programs provide a positive benefit-cost-balance [17, 22].

Clinical symptoms and signs are often unspecific or lacking until the disease has progressed to an advanced stage, and early detection is still unrealistic in the vast majority of patients [9]. Therefore, there is a focus on research within the field of PDAC in order to develop new and improved treatment strategies[7].

1.1.3. Treatment strategies

1.1.3.1. Surgery

Only 15 % of newly diagnosed PDAC tumours are surgically resectable [5, 8]. For operable patients, the prognosis has improved somewhat over the last decades, of which a broader application of multimodal treatment, such as early post-operative mobilisation, optimized analgesia,

[7] https://clinicaltrials.gov and https://www.clinicaltrialsregister.eu (Search "pancreatic cancer")

thrombosis prophylaxis and nutrition, may have contributed [5]. However, even after potentially curative surgery, followed by adjuvant chemotherapy [5, 23], most patients eventually experience locoregional recurrences or metastatic disease. As a result, the median and five-year overall survival is still only 20–25 months [23, 24] and 25 % [8, 24], respectively.

1.1.3.2. Chemotherapy

1.1.3.2.1. General considerations

Eighty five percent of newly diagnosed PDAC tumours are considered unresectable due to locally advanced disease with encasement of large blood vessels or neighbouring organs, or the presence of metastases [8]. Chemotherapy produces moderate objective responses, but is not curative in this setting [5]. Chemotherapy is also used in the adjuvant setting in selected patients who are sufficiently fit after surgery, whereas conclusive evidence is still lacking on the role of neo-adjuvant chemotherapy [17]. Patients who do not tolerate chemotherapy due to poor performance status or severe weight loss, should nevertheless receive supportive care according to best practice guidelines [25].

1.1.3.2.2. Poor compound delivery

PDAC tumours are characterized by a dense fibrotic reaction consisting of, among others, fibroblast and an abundant extracellular matrix, often referred to as *desmoplasia*, with a high interstitial fluid pressure and poor blood supply that results in a nutrient-poor and hypoxic environment [26, 27]. These features may also hamper diffusion of therapeutic compounds into the tissue, and are thought to represent a general mechanism of treatment resistance [28-30]. Efforts to overcome this potential barrier against effective drug delivery have been explored, for example by using inhibitors of sonic

hedgehog signalling or focal adhesion kinase (FAK) aiming at reducing desmoplasia [30], so called stromal depletion therapies. While increased efficacy of chemotherapies were achieved *in vitro*, initial clinical studies were disappointing in terms of improving survival of patients. It has been demonstrated that bacteria [31, 32], fibroblasts [33] and macrophages [34, 35] in the tumour microenvironment might modulate intratumoural drug distribution and metabolism, and it has been suggested that such factors might be equally important mechanisms of treatment resistance as poor drug delivery [33]. Moreover, drug delivery from the vascular compartment into the tumour interstitium is only a part of the whole picture, since transport of chemotherapeutics across cellular membranes is also a prerequisite in order to inhibit growth and kill cancer cells.

Drug transport between the blood plasma, tissues and organs is mainly mediated by *diffusion* and *convection*, with concentration and pressure gradients as their respective driving forces. The amount of drug transported per time unit depends on blood flow, perfusion and the expression of transmembrane influx and efflux transporter proteins in the region of interest, and the hydrophilic/lipophilic properties of the drug and their extent of binding to plasma- and tissue proteins [36, 37].

1.1.3.2.3. Current chemotherapeutic drug regimens

Three main chemotherapeutic drug regimens are the current basis of first and second line palliative treatment of PDAC patients: 1) Gemcitabine monotherapy, 2) gemcitabine combined with nab-paclitaxel, and 3) a combined regimen of folinic acid, 5-fluorouracil (5-FU), irinotecan and oxaliplatin (FOLFIRINOX) [5, 38].

Gemcitabine monotherapy was introduced as first line palliative chemotherapy in 1997, based on a study that showed median overall

survival of 5.7 months, compared to 4.4 months with 5-FU [5, 38]. In addition, the clinical benefit in terms of symptom relief was better with gemcitabine compared to 5-FU, with 23.8 vs 4.8 % responders [38]. From 2011 and onwards, gemcitabine monotherapy was gradually replaced by more effective regimens, but also more toxic, in patients with sufficient performance status who would tolerate a greater toxicity.

In a randomized phase 3 clinical trial where gemcitabine was compared to FOLFIRINOX [39], the authors reported median overall survival of 6.8 and 11.1 months, respectively. FOLFIRINOX was also significantly more toxic, and reduced doses in a modified regime, commonly referred to as "mFOLFIRINOX", was later proposed as an option for some patients [38, 40].

In 2013, a randomized phase 3 trial comparing gemcitabine monotherapy with gemcitabine and albumin-bound paclitaxel (nab-paclitaxel) [41], median overall survival increased from 6.6 months with monotherapy to 8.7 months with the combined regime.

No head-to-head study between gemcitabine/nab-paclitaxel and FOLFIRINOX has been conducted, but both regimens possess individual strengths. A greater survival benefit was reported in the FOLFIRINOX study [39]. In the gemcitabine/nab-paclitaxel study [41], the proportion of older patients was higher. Ultimately, the choice between no chemotherapy, gemcitabine monotherapy, gemcitabine/nab-paclitaxel or FOLFIRINOX comes down to the patient's own preferences and individual risk factors such as age, co-morbidities and performance status [25, 38].

1.1.4. PDAC disease models

In vitro and *in vivo* tumour models are fundamental in basal cancer research projects. *In vitro* cell line models are useful for several reasons, such as identification of the intracellular pathways driving disease development, for high-throughput screening of potential therapeutics, and characterization of cellular drug metabolism and mechanisms of action [42, 43]. Several immortalized PDAC cell lines are available for such research purposes. The cells display a wide range of genotypic and phenotypic traits [44] that might also mirror the variability between PDAC tumours in patients. Several different cell lines, such as BxPC-3, MIA PaCa-2 and PANC-1, have been included in *in vitro* studies of PDAC, and have contributed to an increased understanding of the disease [45]. Cell line models are usually based on two-dimensional (2D) monolayer or multilayer [46] growth on a sterile plastic surface, with direct access to nutrients and other components added to the culture media. Hence, the resulting cellular growth patterns and the microenvironment are quite unlike PDAC tumours in patients, in which an abundant desmoplastic extracellular matrix and multiple other cell types are dominant features [47, 48] . To address some of these shortcomings, three-dimensional (3D) *in vitro* culture systems [49] based on for example collagen, reconstituted basement membranes (Matrigel™) [47], or decellularized matrix scaffolds [50] have been developed. These systems are suitable to study cell-cell interactions and allow chemotherapeutic drug sensitivity testing in a more realistic *in vivo*-like microenvironment, but require more time and resources compared to 2D-cultures [50].

In vivo PDAC models have been established in immunodeficient mice by injecting cell lines or implanting solid tumour pieces from patients, either subcutaneously or orthotopically. Such models are generally referred to as cell-line derived or patient-derived xenografts (PDX) [49], and are superior to *in vitro* models, e.g. in their ability to mimic the systemic pathophysiology of the disease. However, PDAC PDXs have not been able to fully reproduce the desmoplastic reaction seen in patient tumours, and

the clinical relevance of these models have been questioned [27]. In genetically engineered mouse models (GEMM) where PDAC tumours may arise spontaneously, desmoplasia is a more prominent feature. However, several positive results from preclinical GEMM models have also turned out negative in clinical studies [49]. Moreover, mouse studies are labour-intensive, and many researchers therefore still make use of refined *in vitro* 2D or 3D-models of PDAC [51].

1.2. GEMCITABINE

1.2.1. Structure

Gemcitabine, or 2',2'-difluoro-2'-deoxycytidine (dFdC), is a fluorinated analogue of the endogenous pyrimidine nucleoside deoxycytidine (dC) (Figure 1), and as such its transport, metabolism and effects are related to the cellular nucleoside pathways [52, 53].

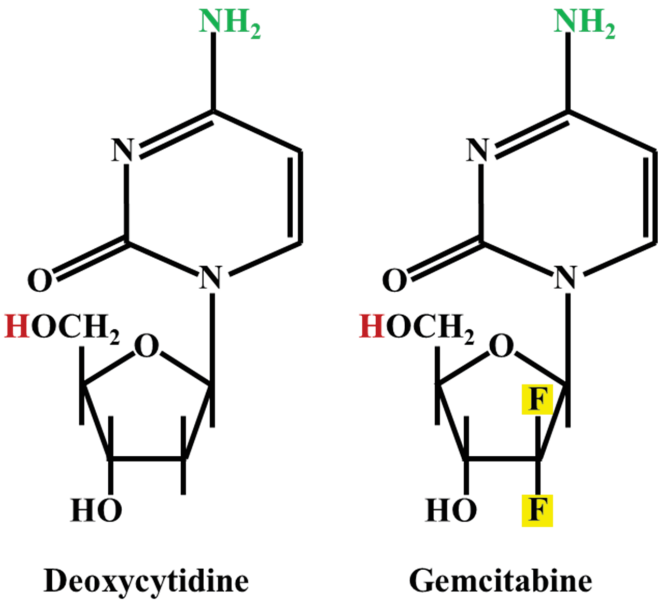

Figure 1. Structure of deoxycytidine (left) and its analogue gemcitabine (right). *The two fluor-atoms in 2'-position indicated in yellow. Positions of metabolic activation (phosphorylation) and inactivation (deamination) are indicated in red and green, respectively.*

1.2.2. Cellular uptake

Gemcitabine enters the cells via transmembrane nucleoside transporter proteins, of which the human equilibrative transporter 1 (hENT1) plays the dominant role, and to a lesser extent, the human concentrative transporters 1 (hCNT1) and 3 (hCNT3) [52, 54]. Equilibrative transporters allow bidirectional transport along the concentration gradient of the substrate,

whereas concentrative transporters are active and utilize sodium co-transport together with the substrate [55]. The particular importance of hENT1 on gemcitabine efficacy is underscored by its correlation with drug uptake and cytotoxicity in cancer cells *in vitro* [56], and on tumour regression and patient survival *in vivo* [54]. Koay and co-workers [29, 57] found that both cellular hENT1-activity and general mass transport properties of the connective tissue are important sources of variable gemcitabine uptake in PDAC tumours.

It has been shown that hENT1 activity in cells [56] and expression in tumour tissues [58, 59] might be a suitable biomarker for prediction of gemcitabine efficacy. Greenhalf and co-workers [59] suggested that in tumours with low hENT1-expression, gemcitabine should be avoided due to a poor anticipated efficacy, and that alternative drug regimens should be considered. Due to the lack of prospective evaluations of hENT1 as a predictive biomarker [18], and suboptimal agreement between immunohistochemistry assessments performed with different antibodies [55, 60], it is not implemented as a routine pre-treatment procedure in most clinics. In 2010, Paproski and co-workers validated an imaging method for assessment of cellular hENT-activity, employing the PET-tracer 3'-deoxy-3'-fluorothymidine (FLT) [56], but to our knowledge this approach has not been developed into clinical use to guide the selection of a suitable therapeutic regimen.

1.2.3. Gemcitabine metabolism

Gemcitabine is subject to extensive systemic and cellular metabolism, either to inactive or active metabolites, and the balance between these two opposing pathways may be a determinant of drug efficacy. Figure 2 illustrates the complexity of this system.

1.2.3.1. Active metabolites and drug targets

The main activation pathway consists of a series of intracellular phosphorylation reactions via nucleoside kinases, of which *deoxycytidine kinase* (dCK), catalysing the initial phosphorylation to gemcitabine monophosphate (dFdCMP), is the rate-limiting step [52, 61]. Expression of dCK in tumour specimen has been suggested as a potential predictive biomarker of gemcitabine response [18]. dFdCMP is further phosphorylated to gemcitabine diphosphate (dFdCDP) and triphosphate (dFdCTP), both of which are pharmacologically active metabolites. A small fraction of dFdCMP is also deaminated by *deoxycytidylate deaminase* (DCTD) to dFdUMP. dFdUMP in turn inhibits *thymidylate synthetase* (TS) responsible for the synthesis of thymidine monophosphate (dTMP) [52], a precursor of thymidine triphosphate (dTTP) (Figure 2). dFdCDP inhibits *ribonucleotide reductase* (RR), an important enzyme regulating nucleotide pool homeostasis by catalysing the reduction of ribonucleotides to deoxyribonucleotides [52, 61]. Overexpression of RR in PDAC tumours has been found to correlate with poor outcome in patients treated with gemcitabine in the adjuvant setting, probably due to an increase in deoxynucleoside triphosphates (dNTPs) [62], including dCTP (Figure 2).

dFdCTP competes directly with dCTP for incorporation into DNA, which results in inhibition of DNA-synthesis through masked chain-termination [52]. The cytotoxic effect of dFdCTP is primarily exerted in the S-phase of the cell cycle [53]. Intracellular dFdCTP concentration in peripheral blood mononuclear cells (PBMC) has been used as a surrogate marker for drug exposure [63] and risk of hematotoxicity [64], and in

cancer cells as a pharmacodynamic endpoint related to inhibition of DNA-synthesis [65] and cytotoxicity [66]. The use of dFdCTP concentrations in these settings is also supported by the fact that the intracellular concentrations of gemcitabine and the other intermediate metabolites are very low, which might preclude their quantification [67].

1.2.3.2. Inactivation

The main elimination pathway of gemcitabine to 2',2'-difluoro-2'-deoxyuridine (dFdU) is catalysed by *cytidine deaminase* (CDA) [68], which is widely expressed in blood, liver and several other tissues [61, 69]. Deamination of dFdCMP to dFdUMP by intracellular *deoxycytidylate deaminase* (DCTD), followed by dephosphorylation, might also represent a minor source of dFdU [52, 68, 70] (Figure 2). Efflux of dFdU from the cells is mediated by multiple different ABC-transporter proteins, and it has been postulated that their activities might indirectly influence cellular gemcitabine sensitivity. The proposed mechanism is that low efflux leads to intracellular accumulation of dFdU, which in turn may inhibit CDA activity. Theoretically, this would allow more gemcitabine to be activated [71]. dFdU itself is considered mainly inactive, and the relevance of suggested active intracellular dFdU-metabolites [72] has been questioned [61].

Other intracellular enzymes may also to some extent promote gemcitabine inactivation. For example, *cytosolic 5'-nucleotidase III* (cN-IIIA) [73], has been shown to dephosphorylate dFdCMP to dFdC and hereby oppose the intracellular accumulation of dFdCTP.

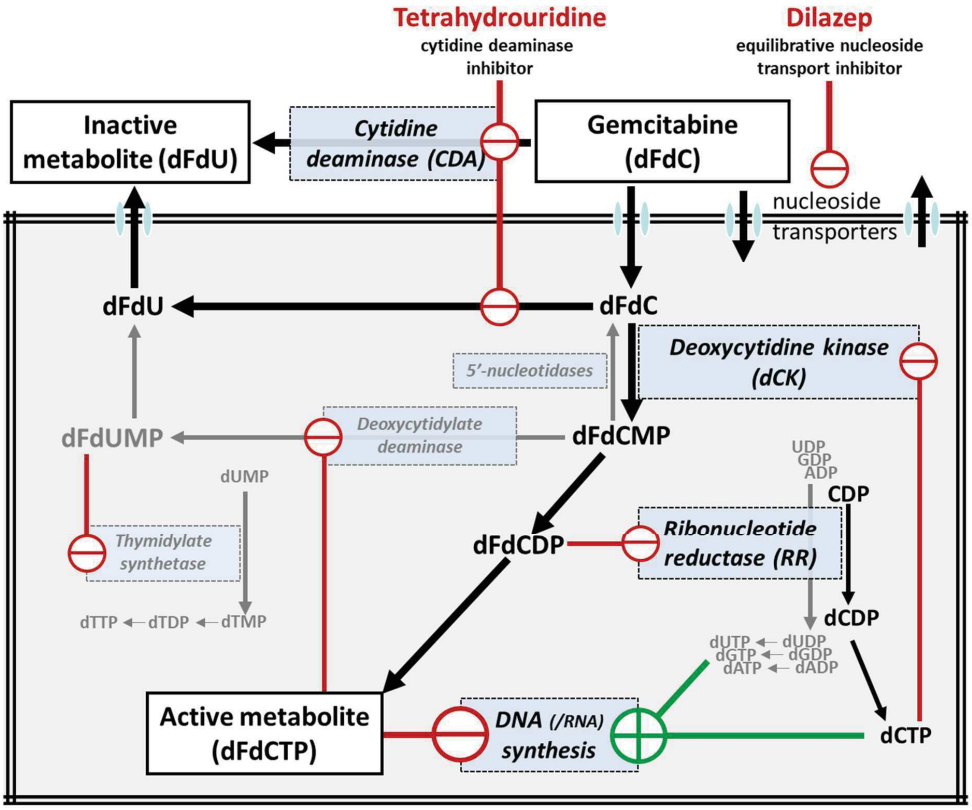

Figure 2. Schematic overview of gemcitabine cellular uptake, metabolic pathways and mechanisms of action. *Arrows indicate transport and enzymatic processes. Examples of the interplay between gemcitabine metabolites and endogenous nucleotides, and of intrinsic regulation and pharmacological inhibition: Red and green lines and corresponding symbols indicate inhibitory and stimulatory actions, respectively.*

ADP: adenosine diphosphate; dADP: deoxyADP; dATP: deoxyadenosine triphosphate; CDA: cytidine deaminase; CDP: cytidine diphosphate; dCDP: deoxyCDP; dCTP; deoxycytidine triphosphate; dCK: deoxycytidine kinase; dFdC; 2',2'-difluoro-2'-deoxycytidine (gemcitabine); dFdCMP: gemcitabine 5'-monophosphate; dFdCDP: gemcitabine 5'-diphosphate; dFdCTP: gemcitabine 5'-triphosphate; dFdU; 2',2'-difluoro-2'-deoxyuridine; dFdUMP; dFdU-5'-monophosphate; DNA: deoxyribonucleic acid; RNA: ribonucleic acid; RR: ribonucleotide reductase

1.2.4. Intrinsic regulation of gemcitabine transport and metabolism

Regulatory mechanisms within the intracellular nucleotide pathways illustrate the interplay between endogenous nucleotides and gemcitabine metabolites. Selected examples are given below and in Figure 2.

1) Inhibition of *ribonucleotide reductase* by dFdCDP results in reduced synthesis of dCTP and other dNTPs. This might increase gemcitabine cytotoxicity via two overlapping mechanisms, referred to as *self-potentiation* [52]:
    a. Reduced feedback-inhibition of dCK by dCTP favours the synthesis of dFdCMP and subsequently results in increased dFdCTP concentrations
    b. The combined effect of reduced dCTP and increased dFdCTP concentration favours incorporation of the latter compound into DNA
2) dFdCTP exerts feedback inhibition on *deoxycytidylate deaminase*, hereby favouring its own activation pathway by limiting the deamination of dFdCMP [52]
3) Several enzymes involved in nucleoside metabolism employ adenosine triphosphate (ATP), cytidine triphosphate (CTP) or uridine triphosphate (UTP) as phosphate donors [74]. In cell cultures, it has been shown that treatment with gemcitabine induces perturbations in the ribonucleotide pools, including ATP, CTP and UTP [75, 76]. Since gemcitabine, being a *nucleoside analogue*, is also metabolised via these enzymes, this could represent another mechanism of "self-modulation", as suggested by van Moorsel and co-workers [66]

1.2.5. Pharmacological modulation of gemcitabine transport and metabolism pathways

Tetrahydrouridine (THU), a CDA-inhibitor [77], and dilazep, an inhibitor of hENT1 and hENT2 [78] (Figure 2), have both been applied as pharmacological modulators in experimental studies involving gemcitabine. THU has been used *in vivo* in mice [79] and in patients [80], and *in vitro* [81] to prolong the half-life of pyrimidine nucleoside analogues in an attempt to increase their efficacy. Moreover, it is routinely used as an additive in blood sample tubes to prevent *ex vivo* deamination of gemcitabine and other nucleoside analogues [82]. Although promising therapeutic results have been achieved by combining THU and nucleoside analogues in leukaemia patients [83, 84], the increase in toxicity may also limit their combined use. To our knowledge, no clinical trial combining gemcitabine with THU has been conducted in PDAC patients.

Dilazep is one of several drugs [85] that has been used to inhibit nucleoside membrane transport *in vitro*, including in PDAC cells treated with gemcitabine [56, 78]. The purpose of employing transport inhibitors has mainly been to isolate individual mechanisms of drug transport. The relevance of such experimental approaches in PDAC is underscored by the importance of hENT1 in cellular gemcitabine uptake [56, 58, 59].

1.2.6. Concentration-time relations

In the following, examples of gemcitabine studies *in vivo* and *in vitro* will be given, with emphasis on drug exposure over time, and on extra- and intracellular concentrations of gemcitabine and its main metabolites.

1.2.6.1. Plasma concentrations

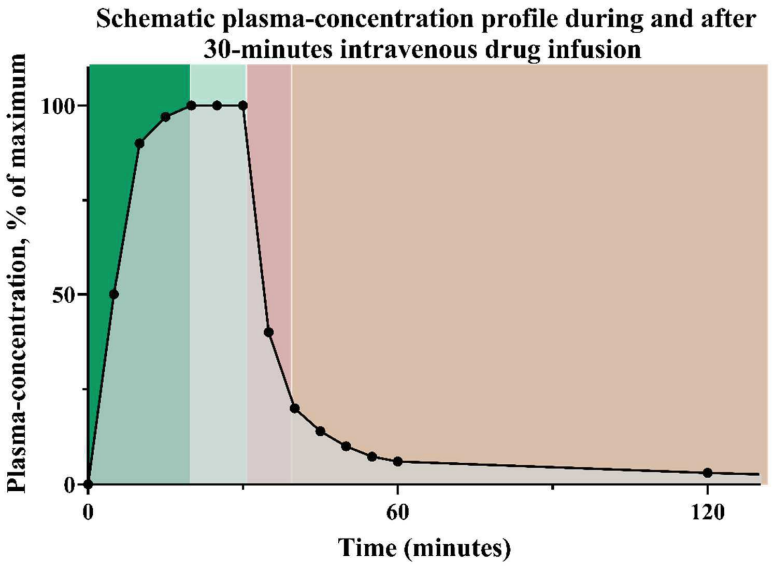

Figure 3. Schematic plasma concentration profile after intravenous drug infusion. *Drug concentrations increase rapidly during drug infusion (dark green), followed by a concentration plateau (light green) with a balance between the dose-rate and distribution/elimination rates. After the infusion is terminated, a rapid initial decline (red, α-phase) is observed when distribution/elimination dominates, followed by a more gradual decline (orange, β-phase) after distributional equilibrium has been reached and drug elimination dominates. The total drug exposure over time is calculated as area under the curve (AUC, shaded area).*

The clinically dominating dosing regimen of gemcitabine in PDAC consists of repeated courses of weekly 30-minutes infusions of 1000 mg/m^2, both when administered as monotherapy [5, 53] and when

combined with nab-paclitaxel [86]. Plasma concentrations (mean±SD) reach a peak plateau of 82±21 µM (21.6±5.6 mg/L) towards the end of the infusion, followed by a rapid elimination with a half-life of 7–18 minutes [69]. Systemic gemcitabine exposure, expressed as area under the curve (AUC) of plasma-concentrations (see schematic in Figure 3), is within 41±12 µM*h (10.8±3.2 mg/L*h) in the majority of patients [69]. Systemic CDA activity is the main route of gemcitabine elimination with dFdU as the sole plasma metabolite. Only 5–10 % of gemcitabine is excreted unchanged in urine [53, 69]. Towards the end of gemcitabine infusions or soon thereafter, dFdU reaches peak concentrations of 106–197 µM (28–52 mg/L) is reached, and subsequently eliminated by renal excretion with a terminal half-life of 33–85 hours [53].

1.2.6.2. Tissue and pericellular concentrations

1.2.6.2.1. *In vivo* gemcitabine and dFdU concentrations

According to *in silico* simulations by Battaglia and co-workers [87], peak gemcitabine concentration around 20 µM could be expected in tumour interstitial fluid in patients receiving gemcitabine 1000 mg/m^2 infusions, followed by a similar elimination rate as from the plasma compartment. As a result, a theoretical tissue-to-plasma AUC ratio of approximately 1/3 could be expected.

To our knowledge, no researchers have directly measured gemcitabine concentrations in PDAC tumour tissue during intravenous drug infusions in human studies. Bapiro and co-workers [88] measured dFdC and dFdU concentrations in plasma and excised pancreatic tumour tissue specimen from mice, 60–75 minutes after intraperitoneal administration of 50 (n=3) or 100 mg/kg (n=3) gemcitabine. Mean dFdC concentrations were 27.0–132.2 µM (7.1–34.8 mg/L) in plasma and 15.2–38.8 µM (4.0–10.2 ng/kg[8]) in tissue, and mean dFdU concentrations were 49.0–72.6 µM (12.9–19.1

[8] Unit conversions from ng/kg tissue based on an assumed tissue density of 1 g/mL (Bapiro et al 2011).

mg/L) in plasma and 42.3–69.2 µM (11.2–18.2 ng/kg) in tissue. Tissue-to-plasma concentration ratios were 0.29–0.56 for dFdC and 0.87–0.95 for dFdU. Neesse and co-workers [89] found comparable concentrations. In both studies [88, 89], gemcitabine concentrations in plasma were high compared to human studies [69], and cannot be directly compared due to different routes of administration. However, relative distribution of gemcitabine between plasma and tissue compartments seemed to fit reasonably well within the *in silico* estimates, as reported by Battaglia and co-workers [87].

1.2.6.2.2. *In vitro* gemcitabine concentrations

Numerous studies of *in vitro* gemcitabine-exposures have been performed. As an illustration, Paproski and co-workers [56] applied three principally different durations of incubation with 0.1–100 µM ^{3}H-gemcitabine:

1) **≤ 45 seconds** in membrane uptake assays,
2) **60 minutes** when assessing uptake and activation / phosphorylation
   and
3) **up to 72 hours** in gemcitabine toxicity assays

Other authors have used conceptually similar gemcitabine exposures [33, 66, 71, 78], with a duration of 24 hours dominating in most studies. In most studies, the rationale for the chosen gemcitabine concentration is not elaborated, whereas in some studies the investigators aimed at concentrations in near proximity to the IC_{50}-limits [90, 91]. Others have chosen the highest drug concentrations possible that did not precipitate in the wells or expose the cells to toxic concentrations of the solvent dimethylsulphoxide (DMSO) [92].

Most researchers prepare spike-solutions based on *a priori* theoretical calculations, and direct quantification of gemcitabine and metabolite concentrations in cell culture media are, with a few exceptions [93], not reported.

1.2.6.3. Intracellular active metabolite concentrations

dFdCTP is the main intracellular metabolite, and its concentration after gemcitabine exposure is used as measure of cellular uptake and activation [56], and has also been related to drug efficacy [63-66]. Due to its high polarity with three phosphate groups, dFdCTP is trapped inside cells and is not found extracellularly [88].

As exemplified by Derissen and co-workers [61], intracellular dFdCTP may be expressed as *ng per mg protein*, *µmol per litre cell volume* or *pmol per 10^6 cells* (hereafter abbreviated as *pmol/10^6*). In our experience, the latter unit, pmol/10^6, is preferred by most researchers. Moreover, it might be a complex task to compare intracellular dFdCTP-concentrations between studies due to exposure with different gemcitabine concentrations and cell lines used. Selected examples from the literature are given below.

1.2.6.3.1. *In vivo* dFdCTP concentrations

In patients, dFdCTP concentrations in mononuclear cells (PBMCs) are commonly used as surrogate marker of gemcitabine exposure and activation. In PBMCs isolated from a patient after a 30-minutes 300 mg/m^2 gemcitabine infusion, Veltkamp and co-workers [94] found a dFdCTP peak concentration of approximately 590 pmol/10^6 two hours after end of the infusion. Abbruzzese and co-workers [95] measured dFdCTP concentrations in PBMCs collected in a phase 1 dose-escalation study with 30-minutes infusions of gemcitabine 22.5 – 1000 mg/m^2. At 350 and 1000 mg/m^2 they found peak dFdCTP concentrations of 284 ± 72 (mean ± SEM) and 224 ± 13 µM, respectively, 30 minutes after the end of infusions. The authors did

not convert concentrations to pmol/10^6, but discussed that variable cell counts between samples may have been a weakness in their study [95]. PBMCs may not reflect the situation in solid tumour cells, in terms of drug exposure to the target and activities in intracellular metabolic pathways [61], but are often preferred as model due to their availability for repeated sampling at multiple time points during and after gemcitabine treatment. Moreover, tumour tissue heterogeneity further complicates the picture. As an example, Koay and co-workers [29] measured dFdCTP incorporation into DNA in tumour tissue specimen excised at the end of intraoperative gemcitabine infusions[9] in 12 patients. They found highly variable concentrations between the different patients, which to some extent could be explained by variable hENT1-expression, vascular supply and different cell numbers in tumour specimens. Bapiro and co-workers [88] also measured dFdCTP concentrations (ng/mg tissue) in tumour tissue from mice one hour after i.p. administration of 100 mg/kg gemcitabine. A considerable variation between the mice was noted, with concentrations of dFdCTP ranging from below the lower limit of quantification (LLOQ) to 30 ng/mg.

1.2.6.3.2. *In vitro* dFdCTP concentrations

Following 24 hours *in vitro* incubation of 19 different cancer cell lines with 1 or 10 µM gemcitabine, van Moorsel and co-workers [66] reported median intracellular dFdCTP concentrations of 450, 614, 816 and 925 pmol/10^6 in ovarian, head-and-neck, lung and colon cancer cell lines, respectively. Nishi and co-workers [96] incubated the leukaemia cell line HL60 for 1.5 hours with 2.0 µM gemcitabine, and primary leukemic cells collected from a patient with chronic lymphocytic leukaemia (CML) for 2.0 hours with 2.0 µM

[9] To our knowledge this trial is the only reported human study in which gemcitabine has been administered intraoperatively and with samples collected from tumours directly after treatment

gemcitabine. Intracellular dFdCTP concentrations were 75 and 20 pmol/10^6 in HL60 and CML cells, respectively.

The time course (kinetics) of dFdCTP accumulation and elimination has also been investigated in a few studies. In general, accumulation of dFdCTP increases when gemcitabine incubation time is increased. Ohmine and co-workers incubated the PDAC cell line PK9 with 1 µM dFdC for 10 min, and 1, 6, 12 and 24 hours. Intracellular dFdCTP increased up to approximately 35 pmol/mg protein at 6 hours (T_{max}), after which a plateau or a small decrease up to 24 hours was noted. A comparable T_{max} was also found in a study of Chinese hamster ovary (CHO) cells by Heinemann and co-workers [97]. Van Haperen and co-workers [75] incubated the ovarian cell line A2780, and the murine and human colon cell lines C26-10 and WiDr with 1, 10 or 100 µM gemcitabine for 4 hours and 24 hours. In all cell lines, higher dFdCTP concentrations were seen with increasing gemcitabine concentrations up to 10 µM, and with 24 hours incubation compared to 4 hours. Moreover, they noted variations in peak dFdCTP concentration from approximately 600 pmol/10^6 in WiDr to 1700 pmol/10^6 in C26-10 at 24 hours, which also reflected different gemcitabine sensitivities between the cell lines. In the same study [75], cellular elimination of dFdCTP was studied after 24 hours incubation with 1 or 10 µM gemcitabine. In all cell lines, peak dFdCTP was seen within 1 hours after terminating drug incubation, followed by a decrease to 0-50 % of the peak concentration after another 24 hours incubation in drug-free medium. In CHO cells, incubated up to 4 hours with 10 µM gemcitabine, Heinemann and co-workers [97] found that dFdCTP was highest immediately after termination of the incubation, and decreased gradually thereafter.

1.2.7. Concluding remarks

Gemcitabine undergoes extensive extra- and intracellular metabolism, and exerts its cytotoxic effects by modulating intracellular nucleotide metabolism and inhibiting DNA synthesis. The relationship between drug exposure and active metabolite accumulation and toxicities has been explored both *in vivo* and *in vitro*, and has exhibited great variability. Whether gemcitabine delivery into PDAC tumour cells represents a liming factor for its efficacy at clinically relevant concentrations, remains to be elucidated.

1.3. SONOPORATION: Ultrasound- and microbubble-assisted drug delivery

Poor chemotherapeutic drug delivery into PDAC tumours may be a general mechanism of treatment resistance, mediated by the dense tissue stroma acting as a barrier against compound diffusion [28-30].

Ultrasound (US) and ultrasound contrast agents, i.e. *microbubbles* (MB), have increasingly been used in order to enhance permeability of biological barriers [98-102]. By exposing gas-filled MB to US pressure waves, they volumetrically oscillate due to increasing and decreasing internal gas-pressures[10], while the surrounding lipid shell stretches and contracts. MBs oscillating close to cell membranes may create transient pores, stimulate endocytosis or, at higher ultrasound intensities, induce microbubble implosions that can destroy membranes [102]. It has also been seen by electron microscopy that MB may directly enter the interior of the cells (Figure 4), or pass through them. These phenomena are commonly referred to as *sonoporation*. The resulting increase in permeability of biological barriers, such as in blood vessels and tumour cell membranes, may facilitate increased extravasation and cellular uptake of drugs [102]. The main mechanisms of such transport are thought to be either passive diffusion through hydrophilic pores along concentration gradients, by direct ultrasound-mediated propulsion or via endocytosis, or a combination [101]. Moreover, it has been shown that different cell types respond differently to sonoporation [103, 104], and that the dominant mechanism of compound uptake depends on the US acoustic pressures [105]. High acoustic pressures may also result in cell membrane disintegration [105] and induce changes in signalling pathways related to cellular growth and viability, in particular when combined with higher MB concentrations [104].

[10] This phenomenon is also called *cavitation*, which may be either *stable* or *inertial*. Stable cavitation is observed at low US acoustic intensities where the MB retain their integrity over time, whereas inertial cavitation at higher intensities involves complete disruption of the MBs

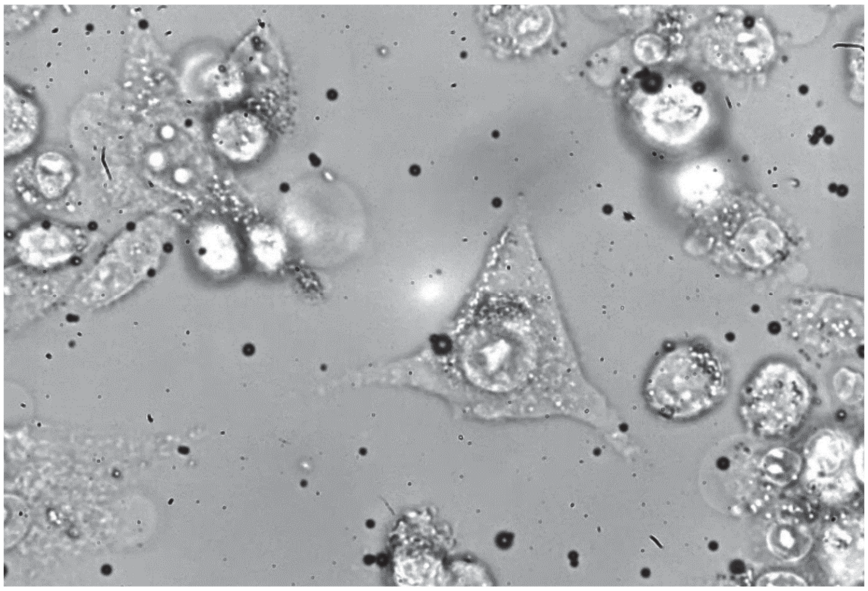

Figure 4. Electron microscopy image displaying the interaction between microbubbles (dark spheres) and pancreatic cancer cells, under the influence of low energy, clinically safe ultrasound intensities. *The bubbles can be seen to merge with, drill into and pass through cells.* (**Original photo** by: Spiros Kotopoulis, University of Bergen / Phoenix Solutions AS)

Uptake of poorly membrane-permeable fluorescent dyes such as fluorescein isothiocyanate (FITC)-labelled dextrans [103] and calcein [104] have served as "model drugs" in many *in vitro* sonoporation-studies. Routine flow-cytometry methods allow distinction between *positive* and *negative* cells[11] and give semiquantitative estimates of amounts of intracellular dye[12] [105]. Despite their widespread application in basal studies of sonoporation, cell-impermeable dyes cannot be regarded as valid model compounds representing all properties of chemotherapeutic drugs. Lammertink and co-workers [101] gave an overview of several *in vitro* cell line[13] and *in vivo* animal studies performed with a

[11] The efficacy of *in vitro* sonoporation is expressed as **% positive cells** in many studies
[12] The signal intensity in positive cells may be expressed as **MFI = mean fluorescence intensity** (De Cock 2015)
[13] Cell lines derived from brain, head-and-neck, breast, liver, kidney and colon cancers

combination of chemotherapeutics and sonoporation. In the majority of *in vitro* studies cell viability, cell death or apoptosis were used as outcome measures, whereas in *in vivo* animal studies the most frequently reported outcomes were tumour volume and survival [106]. Intratumoural drug accumulation has been assessed in only a few studies [101], but none in which gemcitabine was used.

Taken together, it has been demonstrated that sonoporation can increase the permeability of cell membranes, but the underlying mechanisms by which this may improve the outcome of treatment with chemotherapeutics remains incompletely understood. Specifically, the concept of *sonoporation* as a potential method to increase the delivery of gemcitabine and other drugs to PDAC cells needs further exploration. Additionally, in order to bring this concept into clinical use, there is a need to study the efficacy and safety of *sonoporation* at clinically applicable US intensities and MB concentrations.

2. Aims

The overall objective of the project was to evaluate quantitative aspects of gemcitabine delivery and metabolism combined with sonoporation in PDAC patients and in *in vitro* models.

Figure 5 illustrates the overall project and its individual parts.

Specific aims

- To develop and validate liquid chromatography tandem mass spectrometric methods (LC-MS/MS) for quantification of gemcitabine and its main extra- and intracellular metabolites (Paper I & II) and related endogenous nucleotides (Paper II)

- To establish a protocol for collecting and handling blood samples from gemcitabine-treated patients that ensures preanalytical stability of the analytes (Paper I)

- To assess the safety and feasibility of treating PDAC patients with gemcitabine combined with microbubbles and ultrasound, and to evaluate systemic pharmacokinetics of the drug in this setting (Paper III)

- To study the role of intracellular cytidine deaminase activity on gemcitabine metabolism in PDAC cell lines (Paper IV)

- To study uptake and metabolism of gemcitabine in PDAC cell lines exposed to clinically applicable ultrasound intensities and microbubbles (sonoporation) (Paper V)

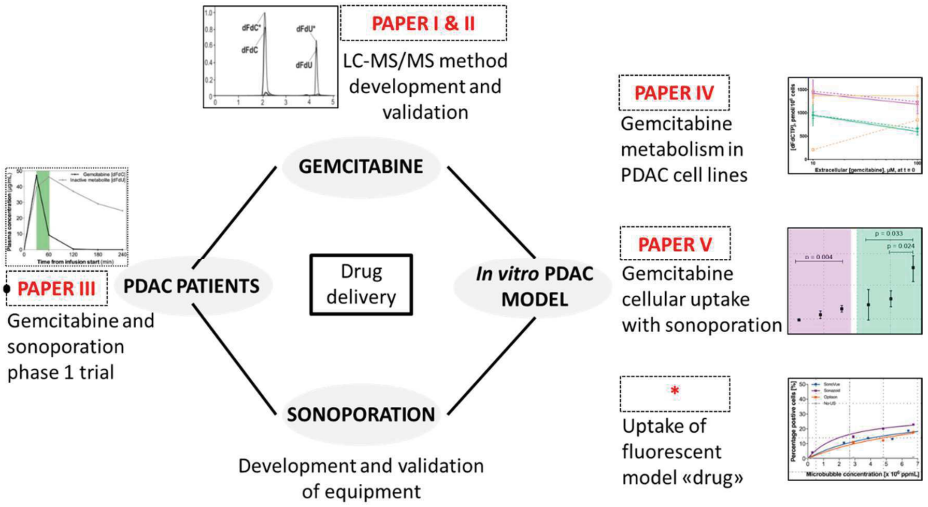

Figure 5. Overview of the project "Drug delivery in pancreatic cancer"

* Data briefly mentioned in Paper V.

3. Methods

Table 1 gives an overview of study designs, main objectives and methods used in the project. In the following, each approach will be briefly explained.

Table 1. Methodological summary of the papers included in the thesis

Paper	Design	Main objectives	Specific methods
I	Method development & validation	Assess preanalytical stability of gemcitabine and dFdU[a] in blood	LC-MS/MS[b]
II	Method development & validation	Quantification of intracellular dFdCTP[c] and endogenous nucleotide triphosphates	LC-MS/MS
III	Clinical phase 1 trial	Evaluate safety and efficacy of gemcitabine and sonoporation in PDAC[d] patients	Gemcitabine infusions Sonoporation LC-MS/MS
IV	*In vitro* cell line study	Assess the regulatory role of intracellular CDA[e] on gemcitabine metabolism in PDAC cell lines	Cell culture LC-MS/MS RT-PCR[f] Western blot
V	*In vitro* cell line study	Assess gemcitabine uptake and retention in PDAC cell lines exposed to sonoporation	Hypoxic bioreactors Sonoporation LC-MS/MS (Flow cytometry)

[a]2',2'-difluoro-2'-deoxyuridine; [b]Liquid chromatography tandem mass spectrometry; [c]Gemcitabine triphosphate; [d]Pancreatic ductal adenocarcinoma; [e]Cytidine deaminase; [f]Real-time polymerase chain reaction

3.1. Study designs and main objectives

3.1.1. Paper I and II – method development and validation

Paper I describes a liquid chromatography tandem mass spectrometry (LC-MS/MS) method for quantification of extracellular gemcitabine and dFdU, and preanalytical stability of the compounds in blood samples from PDAC patients [1]. Paper II describes a LC-MS/MS method for quantification of intracellular dFdCTP and endogenous nucleotide triphosphates (NTPs and dNTPs), including challenges and solutions in sample preparation procedures [2]. The main purpose of both methods (Paper I and II) were to enable quantitative measurements of gemcitabine and its metabolites in subsequent clinical and *in vitro* PDAC model studies. In Paper II, the inclusion of NTPs and dNTPs together with dFdCTP, was based on the idea that their concentrations could be used as an integrated pharmacokinetic-pharmacodynamic measure of gemcitabine efficacy.

3.1.2. Paper III – clinical phase 1 trial

Ten incurable PDAC patients (3 males, 7 females; mean age 59 years) were included in this open-label clinical phase 1 trial [3]. Safety and survival were primary and secondary outcome measures. Patients received intravenous infusions of gemcitabine, followed by intravenous SonoVue® microbubble injections and transabdominal low intensity ultrasound focused at their tumours. Blood samples for pharmacokinetic (PK) evaluations of gemcitabine were collected at the first day of treatment. Radiological response evaluations and assessment of performance status and blood biochemistry were performed regularly. A historical group of 63 PDAC patients treated with gemcitabine alone were used as clinical controls, and data from the literature were used as comparator for gemcitabine PK.

3.1.3. Paper IV and V – *in vitro* cell line studies

Three different PDAC cell lines were used in *in vitro* studies of gemcitabine uptake and metabolism. The purpose of paper IV was to study intracellular

metabolism of gemcitabine with emphasis on CDA-activity with or without tetrahydrouridine (THU), a CDA-inhibitor, in cells with different expression of the enzyme. In paper V we assessed whether *in vitro* sonoporation could facilitate increased cellular uptake and retention of gemcitabine, in cells with operational and inhibited membrane transporters.

3.2. Laboratory methods

3.2.1. Liquid chromatography tandem mass spectrometry (LC-MS/MS)

3.2.1.1. Instrumentation and facilities

LC-MS/MS methods were developed on Agilent 1200 series separation module and Agilent 6410 triple-quad mass spectrometer with electron spray ionization (ESI) at the University of Bergen. The LC-system consisted of a binary pump, a degasser and a thermostated autosampler with a variable volume injector. Chromatographic separation was conducted on a BDS Hypersil C18 column (Paper I) and a Hypercarb column (Paper II). During the project, both methods were transferred to a similar instrument at the Department of Medical Biochemistry and Pharmacology.

3.2.1.2. LC-MS/MS method development and validation

Development and validation of the LC-MS/MS methods were based on protocols within our laboratory that complied with consensual accreditation standards[14]. The general principles of LC-MS/MS method validation, including linearity, within- and between run precision and accuracy, recovery, lower limit of quantification (LLOQ) and stability, have been covered in a recent review by van Nuland and co-workers [107]. The intracellular method validation [2] was particularly challenging, mainly for three reasons:

[14] Internal quality document at https://handbok.helse-bergen.no/eknet/docs/pub/dok21930.htm (last update July 2018)

1) The endogenous nucleotides are structurally very similar, and their intracellular concentrations differed widely
2) All analytes are highly polar with poor retention on conventional reverse phase chromatographic columns. This required introduction of ion-pair agents in the mobile phase in combination with less robust porous graphitic carbon (PGC) columns
3) Preparation of calibration and quality control (QC) standards in cell lysates that already (naturally) contained all the analytes of interest. In order to "strip" the matrix, incubation of the cell lysates with activated charcoal was undertaken prior to addition on the analytes

3.2.2. **Preanalytical sample quality**

3.2.2.1. **Sample collection and preparation**

In paper III, IV and V, four main steps in the sample collection process were undertaken in order to optimize the sample quality:

1) **CDA activity:** Tubes had been spiked with 200 μM THU prior to sample collection, in order to inhibit deamination of gemcitabine
2) **Temperature:** All samples from *in vivo* and *in vitro* experiments were collected in pre-chilled (4 °C) tubes and immediately placed on ice. The purpose was to inhibit cellular membrane transport and enzyme activities in general throughout the sample preparation process

3) **Time:** Cells, mononuclear blood cells (PBMCs) in paper III and PDAC cells in paper IV and V, were isolated and processed as soon as possible after harvest in order to limit post-experimental changes in analyte concentrations. From *in vitro* experiments, adherent PDAC cells were trypsinized at 37 °C for 5 - 8 min, followed by addition of ice-cold (0 - 4 °C) culture media and centrifugation for 5 minutes before isolation. Isolation of PBMCs from patient blood were performed with density gradient centrifugation in Lymphoprep™ Tubes (Figure 6) at 4 °C, which required centrifugation for 25 minutes before careful pipetting of the cell layer

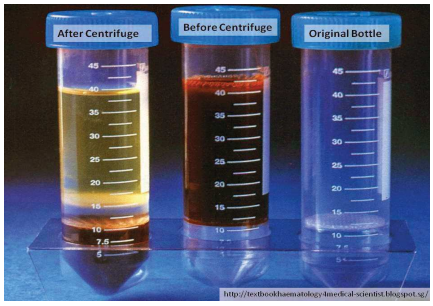

Figure 6. *Isolation of PBMC from whole blood using Lymphoprep ™ Tubes.* (**Image** from: www.textbookhaematology4medical-scientist.blogspot.com)

4) **Inactivation and lysis:** Isolated cells were forcefully dissolved in ice-cold (-20 - 0°C) 60 % methanol (MeOH), snap-frozen in liquid nitrogen, and then transferred to a -80 °C freezer

3.2.2.2. Preanalytical stability of gemcitabine in blood samples

In paper I, we assessed whether the time spent from blood sampling to centrifugation and separation of plasma from blood cells, influenced stability of gemcitabine and dFdU. Figure 7 shows the principal workflow. The purpose was to establish a protocol that allowed collection of multiple samples in succession, followed by centrifugation in a batch rather than one-by-one.

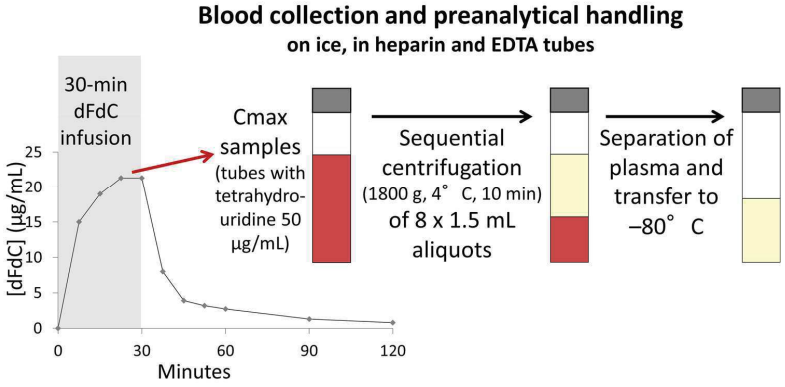

Figure 7. Workflow of sample collection and –processing in the preanalytical study. *Blood was collected from PDAC patients at gemcitabine Tmax in heparin and ethylene-diamine tetra acetic acid (EDTA) tubes collected in rapid succession. Tubes were centrifuged and plasma separated sequentially at eight time points up to 24 hours.* **(Illustration**: from poster presented by TK Bjånes at The European Therapeutic Drug Monitoring Conference, Prague, Czech Republic, August 2014)

3.2.3. Cell culture

Three PDAC cell lines; BxPC-3, MIA PaCa-2 and PANC-1, were used in studies of *in vitro* gemcitabine metabolism and in sonoporation experiments in paper IV and V, respectively. All three cell lines were of human origin, and are commonly used in *in vitro* studies of PDAC. When cultured, they have been shown to display capabilities that resemble the behaviour of tumour cells *in vivo*, including adhesion to extracellular matrix components, migration, invasion and the ability to form tumours [44]. Moreover, mutations in KRAS, TP53, CDKN2A and SMAD4 characteristic for PDAC tumours, have also been found to variable degrees in BxPC-3, MIA PaCa-2 and PANC-1. As such, they may also be considered representative of the diversity seen in pancreatic cancers *in vivo* [44]. Cells were cultured at two different conditions: 1) at normoxia in a) standard culture flasks for expanding cell populations prior to experiments, and b) six-well plates (Figure 8A) for gemcitabine incubation experiments in Paper IV, or 2) in

PetakaG3 ™ LOT[15] hypoxic bioreactors (Figure 8B) for experiments with sonoporation in Paper V.

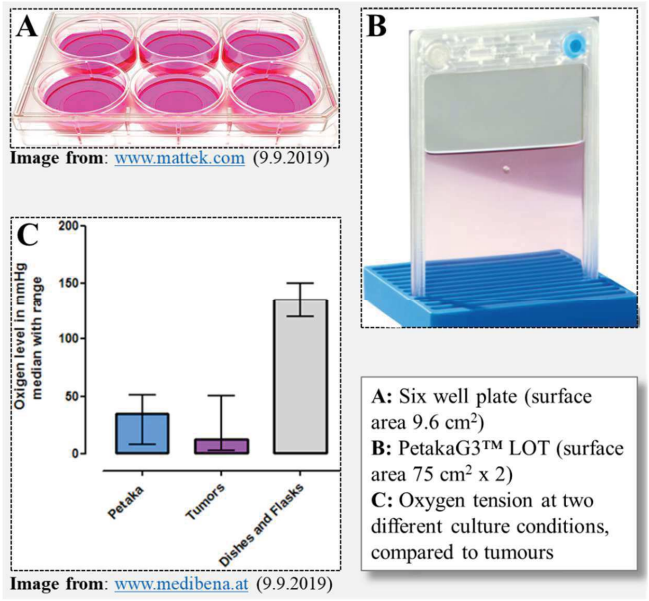

Figure 8. ***Culture conditions in paper IV (A) and paper V (B), and the estimated oxygen tensions compared to tumours (C).***

3.2.4. Gene and protein expression

In paper IV, we assessed the influence of intracellular CDA activity on gemcitabine metabolism in PDAC cells, with or without pharmacological CDA inhibition with 200 µM THU. Expression levels of CDA and other proteins involved in transport, metabolism and mechanism of action of gemcitabine in untreated cells were assessed by a collaborator at the *Centre de Recherche en Cancérologie de Lyon*, Lyon, France. Gene expression was performed with real-time polymerase chain reaction (RT-PCR). For each gene, expression in one individual cell line was calculated as relative to the mean of all three cell lines by the delta-delta cycle threshold (ΔΔCT)-method [108], using 28S mRNA as a housekeeping gene. Protein

[15] LOT = Low Oxygen Transfer. Read more on supplier webpage: http://celartia.com/petaka-options/#LOT-Hypoxia-chamber

expression was assessed by Western blot [109], with beta-actin as loading control in each sample.

3.2.5. **In vitro sonoporation**

Figure 9. *QR-code with link to poster of in vitro optimization of sonoporation conditions (presented at the 51st meeting of the European Pancreatic Club, Bergen, June 2019)*

Prior to the experiments in paper V, comprehensive exploration of multiple different sonoporation parameters was performed; four ultrasound intensities, four microbubble brands and six microbubble concentrations (Figure 9). The membrane-impermeable fluorescent dye calcein was used as an indicator substance, and cells were analysed with flow-cytometry. Calcein *positive* cells were separated from *negative* cells, and the percentage (%) of positive cells within each sample was used as a measure of the amount of cells permeabilized by sonoporation (Figure 9). The ultrasound intensities and microbubble concentrations used in paper V had been shown to result in 30 – 80 % calcein positive cells. In paper V, we assessed gemcitabine and metabolite concentrations in cells with operational and inhibited hENTs, and in cells with inhibited CDA. hENT inhibition was achieved by incubating the cell lines with 100 µM dilazep 20 minutes prior to gemcitabine incubation, whereas CDA inhibition was achieved by co-incubating gemcitabine with 200 µM THU.

3.2.6. **Cell viability**

In Paper V, cells that had been exposed to gemcitabine, sonoporation or both, were reseeded in wells with drug-free media, and their growth was compared to untreated cells for up to ten days post-exposure. Daily snapshots were captured using a Zeiss Vert.A1 microscope with an Axiocam 105 camera and a computer with Zeiss ZEN Pro software. Surface area coverage of cells within each image were calculated with the MIPAR® image analysis software [110].

3.3. **Data processing and Statistics**

Processing of quantitative data was performed with Agilent MassHunter software (LC-MS/MS), SPSS Statistics 21.0 - 24.0 (IBM Inc., Armon, NY, USA) and GraphPad Prism 7 - 8 (San Diego, CA, USA) for Windows.

In papers I and II, calibration curves in LC-MS/MS methods were constructed by linear regression from triplicate values at each data point. Goodness of fit was indicated by R^2. Method performance were expressed as mean and standard deviations (SD) of ten replicates from three (paper II) or five (paper I) different QC concentrations. Coefficients of variation (CV), calculated as SD divided by means, were used as comparator across concentrations.

In the stability experiment in paper I, changes over time from the initial concentrations were related to the LC-MS/MS method performance. This was done in order to discriminate between systematic and random deviation, using an adaptation of the Bland-Altman method [111].

Concentrations of gemcitabine and metabolites in paper I, IV and V were expressed as mean±SD, range (low–high), or as absolute difference or percent (%) compared to baseline. Continuous data in paper III – V were analysed using unpaired two-sided student's t-tests. For comparisons between more than two groups in paper IV, we used analysis of variance (ANOVA) with Bonferroni adjusted post hoc tests. In paper III, patient survival data was analysed with the log-rank test. P-values of less than 0.05 were considered statistically significant.

In paper V, one tailed Pearson's correlation was used to determine trends of gemcitabine and metabolite concentrations with changing ultrasound intensities.

3.4. **Ethical considerations**

The clinical trial (ClinicalTrials.gov number: NCT01674556) was conducted according to the Helsinki Declaration[16] and national regulations, with approval from the Regional Ethics Committee (2011/1601/REK Vest) and the Norwegian Medicines Agency. All patients participating in the clinical trial (Paper III) and those donating blood for testing of gemcitabine stability (Paper I) signed informed consents.

[16] https://www.wma.net/policies-post/wma-declaration-of-helsinki-ethical-principles-for-medical-research-involving-human-subjects/

4. Summary of Results

Table 2. Overview of results

Paper	Main results	Additional results
I	Gemcitabine and dFdU[a] were stable in whole blood for at least four hours when kept on ice with THU[b] added to the collection tubes	LC-MS/MS[c] method for gemcitabine and dFdU in blood samples developed
II	LC-MS/MS method for intracellular dFdCTP[d] and endogenous nucleotide triphosphates developed	
III	Combined treatment of PDAC[e] patients with gemcitabine and sonoporation was safe and feasible	Improved survival compared to historical controls. Similar systemic gemcitabine pharmacokinetics as in literature
IV	Intracellular CDA[f] activity in PDAC cell lines regulated the amount of gemcitabine into the activation pathway	Phenotypical assessment of CDA activity was superior to expression analyses
V	Sonoporation induced increases in gemcitabine uptake in PDAC cells, but pre-existing activities in membrane transporters and intracellular CDA were more important	

[a]2',2'-difluoro-2'-deoxyuridine; [b]Tetrahydrouridine; [c]Liquid chromatography tandem mass spectrometry; [d]Gemcitabine triphosphate; [e]Pancreatic ductal adenocarcinoma; [f]Cytidine deaminase;

4.1. Paper I

Bjånes T, Kamčeva T, Eide T, Riedel B, Schjøtt J, Svardal A. J Pharm Sci 2015; 104(12): 4427-32.

We presented a LC-MS/MS method for gemcitabine and dFdU, and stability assessment of both analytes in blood samples from seven PDAC patients. Linear ranges were 0.125–40.0 and 1.25–80.0 µg/mL for gemcitabine and dFdU, respectively. The method displayed a between run precision CV of 6.5 % or better for gemcitabine QC samples above the LLOQ.

Four hours after blood collection from patients, gemcitabine concentrations were within the 95 % confidence interval (CI) of LC-MS/MS precision. After 24 hours, concentrations showed a greater deviation and tended to drop below the lower boundary of 95 % CI, which indicated analyte instability (Figure 10).

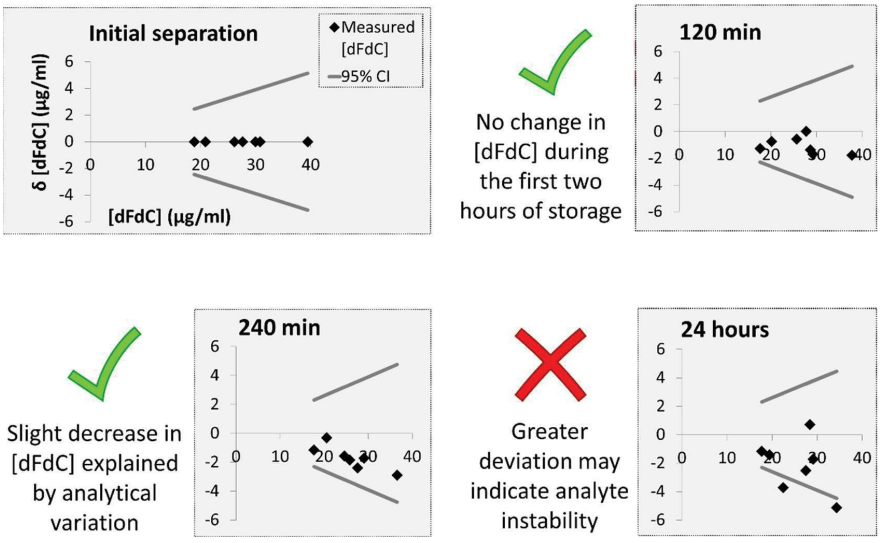

Figure 10. Stability of gemcitabine in blood from PDAC patients. *δdFdC (X-axis) represent the difference from the initial separation. Grey lines represent the upper and lower boundaries of 95 % CI of method performance, based on a between run precision (CV) of 6.5 %.* **(Illustration** from: Poster presented at The European Therapeutic Drug Monitoring Conference, Prague, Czech Republic, August 2014)

4.2. Paper II

Kamčeva T, Bjånes T, Svardal A, Riedel B, Schjøtt J, Eide T. J Chromatogr B Analyt Technol Biomed Life Sci 2015; 1001: 212-20.

We described development and validation of a LC-MS/MS method for quantitative analysis of four ribonucleotide triphosphates (NTPs): ATP, CTP, GTP and UTP; four deoxyribonucleotide triphosphates (dNTPs): dATP, dCTP, dGTP and TTP; and gemcitabine triphosphate (dFdCTP). The linear range for dFdCTP was 0.02–31.3 µM, with a between-run precision from 11.4 % at the lowest to 3.87 % at the highest QC standard. Method validation included charcoal incubation to strip the off nucleotides from the cell matrix before spiking with reference substances when preparing calibration and QC samples.

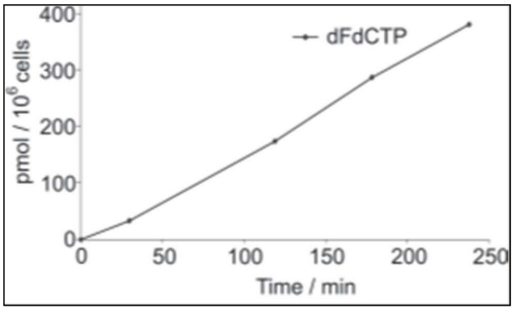

Figure 11. *Concentration course of intracellular dFdCTP in blood mononuclear cells collected from a PDAC patient up to 240 minutes after initiating a 30-minutes infusion of 1000 mg/m^2 gemcitabine.* (**Illustration** from: Paper II)

Sample preparation with solid phase extraction (SPE) and protein precipitation without SPE was also assessed. The absolute recoveries were 20–30 % lower without SPE. However, this was compensated by the presence of ^{13}C,^{15}N-isotope labelled internal standards that were equally affected as their respective analytes.

The method was applied for analyses of dFdCTP concentrations in blood mononuclear cells from PDAC patients treated with gemcitabine. We observed a gradual increase up to 380 pmol/10^6 cells 240 minutes after initiating a 30-minutes gemcitabine infusion (Figure 11). We also measured NTPs and dNTPs 240 minutes after gemcitabine infusions, and observed that all analytes were three to seven times higher than before infusions.

4.3. Paper III

Dimcevski G, Kotopoulis S, Bjånes TK, Hoem D, Schjøtt J, Gjertsen BT, Biermann M, Molven A, Sørbye H, McCormack E, Postema M, Gilja OH. J Control Release 2016; 243; 172-181.

The main results of this phase I clinical trial in ten PDAC patients were that combined treatment with ultrasound, microbubbles and gemcitabine

- was feasible and safe, and with no additional toxicity noted
- seemed to increase the median survival from 8.9 (historical controls, n=63) to 17.6 months (n=10, *p*=0.011). The patients were also able to receive an increased number of treatment cycles; from 8.3±6.0 (historical controls, n=63) to 13.8±5.6 (n=10, *p*=0.008) (Figure 12)
- resulted in similar systemic gemcitabine pharmacokinetic data as described in literature (without sonoporation)

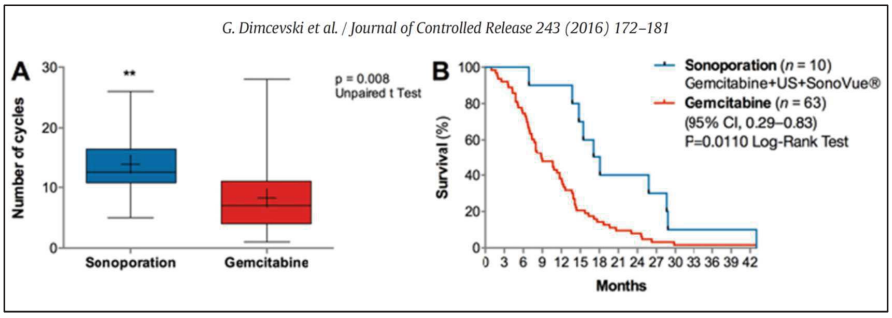

Figure 12. *A: Whisker plot comparing the number of treatment cycles in the two treatment groups (sonoporation + gemcitabine (n=10) and gemcitabine alone (n=63; historical controls)) and B: Survival plot of the two treatment groups. (**Illustration** from: Paper III)*

4.4. Paper IV

Bjånes TK, Jordheim LP, Schjøtt J, Kamceva T, Cros-Perrial E, Langer A, de Garibay GR, Kotopoulis S, McCormack E and Riedel B. Submitted to Drug Metabolism and Disposition September 13th 2019 (Manuscript ID: DMD/2019/089334, ongoing minor revision).

We examined gemcitabine metabolism *in vitro* in three PDAC cell lines, BxPC-3, MIA PaCa-2 and PANC-1, with emphasis on the regulatory role of CDA on intracellular gemcitabine activation. All three cell lines were incubated with 10 or 100 µM gemcitabine for 60 minutes or 24 hours, with or without 200 µM THU. CDA activity and expression varied widely between the three cell lines studied, with low activities in MIA PaCa-2 and PANC-1 compared to BxPC-3.

Our main finding was that intracellular CDA in BxPC-3 mediated an extensive deamination of gemcitabine that seemed to limit the amount gemcitabine available for activation to dFdCTP (Figure 13).

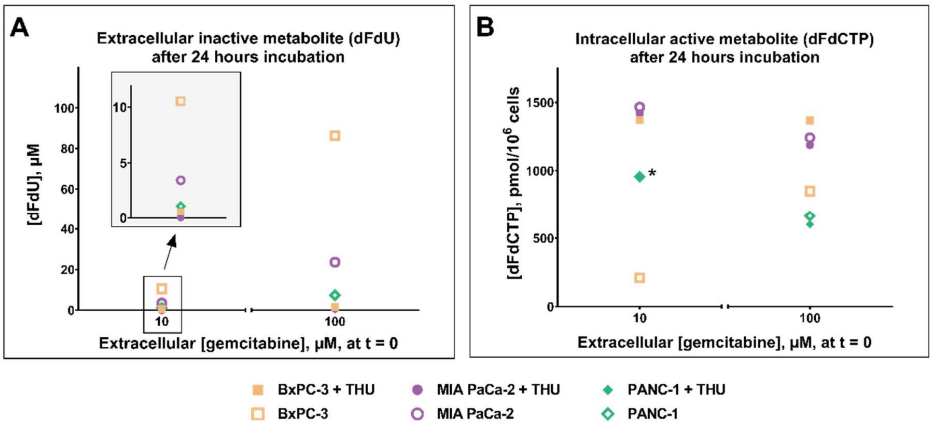

Figure 13. *Extracellular dFdU (A) and intracellular dFdCTP (B) after 24 hours incubation with 10 or 100 µM gemcitabine in BxPC-3 (orange), MIA PaCa-2 (purple) and PANC-1 (green) with (solid lines) or without (dashed lines) THU.* (**Illustration** from: Paper IV).

4.5. Paper V

Bjånes TK, Kotopoulis S, Murvold ET, Kamceva T, Bjørn Tore Gjertsen, Schjøtt J, Riedel B and McCormack E. Manuscript in preparation.

We observed that sonoporation induced moderate increases in gemcitabine uptake in PDAC cells, but that activities in membrane transporters (hENTs) and intracellular CDA were more important determinants of metabolite accumulation. Increasing ultrasound intensities resulted in reduced extracellular gemcitabine concentrations in cell lines with inhibited hENTs (Figure 14).

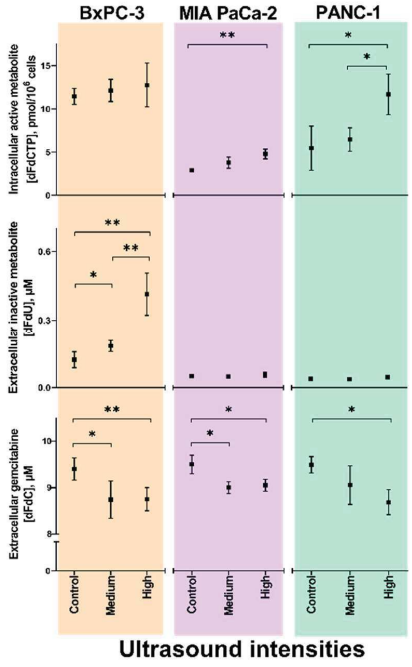

Intracellular dFdCTP concentrations did not change in any of the cell lines with operational hENTs, either with or without inhibited CDA. In cells with inhibited hENTs, but without sonoporation, dFdCTP concentrations were low, 10–30% of baseline. Sonoporation partially restored uptake in these cells, as indicated by moderate increases in dFdCTP in MIA PaCA-2 and PANC-1 (Figure 14, top right). In BxPC-3, gemcitabine was inactivated to dFdU (Figure 14, middle left), and no increase in dFdCTP was seen.

Figure 14. *Effect of sonoporation ("Control", "Medium", "High") on extracellular gemcitabine (bottom line) and dFdU (middle line), and intracellular dFdCTP (top line) concentrations, in cells with inhibited hENTs.* *p<0.05, **p<0.01. (**Illustration** from: poster presented at the 51st meeting of the European Pancreatic Club, Bergen, June 2019).

5. Discussion

Improved treatment of PDAC represents a highly unmet medical need [4, 6, 7] and poor drug delivery is considered to be a major limitation for effective chemotherapeutic treatment [28-30]. Hence, the aims within the current project, combining quantitative assessments of gemcitabine and its main metabolites with *in vivo* and *in vitro* drug-delivery studies in PDAC, may be considered highly relevant.

In accordance with the specific aims within the project, we

I. Developed and validated a LC-MS/MS-method for gemcitabine and dFdU, and demonstrated that the analytes were stable for at least four hours in anticoagulated THU-spiked blood kept on ice. This allows batch centrifugation of samples acquired during this time interval, and is an important prerequisite for quantification of gemcitabine in pharmacokinetic studies in which consecutive blood sampling is performed

II. Developed and validated LC-MS/MS-method for quantitation of intracellular gemcitabine triphosphate and 8 endogenous nucleotide triphosphates, using a porous graphitic column. Moreover, we demonstrated that the treatment of cell supernatants with activated charcoal was an effective method of creating a nucleotide-free matrix that could be used for preparation of internal standards

III. Demonstrated that treatment of PDAC patients with gemcitabine combined with ultrasound and microbubbles was safe and feasible, and potentially clinically beneficial. We found that the systemic pharmacokinetics of gemcitabine was not influenced by intravascular microbubble injections and transabdominal ultrasound. No conclusions could be drawn about local drug delivery to the tumours, since such measures were not part of the study protocol

IV. Demonstrated the role of intracellular cytidine deaminase (CDA) activity in regulating the accumulation of dFdCTP. Our data support the notion

that gemcitabine inactivation by intracellular CDA may represent a protective mechanism against gemcitabine cytotoxicity

V. We demonstrated that increased cellular uptake of gemcitabine did not necessarily result in an increased intracellular accumulation of the active metabolite. *In vitro* sonoporation allowed increased transmembrane transport of gemcitabine in PDAC cell lines, but the effect was negligible in terms of dFdCTP accumulation due to pre-existing nucleoside transporters and intracellular cytidine deaminase activities

There are several limitations within the current project. No PDAC model with a representative tumour microenvironment, such as multiple cell types or abundant desmoplastic stroma [26, 27], was included. Although our findings from the *in vitro* PDAC cell line studies may fit well into existing knowledge of cellular gemcitabine uptake and metabolism, they cannot be generalized to an *in vivo* situation where blood flow and tissue perfusion are also important determinants of drug delivery [36, 37]. Another limitation is that the clinical study was small and based on a historical control group. As a consequence, no general conclusions could be drawn about treatment efficacy. Moreover, the current first-line chemotherapeutic drug regimens used for PDAC, such as nab-paclitaxel [5, 41] or FOLFIRINOX [5, 39], were not included.

Table 3. Overview: Relevance, strengths and limitations within the project

Paper	Relevance	Strengths	Limitations
I	Quantitative analytical method to assess drug delivery *in vivo* and *in vitro*	Validated method Stability testing	Long run-time. Suboptimal sensitivity
II	Quantitative analytical method to assess drug delivery *in vivo* and *in vitro*	Validated method	Long run-time Suboptimal sensitivity (Endogenous nucleotides excluded from the method)
III	First-in-man clinical trial combining chemotherapy with microbubbles and diagnostic intensity US[a]	Commercially available ultrasound equipment and microbubbles used.	Small sample size. Historical control group. Tissue drug concentrations not assessed.
IV	Clarification of mechanism by which intracellular CDA[b] influences *in vitro* gemcitabine metabolism	Direct measurements of extra- and intracellular gemcitabine metabolites	Other gemcitabine-metabolites not measured. No cytotoxicity experiments performed
V	Insight into cellular drug uptake by sonoporation	Clinically applicable US intensities and gemcitabine concentrations	No direct *in vivo* translation

[a]Ultrasound; [b]Cytidine deaminase;

5.1. Methodological considerations

5.1.1. LC-MS/MS

We established two LC-MS/MS methods (Paper I and II) [1, 2] that enabled quantification of gemcitabine and its main inactive and active metabolites in blood cells and in cultured PDAC cell lines. LC-MS/MS is considered the gold standard in pharmacokinetic studies, due to a superior analyte specificity and its ability to quantitate analytes over a broad range of concentrations [107]. The LC-MS/MS methods were used for the generation of data for all papers included in this thesis.

5.1.2. Analyte stability

Gemcitabine is rapidly metabolized to dFdU in blood, and addition of the CDA-inhibitor THU into collection tubes is required to retain gemcitabine until quantification [82]. We added 200 µM (50 µg/mL) THU in blood collection tubes when sampling from PDAC-patients in paper I [1] and III [3] and in the culture media used for collecting cells at the end of *in vitro* experiments in paper IV and V. A concentration of 200 µM THU was primarily based on an *ex vivo* study in human blood by Bowen and co-workers [112]. In paper IV, we demonstrated that the proposed concentration of 200 µM THU effectively blocked *in vitro* deamination of up to 100 µM gemcitabine.

In addition to pharmacological inhibition of CDA, we routinely kept collected samples on ice in order to slow down active transport and intracellular enzyme reactions in cell samples [67]. Most authors emphasize that complete inactivation of transporters and enzyme activities should be performed immediately when analysing cellular nucleotide concentrations [113]. Potassium hydroxide [56, 78], sodium hydroxide [90], perchloric acid (PCA) [76, 93], commercial cell lysis reagents [71] or 60-70 % MeOH [72, 114] have been used to dissolve cell pellets, followed by immediate freezing of the samples. In our experience, forceful dissolution of cell pellets in cold 60 % MeOH followed by snap-freezing in liquid nitrogen, resulted in complete disruption of the cellular integrity and hence represent

a final inactivation of transport and enzyme activities. Cohen and co-workers [115] exemplified the importance of such inactivation on the stability of dFdCTP; in intact PBMCs kept on ice its half-life was only 100 minutes, but with immediate dissolution in PCA and storage of the extracts at -80°C, stability was demonstrated for at least 7 months.

5.1.3. Cell line studies

Several well-known shortcomings of *in vitro* cell lines studies, as described in section 0, also apply to paper IV and V. Specifically, the lack of a more complete dynamic tumour model with other cell types and tissue components that may influence local drug distribution and metabolism [31-35], represent major limitations for the *in vivo* relevance of our results. Nevertheless, we have explored basal mechanisms of gemcitabine transport and metabolism in three different PDAC cell lines, BxPC-3, MIA PaCa-2 and PANC-1 [45], that may also mirror a diversity between tumours [42, 43]. We have highlighted that intracellular drug metabolism should be taken into account in drug delivery studies [116]. This view is further strengthened by the fact that other cell types in PDAC tumours might also influence intratumoural gemcitabine metabolism and distribution, as demonstrated by Hessmann and co-workers [33].

5.1.4. Drug exposure

In the majority of *in vitro* drug incubation studies, the concentration-time profile differs from its profile *in vivo* (Figure 15), unless specialized dynamic bioreactor systems that mimic *in vivo* drug delivery and elimination are used [117].

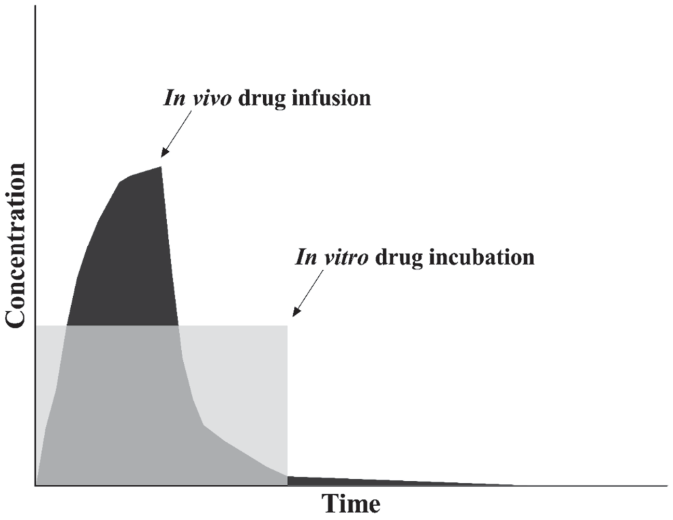

Figure 15. Illustration of typical 1) in vivo and 2) in vitro drug administrations. *1) Displays an increase in concentrations during intravenous drug infusion and a gradual decline after termination. 2) Displays a rectangular concentration-time profile during in vitro drug incubation.*

In paper IV and V, gemcitabine concentrations and duration of *in vitro* incubations were chosen based on two main assumptions.

1. The interstitial/pericellular AUC derived from *in silico* simulations [87] is representative for the *in vivo* tissue exposure during and after intravenous gemcitabine infusions
2. An *in vitro* gemcitabine AUC which is comparable to an *in vivo* interstitial/pericellular AUC would represent the clinically most relevant exposure

Gemcitabine AUC of 41±12 µM*h in plasma from patients [69] would on average result in AUC of 13–14 µM*h in tumour interstitial fluid (i.e. 1/3 of plasma), according to *in silico* simulations [87]. As an example, the *in vitro* exposure used in paper V, 10 µM gemcitabine over 60 minutes (i.e. AUC 10 µM*h), was comparable to the data obtained by the simulations.

However, the lack of an *in vivo* PDAC tumour tissue model in which actual interstitial gemcitabine exposures could be quantified, represents a limitation to the clinical relevance of the *in vitro* results. In particular, the unrestricted compound diffusion within culture media may differ widely from the *in vivo* situation in tumours [26, 27].

5.1.5. Methodological considerations specific to the individual papers

5.1.5.1. Paper I

We demonstrated that gemcitabine and dFdU were stable in blood from PDAC patients for at least four hours when kept on ice, provided that 200 µM THU was added. In a more recent study by Kozo and co-workers [82] gemcitabine (concentrations not stated) and 500 µM THU were spiked into freshly drawn blood, and kept at room temperature (RT) or at 2 – 8 °C. The authors showed that gemcitabine was stable for at least 8 hours at RT. This may indicate that our limit of 4 hours on ice was too strict. However, the studies differed in at least two aspects.

1. The definitions of analyte stability were different: In our study, the analytes were considered stable when the difference from the control sample was not greater than the theoretical deviation seen with the poorest precision of the LC-MS/MS method in samples above LLOQ. Kozo and co-workers made use of an in-house definition of <10% loss as cut-off for analyte stability
2. Our study was performed in blood samples acquired directly from patients at the end of gemcitabine infusions, while Kozo and co-workers used blood spiked with gemcitabine. It has been argued that an inaccurate spike procedure may represent an additional source of variation [118], compared to blood samples from patients treated with the drug

5.1.5.2. Paper II

5.1.5.2.1. Endogenous nucleotides and modification of the LC-MS/MS method

An initial purpose of paper II [2] was to quantify intracellular NTPs and dNTPs ("endogenous nucleotides") together with dFdCTP as an integrated pharmacokinetic/pharmacodynamic measure, based on the potential regulatory action of endogenous nucleotides on gemcitabine cytotoxicity [52, 66]. In paper II, we observed that concentrations of dFdCTP as well as endogenous nucleotides in PBMCs increased up to 240 minutes after initiating gemcitabine infusions [2]. We speculated that the increase in endogenous nucleotides might be explained by a transient upstream accumulation secondary to dFdCTP-induced DNA synthesis inhibition (LP Jordheim, personal communication, August 1st 2014), but had no additional data to support this view. In a few initial *in vitro* 24 hours gemcitabine incubation experiments in MIA PaCa-2, we observed a decrease in most endogenous nucleotides. As an example, a decrease of dATP, dCTP and dGTP with increasing gemcitabine concentrations (Figure 16) was considered to reflect the inhibition of ribonucleotide reductase by dFdCDP [52, 61], as illustrated in Figure 2. However, the sensitivity of the LC-MS/MS-method for dNTPs was challenged, and we also experienced repeated problems with the LC-MS/MS instrument, a >10 years old Agilent 6410[17]. For this reason, we had to abandon further exploration of the nucleotide pools within this project. The LC-MS/MS method was simplified and restricted to quantification of dFdCTP only (Paper IV and V), which allowed shorter run-time and hence, increased sample throughput.

Development of a LC-MS/MS method for analysis of gemcitabine, dFdU and dFdCTP in a single run would have been more rational if

[17] https://www.agilent.com/cs/library/support/documents/f391141304.pdf (Last updated in 2006)

the original plan had not included endogenous nucleotides. Indeed, several LC-MS/MS methods have been published for the simultaneous analysis of all three analytes in plasma[18], blood cells and tissues, with run-times of only 15 minutes [67, 88].

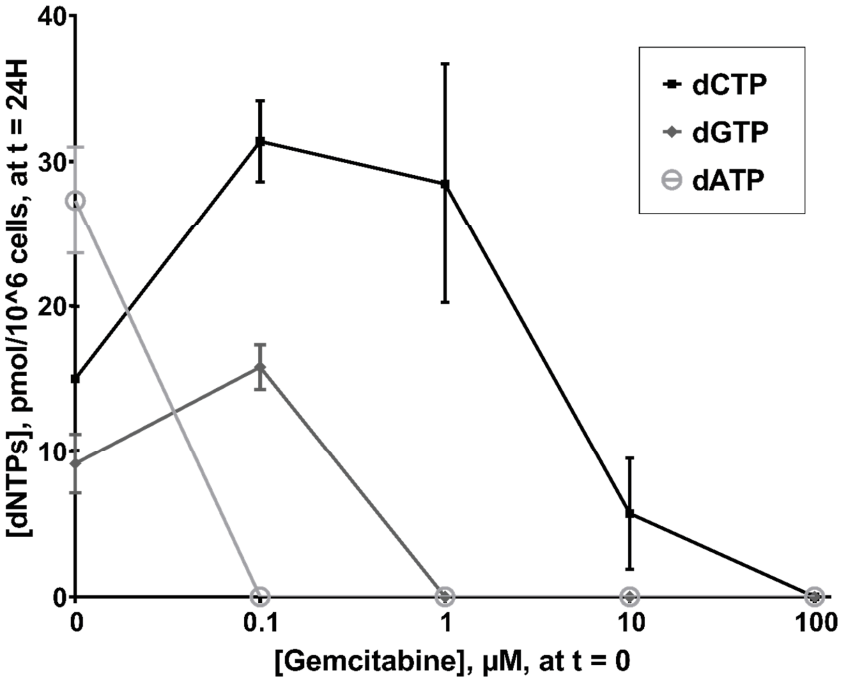

Figure 16. ***Intracellular concentrations of three endogenous nucleotide triphosphates following 24 hours in vitro incubation of MIA PaCa-2 cells with 0 – 100 µM gemcitabine.***

dATP: deoxyadenosine triphosphate, dCTP: deoxycytidine triphosphate, dFdCDP: gemcitabine diphosphate, dGTP: deoxyguanosine triphosphate, LLOQ: lower limit of quantification.

[18] Exception: dFdCTP not detectable in plasma samples

5.1.5.2.2. Porous graphitic carbon (PGC) columns

Porous graphitic carbon (PGC) columns enable separation of structurally very similar analytes, including polar compounds, and have been applied in several nucleotide assays due to this unique property. Challenges with unpredictable analyte retention over time have been described [119]. As a result, the majority of LC-MS/MS methods with PGC have included thorough reconstitution procedures to retain the quality of columns. As a result, the run times have usually been long (up to 2 hours). Bapiro and co-workers [119] recently described a simple solution to these challenges by optimizing the composition of the mobile phases. They found that a 2-minutes maintenance step with 95 % methanol towards the end of each analytical run effectively prevented a gradual loss of retention properties.

With our method [2], each analytical run (total runtime of 68–69 minutes) included a reconditioning phase of 14 minutes. Despite this, we experienced repeated problems with loss of analyte retention. Hence, the study by Bapiro and co-workers [119] may be of great value in future method developments using these columns.

5.1.5.3. Paper III

This small clinical trial (n=10) was the first to explore *in vivo* sonoporation in PDAC patients. An important experience was that the treatment was feasible with commercially available ultrasound equipment, and with ultrasound intensities and microbubbles that were already approved for clinical applications [3, 120]. Due to the encouraging results, the study also paved the way for increased research efforts into drug delivery in PDAC both *in vitro* [90], in pre-clinical studies [106] and into developing larger clinical trials [120]. A limitation in the study design was the use of a historical control group, and as a consequence no firm conclusions could be drawn about survival benefits.

Larger randomized trials are needed in order to explore the clinical outcome of chemotherapy combined with sonoporation.

5.1.5.3.1. Gemcitabine concentrations

We demonstrated that gemcitabine systemic PK in the study patients did not differ from values in the literature. However, we did not measure gemcitabine and –metabolite concentrations in the tumours. Therefore, our data did not prove that sonoporation using low-intensity ultrasound facilitates increased *in vivo* gemcitabine delivery to PDAC tumours in patients. However, since tumour biopsies during (intraoperative) drug administration would be resource demanding, methodically complicated [29, 88] and also ethically challenging, such questions must primarily be addressed in suitable model systems. Indeed, there are currently several ongoing projects at the University of Bergen, briefly mentioned in Section 6.

5.1.5.4. Paper IV

In vivo inactivation through CDA in blood is a well-recognized determinant of gemcitabine elimination kinetics and toxicity [112, 121]. We undertook this *in vitro* study to explore the importance of intracellular CDA on the metabolic fate of gemcitabine in PDAC cell lines. The main finding was that an extensive CDA-mediated inactivation of gemcitabine in BxPC-3 cells limited the intracellular dFdCTP accumulation. We also hypothesized that saturation of dCK was likely to explain a lack of increase in dFdCTP with increasing gemcitabine concentrations in cells with low CDA activities. Although we initially[19] did not perform cytotoxicity experiments following gemcitabine exposure in cells with inhibited CDA, our results supported the notion [122-125] that intracellular conversion to dFdU may represent a mechanism of gemcitabine resistance. Furthermore, the relative mRNA

[19] In a currently ongoing revision of the paper, cell viability experiments are being performed as required by the Journal of Drug Disposition and Metabolism

expression of CDA and other proteins involved in gemcitabine transport and metabolism in BxPC-3, MIA PaCa-2 and PANC-1, was in agreement with previous findings by Funamizu and co-workers [126]. Our observation that protein expression (Western blot) was inferior to phenotypic assessment of CDA activity (i.e. direct measurement of gemcitabine and dFdU), was in agreement with a recently presented expert opinion concerning *in vivo* CDA activity assessments [121].

5.1.5.5. Paper V

5.1.5.5.1. Cell culture in hypoxic bioreactors

The choice of hypoxic bioreactors (Petakas) in sonoporation experiments were done for three main reasons;

1. The bioreactors could be immersed into a water bath that allowed access to the whole surface area for ultrasound exposure
2. The closed system minimized the risk of bacterial contamination during experiments (which included transport across a non-sterile environment)
3. Restricted access to oxygen was considered to resemble the *in vivo* microenvironment in PDAC tumours (Figure 8C)

It has been demonstrated that hypoxia induces a reduction in the expression of ribonucleotide reductase (RR) and intracellular dNTP concentrations in PANC-1 [127]. Since intracellular gemcitabine metabolism and efficacy are also related to the activity of RR and the nucleotide pools [52, 61], hypoxic culture of the PDAC cell lines may represent the most relevant experimental condition for the study of this drug.

5.1.5.5.2. dFdCTP as a measure of cellular gemcitabine uptake

We aimed to assess whether gemcitabine uptake could be facilitated by sonoporation. We initially explored whether direct intracellular quantification of unmetabolized gemcitabine was feasible, but found that the concentrations were less than 1 % of dFdCTP and often below LLOQ of our method (Paper I), even after 24 hours incubation with gemcitabine. Indeed, Heinemann and co-workers [76] also found that after four hours gemcitabine incubation, intracellular concentrations of dFdC, dFdCMP, dFdCDP and dFdCTP accounted for 0.2, 2.4, 5.6 and 89 %, respectively, of the total amount of all metabolites. In compliance with the approach of other researchers [66, 94, 96], we used intracellular dFdCTP as a measure of gemcitabine uptake and intracellular retention, since this metabolite is also related to drug efficacy [63-66].

In sonoporation experiments, the T_{max} of dFdCTP following gemcitabine incubations was perceived as the optimal time point of sampling in order to demonstrate whether gemcitabine uptake was successfully increased. In order to establish T_{max}, we collected cells incubated in drug free medium up to 24 hours after termination of 60 minutes gemcitabine exposure in six well plates. We found that T_{max} of intracellular dFdCTP was achieved immediately after terminating 60 minutes incubation with 10 µM gemcitabine (example in Figure 17), which was in line with previous studies in other cell lines [97]. These data supported our choice of sampling the cells immediately after 60 minutes incubation also from Petakas.

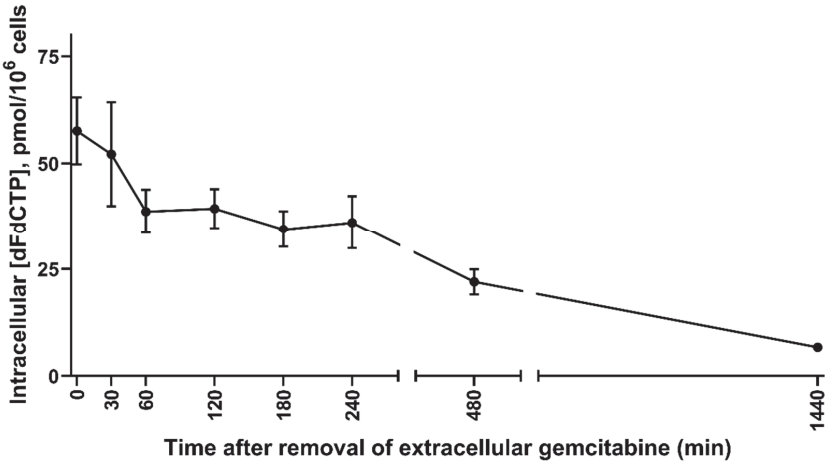

Figure 17. ***Elimination of intracellular dFdCTP from MIA PaCa-2 following termination of 60 minutes incubation with 10 µM gemcitabine.*** *A similar concentration course was also demonstrated in BxPC-3.* (**Illustration from:** Unpublished pilot experiments prior to sonoporation experiments in Paper V)

6. Main conclusions and future perspectives

Overall, our studies contribute to an increased understanding of drug delivery in PDAC. As such, they may provide help for further research to improve the treatment outcome of this disease.

Quantitative assessment of gemcitabine and its main extra- and intracellular metabolites in different matrices enabled elucidation of drug distribution, uptake and metabolism in PDAC. In particular, we showed that gemcitabine delivery through *in vitro* sonoporation depends on the cellular phenotype in terms of membrane transporter and intracellular enzyme activities. The findings are of relevance to improve efficacy of PDAC treatment with gemcitabine, but also to develop sonoporation as a clinical method for delivery of other chemotherapeutics to cancer cells. Furthermore, the *in vitro* findings might question the quantitative importance of sonoporation on cellular drug delivery.

Our studies have addressed several issues that deserve further exploration. In particular, they underpin the need to take mechanisms of drug uptake and metabolism into account. Studies in relevant PDAC models are required. At Haukeland University Hospital and the University of Bergen, the following projects are within our current scope of further advancements within the field:

Evaluation of drug uptake in PDAC tissue models

We suggest that gemcitabine uptake combined with sonoporation should be studied in a PDAC 3D organoid model with multiple cell types and connective tissue components[20]. Using in-house developed scaffold models [50] both *in vitro* and *in vivo* drug delivery studies should be feasible. Furthermore, *in vitro* bioreactors that mimic vascular dynamics is currently under development, and the plan is to culture PDAC organoids within these. An advantage over static *in vitro* systems would be

[20] By using cell lines (PDAC, fibroblasts, endothelial cells etc.) or tumour specimen from PDAC patients

that the transport of chemotherapeutics and microbubbles resemble the *in vivo* situation more closely.

LC-MS/MS development

A LC-MS/MS method comprising gemcitabine, dFdU and dFdCTP in a single run allows a more streamlined process of sample preparation and analysis. Other chemotherapeutics used against PDAC, should also be considered in a new or improved method. Furthermore, validation of the methods for use in tissue samples/homogenates is a prerequisite in order to address questions related to drug distribution and uptake in tumour tissues.

Clinical trial

Larger randomized clinical trials are needed in order to further explore the therapeutic potential of combining sonoporation with gemcitabine or other chemotherapeutics in the treatment of PDAC. Indeed, a protocol of a four-arm randomized clinical trial with FOLFIRINOX or gemcitabine+nab-paclitaxel, with or without sonoporation, has recently been submitted to the regulatory authorities.

7. References

1. Bjanes, T., et al., *Preanalytical Stability of Gemcitabine and its Metabolite 2', 2'-Difluoro-2'-Deoxyuridine in Whole Blood-Assessed by Liquid Chromatography Tandem Mass Spectrometry.* J Pharm Sci, 2015. **104**(12): p. 4427-32.
2. Kamceva, T., et al., *Liquid chromatography/tandem mass spectrometry method for simultaneous quantification of eight endogenous nucleotides and the intracellular gemcitabine metabolite dFdCTP in human peripheral blood mononuclear cells.* J Chromatogr B Analyt Technol Biomed Life Sci, 2015. **1001**: p. 212-20.
3. Dimcevski, G., et al., *A human clinical trial using ultrasound and microbubbles to enhance gemcitabine treatment of inoperable pancreatic cancer.* J Control Release, 2016. **243**: p. 172-181.
4. Maisonneuve, P., *Epidemiology and burden of pancreatic cancer.* Presse Med, 2019. **48**(3 Pt 2): p. e113-e123.
5. Health, T.N.D.o., *Nasjonalt handlingsprogram med retningslinjer for diagnostikk, behandling og oppfølging av pancreaskreft*. 2017.
6. Norway, C.R.o., *Cancer in Norway 2017 - Cancer incidence, mortality, survival and prevalence in Norway*, I.K. Larsen, Editor. 2018, Cancer Registry of Norway: Oslo. p. 104.
7. Bray, F., et al., *Global cancer statistics 2018: GLOBOCAN estimates of incidence and mortality worldwide for 36 cancers in 185 countries.* CA Cancer J Clin, 2018. **68**(6): p. 394-424.
8. Kamisawa, T., et al., *Pancreatic cancer.* Lancet, 2016. **388**(10039): p. 73-85.
9. Gharibi, A., Y. Adamian, and J.A. Kelber, *Cellular and molecular aspects of pancreatic cancer.* Acta Histochem, 2016. **118**(3): p. 305-16.
10. (UICC), U.f.I.C.C., *TNM Classification of Malignant Tumours*. 8th ed. 2016: Wiley Blackwell. 272.
11. Chu, L.C., M.G. Goggins, and E.K. Fishman, *Diagnosis and Detection of Pancreatic Cancer.* Cancer J, 2017. **23**(6): p. 333-342.
12. Toft, J., et al., *Imaging modalities in the diagnosis of pancreatic adenocarcinoma: A systematic review and meta-analysis of sensitivity, specificity and diagnostic accuracy.* Eur J Radiol, 2017. **92**: p. 17-23.
13. Nordaas, I.K., et al., *Computed tomography and transabdominal ultrasound should be considered equal options as parts of the primary diagnostic workup for chronic pancreatitis.* Pancreatology, 2019. **19**: p. S39.
14. Yoshida, T., Y. Yamashita, and M. Kitano, *Endoscopic Ultrasound for Early Diagnosis of Pancreatic Cancer.* Diagnostics (Basel), 2019. **9**(3).
15. Bjørnæs, F.v.I. *Søknader til forskningsrådet 2019*. 2019 May 5th 2019 [cited 2019 July 31st]; Available from: https://public.tableau.com/views/SknadertilForskningsrdet-enkeltsknader/Enkeltsknader?:embed=y&:display_count=yes&publish=yes&:showVizHome=no.
16. Barhli, A., et al., *Prognostic stratification of resected pancreatic ductal adenocarcinoma: Past, present, and future.* Dig Liver Dis, 2018. **50**(10): p. 979-990.
17. McGuigan, A., et al., *Pancreatic cancer: A review of clinical diagnosis, epidemiology, treatment and outcomes.* World J Gastroenterol, 2018. **24**(43): p. 4846-4861.
18. Loosen, S.H., et al., *Current and future biomarkers for pancreatic adenocarcinoma.* Tumour Biol, 2017. **39**(6): p. 1010428317692231.
19. Court, C.M., et al., *Circulating Tumor Cells Predict Occult Metastatic Disease and Prognosis in Pancreatic Cancer.* Ann Surg Oncol, 2018. **25**(4): p. 1000-1008.
20. Bernard, V., et al., *Circulating Nucleic Acids Are Associated With Outcomes of Patients With Pancreatic Cancer.* Gastroenterology, 2019. **156**(1): p. 108-118 e4.
21. Choi, M.H., et al., *Mutation analysis by deep sequencing of pancreatic juice from patients with pancreatic ductal adenocarcinoma.* BMC Cancer, 2019. **19**(1): p. 11.

22. Lo, W., et al., *Screening patients at high risk for pancreatic cancer-Is it time for a paradigm shift?* J Surg Oncol, 2019.
23. Conroy, T. and J.L. Van Laethem, *Combination or single-agent chemotherapy as adjuvant treatment for pancreatic cancer?* Lancet Oncol, 2019. **20**(3): p. 336-337.
24. Riall, T.S., et al., *Pancreaticoduodenectomy with or without distal gastrectomy and extended retroperitoneal lymphadenectomy for periampullary adenocarcinoma--part 3: update on 5-year survival.* J Gastrointest Surg, 2005. **9**(9): p. 1191-204; discussion 1204-6.
25. Health, T.N.D.o., *Nasjonale faglige råd for lindrende behandling i livets sluttfase*. 2018: https://www.helsedirektoratet.no/tema/palliasjon.
26. Perera, R.M. and N. Bardeesy, *Pancreatic Cancer Metabolism: Breaking It Down to Build It Back Up.* Cancer Discov, 2015. **5**(12): p. 1247-61.
27. Cannon, A., et al., *Desmoplasia in pancreatic ductal adenocarcinoma: insight into pathological function and therapeutic potential.* Genes Cancer, 2018. **9**(3-4): p. 78-86.
28. Tod, J., et al., *Tumor-stromal interactions in pancreatic cancer.* Pancreatology, 2013. **13**(1): p. 1-7.
29. Koay, E.J., et al., *Transport properties of pancreatic cancer describe gemcitabine delivery and response.* J Clin Invest, 2014. **124**(4): p. 1525-36.
30. Uzunparmak, B. and I.H. Sahin, *Pancreatic cancer microenvironment: a current dilemma.* Clin Transl Med, 2019. **8**(1): p. 2.
31. Vande Voorde, J., et al., *Nucleoside-catabolizing enzymes in mycoplasma-infected tumor cell cultures compromise the cytostatic activity of the anticancer drug gemcitabine.* J Biol Chem, 2014. **289**(19): p. 13054-65.
32. Geller, L.T., et al., *Potential role of intratumor bacteria in mediating tumor resistance to the chemotherapeutic drug gemcitabine.* Science, 2017. **357**(6356): p. 1156-1160.
33. Hessmann, E., et al., *Fibroblast drug scavenging increases intratumoural gemcitabine accumulation in murine pancreas cancer.* Gut, 2018. **67**(3): p. 497-507.
34. Halbrook, C.J., et al., *Macrophage-Released Pyrimidines Inhibit Gemcitabine Therapy in Pancreatic Cancer.* Cell Metab, 2019. **29**(6): p. 1390-1399 e6.
35. Weizman, N., et al., *Macrophages mediate gemcitabine resistance of pancreatic adenocarcinoma by upregulating cytidine deaminase.* Oncogene, 2014. **33**(29): p. 3812-9.
36. Slordal, L. and O. Spigset, *[Basic pharmacokinetics--distribution].* Tidsskr Nor Laegeforen, 2005. **125**(8): p. 1007-8.
37. Slordal, L. and O. Spigset, *[Basic pharmacokinetics--absorption].* Tidsskr Nor Laegeforen, 2005. **125**(7): p. 886-7.
38. Springfeld, C., et al., *Chemotherapy for pancreatic cancer.* Presse Med, 2019. **48**(3 Pt 2): p. e159-e174.
39. Conroy, T., et al., *FOLFIRINOX versus gemcitabine for metastatic pancreatic cancer.* N Engl J Med, 2011. **364**(19): p. 1817-25.
40. Lambert, A., C. Gavoille, and T. Conroy, *Current status on the place of FOLFIRINOX in metastatic pancreatic cancer and future directions.* Therap Adv Gastroenterol, 2017. **10**(8): p. 631-645.
41. Von Hoff, D.D., et al., *Increased survival in pancreatic cancer with nab-paclitaxel plus gemcitabine.* N Engl J Med, 2013. **369**(18): p. 1691-703.
42. Henderson, M.C., et al., *High-throughput RNAi screening identifies a role for TNK1 in growth and survival of pancreatic cancer cells.* Mol Cancer Res, 2011. **9**(6): p. 724-32.
43. Kim, I., et al., *A drug-repositioning screen for primary pancreatic ductal adenocarcinoma cells identifies 6-thioguanine as an effective therapeutic agent for TPMT-low cancer cells.* Mol Oncol, 2018. **12**(9): p. 1526-1539.
44. Deer, E.L., et al., *Phenotype and genotype of pancreatic cancer cell lines.* Pancreas, 2010. **39**(4): p. 425-35.
45. Collisson, E.A., et al., *Subtypes of pancreatic ductal adenocarcinoma and their differing responses to therapy.* Nat Med, 2011. **17**(4): p. 500-3.

46. Smitskamp-Wilms, E., et al., *Postconfluent multilayered cell line cultures for selective screening of gemcitabine.* Eur J Cancer, 1998. **34**(6): p. 921-6.
47. Froeling, F.E., J.F. Marshall, and H.M. Kocher, *Pancreatic cancer organotypic cultures.* J Biotechnol, 2010. **148**(1): p. 16-23.
48. Gadaleta, E., et al., *A global insight into a cancer transcriptional space using pancreatic data: importance, findings and flaws.* Nucleic Acids Res, 2011. **39**(18): p. 7900-7.
49. Baker, L.A., et al., *Modeling pancreatic cancer with organoids.* Trends Cancer, 2016. **2**(4): p. 176-190.
50. Rozmus, E., *A novel 3D PDAC model system developed with the use of decellularized matrix scaffolds*, in *Department of Biomedicine, Clinical Institute II*. 2019, Bergen.
51. Tuveson, D. and H. Clevers, *Cancer modeling meets human organoid technology.* Science, 2019. **364**(6444): p. 952-955.
52. Wong, A., et al., *Clinical pharmacology and pharmacogenetics of gemcitabine.* Drug Metab Rev, 2009. **41**(2): p. 77-88.
53. SLV, N.M.a. *Summary of product characteristics (SPC) Gemzar*. 2018 15.11.2018 [cited 2019 August 13th]; Available from: https://www.legemiddelsok.no/_layouts/15/Preparatomtaler/Spc/09-6924.pdf.
54. Farrell, J.J., et al., *Human equilibrative nucleoside transporter 1 levels predict response to gemcitabine in patients with pancreatic cancer.* Gastroenterology, 2009. **136**(1): p. 187-95.
55. Pastor-Anglada, M. and S. Perez-Torras, *Nucleoside transporter proteins as biomarkers of drug responsiveness and drug targets.* Front Pharmacol, 2015. **6**: p. 13.
56. Paproski, R.J., J.D. Young, and C.E. Cass, *Predicting gemcitabine transport and toxicity in human pancreatic cancer cell lines with the positron emission tomography tracer 3'-deoxy-3'-fluorothymidine.* Biochem Pharmacol, 2010. **79**(4): p. 587-95.
57. Koay, E.J. and M. Ferrari, *Transport Oncophysics in silico, in vitro, and in vivo. Preface.* Phys Biol, 2014. **11**(6): p. 060201.
58. Elander, N.O., et al., *Expression of dihydropyrimidine dehydrogenase (DPD) and hENT1 predicts survival in pancreatic cancer.* British Journal of Cancer, 2018. **118**(7): p. 947-954.
59. Greenhalf, W., et al., *Pancreatic cancer hENT1 expression and survival from gemcitabine in patients from the ESPAC-3 trial.* J Natl Cancer Inst, 2014. **106**(1): p. djt347.
60. Svrcek, M., et al., *Human equilibrative nucleoside transporter 1 testing in pancreatic ductal adenocarcinoma: a comparison between murine and rabbit antibodies.* Histopathology, 2015. **66**(3): p. 457-62.
61. Derissen, E.J.B., et al., *Intracellular pharmacokinetics of gemcitabine, its deaminated metabolite 2',2'-difluorodeoxyuridine and their nucleotides.* Br J Clin Pharmacol, 2018. **84**(6): p. 1279-1289.
62. Nakagawa, N., et al., *Combined analysis of intratumoral human equilibrative nucleoside transporter 1 (hENT1) and ribonucleotide reductase regulatory subunit M1 (RRM1) expression is a powerful predictor of survival in patients with pancreatic carcinoma treated with adjuvant gemcitabine-based chemotherapy after operative resection.* Surgery, 2013. **153**(4): p. 565-75.
63. Garcia-Cremades, M., et al., *Predicting tumour growth and its impact on survival in gemcitabine-treated patients with advanced pancreatic cancer.* Eur J Pharm Sci, 2018. **115**: p. 296-303.
64. Cattel, L., et al., *Pharmacokinetic evaluation of gemcitabine and 2',2'-difluorodeoxycytidine-5'-triphosphate after prolonged infusion in patients affected by different solid tumors.* Ann Oncol, 2006. **17 Suppl 5**: p. v142-7.
65. Gandhi, V., et al., *Prolonged infusion of gemcitabine: clinical and pharmacodynamic studies during a phase I trial in relapsed acute myelogenous leukemia.* J Clin Oncol, 2002. **20**(3): p. 665-73.
66. van Moorsel, C.J., et al., *Differential effects of gemcitabine on nucleotide pools of 19 solid tumor cell lines.* Adv Exp Med Biol, 1998. **431**: p. 661-5.

67. Jansen, R.S., et al., *Simultaneous quantification of 2',2'-difluorodeoxycytidine and 2',2'-difluorodeoxyuridine nucleosides and nucleotides in white blood cells using porous graphitic carbon chromatography coupled with tandem mass spectrometry.* Rapid Commun Mass Spectrom, 2009. **23**(19): p. 3040-50.
68. Gilbert, J.A., et al., *Gemcitabine pharmacogenomics: cytidine deaminase and deoxycytidylate deaminase gene resequencing and functional genomics.* Clin Cancer Res, 2006. **12**(6): p. 1794-803.
69. Gusella, M., et al., *Equilibrative nucleoside transporter 1 genotype, cytidine deaminase activity and age predict gemcitabine plasma clearance in patients with solid tumours.* Br J Clin Pharmacol, 2011. **71**(3): p. 437-44.
70. Mini, E., et al., *Cellular pharmacology of gemcitabine.* Ann Oncol, 2006. **17 Suppl 5**: p. v7-12.
71. Rudin, D., et al., *Gemcitabine Cytotoxicity: Interaction of Efflux and Deamination.* J Drug Metab Toxicol, 2011. **2**(107): p. 1-10.
72. Veltkamp, S.A., et al., *New insights into the pharmacology and cytotoxicity of gemcitabine and 2',2'-difluorodeoxyuridine.* Mol Cancer Ther, 2008. **7**(8): p. 2415-25.
73. Aksoy, P., et al., *Cytosolic 5'-nucleotidase III (NT5C3): gene sequence variation and functional genomics.* Pharmacogenet Genomics, 2009. **19**(8): p. 567-76.
74. van Haperen, V.W., et al., *Regulation of phosphorylation of deoxycytidine and 2',2'-difluorodeoxycytidine (gemcitabine); effects of cytidine 5'-triphosphate and uridine 5'-triphosphate in relation to chemosensitivity for 2',2'-difluorodeoxycytidine.* Biochem Pharmacol, 1996. **51**(7): p. 911-8.
75. Ruiz van Haperen, V.W., et al., *Schedule dependence of sensitivity to 2',2'-difluorodeoxycytidine (Gemcitabine) in relation to accumulation and retention of its triphosphate in solid tumour cell lines and solid tumours.* Biochem Pharmacol, 1994. **48**(7): p. 1327-39.
76. Heinemann, V., et al., *Gemcitabine: a modulator of intracellular nucleotide and deoxynucleotide metabolism.* Semin Oncol, 1995. **22**(4 Suppl 11): p. 11-8.
77. Xiang, T.X., et al., *Epimer interconversion, isomerization, and hydrolysis of tetrahydrouridine: implications for cytidine deaminase inhibition.* J Pharm Sci, 2003. **92**(10): p. 2027-39.
78. Paproski, R.J., et al., *Human Concentrative Nucleoside Transporter 3 Transfection with Ultrasound and Microbubbles in Nucleoside Transport Deficient HEK293 Cells Greatly Increases Gemcitabine Uptake.* PLoS One, 2013. **8**(2): p. e56423.
79. Beumer, J.H., et al., *Modulation of gemcitabine (2',2'-difluoro-2'-deoxycytidine) pharmacokinetics, metabolism, and bioavailability in mice by 3,4,5,6-tetrahydrouridine.* Clin Cancer Res, 2008. **14**(11): p. 3529-35.
80. Kreis, W., et al., *Tetrahydrouridine: Physiologic disposition and effect upon deamination of cytosine arabinoside in man.* Cancer Treat Rep, 1977. **61**(7): p. 1347-53.
81. Riva, C., et al., *Effect of tetrahydrouridine on metabolism and transport of 1-beta-D-arabinofuranosylcytosine in human cells.* Chemotherapy, 1992. **38**(5): p. 358-66.
82. Kozo, D., et al., *Rapid Homogeneous Immunoassay to Quantify Gemcitabine in Plasma for Therapeutic Drug Monitoring.* Ther Drug Monit, 2017. **39**(3): p. 235-242.
83. Kreis, W., et al., *Therapy of refractory/relapsed acute leukemia with cytosine arabinoside plus tetrahydrouridine (an inhibitor of cytidine deaminase)--a pilot study.* Leukemia, 1991. **5**(11): p. 991-8.
84. Kreis, W., et al., *Effect of tetrahydrouridine on the clinical pharmacology of 1-beta-D-arabinofuranosylcytosine when both drugs are coinfused over three hours.* Cancer Res, 1988. **48**(5): p. 1337-42.
85. Rehan, S., et al., *Thermodynamics and kinetics of inhibitor binding to human equilibrative nucleoside transporter subtype-1.* Biochem Pharmacol, 2015. **98**(4): p. 681-9.
86. EMA, E.M.A. *Summary of product characteristics (SPC) Abraxane*. 2019 June 19th 2019 [cited 2019 August 15th]; Available from:

https://www.ema.europa.eu/en/documents/product-information/abraxane-epar-product-information_en.pdf.
87. Battaglia, M.A. and R.S. Parker, *Pharmacokineticpharmacodynamic modelling of intracellular gemcitabine triphosphate accumulation: translating in vitro to in vivo.* IET Syst Biol, 2011. **5**(1): p. 34.
88. Bapiro, T.E., et al., *A novel method for quantification of gemcitabine and its metabolites 2',2'-difluorodeoxyuridine and gemcitabine triphosphate in tumour tissue by LC-MS/MS: comparison with (19)F NMR spectroscopy.* Cancer Chemother Pharmacol, 2011. **68**(5): p. 1243-53.
89. Neesse, A., et al., *CTGF antagonism with mAb FG-3019 enhances chemotherapy response without increasing drug delivery in murine ductal pancreas cancer.* Proc Natl Acad Sci U S A, 2013. **110**(30): p. 12325-30.
90. Mariglia, J., et al., *Analysis of the cytotoxic effects of combined ultrasound, microbubble and nucleoside analog combinations on pancreatic cells in vitro.* Ultrasonics, 2018. **89**: p. 110-117.
91. Yoshida, T., et al., *Influence of cytidine deaminase on antitumor activity of 2'-deoxycytidine analogs in vitro and in vivo.* Drug Metab Dispos, 2010. **38**(10): p. 1814-9.
92. Bergman, A.M., et al., *Antiproliferative activity, mechanism of action and oral antitumor activity of CP-4126, a fatty acid derivative of gemcitabine, in in vitro and in vivo tumor models.* Invest New Drugs, 2011. **29**(3): p. 456-66.
93. Heinemann, V., et al., *Cellular elimination of 2',2'-difluorodeoxycytidine 5'-triphosphate: a mechanism of self-potentiation.* Cancer Res, 1992. **52**(3): p. 533-9.
94. Veltkamp, S.A., et al., *Quantitative analysis of gemcitabine triphosphate in human peripheral blood mononuclear cells using weak anion-exchange liquid chromatography coupled with tandem mass spectrometry.* J Mass Spectrom, 2006. **41**(12): p. 1633-42.
95. Abbruzzese, J.L., et al., *A phase I clinical, plasma, and cellular pharmacology study of gemcitabine.* J Clin Oncol, 1991. **9**(3): p. 491-8.
96. Nishi, R., T. Yamauchi, and T. Ueda, *A new, simple method for quantifying gemcitabine triphosphate in cancer cells using isocratic high-performance liquid chromatography.* Cancer Sci, 2006. **97**(11): p. 1274-8.
97. Heinemann, V., et al., *Comparison of the cellular pharmacokinetics and toxicity of 2',2'-difluorodeoxycytidine and 1-beta-D-arabinofuranosylcytosine.* Cancer Res, 1988. **48**(14): p. 4024-31.
98. Snipstad, S., et al., *Sonopermeation to improve drug delivery to tumors: from fundamental understanding to clinical translation.* Expert Opin Drug Deliv, 2018. **15**(12): p. 1249-1261.
99. Wang, M., et al., *Sonoporation-induced cell membrane permeabilization and cytoskeleton disassembly at varied acoustic and microbubble-cell parameters.* Sci Rep, 2018. **8**(1): p. 3885.
100. Mullick Chowdhury, S., T. Lee, and J.K. Willmann, *Ultrasound-guided drug delivery in cancer.* Ultrasonography, 2017. **36**(3): p. 171-184.
101. Lammertink, B.H., et al., *Sonochemotherapy: from bench to bedside.* Front Pharmacol, 2015. **6**: p. 138.
102. Lentacker, I., et al., *Understanding ultrasound induced sonoporation: definitions and underlying mechanisms.* Adv Drug Deliv Rev, 2014. **72**: p. 49-64.
103. Bhutto, D.F., et al., *Effect of Molecular Weight on Sonoporation-Mediated Uptake in Human Cells.* Ultrasound Med Biol, 2018. **44**(12): p. 2662-2672.
104. Haugse, R., et al., *Intracellular Signaling in Key Pathways Is Induced by Treatment with Ultrasound and Microbubbles in a Leukemia Cell Line, but Not in Healthy Peripheral Blood Mononuclear Cells.* Pharmaceutics, 2019. **11**(7).
105. De Cock, I., et al., *Ultrasound and microbubble mediated drug delivery: acoustic pressure as determinant for uptake via membrane pores or endocytosis.* J Control Release, 2015. **197**: p. 20-8.

106. Bressand, D., et al., *Enhancing Nab-Paclitaxel Delivery Using Microbubble-Assisted Ultrasound in a Pancreatic Cancer Model.* Mol Pharm, 2019.
107. van Nuland, M., et al., *Bioanalytical LC-MS/MS validation of therapeutic drug monitoring assays in oncology.* Biomed Chromatogr, 2019: p. e4623.
108. Livak, K.J. and T.D. Schmittgen, *Analysis of relative gene expression data using real-time quantitative PCR and the 2(-Delta Delta C(T)) Method.* Methods, 2001. **25**(4): p. 402-8.
109. Hnasko, T.S. and R.M. Hnasko, *The Western Blot.* Methods Mol Biol, 2015. **1318**: p. 87-96.
110. Sosa, J.M., et al., *Development and application of MIPAR™: a novel software package for two- and three-dimensional microstructural characterization.* Integrating Materials and Manufacturing Innovation, 2014. **3**(1): p. 123-140.
111. Bland, J.M. and D.G. Altman, *Statistical methods for assessing agreement between two methods of clinical measurement.* Lancet, 1986. **1**(8476): p. 307-10.
112. Bowen, C., S. Wang, and H. Licea-Perez, *Development of a sensitive and selective LC-MS/MS method for simultaneous determination of gemcitabine and 2,2-difluoro-2-deoxyuridine in human plasma.* J Chromatogr B Analyt Technol Biomed Life Sci, 2009. **877**(22): p. 2123-9.
113. Machon, C., et al., *Use of designed experiments for the improvement of pre-analytical workflow for the quantification of intracellular nucleotides in cultured cell lines.* J Chromatogr A, 2015. **1405**: p. 116-25.
114. Machon, C., et al., *Fully validated assay for the quantification of endogenous nucleoside mono- and triphosphates using online extraction coupled with liquid chromatography-tandem mass spectrometry.* Anal Bioanal Chem, 2014. **406**(12): p. 2925-41.
115. Cohen, S., et al., *Liquid chromatographic methods for the determination of endogenous nucleotides and nucleotide analogs used in cancer therapy: a review.* J Chromatogr B Analyt Technol Biomed Life Sci, 2010. **878**(22): p. 1912-28.
116. Wonganan, P., et al., *Just getting into cells is not enough: mechanisms underlying 4-(N)-stearoyl gemcitabine solid lipid nanoparticle's ability to overcome gemcitabine resistance caused by RRM1 overexpression.* J Control Release, 2013. **169**(1-2): p. 17-27.
117. Kirstein, M.N., et al., *Pharmacodynamic characterization of gemcitabine cytotoxicity in an in vitro cell culture bioreactor system.* Cancer Chemother Pharmacol, 2008. **61**(2): p. 291-9.
118. Reed, G.A., *Stability of Drugs, Drug Candidates, and Metabolites in Blood and Plasma.* Curr Protoc Pharmacol, 2016. **75**: p. 7 6 1-7 6 12.
119. Bapiro, T.E., F.M. Richards, and D.I. Jodrell, *Understanding the Complexity of Porous Graphitic Carbon (PGC) Chromatography: Modulation of Mobile-Stationary Phase Interactions Overcomes Loss of Retention and Reduces Variability.* Anal Chem, 2016.
120. Castle, J., S. Kotopoulis, and F. Forsberg, *Sonoporation for Augmenting Chemotherapy of Pancreatic Ductal Adenocarcinoma.* Methods Mol Biol, 2020. **2059**: p. 191-205.
121. Peters, G.J., et al., *Can cytidine deaminase be used as predictive biomarker for gemcitabine toxicity and response?* Br J Clin Pharmacol, 2019. **85**(6): p. 1213-1214.
122. Bardenheuer, W., et al., *Resistance to cytarabine and gemcitabine and in vitro selection of transduced cells after retroviral expression of cytidine deaminase in human hematopoietic progenitor cells.* Leukemia, 2005. **19**(12): p. 2281-8.
123. Giovannetti, E., et al., *Cytotoxic activity of gemcitabine and correlation with expression profile of drug-related genes in human lymphoid cells.* Pharmacol Res, 2007. **55**(4): p. 343-9.
124. Ohmine, K., et al., *Attenuation of phosphorylation by deoxycytidine kinase is key to acquired gemcitabine resistance in a pancreatic cancer cell line: targeted proteomic and metabolomic analyses in PK9 cells.* Pharm Res, 2012. **29**(7): p. 2006-16.
125. Mameri, H., et al., *Cytidine Deaminase Deficiency Reveals New Therapeutic Opportunities against Cancer.* Clin Cancer Res, 2017. **23**(8): p. 2116-2126.

126. Funamizu, N., et al., *Hydroxyurea decreases gemcitabine resistance in pancreatic carcinoma cells with highly expressed ribonucleotide reductase.* Pancreas, 2012. **41**(1): p. 107-13.
127. Zhang, W., et al., *Analysis of deoxyribonucleotide pools in human cancer cell lines using a liquid chromatography coupled with tandem mass spectrometry technique.* Biochem Pharmacol, 2011. **82**(4): p. 411-7.

8. Original publications

PAPER I

Preanalytical Stability of Gemcitabine and its Metabolite 2′, 2′-Difluoro-2′-Deoxyuridine in Whole Blood—Assessed by Liquid Chromatography Tandem Mass Spectrometry

TORMOD BJÅNES,[1] TINA KAMČEVA,[1] TORUNN EIDE,[2] BETTINA RIEDEL,[1,2] JAN SCHJØTT,[1,2] ASBJØRN SVARDAL[2]

[1]Laboratory of Clinical Biochemistry, Section of Clinical Pharmacology, Haukeland University Hospital, Bergen 5020, Norway
[2]Faculty of Medicine and Dentistry, Institute of Clinical Science, University of Bergen, Bergen 5021, Norway

Received 5 June 2015; revised 18 August 2015; accepted 19 August 2015

Published online in Wiley Online Library (wileyonlinelibrary.com). DOI 10.1002/jps.24638

ABSTRACT: Gemcitabine (2′,2′-difluoro-2′-deoxycytidine, dFdC) and metabolite (2′,2′-difluoro-2′-deoxyuridine, dFdU) quantification is warranted for individualized treatment strategies. Analyte stability is crucial for the validity of such quantification. We therefore studied the impact of the time interval from blood sampling to separation of plasma on gemcitabine stability. Blood from gemcitabine-treated patients was drawn into tetrahydrouridine (THU)-spiked heparin and ethylenediaminetetraacetic acid tubes and kept on ice until separation. Plasma was separated sequentially up to 24 h after sampling and dFdC and dFdU were quantified by liquid chromatography tandem mass spectrometry (LC–MS/MS). The change in plasma concentrations over time was compared with the highest imprecision for concentrations above the lower limit of quantification of the LC–MS/MS method. Analyte concentrations decreased slightly over time, but for samples stored for 4 h on ice, the decline was smaller than the expected analytical imprecision. After 24 h, the maximum decline was 14.0%, which exceeded the expected analytical imprecision. dFdC and dFdU stabilities were acceptable for at least 4 h when THU-spiked whole blood samples were kept on ice. This is within the scope of routine sampling procedures. Further, variations in separation time intervals within this time frame are negligible when interpreting drug concentrations. © 2015 Wiley Periodicals, Inc. and the American Pharmacists Association J Pharm Sci

Keywords: analysis; cancer chemotherapy; clinical pharmacokinetics; HPLC; stability

INTRODUCTION

Gemcitabine (2′,2′-difluoro-2′-deoxycytidine, dFdC) is a nucleoside analog used in chemotherapeutic drug regimens against several human cancers, including pancreatic ductal adenocarcinoma (PDAC).[1] Intra- and interindividual variations in gemcitabine pharmacokinetics are hypothesized to have an impact on drug efficacy.[2–4] Hence, quantification of dFdC and its main metabolite (2′,2′-difluoro-2′-deoxyuridine, dFdU) in plasma is warranted in the development of individualized treatment strategies.[5] The validity of quantitative analyses of dFdC and dFdU relies on both the quality of the analytical method, and on the preanalytical stability of the analytes in blood collection tubes. Several preanalytical aspects have to be taken in to account for dFdC and dFdU plasma concentrations to mirror *in vivo* conditions (Supplementary Fig. S1). *In vitro* deamination of dFdC to dFdU by cytidine deaminase (CDA) is a major issue and can be inhibited by tetrahydrouridine (THU).[11] Assessment of both analytes and of their ratio contributes as a control of the sample quality in this setting. Moreover, both dFdC and dFdU are bidirectionally transported across cellular membranes by nucleoside transporter proteins,[6,7] and distributional changes may occur *ex vivo* before plasma separation is performed. However, data on the magnitude of potential distributional changes in dFdC and dFdU concentrations over time are sparse. In venous blood from eight healthy volunteers, the *in vitro* erythrocyte/plasma partition (EPP) ratio for dFdC was 1–5 in samples incubated with 0.500–100 μg/mL dFdC for 1 h at 37°C.[12] Whether this corresponds to the *in vivo* EPP ratio in patients treated with 30-min gemcitabine infusions is not known.[1,13] The time interval from blood sampling until separation of plasma varied from "without delay"[14] to 1 h[15] in studies reporting dFdC and dFdU plasma concentrations from treated patients, but was not given in most other studies.[16–19] Hence, because of a potential transmembranous transport *ex vivo* (Supplementary Fig. S1), lack of standardization of time to separation could be a source of error when interpreting plasma concentrations of dFdC and dFdU within and across studies. In most studies, blood was kept on ice until centrifugation at 4°C in order to minimize instability of analytes. In one study of [^{3}H]uridine (a human equilibrative nucleoside transporter 1 substrate) transport across isolated red blood cell membranes, the maximum transport velocity (V_{max}) at 0.5°C–0.7°C was found to be 23% of V_{max} at 23°C.[20] In another study, in washed human erythrocytes, V_{max} of [^{3}H]uridine transport at 5°C was only 2% of V_{max} at 25°C.[21] These studies indicate that time, temperature, and enzyme activities are essential factors in transmembrane nucleoside transport and stability *ex vivo* that has to be controlled for.

Therefore, the authors studied the preanalytical stability of dFdC and dFdU in freshly drawn blood samples from

Abbreviations used: CDA, cytidine deaminase; CI, confidence interval; CV, coefficient of variation; dFdC, 2′,2′-difluoro-2′-deoxycytidine; dFdC*, dFdC stable ^{13}C, $^{15}N_2$-isotope; dFdU, 2′,2′-difluoro-2′-deoxyuridine; dFdU*, dFdU stable ^{13}C, $^{15}N_2$-isotope; C_{max}, maximum concentration; EDTA, ethylenediaminetetraacetic acid; EPP, erythrocyte/plasma partition; IS, internal standard; LC–MS/MS, liquid chromatography tandem mass spectrometry; QC, quality control; PDAC, pancreatic ductal adenocarcinoma; THU, tetrahydrouridine.

Correspondence to: Tormod Bjånes (Telephone: +47 55973065; E-mail: tormod.karlsen.bjanes@helse-bergen.no)

This article contains supplementary material available from the authors upon request or via the Internet at http://wileylibrary.com.

Journal of Pharmaceutical Sciences

gemcitabine treated patients in a routine clinical setting at the Oncology Department of the Haukeland University Hospital, using a newly established and validated liquid chromatography tandem mass spectrometric (LC–MS/MS) method.

METHODS

Chemicals and Reagents

Gemcitabine hydrochloride was purchased from Sigma–Aldrich (Oslo, Norway). dFdU and ^{13}C, $^{15}N_2$-isotopes of dFdC (dFdC*, 4-amino-1-[3,3-difluoro-4-hydroxy-5-(hydroxymethyl)oxolan-2-yl][1,3–15N2,2–13C]pyrimidine-2-one hydrochloride)[22] and dFdU (dFdU*, 1-[3,3-difluoro-4-hydroxy-5-(hydroxymethyl) oxolan-2-yl][1,3–15N2,2–13C]pyrimidine-2,4-dione)[22] were purchased from Toronto Research Chemicals (Toronto, ON, Canada). THU was purchased from AH diagnostics AS (Oslo, Norway). HPLC grade methanol (CH_3OH) and acetonitrile (CH_3CN) were obtained from Fisher Scientific (Loughborough, UK). Formic acid (CHOOH) was purchased from Sigma–Aldrich. All solutions were made using ultra-pure water from Milli-Q Advantage A10 Ultrapure Water Purification System. Vacutainer Hemoguard EDTA and heparin tubes were purchased for Medinor AS (Oslo, Norway). HPLC-columns and precolumns were purchased from Matriks AS (Oslo, Norway).

Study Population and Sample Collection

Seven PDAC patients treated with 30-min infusions of gemcitabine 1000 mg/m^2 at the Oncology Department of the Haukeland University Hospital were included. Written informed consent was obtained from all. The protocol was approved by the Regional Committee for Medical and Health Research Ethics.

All blood-handling procedures were performed at ice-cold temperatures (1°C–4°C). Blood was collected into three 6.00 mL heparin and three 6.00 mL ethylenediaminetetraacetic acid (EDTA) vacuum tubes approximately 3 min before gemcitabine infusions were terminated. All tubes had been prefilled with 30.0 μL (300 μg) of a 10.0 mg/mL aquatic solution of the CDA enzyme inhibitor THU. The six tubes were collected in rapid succession, alternating between heparin and EDTA tubes. Blood was pooled to final volumes of 18.0 mL heparin and 18.0 mL EDTA blood. From each sample pool, 1.50 mL aliquots were drawn and centrifuged according to the following time-schedule (time after sampling): "as soon as possible," 15, 30, 45, 60, 120 and 240 min, and 24 h. Thus, eight samples with EDTA plasma and eight with heparin plasma were generated from each patient. Samples centrifuged "as soon as possible" served as baseline samples. Tubes were centrifuged for 10 min at 1800*g* at 4°C, plasma was transferred to 1.00 mL cryotubes and kept on ice until storage at −80 °C. Samples were stored for 3–16 weeks until analysis.

Preparation of Stock Solutions, Calibrator, and Quality Control Samples

Stock solutions (1.00 mg/mL) of dFdC and dFdU for standards and quality controls (QCs) were prepared separately in ultra-pure water, and preserved at −80°C.[23] Prior to spiking to calibration standard solutions, aliquots were thawed and diluted in human plasma to 100 μg/mL. Stock solutions for internal standards (ISs) were prepared in ultra-pure water at concentrations of 1.50 and 2.00 mg/mL for dFdC* and dFdU*, respectively. Prior to adding into spiked plasma samples, ISs were diluted in cold methanol to 20.0 and 26.7 μg/mL for dFdC* and dFdU*, respectively. A 10 mg/mL THU stock solution was prepared in ultra-pure water and stored at −80°C.

Blood for preparation of calibrators was collected from volunteers in the laboratory into 6 mL EDTA tubes prefilled with 300 μg THU, and centrifuged at 1800*g* for 10 min at 4°C. Plasma was pooled and immediately spiked with solutions of dFdC and dFdU, giving seven calibration standards in the ranges 0.125–40.0 μg/mL for dFdC and 1.25–80.0 μg/mL for dFdU. QC samples were prepared from stock solutions separate from those used for calibration standards. Concentrations of QC samples are given in Table 1.

Sample Preparation

Plasma samples (60 μL) were mixed with ice-cold IS methanol solution (90 μL) in 1.5 mL Eppendorf vials, vortexed for 30 s and left on ice for 10 min for protein precipitation. Then, mixtures were vortexed again and centrifuged at 4°C for 5 min at 21,000*g*. Supernatant (100 μL) was transferred to new Eppendorf vials and dried under nitrogen at 37°C for 30–60 min, using TurboVap® LV Concentration Workstation (Caliper LifeSciences, PerkinElmer, Hopkinton, Massachusetts, USA). The residue was dissolved in 100 μL ultra-pure water and

Table 1. QC Sample Concentrations and Assay Performance Data for dFdC and dFdU

Compound	QC Sample	Nominal Concentrations (μg/mL)	Within Run Accuracy (%)	Within Run Precision (CV%)	Between Run Accuracy (%)	Between Run Precision (CV%)
dFdC	LLOQ	0.125	106	4.10	107	11.5
	L	0.500	111	4.70	103	4.90
	M1	10.0	94.5	1.30	84.5	6.50
	M2	20.0	102	2.00	90.3	5.70
	H	30.0	92.7	1.90	98.7	4.90
dFdU	LLOQ	1.25	107	3.20	115	5.20
	L	5.00	109	9.80	98.5	6.80
	M1	20.0	96.6	1.80	82.1	5.80
	M2	40.0	104	2.80	86.4	5.50
	H	60.0	97.6	3.20	102	4.70

dFdC, 2′, 2′-difluoro-2′-deoxycytidine; dFdU, 2′, 2′-difluoro-2′-deoxyuridine; CV, coefficient of variation; LLOQ, lower limit of quantification; L, low; M1, medium 1; M2, medium 2; H, high; QC, quality control.

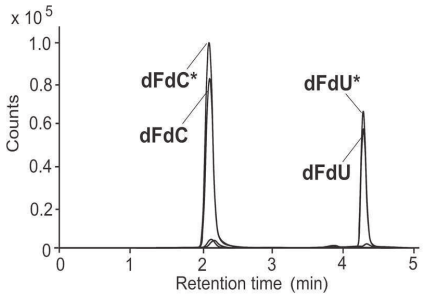

Figure 1. Representative chromatograms of the analytes in a patient sample, with dFdC and dFdU concentrations of 26.2 and 27.3 μg/mL, respectively. dFdC, 2′, 2′-difluoro-2′-deoxycytidine; *dFdC, dFdC stable ^{13}C, $^{15}N_2$-isotope; dFdU, 2′, 2′-difluoro-2′-deoxyuridine; *dFdU, dFdU stable ^{13}C, $^{15}N_2$-isotope.

centrifuged for 5 min at 21,000*g*. Supernatant was transferred to a 1.50 mL vial (Agilent) with a 250 μL insert. During LC–MS/MS method validation, the same procedure had been applied using spiked plasma solutions.

LC–MS/MS Method

The HPLC system consisted of an Agilent 1200 series separation module (Agilent Technologies, Waldbronn, Germany) and a BDS HYPERSIL C18, 3 μm, 100 × 2.1 mm^2 column, coupled with a 10 × 2.1 mm^2 precolumn (Thermo Scientific, Matriks, Oslo, Norway) maintained at 40°C during analysis. The injection volume was 10.0 μL. Mobile phase A was a 0.100% solution of formic acid. Mobile phase B was 100% acetonitrile. The HPLC operated the first 5 min at isocratic conditions of 4.00% mobile phase B, followed by a washing step with 100% B from 5.10 to 10.1 min and from 10.2 to 20.1 min with 4.00% mobile phase B. Total run time was 20.3 min. An Agilent Technologies 6410 triple-quad mass spectrometer (Agilent Technologies Inc., Santa Clara, California) was operated at positive ion electrospray ionization and the MS was applied in MRM mode. Precursor and product ion scan parameters (*m/z*) were 264.0 → 112.0 for dFdC, 267.1 → 115.1 for *dFdC, 265.1 → 112.9 for dFdU and 268.1 → 116.1 for *dFdU. Representative chromatograms of the analytes in a patient sample are shown in Figure 1, with dFdC and dFdU concentrations of 26.2 and 27.3 μg/mL, respectively. dFdC and dFdU eluted at 2.30 and 4.20 min, respectively.

The method was validated over the ranges of 0.125–40.0 and 1.25–80.0 μg/mL for dFdC and dFdU, respectively. Linear correlation coefficients (R^2) from seven calibrators analyzed in triplicate in freshly prepared plasma were 0.975 and higher (data not shown). Recoveries were assessed using control plasma samples and water spiked with working solutions of dFdC and dFdU to five QC-sample concentrations. Each spike level was processed and analyzed in ten replicates. Recoveries of analytes were calculated in relation to peaks in ultra-pure water, using heights of corresponding peaks for comparison, and expressed as mean of 10 replicates. Across all QC concentrations the recoveries [mean (SD)] were 102 (6.71)% and 103 (4.91)% for dFdC and dFdU, respectively. Precision and accuracy were determined by analyzing 10 replicates each of the five QC samples, along with a front calibration curve. Within run accuracy was calculated as a relative ratio (%) of the mean concentration ($N = 10$) per analytical run and the nominal concentration. Between run accuracy was calculated as a relative ratio (%) of the mean concentration of 10 analytical runs and the nominal concentration. Within and between run precision were expressed as coefficient of variation (CV). Table 1 summarizes assay performance data of the LC–MS/MS method.

After three freeze–thaw cycles of QC samples, maximum deviations were 9.70% and 4.90% for dFdC and dFdU, respectively. In five patient samples, the maximum deviations after as much as five freeze–thaw cycles were 9.40% and 8.50% for dFdC and dFdU, respectively. All patient samples were processed within one freeze–thaw cycle. Autosampler stability of QC and patient samples were tested up to 48 h. 80% of all concentrations deviated less than 2.00%, and the highest deviation across all concentrations was 5.60%.

Data Processing and Statistics

Data were processed using Agilent MassHunter software, Microsoft Office Excel 2010 and IBM SPSS Statistics 21.0. Variations of data were expressed as SD of repeated measurements, and as CV. Plasma concentrations from the preanalytical stability study were visualized in relation to the method precision performance in differential plots based on the Bland-Altman approach.[24] The absolute differences between subsequent concentrations and the initial concentrations, δ[dFdC] (*Y*-axis), measured in each individual patient were plotted against the respective initial concentrations (*X*-axis). Positive δ[dFdC] values indicated that concentrations were higher than the baseline concentrations, whereas negative values indicated lower concentrations. 95% confidence intervals (CIs), which indicated the maximum expected analytical variation was outlined within each differential plot. The construction of the CI was based on the highest CV obtained during validation of non-LLOQ QC samples. Analytes were considered to be stable if all concentrations were within the 95% CI of the expected analytical variation.

RESULTS AND DISCUSSION

dFdC and dFdU in Blood Samples from Patients Treated with Gemcitabine

Blood samples from seven PDAC patients were collected approximately 3 min before the end of 30-min gemcitabine infusions, that is, at the expected dFdC maximum concentrations (C_{max}). Median delay from sampling until the first centrifugation was 7 min (range 6–17). Separated plasma samples were stored at −80°C for 3–16 weeks until analysis, which was well within the limits of the analyte stability demonstrated by Freeman et al.,[25] that is, at least eight and 21 months at −20°C and −70°C, respectively, for both dFdC and dFdU.

In samples from all seven patients, dFdC and dFdU concentrations at baseline in heparin plasma were dFdC 27.7 μg/mL (18.9–39.5) and 29.7 μg/mL (13.8–39.9), respectively, and did not differ from those in EDTA plasma [dFdC 27.2 μg/mL (18.9–36.6); dFdU 29.6 μg/mL (13.4–40.1)]. Mean relative heparin/EDTA concentrations in all samples from each patient were 101% (data not shown), indicating that the two anticoagulants could be used interchangeably in this setting.

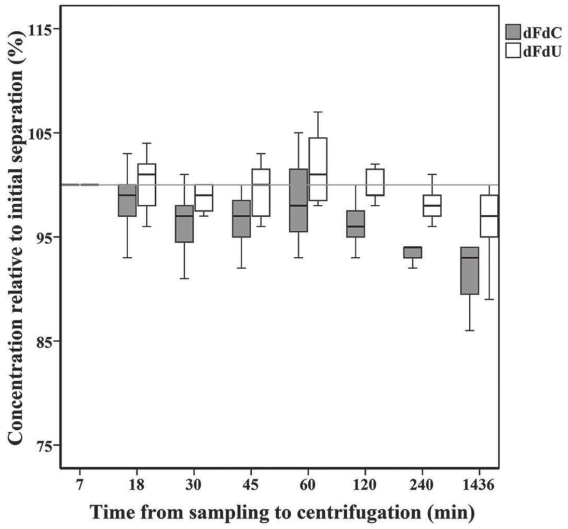

Figure 2. Boxplot showing concentrations (%) relative to those at initial separation (100%, reference), of dFdC and dFdU in heparin plasma from seven patients. dFdC, 2′, 2′-difluoro-2′-deoxycytidine; dFdU, 2′, 2′-difluoro-2′-deoxyuridine.

Concentrations of dFdC and dFdU were in accordance with previous studies of gemcitabine pharmacokinetics following infusions of 800–1000 mg/m^2: in eight patients with advanced breast cancer,[26] six patients with pancreatic cancer[17] and five patients with other solid tumors.[2] Plasma concentrations, analyzed in triplicate, from one patient are presented in Supplementary Table S1. The CVs of mean concentrations at each individual time-point in this patient were 0.600%–5.70%, which was in agreement with data from spiked samples (Table 1) and demonstrated the validity of the LC–MS/MS method in clinical samples.

We assessed the stability of dFdC and dFdU in whole blood samples during storage for 0–24 h until separation of plasma. First, we studied whether CDA activity was inhibited effectively. We calculated dFdC/dFdU concentration ratios as a function of time. The mean change from the first (7 min) to the last (24 h) sample in all patients was less than 4.50% (data not shown). Hence, adding THU in a concentration of 50 μg/mL blood prevented deamination effectively, which was in accordance with data from Bowen et al.[11] Second, we investigated whether concentrations of dFdC and dFdU in plasma remained unchanged following storage of whole blood at ice-cold temperature, to indirectly address whether transmembrane transport (Supplementary Fig. S1) was inhibited effectively. The dFdC and dFdU concentrations in heparin plasma from all seven patients, calculated as % from the concentrations obtained at baseline (100%), are shown in Figure 2. There was no change in the concentrations of dFdC and dFdU during the first 2 h of storage. However, dFdC tended to decrease as a function of further storage time. The mean dFdC concentrations after 240 min and 24 h were 94.0% (SD 2.00%) and 93.0% (SD 6.00%), respectively, compared with the baseline concentrations (100%, initial separation). To visualize the change in concentrations in relation to the analytical imprecision, we constructed differential plots based on the Bland-Altman method[24] and included lines indicating the 95% CIs (Figs. 3a–3d) based on an analytical imprecision (CV) of 6.50%. This CV represented the highest variation for dFdC in QC samples at concentrations ranging from 0.500 to 30.0 μg/mL (Table 1), excluding LLOQ, which was

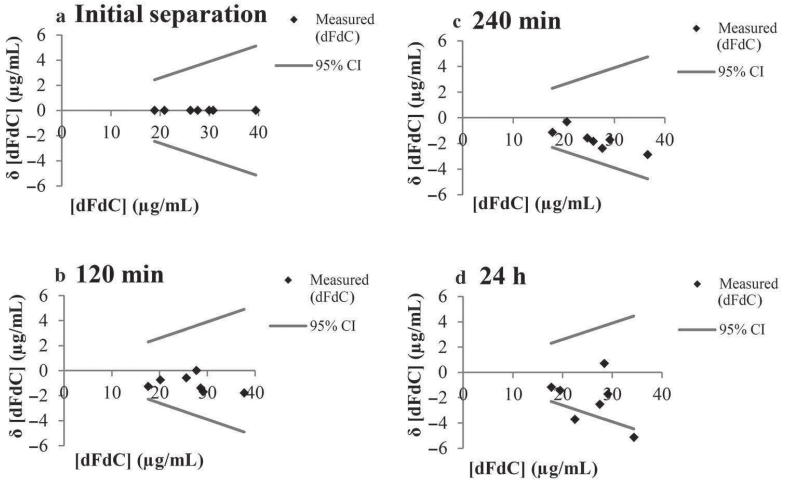

Figure 3. Differential plots of [dFdC] (*X*-axis, measured concentrations) versus δ[dFdC] (*Y*-axis, difference from initial separation) in heparin plasma from patients (n = 7). Gray lines indicate 95% CIs of [dFdC] based on an analytical CV of 6.50%. (a) Initial separation (at 7 min). (b) Separation at 120 min. (c) Separation at 240 min. (d) Separation at 24 h. dFdC, 2′, 2′-difluoro-2′-deoxycytidine; dFdU, 2′, 2′-difluoro-2′-deoxyuridine; CI, confidence intervals; CV, coefficient of variation.

considered to be less relevant for comparison with samples acquired at C_{max}. Data from the supplementary Table S1 supported our choice of using the highest CV from non-LLOQ QC samples when constructing the 95% CI in Figures 3a–3d. In Figures 3a and 3b, dFdC concentrations up to 120 min were within the 95% CI. After 240 min, all δ[dFdC] were below zero but within the 95% CI (Fig. 3c). Hence, analytical variation within the boundaries of the described method imprecision could not be ruled out. After 24 h, two of the seven concentrations were outside the 95% CI, differing 13.0%–14.0% from their respective baseline concentrations (Fig. 3d). Therefore, based on the definition of stability used in our study, a time interval of 24 h until separation of plasma was considered not to be acceptable to be included into a routine blood sampling procedure. In the same samples, the corresponding dFdU concentrations were 7.00%–11.0% lower than at baseline (data not shown), which indicated that the decline in dFdC after 24 h was not caused by incomplete CDA inhibition. Increased variation of concentrations in blood samples stored over time could reflect analyte instability.[27] Whether these deviations in the concentrations were caused by analytical variation exceeding the expected 95% CIs calculated from spiked QC samples cannot be ruled out. This may underline the challenge of distinguishing preanalytical variations from analytical variations in a newly established method, where for which performance calculations are mainly based on data from spiked QC samples.

General pharmacokinetic data for gemcitabine[1,13] indicate that a distributional steady state between plasma and blood cells may not be achieved during a 30-min gemcitabine infusion. Thus, our data on analyte stability over at least 4 h may preferentially be explained by efficiently inhibited transmembranous transport due to low temperatures during storage of blood. This notion is in accordance with findings in previous *in vitro* studies of [^{3}H]uridine-transport.[20,21] Alternatively, dFdC and dFdU were already evenly distributed between blood cells and plasma at the time of the first sample separation. However, as we did not analyze intracellular concentrations of dFdC and dFdU, we could not calculate EPP ratios to further elucidate these options.

Taken together, we demonstrated the validity of a newly established and validated LC–MS/MS method for the quantification of dFdC and dFdU, and showed that plasma concentrations of these analytes in both heparin and EDTA blood samples spiked with THU to a final concentration of 50.0 μg/mL blood and kept on ice during storage, were stable for at least 4 h until plasma was separated. This time interval allows batch-centrifugation of samples acquired at different timepoints from different patients, and of samples collected consecutively from single patients for pharmacokinetic evaluations. During this time interval, the risk of introducing a preanalytical bias due to variation in time until centrifugation seems to be negligible.

CONCLUSIONS

Our study showed that storage of whole blood samples for up to at least 4 h until centrifugation, provided that the samples were spiked with THU and kept on ice, may not be an important factor of variance when comparing results within or across studies of gemcitabine plasma pharmacokinetics. Our findings encourage further use of the established preanalytical procedures and the LC–MS/MS method, in future studies of individualized treatment strategies with gemcitabine.

ACKNOWLEDGMENTS

The authors would like to thank the patients from the outpatient oncology unit at the Haukeland University Hospital for their participation, the staff at the outpatient clinic and at the Laboratory of clinical biochemistry for assistance with patient recruitment and blood sampling, and Marit Sylte, PhD, and Steinar Hustad, PhD, for valuable scientific advice.

REFERENCES

1. Norwegian Medicines Agency. Summary of product characteristics (SPC) Gemzar. Last update August 8, 2013. Accessed May, 2015, at: http://www.legemiddelverket.no.
2. Abbruzzese JL, Grunewald R, Weeks EA, Gravel D, Adams T, Nowak B, Mineishi S, Tarassoff P, Satterlee W, Raber MN, Plunkett. 1991. A phase I clinical, plasma, and cellular pharmacology study of gemcitabine. J Clin Oncol 9(3):491–498.
3. Wong A, Soo RA, Yong WP, Innocenti F. 2009. Clinical pharmacology and pharmacogenetics of gemcitabine. Drug Metab Rev 41(2):77–88.
4. Venook AP, Egorin MJ, Rosner GL, Hollis D, Mani S, Hawkins M, Byrd J, Hohl R, Budman D, Meropol NJ, Ratain MJ. 2000. Phase I and pharmacokinetic trial of gemcitabine in patients with hepatic or renal dysfunction: Cancer and Leukemia Group B. 9565. J Clin Oncol 18(14):2780–2787.
5. Kotopoulis S, Dimcevski G, Gilja OH, Hoem D, Postema M. 2013. Treatment of human pancreatic cancer using combined ultrasound, microbubbles, and gemcitabine: A clinical case study. Med Phys 40(7):072902.
6. Farrel JJ, Elsaleh H, Garcia M, Lai R, Ammar A, Regine WF, Abrams R, Benson AB, Macdonald J, Cass CE, Dicker AP, Mackey JR. 2009. Human equilibrative nucleoside transporter 1 levels predict response to gemcitabine in patients with pancreatic cancer. Gastroenterology 136(1):187–195.
7. Tanaka M, Javle M, Dong X, Eng C, Abbruzzese JL, Li D. 2010. Gemcitabine metabolic and transporter gene polymorphisms are associated with drug toxicity and efficacy in patients with locally advanced pancreatic cancer. Cancer 116(22):5325–5335.
8. Galmarini CM, Mackey JR, Dumontet C. 2001. Nucleoside analogues: Mechanisms of drug resistance and reversal strategies. Leukemia 15(6):875–890.
9. Neff T, Blau CA. 1996. Forced expression of cytidine deaminase confers resistance to cytosine arabinoside and gemcitabine. Exp Hematol 24(11):1340–1346.
10. Plunkett W, Huang P, Xu YZ, Heinemann V, Grunewald R, Gandhi V. 1995. Gemcitabine: Metabolism, mechanisms of action, and self-potentiation. Semin Oncol 22(4, Suppl 11):3–10.
11. Bowen C, Wang S, Licea-Perez H. 2009. Development of a sensitive and selective LC-MS/MS method for simultaneous determination of gemcitabine and 2,2-difluoro-2-deoxyuridine in human plasma. J Chromatogr B Analyt Technol Biomed Life Sci 877(22):2123–2129.
12. Dumez H, Guetens G, De Boeck G, Highley MS, de Bruijn EA, van Oosterom AT, Maes RA. 2005. In vitro partition of docetaxel and gemcitabine in human volunteer blood: The influence of concentration and gender. Anticancer Drugs 16(8):885–891.
13. Eli Lilly Company. Highlights of prescribing information Gemzar (gemcitabine for injection). Last update June 2014. Accessed May, 2015, at: http://pi.lilly.com/us/gemzar.pdf.
14. Khoury H, Deroussent A, Reddy LH, Couvreur P, Vassal G, Paci A. 2007. Simultaneous determination of gemcitabine and gemcitabine-squalene by liquid chromatography-tandem mass spectrometry in human plasma. J Chromatogr B Analyt Technol Biomed Life Sci 858(1–2):71–78.

15. Maring JG, Wachters FM, Slijfer M, Maurer JM, Boezen HM, Uges DR, de Vries EG, Groen HJ. 2010. Pharmacokinetics of gemcitabine in non-small-cell lung cancer patients: Impact of the 79A>C cytidine deaminase polymorphism. Eur J Clin Pharmacol 66(6): 611–617.
16. Marangon E, Sala F, Caffo O, Galligioni E, D'Incalci M, Zucchetti M. 2008. Simultaneous determination of gemcitabine and its main metabolite, dFdU, in plasma of patients with advanced non-small-cell lung cancer by high-performance liquid chromatography-tandem mass spectrometry. J Mass Spectrom 43(2):216–223.
17. Nakata B, Amano R, Nakao S, Tamura T, Shinto O, Hirakawa T, Okita Y, Yamada N, Hirakawa K. 2010. Plasma pharmacokinetics after combined therapy of gemcitabine and oral S-1 for unresectable pancreatic cancer. J Exp Clin Cancer Res 29:15–21.
18. Masumori N, Kunishima Y, Hirobe M, Takeuchi M, Takayanagi A, Tsukamoto T, Itoh T. 2008. Measurement of plasma concentration of gemcitabine and its metabolite dFdU in hemodialysis patients with advanced urothelial cancer. Jpn J Clin Oncol 38(3):182–185.
19. Grunewald R, Katarjian H, Du M, Faucher K, Tarassoff P, Plunkett W. 1992. Gemcitabine in leukemia: A phase I clinical, plasma, and cellular pharmacology study. J Clin Oncol 10(3):406–413.
20. Takano M, Kimura E, Suzuki S, Nagai J, Yumoto R. 2010. Human erythrocyte nucleoside transporter ENT1 functions at ice-cold temperatures. Drug Metab Pharmacokinet 25(4):351–360.
21. Plagemann PG, Wohlhueter RM. 1984. Effect of temperature on kinetics and differential mobility of empty and loaded nucleoside transporter of human erythrocytes. J Biol Chem 259(14):9024–9027.
22. International Union of Pure and Applied Chemistry (IUPAC), Organic Chemistry Division, Commision on Nomenclature of Organic Chemistry. 1978. Section H: Isotopically Modified Compounds. Accessed May, 2015, at: http://www.chem.qmul.ac.uk/iupac/sectionH/.
23. Jansen RS, Rosing H, Schellens JH, Beijnen JH. 2009. Simultaneous quantification of 2′,2′-difluorodeoxycytidine and 2′,2′-difluorodeoxyuridine nucleosides and nucleotides in white blood cells using porous graphitic carbon chromatography coupled with tandem mass spectrometry. Rapid Commun Mass Spectrom 23(19):3040–3050.
24. Bland JM, Altman DG. 1986. Statistical methods for assessing agreement between two methods of clinical measurement. Lancet 1:307–310.
25. Freeman KB, Anliker S, Hamilton M, Osborne D, Dhahir PH, Nelson R, Allerheiligen SRB. 1995. Validated assays for the determination of gemcitabine in human plasma and urine using high-performance liquid chromatography with ultraviolet detection. J Chromatogr B 665:171–181.
26. Czejka M, Ostermann E, Muric L, Heinz D, Schueller J. 2005. Pharmacokinetics of gemcitabine combined with trastuzumab in patients with advanced breast cancer. Onkologie 28(6–7):318–322.
27. Peters FT. 2008. Stability of analytes in biosamples—An important issue in clinical and forensic toxicology? Anal Bioanal Chem 388(7):1505–1519.

SUPPLEMENTAL FIGURE S1. Outline of essential mechanisms of relevance for pharmacokinetic monitoring of gemcitabine

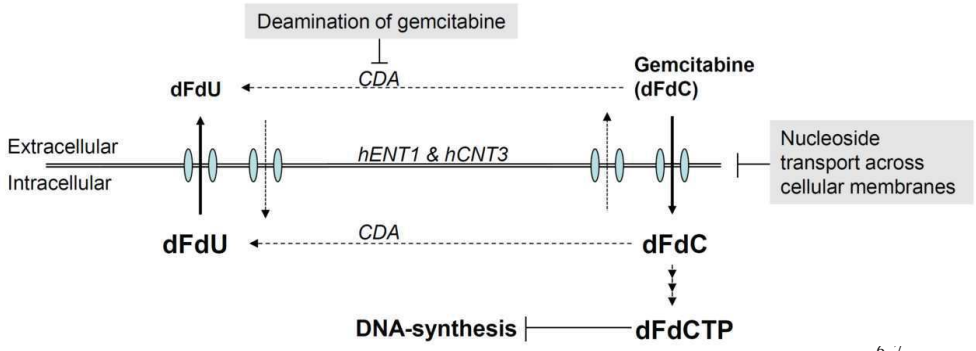

Gemcitabine (dFdC) is transported across cellular membranes via hENT1 and hCNT[6, 7], and is subject to two enzymatic processes: stepwise phosphorylation to active metabolites, or rapid deamination to inactive dFdU by CDA[2, 8-10]. CDA is also highly active extracellularly. In pharmacokinetic studies, the transport mechanisms and enzymatic activities involved in these processes need to be minimized, such that the measured drug-/metabolite-concentrations ex vivo mirror the concentrations in vivo. Time, temperature and the use of enzyme inhibitor are essential factors for the preanalytical stability of gemcitabine.

hENT1: Human equilibrative nucleoside transporter 1; hCNT3: human concentrative nucleoside transporter 3; dFdC: 2', 2'-difluoro-2'-deoxycytidine; dFdCTP: 2', 2'-difluoro-2'-deoxycytidine-5'-triphosphate (active metabolite); dFdU: 2',2'-difluoro-2'-deoxyuridine; CDA: cytidine deaminase;

SUPPLEMENTAL TABLE. Concentrations of dFdC and dFdU in heparin and EDTA plasma from one patient, separated from whole blood at different time intervals. Samples were run in triplicate.

Time (min)	dFdC				dFdU			
	Heparin		EDTA		Heparin		EDTA	
	Mean conc. (µg/ml)	CV (%)	Mean conc. (µg/ml)	CV (%)	Mean conc. (µg/ml)	CV (%)	Mean conc. (µg/ml)	CV (%)
7	20.87	4.22	19.99	1.87	13.85	3.67	13.37	0.86
18	20.47	3.71	20.90	5.21	13.78	3.18	13.96	5.05
30	20.29	3.52	19.58	1.48	13.73	3.64	13.22	2.89
45	20.96	5.70	20.63	3.58	14.30	5.34	13.83	2.82
60	20.61	3.45	20.07	5.09	14.09	2.52	13.61	3.77
120	20.14	3.63	19.41	4.71	13.78	3.83	13.16	3.52
239	20.56	2.68	19.60	1.84	14.03	2.31	13.25	0.60
1423	19.46	2.14	18.68	3.65	13.44	1.63	12.99	3.66

dFdC: 2', 2'-difluoro-2'-deoxycytidine; dFdU: 2', 2'-difluoro-2'-deoxyuridine; CV: coefficient of variation; EDTA: ethylene-diamine-tetraacetic acid

PAPER II

Journal of Chromatography B, 1001 (2015) 212–220

Contents lists available at ScienceDirect

Journal of Chromatography B

journal homepage: www.elsevier.com/locate/chromb

Liquid chromatography/tandem mass spectrometry method for simultaneous quantification of eight endogenous nucleotides and the intracellular gemcitabine metabolite dFdCTP in human peripheral blood mononuclear cells

Tina Kamčeva[a,*], Tormod Bjånes[a], Asbjørn Svardal[b], Bettina Riedel[a,b], Jan Schjøtt[a,b], Torunn Eide[b]

[a] Laboratory of Clinical Biochemistry, Section of Clinical Pharmacology, Haukeland University Hospital, 5020 Bergen, Norway
[b] Faculty of Medicine and Dentistry, Institute of Clinical Science, University of Bergen, 5021 Bergen, Norway

ARTICLE INFO

Article history:
Received 19 January 2015
Received in revised form 17 July 2015
Accepted 18 July 2015
Available online 3 August 2015

Keywords:
Nucleotides
Gemcitabine
dFdCTP
PBMC
LC–MS/MS

ABSTRACT

Quantification of endogenous nucleotides is of interest for investigation of numerous cellular biochemical processes, such as energy metabolism and signal transduction, and may also be applied in cancer and antiretroviral therapies in which nucleoside analogues are used. For these purposes we developed and validated a sensitive and high accuracy ion-pair liquid chromatography tandem mass spectrometry (IP LC–MS/MS) method for simultaneous quantification of eight endogenous nucleotides (ATP, CTP, GTP, UTP, dATP, dCTP, dGTP, dTTP) and 2′,2′-difluoro-2′-deoxycytidine triphosphate (dFdCTP), an intracellular metabolite of the nucleoside analogue gemcitabine. The assay was validated using 200 μL aliquots of peripheral blood mononuclear cell (20×10^6 cells/ml, 4×10^6 cells) extracts, pretreated with activated charcoal and spiked with unlabeled nucleotides, deoxynucleotides and dFdCTP. Analytes were extracted by simple precipitation with cold 60% methanol containing isotope labeled internal standards and separated on a porous graphitic carbon column. For method validation, the concentration ranges were: 0.125–20.8 pmol injected for deoxynucleotides, 0.25–312.5 pmol injected for dFdCTP and 5–3200 pmol injected for nucleotides. The highest coefficients of variation (CV) were 12.1% for within run assay and 11.4% for between run assay, both representing the precision at the lowest analyte concentrations. The method was applied to monitor dFdCTP and changes in endogenous nucleotides in patients who were receiving gemcitabine infusions.

1. Introduction

Nucleosides and nucleotides are involved in important cellular processes, such as polymerase-mediated synthesis of nucleic acids, cellular signal transduction, enzyme regulation and metabolism. Alterations in the size or composition of the intracellular nucleotide pool affect essential biologic functions including cellular growth

Abbreviations: ACN, acetonitrile; AcOH, acetic acid; ATP, adenosine 5′-triphosphate; BRA, between run accuracy; BRP, between run precision; Br-ATP, 8-bromoadenosine 5′-triphosphate; CD, cytidinedeaminase; CE, collision energy; CTP, cytidine 5′-triphosphate; CV, coefficient of variation; dATP, 2′-deoxyadenosine 5′-triphosphate; dCK, deoxycytidine kinase; dCMP, deoxycytidine-5′-monophosphate; dCTP, 2′-deoxycytidine 5′-triphosphate; DEA, diethylamine; dFdC, 2′,2′-difluoro-2′-deoxycytidine, gemcitabine; dFdCTP, 2′,2′-difluoro-2′-deoxycytidine triphosphate, gemcitabine triphosphate; dFdU, 2′,2′-difluoro-2′-deoxyuridine; dGTP, 2′-deoxyguanosine 5′-triphosphate; DNA, deoxyribonucleic acid; dNTP, deoxyribonucleoside triphosphate; FV, fragmentor voltage; GTP, guanosine 5′-triphosphate; HA, hexylamine; HPLC, high performance liquid chromatography; IE, ion-exchange (chromatography); IP, ion-pair (chromatography); IS, internal standard; LC, liquid chromatography; LC–MS/MS, liquid chromatography coupled with tandem mass spectrometry; LLOQ, lower limit of quantitation; MeOH, methanol; MRM, multiple reaction mode; MS, mass spectrometry; NTP, nucleoside triphosphate; PBMC, peripheral blood mononuclear cells; PBS, phosphate buffered saline; PGC, porous graphitic carbon; QC, quality control; RR, ribonucleotide reductase; SPE, solid phase extraction; THU, tetrahydrouridine; dTTP, 2′-deoxythymidine triphosphate; UTP, uridine 5′-triphosphate; UV, ultra-violet; WAX, weak anion-exchange (chromatography); WRA, within run accuracy; WRP, within run precision.

* Corresponding author. Fax: +47 55 290718.
E-mail addresses: Tina.Kamceva@k2.uib.no, tina@vinca.rs (T. Kamčeva), tormod.karlsen.bjanes@helse-bergen.no (T. Bjånes), Asbjorn.Svardal@k2.uib.no (A. Svardal), bettina.marie.riedel@helse-bergen.no (B. Riedel), jan.didrik.schjott@helse-bergen.no (J. Schjøtt), Torunn.Eide@k2.uib.no (T. Eide).

http://dx.doi.org/10.1016/j.jchromb.2015.07.041
1570-0232/

and differentiation, DNA replication and repair, immunocompetence and chromosome stability and can lead to spontaneous or induced mutability [1]. As such, analysis of nucleotides and deoxynucleotides may not only be of interest in genetic and molecular biology research, but also in studies involving nucleoside analogues used in anti-cancer, anti-viral and immunosuppressive therapies [2]. To elucidate intracellular pharmacokinetics of nucleoside analogues and their effect on the endogenous nucleotide pool, it is necessary to possess a sensitive assay for simultaneous quantification of both endogenous nucleotides and intracellular metabolites of the nucleoside analogue of interest.

There are several challenges in quantification of nucleotides in cellular matrices. Firstly, their concentrations vary among different cell types and are generally very low, in the range of 77–3532 pmol/10^6 cells for nucleoside triphosphates (NTPs) and 0.7–69 pmol/10^6 cells for deoxynucleoside triphosphates (dNTPs) [3–7]. Secondly, they resemble each other in their chemical structure which requires highly selective methods for their quantification. Thirdly, nucleotides have poor retention when separated by conventional reverse phase high performance liquid chromatography (HPLC) due to their high hydrophilicity, and a majority of assays developed for their quantification are based on anion-exchange or ion-pair (IP) chromatography [8–15]. However, poor lot to lot reproducibility and instability of ion-exchange columns, as well as the use of high salt concentrations incompatible with mass spectrometry (MS), limit the application of strong anion exchange mechanism for this purpose [16,17]. High salt concentrations can be avoided by weak anion exchange (WAX) chromatography which utilizes the change of eluent pH for compound separation [12,18]. Ion-pair chromatography on reversed phase columns have high efficiency and greater versatility than fixed-site ion exchanger [19,20], but main disadvantages are low volatility of IP agents used and the significant ion-suppression they can cause. Still, IP agents are necessary to reduce peak tailing characteristic for NTPs, and a compromise has been made by separation on porous graphitic carbon (PGC) columns using low concentrations of these agents [12,17]. An alternative to circumvent MS compatibility issues is to dephosphorylate nucleotides to nucleosides prior to analysis, but the method requires laborious and time-consuming sample preparation [17]. Hydrophilic interaction chromatography (HILIC) methods which utilize MS-compatible buffers have recently been developed. This technique has generally yielded poor separation and unsatisfactory peak shapes for di- and triphosphorylated analytes, and HILIC columns are not straightforward to optimize [21–23].

We describe a sensitive IP LC–MS/MS method for separation and quantification of 8 endogenous nucleotides (ATP, CTP, GTP, UTP, dATP, dCTP, dGTP and dTTP) and 2′,2′-difluoro-2′-deoxycytidine triphosphate (dFdCTP), the active metabolite of gemcitabine, in peripheral blood mononuclear cells (PBMC). The method has been validated for sensitive and accurate determination of all analytes and innovative steps in preparation of standards are described.

2. Experimental

2.1. Chemicals and reagents

Adenosine 5′-triphosphate (ATP) disodium salt hydrate, cytidine 5′-triphosphate (CTP) disodium salt hydrate, guanosine 5′-triphosphate (GTP) sodium salt hydrate, uridine 5′-triphosphate (UTP) trisodium salt hydrate, 2′-deoxyadenosine 5′-triphosphate (dATP) disodium salt, 2′-deoxycytidine 5′-triphosphate (dCTP) disodium salt, 2′-deoxyguanosine 5′-triphosphate (dGTP) sodium salt hydrate, thymidine 5′-triphosphate (dTTP) sodium salt and 8-bromoadenosine 5′-triphosphate (Br-ATP) sodium salt were purchased from Sigma–Aldrich (Oslo, Norway). Gemcitabine triphosphate (dFdCTP) ditriethylamine was manufactured by Toronto Research Chemicals (ON, Canada). 100 mM solutions of stable isotope labeled sodium salts of adenosine-$^{13}C_{10}$,$^{15}N_5$ 5′-triphosphate ($ATP_{13C,15N}$), cytidine-$^{13}C_9$,$^{15}N_3$ 5′-triphosphate ($CTP_{13C,15N}$), guanosine-$^{13}C_{10}$,$^{15}N_5$ 5′-triphosphate ($GTP_{13C,15N}$), uridine-$^{13}C_9$,$^{15}N_2$ 5′-triphosphate ($UTP_{13C,15N}$), 2′-deoxyadenosine-$^{13}C_{10}$,$^{15}N_3$ 5′-triphosphate ($dATP_{13C,15N}$), 2′-deoxycytidine-$^{13}C_9$,$^{15}N_3$ 5′-triphosphate ($dCTP_{13C,15N}$), 2′-deoxyguanosine-$^{13}C_{10}$,$^{15}N_5$ 5′-triphosphate ($dGTP_{13C,15N}$), thymidine-$^{13}C_{10}$,$^{15}N_2$ 5′-triphosphate ($dTTP_{13C,15N}$) in 5 mM Tris buffer were purchased from ISOTEC, Sigma–Aldrich (Oslo, Norway). 30% ammonium hydroxide solution (NH_4OH), phosphate buffered saline (PBS) and IP reagents hexylamine (HA) and diethylamine (DEA), were also purchased from Sigma–Aldrich (Oslo, Norway). Ammonium acetate (NH_4OAc) was purchased from KeboLab (Bromma, Sweden), acetic acid (AcOH) from Merck (Darmstadt, Germany) and tetrahydrouridine (THU) from BioVision (Milpitas, CA, USA). HPLC grade acetonitrile (ACN) and methanol (MeOH) were provided by Fisher Scientific (Oslo, Norway). The activated charcoal was manufactured by Merck (Darmstadt, Germany) and purchased from VWR International AS (Oslo, Norway). The water (analytical grade) was produced in our laboratory via a Milli-Q (Millipore Corporation, MA, USA) deionized water system.

2.2. Instrumentation

2.2.1. Chromatography

The HPLC system was an Agilent 1200 series (Waldbronn, Germany) with a binary pump, a degasser, a variable volume injector and a thermostated autosampler. Chromatographic separation was conducted at 30 °C, on a Hypercarb column 100 mm × 2.1 mm, 5 μm (Thermo Fisher Scientific, Waltham, MA, USA) connected to a guard column of the same type (10 mm × 2.1 mm, 5 μm). Mobile phase A was 5 mM hexylamine (HA) and 0.5% diethylamine (DEA) in water, with pH adjusted to 10 with acetic acid (AcOH). Mobile phase B was 50:50 acetonitrile (ACN):water (v:v) [3]. The gradient was as follows: 0–24% B for 15 min, 24% B for 20 min, 24–50% B for 10 min and 100% B for 9 min. The flow rate was 0.25 mL/min and all peaks were eluted in 51 min. The injection volume was 5 μL and effluent from the column was directed into the mass spectrometer in the time interval between 20 and 51 min, otherwise to waste. The column was reconditioned between subsequent analyses with 100% A for 14 min (flow rate 0.75 mL/min), resulting in a total run time of 68 min.

2.2.2. Mass spectrometry

The MS was an Agilent 6410 Triple Quad LC–MS (Agilent Technologies Inc., Santa Clara, CA, USA). The acquisition settings were optimized for NTPs, dNTPs, their stable isotopes, Br-ATP and dFdCTP. Depending on the analyte, the MS was operated in positive or negative ion multiple reaction mode (MRM) with different mass spectral settings, divided into six time segments (Table 1). Source parameters were as follows: gas temperature 350 °C, gas flow 13 L/min and nebulizer pressure 60 psi. Capillary voltage was 6000 V in negative mode and 4000 V in positive mode. MassHunter software was used for LC–MS/MS system control, data acquisition and data processing.

2.3. Sample preparation

2.3.1. Isolation of PBMC and preparation of cell supernatant

Isolation of PBMCs was performed with slight modifications of the procedure described by Losa et al. [20]. Clinical samples were collected from patients during treatment with gemcitabine infusion in an experimental treatment protocol (ClinicalTrials.gov

Table 1
Mass spectral settings (fragmentor voltage, collision energy, dwell time) for multiple reaction mode (MRM) divided in time segments when negative or positive mode was applied.

Time segment (min)	Mode	Analyte	MRM (*m*/*z*)	FV (V)	CE (eV)	Dwell time (ms)
I	−	CTP	481.8 → 158.9	135	28	120
20–25		UTP	482.9 → 158.9	140	28	160
		$UTP_{13C,15N}$	494.0 → 159.0	140	28	160
		dCTP	465.9 → 158.8	135	24	400
		$dCTP_{13C,15N}$	478.0 → 159.0	135	24	400
II	+	dFdCTP	504.1 → 326.1	200	15	300
25-32						
III	−	dTTP	481.0→158.9	135	22	840
32–45.5		$dTTP_{13C,15N}$	493.0 → 159.0	135	22	840
		GTP	521.9 → 158.8	155	28	800
		$GTP_{13C,15N}$	537.0 → 159.0	155	28	800
IV	+	ATP	581.0 → 136.1	125	28	125
45.5–47.3		$ATP_{13C,15N}$	596.2 → 146.1	125	28	125
		dGTP	580.9 → 152.1	100	28	375
		$dGTP_{13C,15N}$	596.2 → 162.1	100	28	375
V	−	dATP	489.9 → 158.9	130	28	500
47.3–49		$dATP_{13C,15N}$	505.0 → 159.0	130	28	500
VI	+	Br-ATP	660.9 → 215.7	125	25	200
49–51						

Identifier: NCT01674556), which included pharmacokinetic analyses in plasma and nucleotide pool quantification in PBMC [16]. To prevent analyte metabolism ex vivo, PBMC isolation was performed on ice and cells were lysed as quickly as possible. In addition, all tubes (6 mL) had been prefilled with 300 μg (30 μL) of a 10 mg/mL aquatic solution of aquatic solution of tetrahydrouridine (THU) to effectively inhibit the deamination of 2′,2′-difluoro-2′-deoxycytidine (dFdC) via cytidine deaminase [24]. From each patient who was available for sampling ($n = 4$) 10 mL blood was collected into cold heparinized vacutainer tubes at six time-points (before and 30, 60, 120, 180 and 240 min after initiating gemcitabine infusion), diluted with cold 10 mL 0.01 M phosphate buffered saline (PBS), transferred into cold 50 mL Lymphoprep Tubes™ (Axis Shield, Norway) prefilled with 10 ml Lymphoprep medium, and centrifuged for 25 min at 1000×*g* at 4 °C. The layer of PBMCs above the Lymphoprep medium was gently harvested, washed twice in ice-cold PBS, dissolved in 500 μL 60% MeOH solution, vortexed vigorously and frozen in liquid N_2 to lyse the cells effectively. In cell samples prepared from buffy coats the final sample volume was adjusted to achieve a standardized concentration of 20×10^6 cells/mL MeOH. Samples were kept at −80 °C until analyses. Special attention was given to avoid contamination by other blood cells, as this has been shown to introduce variations in matrix effects and cause ion suppression [25]. Before the final centrifugation, 100–300 μL of the cell suspension was removed, and cells were counted on an ADVIA 2120 (Siemens Medical, Erlangen, Germany) to be able to relate the measured nucleotide concentrations to the cell number in each sample. Prior to analyses, cell lysates were vortexed and centrifuged at 21,000×*g* at 4 °C for 5 min, and precipitates were discarded.

PBMCs for stock solutions used in the validation procedure were isolated from 50 mL buffy coats in blood acquired from blood donors. To prepare nucleotide-free matrix, PBMC cell lysate was treated with activated charcoal prior to spiking with the predefined concentrations of analytes. This method known as "matrix stripping", was successfully used in our previous analytical methods for preparation of folate free matrix [26–28]. The charcoal suspension (40 mg per mL cell supernatant) was mixed for 5 min and centrifuged at 21,000×*g* for 5 min. The supernatant was collected and stored at −80 °C until analysis.

2.3.2. Preparation of standards

Stock solutions containing all NTPs, dNTPs and dFdCTP were prepared in charcoal treated cell supernatant to the following concentrations: 8 mM ATP, 0.4 mM CTP, 0.8 mM GTP, 2 mM UTP, 0.026 mM dATP, 0.014 mM dCTP, 0.01 mM dGTP, 0.052 mM dTTP and 1.42 mM dFdCTP. Calibration (C) and quality control (QC) solutions were prepared individually by spiking carbon treated cell supernatant with stock solution to yield spiked concentrations in the ranges: 10–320 μM for ATP, 0.5–16 μM for CTP, 1–32 μM for GTP, 2.5–80 μM for UTP, 0.03–1.10 μM for dATP, 0.01–0.56 μM for dCTP, 0.01–0.40 μM for dGTP, 0.06–2.10 μM for dTTP and 0.02–31.25 μM for dFdCTP. To recalculate the amount of analytes as pmol per 10^6 PBMCs, the concentration values given in μM should be multiplied by 50. One ml aliquots of stock, calibration and quality control solutions were stored at −80 °C. ISs stock solution was prepared in water by diluting 100 mM commercially available solutions of isotope labeled NTPs and dNTPs to the following concentrations: 200 μM $ATP_{13C,15N}$, 20 μM $GTP_{13C,15N}$, 50 μM $UTP_{13C,15N}$, 0.65 μM $dATP_{13C,15N}$, 0.35 μM $dCTP_{13C,15N}$, 0.25 μM $dGTP_{13C,15N}$ and 1.3 μM $dTTP_{13C,15N}$. Working IS solution was prepared by diluting stock solution to 1:100 in MeOH and 1 mL aliquots were stored at −80 °C.A 0.17 mM stock solution of Br-ATP, which is used as the IS for dFdCTP, was prepared in mobile phase A and 1 mL aliquots were stored at −80 °C.

2.3.3. Nucleotide extraction

As SPE is time consuming and may cause less accuracy [3,17,29,30], we decided to investigate whether this step could be excluded. Both procedures, without SPE and with SPE, were performed for comparison. Without SPE: calibration solutions, QC solutions, Br-ATP stock solution, internal standards working solutions and carbon treated cell supernatants were thawed at room temperature. 200 μL calibration and QC solution, 80 μL internal standard working solution and 10 μL of Br-ATP solution were vigorously vortexed and evaporated to dryness under nitrogen gas flow using TurboVap® LV Concentration Workstation (Caliper LifeSciences, PerkinElmer, MA, USA) at 37 °C. Dried residues were resuspended in 100 μL mobile phase A, vortexed, centrifuged at 21,000×*g* for 5 min, transferred to a 1.5 mL vial (Agilent technologies) with a 250 μL insert and placed in an autosampler (4 °C) until analysis. With SPE: 200 μL calibration and QC solution, 80 μL inter-

Table 2
Assay performance data for ATP, CTP, GTP, UTP, dATP, dCTP, dGTP, dTTP and dFdCTP obtained at three concentrations level, low, medium and high in 10 replicates.

Analyte	Nominal conc. (μM)	Within run acc. (% deviation)	Within run precision (% CV)	Between run acc. (% deviation)	Between run precision (% CV)
ATP	20	101.99	2.40	103.12	4.73
	72	107.84	1.98	101.86	3.45
	288	105.98	5.99	96.54	3.71
CTP	1	102.71	5.45	101.39	5.46
	3.6	106.03	2.21	99.13	4.77
	14.4	105.52	7.31	94.06	4.23
GTP	2	104.56	3.26	104.42	6.14
	7.2	103.73	2.03	98.01	4.48
	28.8	106.91	6.80	96.07	4.57
UTP	5	106.43	2.18	106.41	4.67
	18	102.53	2.31	96.51	4.91
	72	105.71	7.34	97.52	3.52
dATP	0.065	101.52	9.08	90.72	11.35
	0.234	104.33	3.88	101.44	4.24
	0.936	105.27	6.05	96.80	4.12
dCTP	0.035	103.54	10.59	105.05	8.43
	0.126	104.67	2.96	99.29	4.98
	0.504	105.20	6.73	93.58	4.75
dGTP	0.025	105.04	3.12	103.40	5.75
	0.09	103.06	2.65	99.13	3.76
	0.504	105.04	6.78	97.09	2.86
dTTP	0.117	102.34	6.44	105.65	4.47
	0.468	99.30	8.31	94.26	6.10
	1.80	98.01	2.30	105.65	4.00
dFdCTP	0.05	105.70	12.08	100.47	11.44
	1.125	101.08	5.25	86.96	11.35
	28.125	103.70	3.95	96.86	3.87

nal standard working solution, 10 μL of Br-ATP solution and 60% MeOH solution were added to a final sample volume of 2 mL. SPE was performed using weak anion exchange columns OASIS®WAX 60 mg, 60 μm (Waters, Milford, USA), as described by Cohen et al. [3]. WAX columns were first conditioned with 2 mL MeOH, washed with 2 mL NH_4OAc (50 mM, pH 4.5 adjusted with AcOH), loaded with 2 mL samples and washed again with 2 mL NH_4OAc. Analytes were eluted in separate tubes by applying 2 mL MeOH:H_2O:NH_4OH (80:15:5 v/v) mixture on the WAX columns. Eluates were evaporated to dryness, reconstituted in 100 μL mobile phase A, vortexed, centrifuged at 21,000×*g* for 5 min, transferred to a 1.5 mL vial (Agilent technologies) with 250 μL insert and placed in autosampler (4 °C) until analyzed.

2.4. Method validation

The method was validated by carrying out tests of linearity, within- and between run precision and recovery, lower limit of quantitation (LLOQ) and stability. To evaluate the matrix effects in charcoal treated cell supernatant and in an original matrix, both were spiked with stable isotopes (ISs), dFdCTP and Br-ATP to known concentrations. Three concentration levels as those given in the Table 2 for QC samples were evaluated. The matrix effect in these two matrices was considered similar if the corresponding peak areas in charcoal treated and untreated cell supernatant did not deviate more than 25% [31]. The linearity curves were obtained by analyzing PBMC lysate containing dFdCTP and eight NTPs and dNTPs at six concentration levels in the ranges given in Section 2.3.2. All calibration curves were constructed from data obtained in triplicate. Calibration curves for each analyte were obtained as plots of relative intensities (ratios of analyte and corresponding IS peak areas) versus relative concentrations (ratios of analyte and IS concentrations) by linear regression using a weighting factor of the reciprocal of the relative concentration ($1/x$). The within run precision (WRP) and within run accuracy (WRA) were determined by measuring ten replicates of QC samples at three concentration levels (20, 72 and 288 μM for ATP; 1.0, 3.6 and 14.4 μM for CTP; 2.0, 7.2 and 28.8 μM for GTP; 5, 18 and 72 μM for UTP; 0.07, 0.23 and 0.94 μM for dATP; 0.04, 0.13 and 0.50 for dCTP; 0.03, 0.09 and 0.36 μM for dGTP; 0.13, 0.478 and 1.80 μM for dTTP; and 0.05, 1.13 and 28.13 μM for dFdCTP). For between run precision (BRP) and between run accuracy (BRA), ten replicates of QC samples at the same three concentrations were analyzed during a 2-week period. WRP and BRP were reported as coefficients of variation (CVs), which represented the ratio of standard deviations and mean values of 10 within run or between run samples, multiplied by 100. WRA and BRA were expressed as ratios of mean values and nominal concentrations in per cent. Recovery data at low, medium and high concentrations were calculated as ratios of peak areas of each analyte from chromatograms obtained by the methods described in Section 2.3.3 (with and without SPE steps) and peak areas of corresponding analytes at the same concentrations in 60% MeOH solution. Data were obtained from six replicates at each concentration and all results are presented in per cents. Stability of NTPs and dNTPs was assessed in stock and working solutions stored at −80 °C for 3 months, in samples after two freeze and thaw cycles and in processed samples at autosampler temperature (4 °C) after 48 h. Analytes were considered stable if the determined concentrations did not deviate more than +15 % from the concentration determined at time zero.

2.5. Quantification of gemcitabine (dFdC) and its metabolite dFdU in plasma

Plasma supernatant from Lymphoprep tubes (Section 2.3.1) was collected and prepared for analysis on an in-house developed LC–MS/MS method for quantification of dFdC and 2′,2′-difluoro-2′-deoxyuridine (dFdU) (manuscript submitted). Samples (60 μL) were mixed with ice cold methanol solution (90 μL), containing stable ^{13}C,$^{15}N_2$-isotopes of dFdC and dFdU, and left on ice for protein precipitation. After centrifugation (21,000×*g*, 5 min, 4 °C), 100 μL supernatant was transferred to a new Eppendorf vial, dried under nitrogen flow, reconstituted in 100 μL ultra-pure water, transferred to a vial (Agilent) and placed in the autosampler (4 °C). Separation of sample components was performed on a BDS HYPERSIL C18, 3 μm, 100 × 2.1 mm column, coupled with a 10 × 2.1 mm precolumn (Thermo Scientific, Matriks, Oslo) maintained at 40 °C during analysis. Mobile phase A was a 0.1% solution of formic acid. Mobile phase B was 100% acetonitrile. The HPLC system was set up to operate the first 5 min at a flow rate of 0.2 mL/min at isocratic conditions of 4% mobile phase B, followed by a washing step with 100% B from 5.1 to 10.1 min at a flow rate of 0.3 mL/min. From 10.2 to 20.1 min the flow rate with 4% mobile phase B was 0.3 mL/min, and at 20.2 min it was returned to 0.2 mL/min. The total run time was 20.3 min. The injection volume was 10 μL. The capillary voltage was 6000 V, gas temperature was 350 °C and the flow rate was set to 13 L/min.

3. Results and discussion

We present a method for simultaneous quantification of 8 endogenous NTPs and dNTPs and the active metabolite of gemcitabine, dFdCTP. One of the main goals in developing this method was to simplify the sample preparation procedure and, if possible, to avoid SPE. PBMC supernatant naturally contained all NTPs and dNTPs, and using unlabeled standards to prepare solutions with known concentration of analytes was not possible. Isotope labeled standards could be used as analytes, but this would limit the choice of internal standard and lead to higher deviations in recovery results [3]. Hence, it was of importance to find conditions

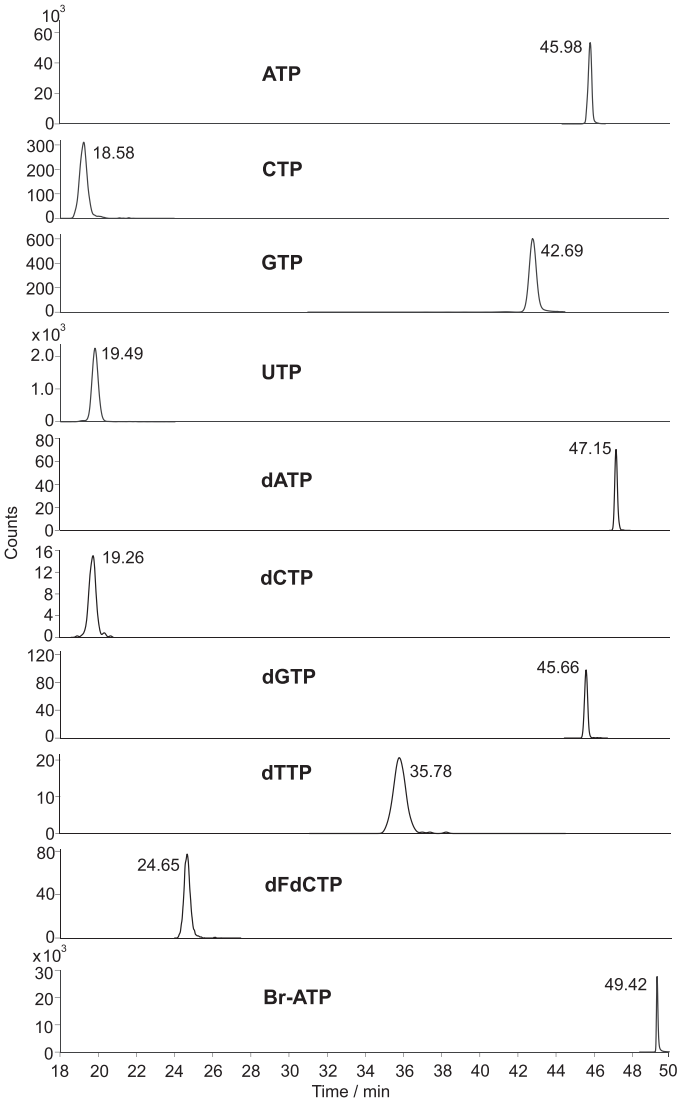

Fig. 1. Multiple reaction mode (MRM) ion chromatograms of NTPs, dNTPs and dFdCTP of a spiked cell supernatant at concentrations corresponding to LLOQ. Concentration of Br-ATP, used as IS for dFdCTP, was 17 μM.

under which endogenous nucleotides could be effectively removed. In our previous analytical methods, the activated charcoal treatment was successfully used for preparing folate-free serum [26,27], and we adjusted the same procedure to prepare nucleotide-free cell supernatant. Incubation of cell supernatant with activated charcoal (40 mg/mL, 5 min) effectively removed the traces of isotope labeled nucleotides at concentrations which were higher than those expected for endogenous nucleotides. Peak areas of endogenous NTPs decreased to less than 1% of corresponding peak areas before the treatment, while peaks of dNTP could not even be detected (data not shown). This innovative approach influenced other important aspects of the method. Firstly, we prepared calibration solutions by spiking carbon treated cell matrix to known concentrations of unlabeled analytes and used $^{13}C,^{15}N$ isotopes of compounds as their internal standards. This is one of the most important advantages of our method, because internal standards had identic separation, ionization and fragmentation patterns which resulted in high precision and accuracy, particularly at low concentrations [32]. Exceptions were made for dFdCTP, where Br-ATP was used as an internal standard instead of very expensive stable isotope labeled dFdCTP. In the case of CTP, $^{13}C,^{15}N$ isotope of UTP was chosen as internal standard because stable isotope labeled CTP and UTP had the same transitions and we did not achieve baseline separation between them. Secondly, the choice of internal standards simpli-

fied the nucleotide extraction step. Interferences originating from cellular matrix which influence recovery of analytes and internal standards were greatly reduced, and additional steps for "cleaning" of the matrix, for example by time-consuming SPE, was unnecessary. Finally, dGTP, ATP and dFdCTP were analyzed in positive mode, while all the other NTPs and dNTPs had more efficient ionization in negative mode. By using isotope labeled internal standards for each analyte (except for dFdCTP and CTP) it was possible to quantify all compounds by chromatographic separation in defined time segments (Table 1), where the mass spectrometer was operated in either negative or positive mode. Using Br-ATP as IS for all analytes, as described by Cohen et al. [3], would have required a LC–MS/MS instrument which is able to switch between negative and positive mode rapidly. As the Agilent 6410A instrument does not have this ability, we would have had to run each sample in positive and negative mode separately and the run-time would have been doubled.

3.1. Chromatography

PGC chromatography has abilities to retain polar and ionic compounds. However, it is necessary to introduce low concentration of ion pair agents (DEA) to reduce peak tailing, characteristic for triphosphates. Variations in retention times between analytical runs required an additional preconditioning step (see Section 2.2.1) [17,33–35]. The analytes and their corresponding ISs had the following retention times: 18.6 min for CTP, 19.3 for dCTP and dCTP*, 19.5 for UTP and UTP*, 24.6 min for dFdCTP, 35.8 min for dTTP and dTTP*, 42.7 min for GTP and GTP*, 45.7 min for dGTP and dGTP*, 46.0 min for ATP and ATP*, 47.2 for dATP and dATP* and 50 min for BrATP, where the asterisk (*) represents isotope labeled compounds. MRM ion chromatograms of all analytes at LLOQ concentrations are presented in Fig. 1.

3.2. Mass spectrometry

Negative ionization mode is the most common ionization mode described for the analysis of triphosphorylated nucleotides, characterized by loss of a pyrophosphate group [16,36,37]. In the present method dFdCTP, ATP, dGTP and BrATP were analyzed in positive mode. ATP and dGTP have the same molecular weight and mass transition during analysis (m/z 506 → 159.09), but in the presence of an ion pair agent the fragmentation pathway is modified. DEA adducts of ATP and dGTP have different transitions, with the daughter ion from adenine at m/z = 136 and from guanine at m/z = 152. Hence, detection of positive ions and the addition of DEA in the mobile phase in this case enabled simultaneous determination of ATP and dGTP [3,16]. dFdCTP was found to give a better signal in positive than in negative mode and BrATP was used as internal standard for its quantification. As our instrument does not have the ability to switch rapidly between negative and positive ionization modes, careful determination of time segments (Table 1) and standardization of retention times was required.

3.3. Validation

To validate the activated charcoal treatment the peak areas of ISs and dFdCTP at three concentrations in charcoal treated and original cell supernatant were compared. The corresponding results did not deviate more than 15.12% for high, 21.24% for medium and 24.81% for low concentrations, and the matrix effect in original and surrogate – charcoal treated cell supernatant was confirmed as similar.

A concentration–response calibration curve for each analyte was determined in triplicate for six concentration levels over the defined ranges. The method exhibited excellent linearity with correlation coefficients ranging from 0.9991 to 0.9998.

The LLOQs, estimated as the minimum analyte concentration providing signal to noise ratio of at least 10 measured in peak-to-peak mode, were 10.17 μM for ATP, 0.52 μM for CTP, 1.13 μM for GTP and 2.89 μM for UTP, 0.033 μM for dATP, 0.018 μM for dCTP, 0.013 μM for dGTP, 0.062 μM for dTTP and 0.062 μM for dFdCTP. To recalculate the amount of analytes as pmol injected, the concentration values given in μM should be multiplied by 10. The between-run precision of the assay was less than 11.15% for all compounds and the accuracy was in the range of 82.7–119.8%. The LLOQs for NTPs were tested to the concentrations that are sufficient for application of the method and the values could be set

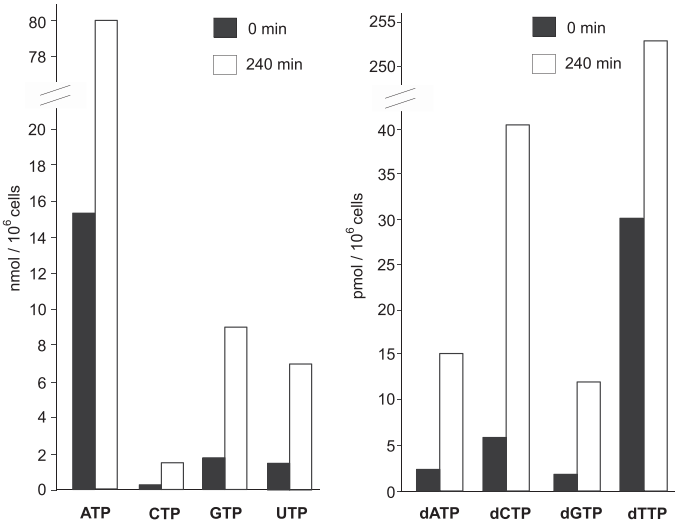

Fig. 2. Concentrations of NTPs (nmol/10^6 cells) and dNTPs (pmol/10^6 cells) extracted from PBMCs from pancreatic cancer patient before and 240 min after initiating a 30-min gemcitabine infusion.

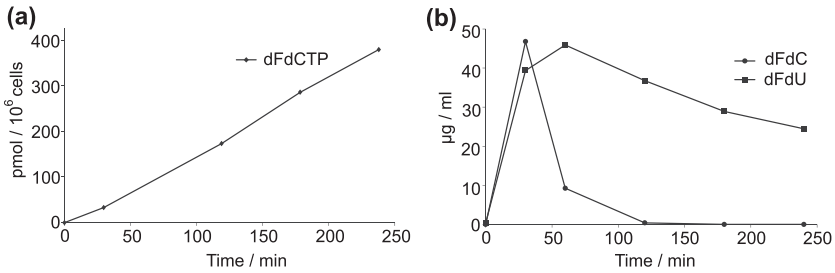

Fig. 3. (a) Concentrations of dFdCTP in PBMCs (pmol/10^6 cells) obtained from a pancreatic cancer patient acquired at different time points after initiating a 30-min gemcitabine infusion. Results were obtained by the described method, during the same analytical run and from the same samples in which all NTPs and dNTPs were determined (Fig. 2). (b) Concentrations of dFdC and dFdU (μg/mL) versus time, determined in plasma from the same blood samples using another analytical method (shortly described in Section 2.5).

Table 3
Recovery data for all NTPs and dNTPs at three concentration levels (QClow, QCmed and QChigh) and their ISs, calculated for two sample preparation methods, one including protein precipitation with 60% MeOH, evaporation and resuspension in mobile phase A (Without SPE) and the method including additional solid phase extraction (With SPE) step.

Compound	Recovery (With SPE) (%)			Recovery (Without SPE) (%)		
	QClow	QCmed	QChigh	QClow	QCmed	QChigh
ATP	99.5	99.7	100.9	71.7	79.0	81.6
CTP	104.0	105.7	106.1	68.3	70.6	73.4
GTP	95.9	95.5	104.7	66.8	70.7	72.4
UTP	101.9	110.6	102.5	67.6	70.6	73.7
dATP	95.1	98.4	115.6	59.2	69.2	69.6
dCTP	107.8	108.1	107.4	59.9	69.9	75.5
dGTP	94.2	96.0	95.1	65.8	70.7	88.6
dTTP	102.1	90.7	121.8	73.8	80.3	67.0
dFdCTP	111.1	112.0	118.2	59.2	66.7	77.3
ATP*	100.1	97.0	101.6	74.5	75.4	91.9
GTP*	98.1	93.5	108.4	67.0	66.7	74.1
UTP*	101.5	106.2	106.5	66.5	65.7	73.8
dATP*	95.1	98.4	115.6	59.2	69.2	69.6
dCTP*	104.5	101.7	109.4	64.5	66.2	75.9
dGTP*	99.1	94.6	93.6	68.1	66.9	89.2
dTTP*	97.9	70.5	121.9	71.0	70.2	72.8
BrATP	101.78	95.53	107.63	73.8	72.82	77.41

lower. These values suggest that our assay is more sensitive than previously published methods [3,36,37], even though the sample preparation was simplified.

The assay within- and between run precision and accuracy data are summarized in Table 2 for all analytes at three concentrations levels. The within run accuracy ranged from 98.01 to 107.84%, while the between run accuracy ranged from 86.96 to 106.41%. The standard relative deviation was not higher than 12.08% for within run precision and 11.44% for between run precision.

The extraction recovery data were calculated for two types of extraction, described in Section 2.3.3. The first one was a simple protein precipitation with 60% MeOH, evaporation of the supernatant and resuspension in mobile phase A ("without SPE"). The second approach included precipitation, solid phase extraction on a WAX column, evaporation and resuspension ("with SPE"). Recovery data for all analytes at three concentrations and IS are presented in Table 3. When calculating recovery according to peak areas, the "without SPE" procedure resulted in recoveries ranging from 59.2% to 91.9%. In the "with SPE" procedure the recoveries ranged from 94.2% to 121.8%. Lower recovery for the first method was expected and can be explained by a higher ion suppression originating from a more complex matrix. However, as the analytes and their ^{13}C,^{15}N isotopes are affected equally by the cell matrix, the quantification of each NTP and dNTP could be determined more accurately than in the method reported by Cohen et al. [3]. This fast, sensitive and relatively simple method for nucleotide extraction may be a better choice than one including SPE, which is time consuming, more expensive and includes more experimental steps that could lead to higher inaccuracy.

Stability of NTPs and dNTPs in stock and working solutions, prepared in cellular lysis extract remained stable for at least 3 months at −80 °C, as has been reported also earlier [3]. Short term stability at room temperature and long term stability in original matrix at freezer (−80 °C) were not assessed because the described sample preparation requires immediate handling of the samples, including adding of MeOH and freezing in liquid nitrogen, in order to reduce the potential of introducing a preanalytical bias, such as analyte metabolism ex vivo. Samples (in 60% MeOH) remained stable between two freeze–thaw cycles, as the concentration of the analytes did not deviate more than 15%. Stability of NTPs and dNTPs in processed samples (in reconstitution solution) maintained during 48 h at 4 °C was acceptable since responses did not deviate more than 12.3% from initial values.

3.4. Application of the method

Nucleotides were extracted from PBMCs isolated from blood drawn at different time points (0–240 min) after initiating a 30-min infusion of gemcitabine (2′,2′-difluoro-2′-deoxycytidine, dFdC) given to pancreatic cancer patients. All NTPs and dNTPs, as well as dFdCTP were quantified using the described method, and their concentrations (given in μM) were recalculated in relation to the number of PBMCs in each analyzed sample. In Fig. 2, concentrations of NTPs and dNTPs given in pmol/10^6 cells before and 240 min after gemcitabine infusion are presented. In samples acquired before treatment (t = 0 min) all nucleotides except ATP and GTP were within expected ranges according to literature values [38]. We speculate that the high amounts of ATP and GTP in untreated cells may be due to variations of intrinsic NTP pools dependent on cell types or to the method of cell culturing [39]. In our study PBMCs were isolated from venous blood samples in patients treated with gemcitabine infusions, while most published data are based on measurements in solid tumor and in cultured leukemia cells lines incubated with the drug. Four hours after initiating a gemcitabine infusion, all NTPs and dNTPs increased significantly (Fig. 2), which is in agreement with results from studies with cell cultures [38,40].

Concentrations versus time of intracellular dFdCTP in PBMCs from samples of one patient are given in Fig. 3(a). Gemcitabine and its main metabolite, dFdU were quantified in plasma samples acquired simultaneously and a concentration versus time profile is presented in Fig. 3(b). As has been shown in previous studies, dFdC in plasma peaked at the end of a 30-min after infusion, while dFdU peaked after another 30 min and was eliminated slowly [41].

However, the concentration plateau of dFdCTP was not reached within the first 4 h after infusion. An explanation for this finding is not readily apparent as different nucleoside membrane transporter genotypes and different infusion rates (8–50 mg/m^2/min) affect the rate and extent of dFdCTP accumulation [42], and these factors were not assessed in our preliminary study. We suggest the presented LC–MS/MS method to be a useful tool in future studies of the nucleotide pool and of intracellular gemcitabine pharmacology.

4. Conclusion

A sensitive and accurate ion-pair LC–MS/MS method on a porous graphitic column was developed and validated for simultaneous quantification of 8 endogenous nucleotides and the most important active metabolite of gemcitabine, dFdCTP, in PBMCs. During validation of the method, cell supernatant was treated with a ctivated charcoal to remove traces of endogenous NTPs and dNTPs, so that unlabeled compounds could be used as spike solutions and ^{13}C,^{15}N isotopes as internal standards. This method is applicable in cellular biology and pharmacological studies, and may be further evaluated for the investigation of the nucleotide pool and of intracellular gemcitabine pharmacokinetics and pharmacodynamics in blood cells acquired from patients treated with this drug.

Acknowledgements

The authors would like to thank the patients for their participation in our project, Bjørn Tore Gjertsen at the Clinical trials unit at Haukeland University Hospital for expert medical advice, and Wenche Hauge Eilifsen for valuable assistance in blood sampling and PBMC isolation.

References

[1] P. Rai, Oxidation in the nucleotide pool, the DNA damage response and cellular senescence: defective bricks build a defective house, Mutat. Res. 703 (2010) 71–81.
[2] L.P. Jordheim, D. Durantel, F. Zoulim, C. Dumontet, Advances in the development of nucleoside and nucleotide analogues for cancer and viral diseases, Nat. Rev. Drug Discov. 12 (2013) 447–464.
[3] S. Cohen, M. Megherbi, L.P. Jordheim, I. Lefebvre, C. Perigaud, C. Dumontet, J. Guitton, Simultaneous analysis of eight nucleoside triphosphates in cell lines by liquid chromatography coupled with tandem mass spectrometry, J. Chromatogr. B Anal. Technol. Biomed. Life Sci. 877 (2009) 3831–3840.
[4] S. Palmer, S. Cox, Comparison of extraction procedures for high-performance liquid chromatographic determination of cellular deoxynucleotides, J. Chromatogr. A 667 (1994) 316–321.
[5] K. Smid, C.J. Van Moorsel, P. Noordhuis, D.A. Voorn, G.J. Peters, Interference of gemcitabine triphosphate with the measurements of deoxynucleotides using an optimized DNA polymerase elongation assay, Int. J. Oncol. 19 (2001) 157–162.
[6] D. Di Pierro, B. Tavazzi, C.F. Perno, M. Bartolini, E. Balestra, R. Calio, B. Giardina, G. Lazzarino, An ion-pairing high-performance liquid chromatographic method for the direct simultaneous determination of nucleotides, deoxynucleotides, nicotinic coenzymes, oxypurines, nucleosides, and bases in perchloric acid cell extracts, Anal. Biochem. 231 (1995) 407–412.
[7] B. Roy, C. Beuneu, P. Roux, H. Buc, G. Lemaire, M. Lepoivre, Simultaneous determination of pyrimidine or purine deoxyribonucleoside triphosphates using a polymerase assay, Anal. Biochem. 269 (1999) 403–409.
[8] R. Nishi, T. Yamauchi, T. Ueda, A new, simple method for quantifying gemcitabine triphosphate in cancer cells using isocratic high-performance liquid chromatography, Cancer Sci. 97 (2006) 1274–1278.
[9] J.L. Abbruzzese, R. Grunewald, E.A. Weeks, D. Gravel, T. Adams, B. Nowak, S. Mineishi, P. Tarassoff, W. Satterlee, M.N. Raber, et al., A phase I clinical, plasma, and cellular pharmacology study of gemcitabine, J. Clin. Oncol. Off. J. Am. Soc. Clin. Oncol. 9 (1991) 491–498.
[10] R. Grunewald, J.L. Abbruzzese, P. Tarassoff, W. Plunkett, Saturation of 2′,2′-difluorodeoxycytidine 5′-triphosphate accumulation by mononuclear cells during a phase I trial of gemcitabine, Cancer Chemother. Pharmacol. 27 (1991) 258–262.
[11] R.W. Sparidans, M. Crul, J.H. Schellens, J.H. Beijnen, Isocratic ion-exchange chromatographic assay for the nucleotide gemcitabine triphosphate in human white blood cells, J. Chromatogr. B Anal. Technol. Biomed. Life Sci. 780 (2002) 423–430.
[12] R.S. Jansen, H. Rosing, J.H. Schellens, J.H. Beijnen, Simultaneous quantification of 2′,2′-difluorodeoxycytidine and 2′,2′-difluorodeoxyuridine nucleosides and nucleotides in white blood cells using porous graphitic carbon chromatography coupled with tandem mass spectrometry, Rapid Commun. Mass Spectrom. 23 (2009) 3040–3050.
[13] M. Gebelein, G. Merdes, M.R. Berger, Nucleotide preparation from cells and determination of nucleotides by ion-pair high-performance liquid chromatography, J. Chromatogr. 577 (1992) 146–150.
[14] T. Ryll, R. Wagner, Improved ion-pair high-performance liquid chromatographic method for the quantification of a wide variety of nucleotides and sugar-nucleotides in animal cells, J. Chromatogr. 570 (1991) 77–88.
[15] T. Uesugi, K. Sano, Y. Uesawa, Y. Ikegami, K. Mohri, Ion-pair reversed-phase high-performance liquid chromatography of adenine nucleotides and nucleoside using triethylamine as a counterion, J. Chromatogr. B Biomed. Sci. Appl. 703 (1997) 63–74.
[16] S. Cohen, L.P. Jordheim, M. Megherbi, C. Dumontet, J. Guitton, Liquid chromatographic methods for the determination of endogenous nucleotides and nucleotide analogs used in cancer therapy: a review, J. Chromatogr. B Anal. Technol. Biomed. Life Sci. 878 (2010) 1912–1928.
[17] R.S. Jansen, H. Rosing, J.H. Schellens, J.H. Beijnen, Mass spectrometry in the quantitative analysis of therapeutic intracellular nucleotide analogs, Mass Spectrom. Rev. 30 (2011) 321–343.
[18] S.A. Veltkamp, M.J. Hillebrand, H. Rosing, R.S. Jansen, E.R. Wickremsinhe, E.J. Perkins, J.H. Schellens, J.H. Beijnen, Quantitative analysis of gemcitabine triphosphate in human peripheral blood mononuclear cells using weak anion-exchange liquid chromatography coupled with tandem mass spectrometry, J. Mass Spectrom. 41 (2006) 1633–1642.
[19] M. Cichna, M. Raab, H. Daxecker, A. Griesmacher, M.M. Muller, P. Markl, Determination of fifteen nucleotides in cultured human mononuclear blood and umbilical vein endothelial cells by solvent generated ion-pair chromatography, J. Chromatogr. B Anal. Technol. Biomed. Life Sci. 787 (2003) 381–391.
[20] R. Losa, M.I. Sierra, M.O. Gion, E. Esteban, J.M. Buesa, Simultaneous determination of gemcitabine di- and triphosphate in human blood mononuclear and cancer cells by RP-HPLC and UV detection, J. Chromatogr. B Anal. Technol. Biomed. Life Sci. 840 (2006) 44–49.
[21] E. Johnsen, S.R. Wilson, I. Odsbu, A. Krapp, H. Malerod, K. Skarstad, E. Lundanes, Hydrophilic interaction chromatography of nucleoside triphosphates with temperature as a separation parameter, J. Chromatogr. A 1218 (2011) 5981–5986.
[22] N.L. Padivitage, M.K. Dissanayake, D.W. Armstrong, Separation of nucleotides by hydrophilic interaction chromatography using the FRULIC-N column, Anal. Bioanal. Chem. 405 (2013) 8837–8848.
[23] K. Burgess, D. Creek, P. Dewsbury, K. Cook, M.P. Barrett, Semi-targeted analysis of metabolites using capillary-flow ion chromatography coupled to high-resolution mass spectrometry, Rapid Commun. Mass Spectrom. 25 (2011) 3447–3452.
[24] C. Bowen, S. Wang, H. Licea-Perez, Development of a sensitive and selective LC–MS/MS method for simultaneous determination of gemcitabine and 2,2-difluoro-2-deoxyuridine in human plasma, J. Chromatogr. B Anal. Technol. Biomed. Life Sci. 877 (2009) 2123–2129.
[25] G. Shi, J.T. Wu, Y. Li, R. Geleziunas, K. Gallagher, T. Emm, T. Olah, S. Unger, Novel direct detection method for quantitative determination of intracellular nucleoside triphosphates using weak anion exchange liquid chromatography/tandem mass spectrometry, Rapid Commun. Mass Spectrom. 16 (2002) 1092–1099.
[26] R. Hannisdal, A. Svardal, P.M. Ueland, Measurement of folate in fresh and archival serum samples as p-aminobenzoylglutamate equivalents, Clin. Chem. 54 (2008) 665–672.
[27] R. Hannisdal, P.M. Ueland, A. Svardal, Liquid chromatography-tandem mass spectrometry analysis of folate and folate catabolites in human serum, Clin. Chem. 55 (2009) 1147–1154.
[28] N.C. v, d. Merbel, Quantitative determination of endogenous compounds in biological samples using chromatographic techniques, Trends Anal. Chem. 27 (2008) 924–933.
[29] R.L. Claire 3rd, Positive ion electrospray ionization tandem mass spectrometry coupled to ion-pairing high-performance liquid chromatography with a phosphate buffer for the quantitative analysis of intracellular nucleotides, Rapid Commun. Mass Spectrom. 14 (2000) 1625–1634.
[30] C. Crauste, I. Lefebvre, M. Hovaneissian, J.Y. Puy, B. Roy, S. Peyrottes, S. Cohen, J. Guitton, C. Dumontet, C. Perigaud, Development of a sensitive and selective LC/MS/MS method for the simultaneous determination of intracellular 1-beta-D-arabinofuranosylcytosine triphosphate (araCTP), cytidine triphosphate (CTP) and deoxycytidine triphosphate (dCTP) in a human follicular lymphoma cell line, J. Chromatogr. B Anal. Technol. Biomed. Life Sci. 877 (2009) 1417–1425.
[31] W.A. Korfmacher, Using Mass Spectrometry for Drug Metabolism Studies, CRC Press, Boca Raton, FL, 2005.
[32] J.J. Pitt, Principles and applications of liquid chromatography-mass spectrometry in clinical biochemistry, The Clinical biochemist, Rev. Aust. Assoc. Clin. Biochem. 30 (2009) 19–34.
[33] R.S. Jansen, H. Rosing, J.H. Schellens, J.H. Beijnen, Retention studies of 2′-2′-difluorodeoxycytidine and 2′-2′-difluorodeoxyuridine nucleosides and nucleotides on porous graphitic carbon: development of a liquid

chromatography-tandem mass spectrometry method, J. Chromatogr. A 1216 (2009) 3168–3174.
[34] S. Rinne, A. Holm, E. Lundanes, T. Greibrokk, Limitations of porous graphitic carbon as stationary phase material in the determination of catecholamines, J. Chromatogr. A 1119 (2006) 285–293.
[35] M. Pabst, A. Kohn, Implementation of transition moments between excited states in the approximate coupled-cluster singles and doubles model, J. Chem. Phys. 129 (2008) 214101.
[36] G. Hennere, F. Becher, A. Pruvost, C. Goujard, J. Grassi, H. Benech, Liquid chromatography-tandem mass spectrometry assays for intracellular deoxyribonucleotide triphosphate competitors of nucleoside antiretrovirals, J. Chromatogr. B Analyt. Technol. Biomed. Life Sci. 789 (2003) 273–281.
[37] J. Klawitter, V. Schmitz, J. Klawitter, D. Leibfritz, U. Christians, Development and validation of an assay for the quantification of 11 nucleotides using LC/LC-electrospray ionization-MS, Anal. Biochem. 365 (2007) 230–239.
[38] C.J. van Moorsel, A.M. Bergman, G. Veerman, D.A. Voorn, V.W. Ruiz van Haperen, J.R. Kroep, H.M. Pinedo, G.J. Peters, Differential effects of gemcitabine on ribonucleotide pools of twenty-one solid tumour and leukaemia cell lines, Biochim. Biophys. Acta 1474 (2000) 5–12.
[39] E. Smitskamp-Wilms, H.M. Pinedo, G. Veerman, V.W. Ruiz van Haperen, G.J. Peters, Postconfluent multilayered cell line cultures for selective screening of gemcitabine, Eur. J. Cancer 34 (1998) 921–926.
[40] L.P.J. Christelle Machon, Jean-Yves Puy, Isabelle Lefebvre, Charles Dumontet, Jerome Guitton, Fully validated assay for the quantification of endogenous nucleoside mono- and triphosphates using online extraction coupled with liquid chromatography–tandem mass spectrometry, Anal. Bioanal. Chem. 406 (2014) 2925–2941.
[41] M. Czejka, E. Ostermann, L. Muric, D. Heinz, J. Schueller, Pharmacokinetics of gemcitabine combined with trastuzumab in patients with advanced breast cancer, Onkologie 28 (2005) 318–322.
[42] A. Khatri, B.W. Williams, J. Fisher, R.C. Brundage, V.J. Gurvich, L.G. Lis, K.M. Skubitz, A.Z. Dudek, E.W. Greeno, R.A. Kratzke, J.K. Lamba, M.N. Kirstein, SLC28A3 genotype and gemcitabine rate of infusion affect dFdCTP metabolite disposition in patients with solid tumours, Br. J. Cancer 110 (2014) 304–312.

PAPER III

Journal of Controlled Release 243 (2016) 172–181

Contents lists available at ScienceDirect

Journal of Controlled Release

journal homepage: www.elsevier.com/locate/jconrel

A human clinical trial using ultrasound and microbubbles to enhance gemcitabine treatment of inoperable pancreatic cancer☆

Georg Dimcevski [a,b,*], Spiros Kotopoulis [a,b], Tormod Bjånes [c], Dag Hoem [d], Jan Schjøtt [c,e], Bjørn Tore Gjertsen [f,g], Martin Biermann [h,b], Anders Molven [i,j], Halfdan Sorbye [k,e], Emmet McCormack [e,g], Michiel Postema [l,m], Odd Helge Gilja [a,b]

[a] National Centre for Ultrasound in Gastroenterology, Haukeland University Hospital, Bergen, Norway
[b] Department of Clinical Medicine, University of Bergen, Bergen, Norway
[c] Laboratory of Clinical Biochemistry, Section of Clinical Pharmacology, Haukeland University Hospital, Bergen, Norway
[d] Department of Surgical Sciences, Haukeland University Hospital, Norway
[e] Department of Clinical Science, University of Bergen, Bergen, Norway
[f] Centre for Cancer Biomarkers, CCBIO, Department of Clinical Science, University of Bergen, Bergen, Norway
[g] Department of Internal Medicine, Hematology Section, Haukeland University Hospital, Bergen, Norway
[h] Department of Radiology, Haukeland University Hospital, Bergen, Norway
[i] Department of Pathology, Haukeland University Hospital, Bergen, Norway
[j] Gade Laboratory for Pathology, Department of Clinical Medicine, University of Bergen, Bergen, Norway
[k] Department of Oncology, Haukeland University Hospital, Bergen, Norway
[l] Institute of Fundamental Technological Research, Polish Academy of Sciences, Warszawa, Poland
[m] School of Electrical and Information Engineering, Chamber of Mines Building, University of the Witwatersrand, Johannesburg, South Africa

ARTICLE INFO

Article history:
Received 2 July 2016
Received in revised form 7 October 2016
Accepted 10 October 2016
Available online 12 October 2016

Keywords:
Ultrasound
Microbubbles
Sonoporation
Pancreatic cancer
Image-guided therapy
Clinical trial

ABSTRACT

Background: The primary aim of our study was to evaluate the safety and potential toxicity of gemcitabine combined with microbubbles under sonication in inoperable pancreatic cancer patients. The secondary aim was to evaluate a novel image-guided microbubble-based therapy, based on commercially available technology, towards improving chemotherapeutic efficacy, preserving patient performance status, and prolonging survival.
Methods: Ten patients were enrolled and treated in this Phase I clinical trial. Gemcitabine was infused intravenously over 30 min. Subsequently, patients were treated using a commercial clinical ultrasound scanner for 31.5 min. SonoVue® was injected intravenously (0.5 ml followed by 5 ml saline every 3.5 min) during the ultrasound treatment with the aim of inducing sonoporation, thus enhancing therapeutic efficacy.
Results: The combined therapeutic regimen did not induce any additional toxicity or increased frequency of side effects when compared to gemcitabine chemotherapy alone (historical controls). Combination treated patients ($n = 10$) tolerated an increased number of gemcitabine cycles compared with historical controls ($n = 63$ patients; average of 8.3 ± 6.0 cycles, *versus* 13.8 ± 5.6 cycles, $p = 0.008$, unpaired *t*-test). In five patients, the maximum tumour diameter was decreased from the first to last treatment. The median survival in our patients ($n = 10$) was also increased from 8.9 months to 17.6 months ($p = 0.011$).
Conclusions: It is possible to combine ultrasound, microbubbles, and chemotherapy in a clinical setting using commercially available equipment with no additional toxicities. This combined treatment may improve the clinical efficacy of gemcitabine, prolong the quality of life, and extend survival in patients with pancreatic ductal adenocarcinoma.

1. Introduction

A diagnosis of pancreatic ductal adenocarcinoma (PDAC) carries one of the most dismal prognoses in all of medicine. Currently the 4th most lethal cancer in the western world, it has an average 5-year survival of approximately 5% and is predicted within the decade to become the second greatest cause of cancer death [1]. Surgery provides the only possibility for cure, however >85% of newly diagnosed pancreatic tumours are considered unresectable due to locally advanced disease with encasement of large blood vessels or metastasis. Furthermore, the prevalence of extreme desmoplasia generally renders the disease resistant to chemo-radiative approaches [2]. Untreated, locally advanced PDAC patients have a median survival of 6–10 months and 3–5 months for

☆ ClinicalTrials.gov number: NCT01674556

* Corresponding author at: Department of Medicine, Haukeland University Hospital, 5021 Bergen, Norway.
E-mail address: Georg.dimcevski@helse-bergen.no (G. Dimcevski).

http://dx.doi.org/10.1016/j.jconrel.2016.10.007

patients with metastatic disease [3–5] highlighting the immediate and dire need for novel therapeutic interventions.

Gemcitabine has been the standard chemotherapeutic used in recent years and the most effective single agent. Compared to 5-fluorouracil, gemcitabine extends the survival by approximately one month whilst also improving clinical symptoms [6]. Recently, FOLFIRINOX (bolus and infusion of 5-fluorouracil, leucovorin, irinotecan, and oxaliplatin) emerged as a new chemotherapeutic option for patients with metastatic pancreatic cancer and an Eastern Cooperative Oncology Group (ECOG) performance status of 0–1. For this cohort of patients FOLFIRINOX is now the reference treatment. However, owing to the demonstrable toxicities and side effects of this therapy, gemcitabine is still the standard of care in patients with poor performance status or contraindication to FOLFIRINOX [7]. Furthermore, the combination of nanoparticle albumin-bound paclitaxel (nab-paclitaxel) and gemcitabine provides another new therapeutic option resulting with improved median survival of 1.8 months, compared to gemcitabine alone [8]. Despite these novel interventions, the reported increases in survival are minimal and we continue our wait for a therapy that will impact survival, provide a bridge to reductive surgery and ultimately cure PDAC.

Diagnostic ultrasound (US) imaging has been used in the clinic for > 50 years [9,10], with detection of pancreatic lesions dating back to the late 1960s [11]. Over the past 30 years, the use of ultrasound to detect PDAC has significantly increased [11–13]. Contrast-enhanced ultrasound uses stabilised gas microbubbles (MBs) to enhance the signal-to-noise ratio of the vasculature and allows clinicians to better visualise tissue perfusion. Twenty years ago, researchers discover that upon application of ultrasound these microbubbles volumetrically oscillate. If these oscillating microbubbles were in the vicinity of cells, small pores could be formed increasing the uptake of macromolecules significantly [14–16]. Henceforth, the use of ultrasound and microbubbles to invoke biomechanical effects that increase the permeability of the vascular barrier and/or the extravasation of drug in a specific location is now commonly known as “sonoporation”.

Numerous researchers have shown *in vitro* and *in vivo* that sonoporation is a viable technique to improve drug delivery and improve therapeutic efficacy in various cell lines derived from pharyngeal [17], glioma [18], prostate [19,20], melanoma [21], and pancreatic cancer [22]. Sonoporation has also been used to open the blood brain barrier [23,24]. In general, sonoporation research is split into two camps: A) high-intensity, *i.e.*, using inertial cavitation [9,25–27] and/or taking advantage of the thermal effects [28,29], and B) low-intensity, *i.e.*, using stable cavitation [30,31] and non-thermal effects [32–34].

The use of high-intensity ultrasound without MB has previously been evaluated clinically and shown considerable success for pain therapy [35,36], ablation of breast fibroadenomas [37], opening the blood-brain barrier [38] and treatment of pancreatic adenocarcinoma [39]. Nevertheless, to our knowledge, there has been no clinical trial evaluating the efficacy of low-intensity ultrasound in combination with microbubbles to improve the chemotherapeutic efficacy in patients with PDAC.

We have previously demonstrated *in vitro* and preclinically in an orthotopic model of PDAC, enhanced treatment effects of gemcitabine with concurrent exposure to SonoVue® MB and US at low acoustic intensities [40]. Based on these preclinical results we initiated an open label phase I, single centre, safety evaluation study in PDAC patients by combining an ultrasound contrast agent and gemcitabine under sonication at clinical diagnostic conditions.

The primary objective of this study was to evaluate the safety and potential toxicity of gemcitabine combined with ultrasound contrast agent under ultrasound treatment in inoperable pancreatic cancer patients. The secondary objective was to evaluate a novel image-guided microbubble-based therapy, based on commercially available technology, towards improving chemotherapeutic efficacy, preserving patient performance status and prolonging survival.

2. Material and methods

2.1. Subjects

Over a 23-month period (January 2012–November 2013), we recruited ten consecutive voluntary patients with inoperable pancreatic cancer (ICD-10 C25.0–3) at Haukeland University Hospital. All had histologically verified, locally advanced (non-resectable Stage III) or metastatic (Stage IV) pancreatic adenocarcinoma. Needle biopsies were obtained either from the primary tumour or from a metastatic lesion. The tissue was processed in the diagnostic pathology laboratory according to standard routines (formalin-fixation, paraffin-embedment, staining with hematoxylin and eosin). The histology was evaluated by a senior pathologist with special competence in gastrointestinal pathology. Patients were ambulatory with an Eastern Cooperative Oncology Group (ECOG) performance status 0–1 (Table 1). Patients had to meet the standard criteria at our hospital for treatment with gemcitabine and no known intolerance to gemcitabine or SonoVue® (Bracco Imaging Scandinavia AB, Oslo, Norway) ultrasound contrast agent [45].

Historical data from PDAC patients undergoing equal gemcitabine treatment following the same inclusion and exclusion criteria, between 2009 and 2011 at Haukeland University Hospital, were used for comparison of treatment tolerance, safety, and overall survival. The only difference in treatment between the historical control group and our treated group was the addition of ultrasound and microbubbles following chemotherapeutic infusion. Gemcitabine was considered the standard of care for the treatment time period of the control patients and throughout this clinical study.

2.2. Chemotherapeutic and microbubble dosage

Two experienced oncologists, not participating in the study, were responsible for the chemotherapeutic treatment. The only divergence from normal administration practice was relocation to the research unit. We used the standard recommended treatment protocol of

Table 1
Clinico-pathological characteristics of all pancreatic cancer patients. There was no statistically significant difference between the sonoporation treated cohort and historical control group in age, body mass index and blood chemistry. CA19-9 was not recorded in the historical control cohort.

	Sonoporation ($n = 10$)		Control ($n = 63$)
Variables (unit)	Start of treatment	End of treatment	Start of treatment
Age (years)	58.8 (±9.8)	59.5 (±10)	64.8 (±14.0)
Gender (%) (male/female)	30/70		54/46
Body Mass Index (kg/m^2)	23.7 (±4.3)	23.9 (±5.1)	22.9 (±3.05)
ECOG performance status (%)			
0	50	10	71
1	50	80	29
2	0	10	
Histological type	Adenocarcinoma		
Stage			
Locally advanced	70	NA	55
Metastatic	30		45
Blood chemistry			
B-hemoglobin (g/dL)	13.4 (±1.5)	11.9 (±0.9)	12.6 (±1.5)
ALAT (U/L)	45.2 (±21.8)	59.7 (±42.9)	71.2 (±59.6)
LD (mg/dL)	151.4 (±27.6)	209.6 (±46.0)	177.7 (±49.4)
Bilirubin (μmol/L)	14.5 (±8.46)	7.3 (±4.0)	37.3 (±66.0)
CA 125 (U/mL)	54.1 (±39.6)	62 (±60.1)	90.0 (±100.5)
CA19-9 (U/mL)[a]	248.5 (±380.8)	117.1 (±202.9)	NA

Comments:
Obligatory lab values for chemotherapy inclusion: B-Hemoglobin >10, Neutrophils (polymorphoneuclear leukocytes) >3.5, Platelets >150, Bilirubin >75.
[a] One sonoporation treated patient exhibited abnormally high CA19-9 values at 4608 U/mL hence not included in average CA19-9 values.

gemcitabine hydrochloride (Gemzar®, Eli Lilly & Co., Indianapolis, USA) [45]. Specifically, an initial phase of intravenous gemcitabine infusion was administered at a frequency of one cycle per week for seven weeks followed by a one-week pause. Subsequent cycles of infusions were given once weekly for 3 consecutive weeks out of every 4 weeks. Treatment pauses or any dose adjustments were administered according to standard guidelines [43,45]. Chemotherapy was continued as long as the treatment was beneficial [46]. The patients were monitored according to the requirements for Phase I studies [47].

Maximum plasma concentration of gemcitabine is achieved after 30 min at which point sonoporation with Sonovue® was initiated to ensure maximal possible tumour exposures [48]. Clinically approved SonoVue® ultrasound contrast agent was used as the microbubble for sonoporation [49]. Ethical approval limited treatment to the use of a single vial of microbubbles, paralleling traditional imaging protocols. Due to the acoustic emission limitations of the clinical diagnostic scanner (*c.f.,* Section 2.4) we chose to maximise the treatment time to achieve the longest active sonoporation time (*i.e.*, time when ultrasound waves and microbubbles were present). The expected *in-vivo* life time of microbubbles was 4–5 min, hence we chose to inject boluses every 3.5 min to ensure microbubbles were present continuously throughout the whole treatment. Previous experience [50] showed that we were able to detect microbubble using non-linear ultrasound imaging using 0.5 ml boluses [51]. Due to these requirements, microbubble dosage results in 0.5 ml of SonoVue® followed by 5-ml saline every 3.5 min, immediately after the end of the intravenous infusion of gemcitabine [43]. A complete vial was used in 31.5 min. The total dose of contrast agent used throughout each treatment was within standard clinical practice [52].

2.3. Ultrasound scanner configuration

In our previous studies we determined that sonoporation had a significant therapeutic effect when using long pulse durations, specifically 40 μs pulses every 100 μs (*i.e.,* a duty cycle of 40%) [41,44]. This resulted in minimal acoustic energy deposition within FDA and IEC guidelines and maximum therapeutic efficacy [53,54]. In this clinical study, an unmodified clinical diagnostic ultrasound scanner (LOGIQ 9, GE Healthcare, Waukesha, WI) in combination with a 4C curvilinear probe (GE Healthcare) was used to apply the therapeutic ultrasound. Unfortunately, it is not possible to generate such long duty cycles with an unmodified clinical diagnostic machine, due to technical limitations. In addition, such long duty cycles would severely degrade the image resolution. Hence, we attempted to maximise the ultrasonic duty cycle emitted by the clinical machine, whilst keeping linear waves, to avoid bubble destruction and energy deposition at higher harmonics.

In order to determine the ideal settings, the machine was characterised and calibrated in a bespoke, automated, 3-axis ultrasound characterisation chamber filled with filtered, degassed, deionised water. To waterproof the probe prior to submersion, the transmission surface was covered in AQUASONIC® ultrasound transmission gel (Parker Laboratories, Fairfield, NJ), and subsequently covered using a latex ultrasound probe cover (Sheathing Technologies, Inc., Morgan Hill, CA). The probe was locked in place and a range of acoustic emission conditions were evaluated with the aim of reaching the longest duty cycle with linear waves (*i.e.*, minimum amount of harmonics) at a de-rated MI of 0.2. The ultrasound emission conditions were characterised following FDA and IEC ultrasound guidelines [53,54]. To achieve the maximum pulse repetition rate the packet size was maximized. Whilst this reduced the frame rate substantially, it resulted in increasing the pulse repetition significantly higher than possible with a frame rate increase alone. Knowing that each patient would have a different tumour depth and size, various focal and image depths were calibrated to ensure all patients were treated with identical conditions. The ultrasound scanner configuration was programmed to maximise the duty cycle, with short broadband linear pulse in order excite as many microbubbles as possible for the longest period possible. These acoustic emission conditions were considered optimal in relation to the limitations of the clinical ultrasound system emission configuration conditions. The device optimized acoustic conditions resulted in a derated MI of 0.2 (0.27 MPa peak-negative pressure), a 0.3% duty cycle with a center emission frequency of 1.9 MHz, and a spatial-peak temporal-average intensity of 0.25 mW/(cm) [2]. Specifically, the beamformed ultrasound bursts consisted of 4 cycles (2.1 μs) every 21 ms, *i.e.*, a transmission duty cycle of 1%. Following the completion of the 12 ultrasound packet transmissions, there was a transmission pause allowing for echo capture and image reconstruction resulting in an overall duty cycle of 0.3%. The center frequency of 1.9 MHz was ideal as it was close to the natural resonance of the SonoVue® microbubbles [55]. At an MI of 0.2, only stable cavitation was expected to be induced throughout treatment. These acoustic emission conditions resulted in a 1-cm thick treatment slice based on a −3 dB contour [43].

To make sure that treatment only occurred at the target, *i.e.,* the tumour, the image plane and non-linear contrast region of interest (ROI) was limited to the tumour area +1 cm surrounding area. We avoided treating any liver or bowel area. The acoustic focal depth was placed at the centre of the tumour. The expected treatment height, based on a −3 dB contour was 3 cm above and below the acoustic focus depth.

This image-guided therapy model is based on the expectation that treatment only occurs where the ultrasound and microbubbles are present, *i.e.*, what is being imaged.

The ultrasound probe was re-calibrated every six months to ensure acoustic consistency. The exact acoustic conditions and the ultrasound field map are thoroughly described in our previous publication [43].

2.4. Transabdominal ultrasound

Routine abdominal US imaging [56] was performed during the last 10 min ($T = 20$ min) of chemotherapeutic delivery using the same LOGIQ 9 clinical diagnostic ultrasound scanner as for treatment. The ultrasound probe was attached to a ball-head mount allowing for initial free-hand scanning. Once in the optimal position for treating the tumour, with the largest diameter targeted, the ball-head mount was locked and the ultrasound probe was kept in this position till completion of the treatment [43] (*c.f.,* Fig. 1). The optimal treatment position of the 4C clinical diagnostic ultrasound probe to ensure a clear acoustic path to the tumour without any obstructions such as stomach and bowel air varied per patient. This was achieved by following established diagnostic protocols for imaging the pancreas [56,57]. In general, the probe was positioned in the epigastric region with the acoustic propagation path pointing towards the pancreatic tumour. The azimuth and elevation of the probe was adjusted to avoid any air pockets and liver tissue. The patients were allowed to lie in their most comfortable position prior to locating the tumour and locking the transducer in place. The patients were consulted if any discomfort was felt, and pressure adjustments were made if necessary. The large vasculature near the primary tumour was visualized using non-linear contrast mode in order to validate that microbubbles were being sonicated near the target tumour. Patient breathing allowed for passive scanning of the tumour, as with each breath the tumour would move through the acoustic field. The amount of passive scanning varied per patient breathing volume. Breathing based passive scanning ranged between 1 and 3 cm at the tumour level.

The total duration of combined ultrasound and microbubble treatment was 31.5 min. Fig. 1 shows the experimental setup used to combine chemotherapy, ultrasound, and microbubbles. Panel A shows the time course of each treatment cycle whilst Panel B shows a photograph of the ultrasound positioned to treat the tumour.

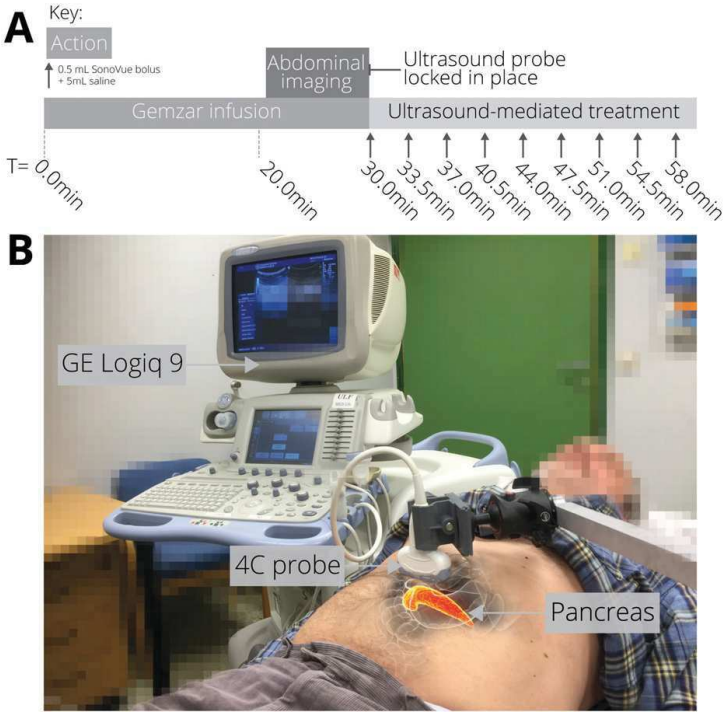

Fig. 1. (A) Treatment procedure flow chart with timings of chemotherapeutics, ultrasound exposure, and microbubble infusion. Using the current protocol, the treatment duration was 61.5 min. The first 30 min were reserved for chemotherapeutic infusion and the last 31.5 min were reserved for ultrasound and microbubble treatment. Abdominal imaging was performed for the last 10 min of infusion. Every 3.5 min, 0.5 ml of SonoVue® microbubbles were injected. (B) Photograph of patient with PDAC undergoing treatment using a clinically available diagnostic scanner. The ultrasound probe was locked in position using a mechanical arm targeted at the primary tumour for the full 31.5 min of ultrasound and microbubble treatment.

2.5. Pharmacokinetic evaluations

Analytical methods for pharmacokinetic (PK) evaluations were developed in parallel to the clinical study [58]. Whole blood samples were collected sequentially into prechilled heparinized tubes at the following time-points: $T = 0$, 30, 60, 120, 180 and 240 min. Tubes were spiked with the cytidine deaminase inhibitor tetrahydrouridine to prevent deamination of gemcitabine to dFdU [58]. Plasma and mononuclear cells were separated from whole blood as described previously. Concentrations of gemcitabine and dFdU were measured in plasma using in-house LC-MS/MS methods [58].

2.6. Monitoring

All patients underwent dual-phase computed tomography (CT) imaging ≤3 weeks before study inclusion. Routine abdominal CT was performed every 8th week where maximum tumour diameter was quantified by independent radiologists. Tumour size and development was characterised according to the Response Evaluation Criteria in Solid Tumours (RECIST). Positron emission tomography (PET) imaging with F-18-fluoro-deoxyglucose (FDG) was performed prior to the treatment to determine if metastases were present.

Assessment of clinical state during the treatment also included an evaluation of the clinical benefit response and if surgical resection could be performed [46,59]. ECOG performance status was used as a proxy to monitor the effectiveness of the combined treatment. The ECOG scale describes patients' level of functioning in terms of their ability to care for themselves, daily activity, and physical ability [46]. An ECOG grade of 0 indicates a patient who is fully active and able to carry on all pre-disease performance without restriction. An ECOG grade of 1 indicates that a patient is restricted in physical strenuous activity but ambulatory and able to carry out work of a light or sedentary nature, *e.g.*, light house work, office work. An ECOG grade of 2 indicates a patient is ambulatory and capable of all self-care but unable to carry out any work activities. The patient is up and about >50% of waking hours. An ECOG grade of 3 indicates a patient capable of limited self-care and confided to bed or chair >50% of waking hours. Hence, the longer a patient stayed below an ECOG grade of 3, the more effective the treatment was considered indicating an extended period of well-being. When a patient reaches an ECOG grade of 3, they are no-longer able to undergo gemcitabine chemotherapy.

Select patients also underwent diagnostic contrast-enhanced ultrasound following established clinical procedures [60]. Blood analysis was performed to evaluate if there was any acute toxicity.

2.7. Statistical analysis

The results are expressed as mean values ± SD, unless otherwise indicated. Continuous data was analysed using *t*-tests, or Mann-Whitney tests if data were not normally distributed. Gehan-Breslow-Wilcoxon test and Log-rank (Mantel-Cox) test were used to compare survival. Variance is expressed through 95% confidence intervals. $p < 0.05$ was considered statistical significant. Patients removed from the study due to improvement were considered as intention to treat in the survival statistical analysis.

3. Results

3.1. Tumour targeting

The established guidelines for imaging the pancreas [56,57] allowed us to target the primary PDAC tumour, independent of tumour depth and size. Fig. 2 shows four representative ultrasound images of the PDAC tumours from our treated patient cohort captured prior to switching the diagnostic ultrasound scanner settings to "treatment mode". In these images tumour depths ranges from 3.1 cm to 8.9 cm indicating that shallow or deep tumour did not inhibit tumour visualisation or targeting.

3.2. Toxicity evaluation

The direct parameters used to evaluate the toxicity of our treatment were clinical parameters including vital signs, ECG and blood chemistry. Overall, all data indicated that gemcitabine in combination with US did not induce any unexpected deviation or additional toxicities than chemotherapy alone.

One patient was hospitalised for a serious adverse event (SAE) unrelated to protocol therapy. Four SAEs occurred during protocol therapy. Two patients had symptoms indicating biliary obstruction and necessitated hospitalisation and rescheduling of the treatment. One was treated for pneumonia and one had fever due to cholangitis. The most frequent possibly treatment-related toxicities *i.e.,* adverse events (AE) were abdominal pain ($n = 9$), nausea ($n = 7$), fever ($n = 6$), neutropenia ($n = 6$), and fatigue ($n = 6$) as described in Fig. 3. These events were registered as possibly related to protocol therapy. Since all the reported toxicities are expected side effects of gemcitabine, they were evaluated as gemcitabine related. All other AE were probably related to progression of underlying disease. There were no treatment-related deaths.

3.3. Blood biochemistry

No additional toxicity was observed. Blood values changed as expected. CA 19-9 and CA 125 levels decreased in 5 out of 8 patients measured, and 7 of the 10 patients, respectively.

When evaluating the levels of cancer marker CA 125 we observed a decline following combined treatment. A total of four out of ten patients went from elevated to normal counts and only a single patient went from normal to elevated counts. Whilst fewer measurements were made in the CA 19-9 counts a similar trend was also observed where three patients went from elevated counts to normal counts, five patients showed a decrease, two patients showed an increase, and only a single patient went from normal to elevated counts. No correlation between tumour size change and cancer marker count was observed (Supplemental Fig. 1).

Bilirubin, LD, ALAT and other liver parameters were in line with the expected variation under gemcitabine treatment. These were all considered to be normal blood biochemistry changes as expected from chemotherapy and disease course.

3.4. Clinical benefit and response assessment

The following methods were applied to evaluate the responses in the ten patients: RECIST, tumour size, ECOG grade and treatment cycles [59,61].

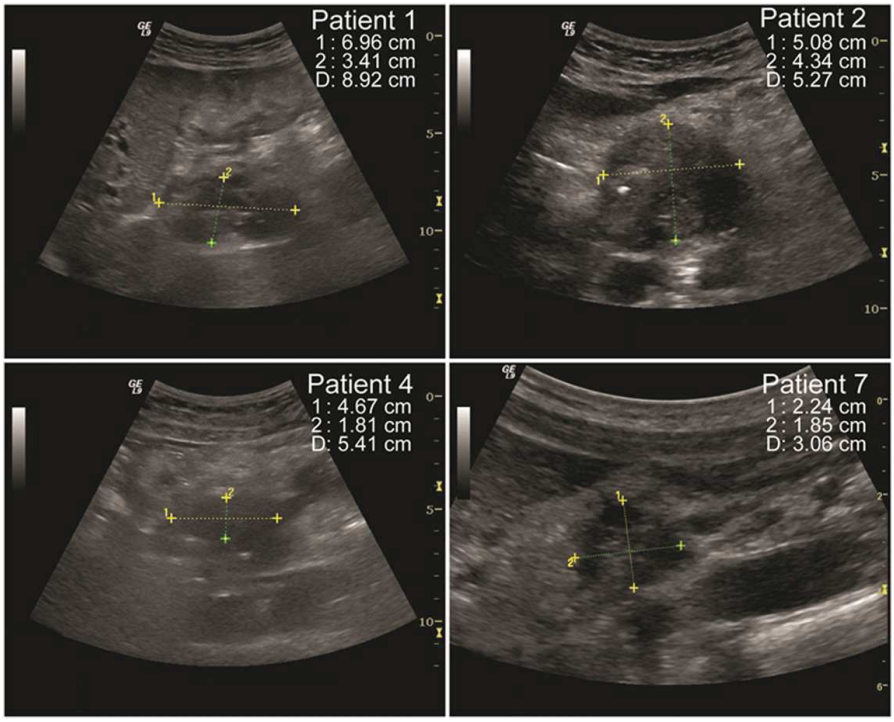

Fig. 2. Representative ultrasound images showing the PDAC tumour in four of the ultrasound and microbubble treated patients. Tumour height and width are indicated by the yellow and green dotted lines. The ultrasound transducer was positioned to ensure no obstructions of the acoustical beam path to the tumour. This resulted in a unique ultrasound probe position per patient and treatment. Distance 1 and 2 indicate the tumour width and height respectively. Value D indicated the tumour centroid depth.

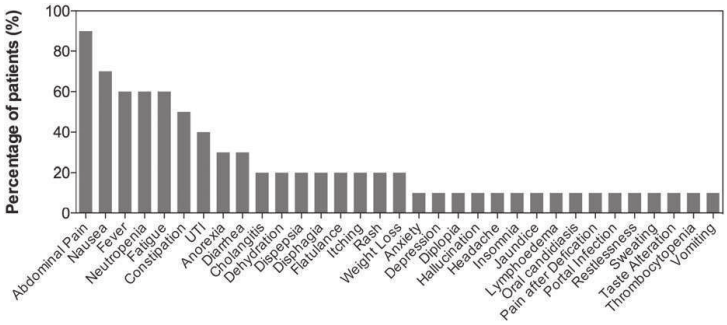

Fig. 3. Percentage of patients with PDAC treated with sonoporation that experienced a given adverse event. This graph shows all the adverse events experienced by all patients regardless of severity grade, or direct correlation to the treatment. All adverse events were already associated with gemcitabine treatment alone, indicating that addition of ultrasound and microbubbles did not induce or increase the frequency of new adverse events.

The patients considered to be positive clinical responders were regularly evaluated by the Dept. of Oncology for FOLFIRINOX treatment or consolidative radiation therapy and surgery. After 12 treatment cycles, one patient was down-staged from 8.6 cm to 4.2 cm in tumour size and thereby became available for potentially curative therapy. She was removed from the clinical trial and underwent radiation therapy and subsequent pancreatectomy. Five patients exhibited partial responses as evidenced by reduction in tumour diameter. As a result, they were offered either consolidative radiation therapy or FOLFIRINOX treatment.

Fig. 4 shows the effect of our combined treatment on the tumour size. The green lines indicate the patient tumour size recession or stabilization from the start to the end of the treatment, whereas the red lines indicate tumour size increase. When the line ends, this indicates that the patient was removed from the clinical trial.

An average of 13.8 ± 5.6 and median 12.5 (range 5–26) treatment cycles of protocol therapy were delivered per patient. In comparison, our historical control group treated with the same chemotherapeutic protocol of gemcitabine alone received an average of 8.3 ± 6.0 and median 7 (range 1–28) treatment cycles ($p = 0.008$). Fig. 5A shows a whisker plot depicting the number and range of treatment cycles.

Fig. 5B shows the survival curve of the combined treatment group compared to the historical control group. The number of treatment cycles and days of survival in our patient group are summarised in Table 2. Both Gehan-Breslow-Wilcoxon test and Log-rank (Mantel-Cox) test showed that the survival was significantly different with $p = 0.0043$ and $p = 0.011$, respectively.

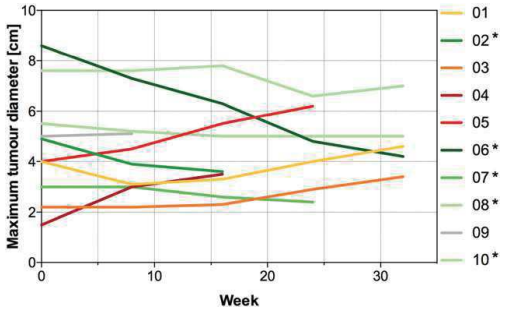

Fig. 4. Maximum tumour size as function of time for all ten patients with inoperable pancreatic adenocarcinoma. Green lines indicate tumour size recession or stabilization. Red/orange or grey lines indicate tumour size increase. Colour gradient indicates linear regression fit of tumour growth gradient (lighter = shallower). Five out of ten patients (50%) showed tumour size reduction during treatment. A reduction in tumour size may allow for surgical resection; the only current curative option. The star (*) indicates which patients showed tumour size reduction and were evaluated for consolidative radiation therapy or FOLFIRINOX treatment.

3.5. Gemcitabine pharmacokinetics

Concentration profiles of gemcitabine and dFdU in plasma samples were in accordance with previous studies of gemcitabine-infusions of 800–1000 mg/m^2 administered to breast, lung, pancreatic and patients with various other solid tumours [48,62]. This demonstrates that the combination regimen did not seem to alter the systemic pharmacokinetics of gemcitabine. A representative concentration profile from one of the patients is shown in Supplemental Fig. 2.

4. Discussion

To our knowledge, this is the first human trial evaluating the use of low intensity ultrasound and microbubbles to treat cancer. All previous studies have only been performed *in vitro* or pre-clinically. Clinical studies using ultrasound for therapy have been focused on high-intensity ultrasound without microbubbles, or for pain treatment. Hence the effect of low intensity sonoporation therapy for PDAC in humans is unknown [44,63–65].

In our previous study [43], we presented the experimental protocol focusing on the technical aspects of implementing low-intensity sonoporation using a clinical diagnostic ultrasound scanner. We also presented pilot results of five patients briefly discussing the number of cycles and tumour sizes. In the current work we present the final results and clinical data of all 10 patients, including a comparison of overall survival. In addition, we provide a toxicity report regarding the safety of the study following 138 treatment cycles.

The primary aim of this Phase I study was to evaluate the safety and potential toxicity, when combing microbubbles, ultrasound, and a chemotherapeutic agent in patients with PDAC. Hence, in this clinical trial we only evaluated a total of ten patients, as required by the NMA. Overall, all data clearly indicated that this combination did not induce any additional toxicities.

4.1. Cancer markers

These results indicate that chemotherapy in combination with microbubbles and ultrasound may have a positive impact on tumour development. It is well known that there are correlations between CA 19-9 decline and both overall survival and time to treatment failure in patients treated with gemcitabine alone [66]. The limited number of patients in our Phase-I-trial does not allow us to make any further conclusions.

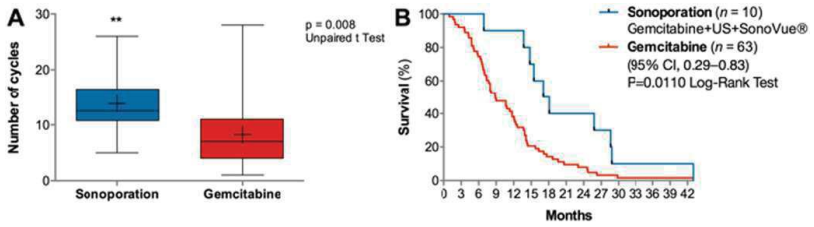

Fig. 5. (A) Whisker plot comparing the number of treatment cycles undergone in patients with pancreatic adenocarcinoma. Patients treated with sonoporation showed a statistically significant increase in number of treatment cycles ($p = 0.008$, unpaired *t*-test) indicating inhibited tumour progression and extended period of well-being (B) Survival plot comparing patients treated with ultrasound, microbubbles, and gemcitabine *vs* gemcitabine alone. The survival curve indicated that the combined treatment group had near twice as high median survival compared to treatment with gemcitabine alone; from a median of 8.9 months to 17.6 months ($p = 0.011$, Log Rank test).

4.2. Adverse events

In our present work, we present all adverse events experienced by the patients independent of grade and severity (Fig. 3). This also includes adverse events due to the actual malignancy, or personal experiences. Other clinical studies typically only register adverse events that can be directly correlated to the treatment itself, with occurrences above 10% and grades ≥3 [45]. As adverse events are rarely registered clinically, we were unable to directly compare with our historical group. To aid comparison we have compared to values available in literature (*c.f.*, Supplemental Fig. 3). In this Figure, we observe a 40% difference of abdominal pain. The primary symptoms of pancreatic cancer are abdominal pain and weight loss [67], as a result this symptom is rarely recorded. Nine out of our ten patients exhibited abdominal pain prior to treatment, hence we do not attribute this adverse event as treatment related. In contrast, in studies where weight loss was recorded, it was observed in nearly all patients. In our treated patient cohort, only 20% (2 patients) exhibited weight loss. Throughout this study all AE had already been previously associated with gemcitabine chemotherapy alone. This strongly suggests that there is no additional toxicity when combining ultrasound and microbubbles with gemcitabine chemotherapy.

4.3. Overall survival and well being

When the patients' health deteriorates, and their ECOG status rises above 2, they are no longer able to undergo therapy. Hence, number of treatment cycles indirectly represents the physical well-being of the patients. Our clinical trial group was able to undergo 66% more cycles than the historical control group. It is important to note that the analysis of treatment cycles is biased against the sonoporation group as four out of ten patients were removed from the study due to reduction of the tumour size. If these patients had continued treatment, the number of treatment cycles would be higher. This suggests that chemotherapy in combination with ultrasound and microbubbles may prolong the physical health and ambulatory status of patients with pancreatic cancer. Due to the study design, our data may not be directly comparable to the historical control cohort; hence these results should be interpreted with caution.

Table 2
Number of cycles and days survival as of diagnosis for patients with pancreatic cancer treated with ultrasound, microbubbles, and gemcitabine. The number of treatment cycles ranged from 5 to 26 cycles whereas survival ranged from 207 to over 1333 days.

Patient	Number of treatment cycles	Days survival
P1	26	443
P2[a]	11	207
P3	10	774
P4	16	513
P5	16	859
P6[a]	11	412
P7[a]	12	1333
P8[a]	18	543
P9	5	464
P10[a]	13	865
Average	13.8	641
Median	12.5	528
SD	5.7	322

[a] Patients removed from the study due to improvement.

When evaluating survival, our results showed a mean survival of 21.4 months and median survival of 17.6 months. This was significantly longer than our historical control group (8.9 months) and literature values (6.7 months) [5]. Whilst these results should be interpreted carefully, we argue that chemotherapy in combination with ultrasound and microbubbles probably increases survival in patients with pancreatic cancer.

4.4. Other chemotherapeutic options

Whilst gemcitabine is no longer considered at the forefront of chemotherapeutic treatment for PDAC, it was the first choice treatment when this clinical trial was initiated [68]. Other drugs and drug-combinations such as FOLFIRINOX and Gemcitabine + nab-Paclitaxel are now considered state-of-the-art [7,8]. As this trial was initiated using Gemcitabine we could not modify the protocol when other drugs and drug combinations reached the forefront of PDAC chemotherapeutic treatment. Gemcitabine is still commonly used worldwide for the treatment of PDAC, hence this protocol may allow for easier implementation.

When we compare median survivals of these patient groups from literature we see that FOLFIRINOX results in median survival of 11.7 months while gemcitabine + nab-Paclitaxel give a median survival of 12.2 months [69]. The observed median survival in our study far surpassed both these values using a less effective drug (Graphical Abstract). As sonoporation is not limited to any specific drug, inducing sonoporation with a more effective chemotherapeutic may further improve the therapeutic efficacy. In the case of combined chemotherapeutics, sonoporation could either be induced during or after infusion of all drugs, or at a time point where all chemotherapeutics are in the bloodstream.

4.5. Tumour perfusion

PDAC is well known to be a hypovascular tumour [70], meaning it has less perfusion than the tissue surrounding it. This is falsely correlated to no perfusion. Nevertheless, in the clinical field it is well known that PDAC still exhibits perfusion. An example of such hypovascular perfusion can be seen the Supplemental video 1 and Fig. 6. Fig. 6 shows a B-Mode image, contrast-enhanced image, and a perfusion curve of the aorta, healthy pancreatic tissue and the primary PDAC tumour. Microbubbles can be clearly distinguished in the primary PDAC tumour when comparing the primary PDAC tumour area in Fig. 6 A *vs.* B. The perfusion curve Fig. 6C, depicts non-linear contrast echo amplitude as

a function of time for three regions of interest (ROI). The results validate that microbubbles enter the PDAC tumour. At $T = 0$, *i.e.*, the time of injection, no microbubbles are present (*i.e.*, −68 dB is the base line). At around 25 s the aorta is the first ROI to reach maximum perfusion, as expected. The pancreas reaches maximum perfusion at around 27 s, whilst the PDAC tumour reaches maximum perfusion at around 32 s. The aorta shows the highest nonlinear echo amplitude, followed by the pancreatic tissue. The PDAC has the lowest nonlinear echo amplitude whilst still being 26 dB higher than the baseline, but only 5–10 dB lower than the pancreas. This indicates the tumour has lower perfusion than the surrounding tissue, yet is sufficiently perfused to allow microbubbles to enter.

It is important to note that our historical control group treated with gemcitabine alone has a median survival of 8.9 months, which is slightly higher than that previously reported in literature (6.7 months) [3,5,71] indicating that our historical control group was not negatively biased.

4.6. Potential mechanisms of sonoporation in vivo

In vitro, sonoporation is typically evaluated on a cell monolayer allowing direct contact between the target cell line and microbubbles. *In vivo*, the microbubbles flow through the vasculature and capillaries allowing direct contact only with endothelial cells, resulting in enhanced uptake only by these cells or, in some cases, in deeper cell layers [72,73]. We believe that the therapeutic efficacy observed in this Phase I clinical trial cannot only be attributed to the potential increase of gemcitabine uptake in the endothelial cell walls. The interaction between the vascular barrier and microbubbles may result in increased fenestration size allowing deeper drug penetration [74]. It is also known that ultrasound in combination with microbubbles can increase intracellular stress signalling [75]. This increased stress, in combination with the chemotherapeutic may result in enhanced drug sensitivity. Nevertheless, further work needs to be performed, pre-clinically and clinically to ascertain the true mechanisms behind the improved therapeutic efficacy.

4.7. Limitations

Whilst all these results show great promise, we cannot make global assertions on the efficacy of ultrasound-enhanced chemotherapy based on this study. To further understand and validate these results it is paramount to perform mechanistic experimental studies and examine a larger patient cohort in a prospective randomized controlled Phase II trial.

The tumour size reduction was measured using the maximum tumour diameter. Whilst this method gives a representative overview of

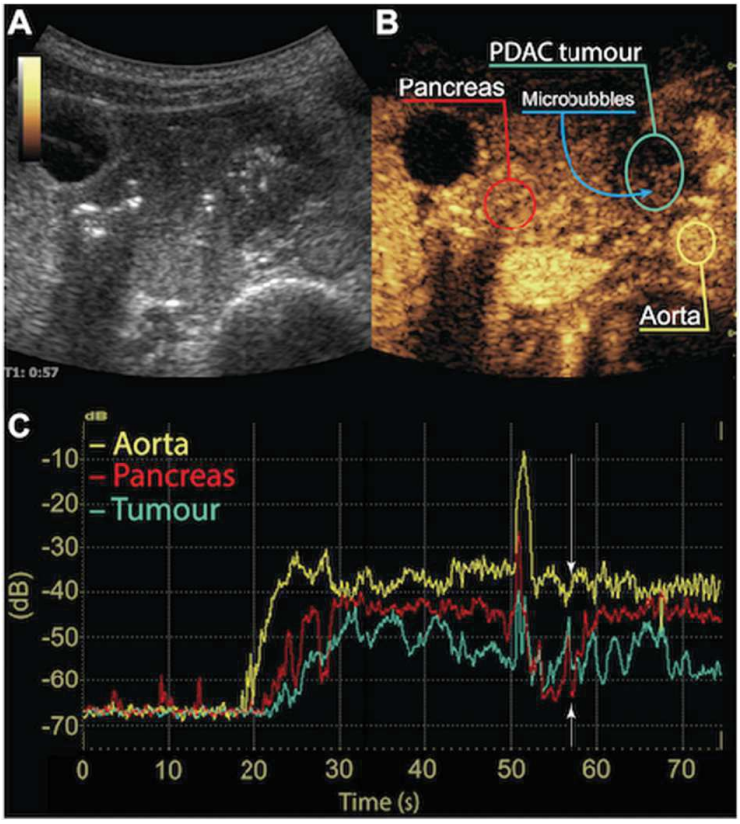

Fig. 6. Contrast-enhanced ultrasound of the PDAC tumour in Patient 7. Panel A: B-mode image. Panel B: Contrast-Enhanced image using SonoVue® microbubbles. Pancreatic tissue, the PDAC tumour and aorta have been labeled. Microbubbles can be clearly distinguished in the PDAC tumour when comparing to the B-Mode image. Panel C: Perfusion curve depicting non-linear echo amplitude as a function of time for the three regions of interest: Aorta (yellow), pancreatic tissue (red) and PDAC tumour (cyan). The PDAC tumour exhibits a longer time-to-peak and lower perfusion than both the aorta and pancreas, yet is still adequately perfused for microbubbles to enter. Panels A and B are freeze frames of late phase perfusion, 57 s after microbubbles injection (*c.f.*, white arrows in Panel C).

tumour progression it does not take into account the 3D structural change of the tumour. In our opinion, future work should address the treatment effect on the tumour volume and not only the maximal diameter.

The primary limitations of this study are that only a single 2D slice of the tumour was treated. Using a 3D ultrasound probe with further optimized acoustic conditions and modifying the microbubble type and concentration may improve the therapeutic efficacy [44].

The ultrasound emission conditions used here were severely limited by the clinical diagnostic scanner. In previous studies, longer duty cycles have shown to have a better therapeutic effect than short duty cycles [76]. Future work should aim to determine the ultrasound conditions that induce the highest therapeutic effect and to allow implementation of such conditions in the clinic.

There is currently no consensus on what is considered an ideal microbubble dose. At high dosages, the microbubbles may interact more with each other than the cells due to secondary Bjerknes forces [42], whereas at low concentrations, there may not be enough microbubbles to interact with the cells. Future work should evaluate and optimise the microbubble type and dosage.

In the field of sonoporation, it is typically assumed that the enhanced effect is due to the increase in local drug concentrations. In our work, we did not evaluate if the local drug concentration was increased and if this could be the reason for the enhanced effect. Future work should evaluate if there is an increase in local drug concentration, or if the improved therapeutic efficacy is due to increase or decrease in perfusion, or other intracellular responses.

5. Conclusion

In conclusion, our study indicated that chemotherapy in combination with ultrasound and microbubbles seems to be safe. No additional toxicity was observed when compared to chemotherapy alone. In our patient cohort, sonoporation has the additional benefit of improving the number of treatment cycles the patients were able to undergo and correspondingly extending the period of well-being. Significantly increased survival was also observed compared to a historical cohort of patients. Acknowledging the small treatment group with sub-optimal treatment conditions in this study, a larger study with improved acoustic conditions and microbubble delivery is essential to improve our understanding and validating our results. Nevertheless, in our opinion these novel results show great promise for ultrasound and microbubble enhanced therapy.

Supplementary data to this article can be found online at http://dx.doi.org/10.1016/j.jconrel.2016.10.007.

Ethical considerations

The protocol was approved by the Regional Ethics Committee (2011/1601/REK vest) and the Norwegian Medicines Agency (NMA). The study was performed in accordance with the Helsinki Declaration. All subjects signed an informed consent.

Conflict of interest disclosure statement

I declare no conflict of interest Georg Dimcevski, Date: 06/10/2016, Bergen Norway.

Acknowledgements

This study has received initial financial support from the Norwegian Cancer Society (11007001), Helse Vest (911779), and MedViz (03-2014) (http://medviz.uib.no/), a research consortium from Haukeland University Hospital, University of Bergen and Christian Michelsen Research AS. We give our special acknowledgement to our chemotherapy administrating oncologists Nils Glenjen and Hämmerling Katrin. And special thanks to our nurses (Hilde Sælensminde, Torill Våge, Marianne Lehmann, Mari Holsen, Elisabeth Bjerkan) at the Clinical Trial Unit at Haukeland University Hospital for taking care of our patients.

References

[1] World Cancer Report. 2014.
[2] A. Neesse, P. Michl, K.K. Frese, C. Feig, N. Cook, M.A. Jacobetz, M.P. Lolkema, M. Buchholz, K.P. Olive, T.M. Gress, D.A. Tuveson, Stromal biology and therapy in pancreatic cancer, Gut 60 (2011) 861–868.
[3] Kreftregisteret, Cancer in Norway, 2010.
[4] N. Alexakis, C. Halloran, M. Raraty, P. Ghaneh, R. Sutton, J.P. Neoptolemos, Current standards of surgery for pancreatic cancer, Br J Surg 91 (2004) 1410–1427.
[5] M. Malvezzi, P. Bertuccio, F. Levi, V.C. La, E. Negri, European cancer mortality predictions for the year 2013, Ann. Oncol. 24 (2013) 792–800.
[6] H.A. Burris III, M.J. Moore, J. Andersen, M.R. Green, M.L. Rothenberg, M.R. Modiano, M.C. Cripps, R.K. Portenoy, A.M. Storniolo, P. Tarassoff, R. Nelson, F.A. Dorr, C.D. Stephens, D.D. Von Hoff, Improvements in survival and clinical benefit with gemcitabine as first-line therapy for patients with advanced pancreas cancer: a randomized trial, J. Clin. Oncol. 15 (1997) 2403–2413.
[7] T. Conroy, C. Gavoille, E. Samalin, M. Ychou, M. Ducreux, The role of the FOLFIRINOX regimen for advanced pancreatic cancer, Curr. Oncol. Rep. 15 (2013) 182–189.
[8] S.M. Hoy, Albumin-bound paclitaxel: a review of its use for the first-line combination treatment of metastatic pancreatic cancer, Drugs 74 (2014) 1757–1768.
[9] B.B. Goldberg, R. Gramiak, A.K. Freimanis, Early history of diagnostic ultrasound: the role of American radiologists, AJR Am. J. Roentgenol. 160 (1993) 189–194.
[10] S. Ødegaard, Gilja OH, Gregersen H, Basic and New Aspects of Gastrointestinal Ultrasonography, 2005.
[11] B.J. Ostrum, B.B. Goldberg, H.J. Isard, A-mode ultrasound differentiation of soft-tissue masses, Radiology 88 (1967) 745–749.
[12] G.A. Zamboni, M.C. Ambrosetti, M. D'Onofrio, M.R. Pozzi, Ultrasonography of the pancreas, Radiol. Clin. N. Am. 50 (2012) 395–406.
[13] Y. Wei, X.L. Yu, P. Liang, Z.G. Cheng, Z.Y. Han, F.Y. Liu, J. Yu, Guiding and controlling percutaneous pancreas biopsies with contrast-enhanced ultrasound: target lesions are not localized on B-mode ultrasound, Ultrasound Med. Biol. 41 (2015) 1561–1569.
[14] D.L. Miller, J. Quddus, Sonoporation of monolayer cells by diagnostic ultrasound activation of contrast-agent gas bodies, Ultrasound Med. Biol. 26 (2000) 661–667.
[15] J. Wu, J.P. Ross, J.F. Chiu, Reparable sonoporation generated by microstreaming, J. Acoust. Soc. Am. 111 (2002) 1460–1464.
[16] S. Bao, B.D. Thrall, D.L. Miller, Transfection of a reporter plasmid into cultured cells by sonoporation in vitro, Ultrasound Med. Biol. 23 (1997) 953–959.
[17] B.H. Lammertink, C. Bos, K.M. van der Wurff-Jacobs, G. Storm, C.T. Moonen, R. Deckers, Increase of intracellular cisplatin levels and radiosensitization by ultrasound in combination with microbubbles, J. Control. Release 238 (2016) 157–165.
[18] M. Derieppe, K. Rojek, J.M. Escoffre, B.D. de Senneville, C. Moonen, C. Bos, Recruitment of endocytosis in sonopermeabilization-mediated drug delivery: a real-time study, Phys. Biol. 12 (2015) 046010.
[19] v. WA, S. PC, A. Healey, S. Kvale, N. Bush, J. Bamber, d.L. DC, Acoustic cluster therapy (ACT) enhances the therapeutic efficacy of paclitaxel and Abraxane(R) for treatment of human prostate adenocarcinoma in mice, J. Control. Release 236 (2016) 15–21.
[20] S. Eggen, S.M. Fagerland, Y. Morch, R. Hansen, K. Sovik, S. Berg, H. Furu, A.D. Bohn, M.B. Lilledahl, A. Angelsen, B. Angelsen, D.C. de Lange, Ultrasound-enhanced drug delivery in prostate cancer xenografts by nanoparticles stabilizing microbubbles, J. Control. Release 187 (2014) 39–49.
[21] I. Lentacker, B. Geers, J. Demeester, S.C. De Smedt, N.N. Sanders, Design and evaluation of doxorubicin-containing microbubbles for ultrasound-triggered doxorubicin delivery: cytotoxicity and mechanisms involved, Mol. Ther. 18 (2010) 101–108.
[22] B. Theek, M. Baues, T. Ojha, D. Mockel, S.K. Veettil, J. Steitz, v. BL, G. Storm, F. Kiessling, T. Lammers, Sonoporation enhances liposome accumulation and penetration in tumors with low EPR, J. Control. Release 231 (2016) 77–85.
[23] M. Bazan-Peregrino, C.D. Arvanitis, B. Rifai, L.W. Seymour, C.C. Coussios, Ultrasound-induced cavitation enhances the delivery and therapeutic efficacy of an oncolytic virus in an in vitro model, J. Control. Release 157 (2012) 235–242.
[24] N. McDannold, C.D. Arvanitis, N. Vykhodtseva, M.S. Livingstone, Temporary disruption of the blood-brain barrier by use of ultrasound and microbubbles: safety and efficacy evaluation in rhesus macaques, Cancer Res. 72 (2012) 3652–3663.
[25] S.M. Fix, M.A. Borden, P.A. Dayton, Therapeutic gas delivery via microbubbles and liposomes, J. Control. Release 209 (2015) 139–149.
[26] F. Prieur, A. Pillon, J.L. Mestas, V. Cartron, P. Cebe, N. Chansard, M. Lafond, C. Lafon, Enhancement of fluorescent probe penetration into tumors in vivo using unseeded inertial cavitation, Ultrasound Med. Biol. 42 (2016) 1706–1713.
[27] I. Lentacker, B. Geers, J. Demeester, S.C. De Smedt, N.N. Sanders, Design and evaluation of doxorubicin-containing microbubbles for ultrasound-triggered doxorubicin delivery: cytotoxicity and mechanisms involved, Mol. Ther. 18 (2010) 101–108.
[28] B.D. de Senneville, C. Moonen, M. Ries, MRI-Guided HIFU methods for the ablation of liver and renal cancers, Adv. Exp. Med. Biol. 880 (2016) 43–63.
[29] Ebbini ES, ter HG. Ultrasound-guided therapeutic focused ultrasound: current status and future directions. Int. J. Hyperth. 2015;31:77–89.
[30] G. Shapiro, A.W. Wong, M. Bez, F. Yang, S. Tam, L. Even, D. Sheyn, S. Ben-David, W. Tawackoli, G. Pelled, K.W. Ferrara, D. Gazit, Multiparameter evaluation of in vivo gene delivery using ultrasound-guided, microbubble-enhanced sonoporation, J. Control. Release 223 (2016) 157–164.

[31] I. De C, G. Lajoinie, M. Versluis, D.S. SC, I. Lentacker, Sonoprinting and the importance of microbubble loading for the ultrasound mediated cellular delivery of nanoparticles, Biomaterials 83 (2016) 294–307.
[32] M. Postema, S. Kotopoulis, A. Delalande, Odd Helge Gilja. Sonoporation: why microbubbles create pores, Ultraschall in Med 2012 33 (1) (2016) 97–98.
[33] v. RT, I. Skachkov, I. Beekers, L. KR, V. JD, K. TJ, D. Bera, Y. Luan, v. der Steen AF, d. JN, K. Kooiman, Viability of endothelial cells after ultrasound-mediated sonoporation: influence of targeting, oscillation, and displacement of microbubbles, J. Control. Release 238 (2016) 197–211.
[34] A. Delalande, C. Leduc, P. Midoux, M. Postema, C. Pichon, Efficient gene delivery by sonoporation is associated with microbubble entry into cells and the clathrin-dependent endocytosis pathway, Ultrasound Med. Biol. 41 (2015) 1913–1926.
[35] M. Chan, K. Dennis, Y. Huang, C. Mougenot, E. Chow, C. DeAngelis, J. Coccagna, A. Sahgal, K. Hynynen, G. Czarnota, W. Chu, Magnetic resonance-guided high-intensity-focused ultrasound for palliation of painful skeletal metastases: a pilot study, Technol Cancer Res Treat (2016).
[36] A. Waspe, Y. Huang, R. Endre, J. Amaral, J. de Ruiter, F. Campbell, C. Mougenot, K. Hynynen, G. Czarnota, J. Drake, M. Temple, Magnetic resonance guided focused ultrasound for noninvasive pain therapy of osteoid osteoma in children, Journal of Therapeutic Ultrasound 3 (Suppl 1) (2015) O48 2015.
[37] K. Hynynen, O. Pomeroy, D.N. Smith, P.E. Huber, N.J. McDannold, J. Kettenbach, J. Baum, S. Singer, F.A. Jolesz, MR imaging-guided focused ultrasound surgery of fibroadenomas in the breast: a feasibility study, Radiology 219 (2001) 176–185.
[38] A. Carpentier, M. Canney, A. Vignot, V. Reina, K. Beccaria, C. Horodyckid, C. Karachi, D. Leclercq, C. Lafon, J.Y. Chapelon, L. Capelle, P. Cornu, M. Sanson, K. Hoang-Xuan, J.Y. Delattre, A. Idbaih, Clinical trial of blood-brain barrier disruption by pulsed ultrasound, Sci. Transl. Med. 8 (2016) 343re2.
[39] M. Anzidei, B.C. Marincola, M. Bezzi, G. Brachetti, F. Nudo, E. Cortesi, P. Berloco, C. Catalano, A. Napoli, Magnetic resonance-guided high-intensity focused ultrasound treatment of locally advanced pancreatic adenocarcinoma: preliminary experience for pain palliation and local tumor control, Investig. Radiol. 49 (2014) 759–765.
[40] A. Delalande, S. Kotopoulis, T. Rovers, C. Pichon, M. Postema, Sonoporation at a low mechanical index, Bubble Science, Engineering & Technology 3 (2011) 3–12.
[41] A. Delalande, S. Kotopoulis, M. Postema, P. Midoux, C. Pichon, Sonoporation: mechanistic insights and ongoing challenges for gene transfer, Gene 525 (2013) 191–199.
[42] S. Kotopoulis, M. Postema, Microfoam formation in a capillary, Ultrasonics 50 (2010) 260–268.
[43] S. Kotopoulis, G. Dimcevski, O.H. Gilja, D. Hoem, M. Postema, Treatment of human pancreatic cancer using combined ultrasound, microbubbles, and gemcitabine: a clinical case study, Med. Phys. 40 (2013) 072902.
[44] S. Kotopoulis, A. Delalande, M. Popa, V. Mamaeva, G. Dimcevski, O.H. Gilja, M. Postema, B.T. Gjertsen, E. McCormack, Sonoporation-enhanced chemotherapy significantly reduces primary tumour burden in an orthotopic pancreatic cancer xenograft, Mol. Imaging Biol. 16 (2014) 53–62.
[45] Highlights of Prescribing Information: Gemzar, Eli Lilly and Company, Indianapolis, Indiana, 2010.
[46] M.M. Oken, R.H. Creech, D.C. Tormey, J. Horton, T.E. Davis, E.T. McFadden, P.P. Carbone, Toxicity and response criteria of the eastern cooperative oncology group, Am. J. Clin. Oncol. 5 (1982) 649–655.
[47] European Medicines Agency, Guideline for good clinical practice, ICH Topic E 6 (R1) (2002).
[48] L.S. Tham, L.Z. Wang, R.A. Soo, H.S. Lee, S.C. Lee, B.C. Goh, N.H. Holford, Does saturable formation of gemcitabine triphosphate occur in patients? Cancer Chemother. Pharmacol. 63 (2008) 55–64.
[49] M. Schneider, Characteristics of SonoVue®, Echocardiography 16 (1999) 743–746.
[50] S. Schafer, K. Nylund, F. Saevik, T. Engjom, M. Mezl, R. Jirik, G. Dimcevski, O.H. Gilja, K. Tonnies, Semi-automatic motion compensation of contrast-enhanced ultrasound images from abdominal organs for perfusion analysis, Comput. Biol. Med. 63 (2015) 229–237.
[51] F. Piscaglia, C. Nolsoe, D. CF, C. DO, G. OH, B. NM, T. Albrecht, L. Barozzi, M. Bertolotto, O. Catalano, M. Claudon, C. DA, C. JM, M. D'Onofrio, D. FM, J. Eyding, M. Giovannini, M. Hocke, A. Ignee, J. EM, K. AS, N. Lassau, E. Leen, G. Mathis, A. Saftoiu, G. Seidel, S. PS, H. GT, D. Timmerman, W. HP, The EFSUMB Guidelines and Recommendations on the Clinical Practice of Contrast Enhanced Ultrasound (CEUS): update 2011 on non-hepatic applications, Ultraschall Med. (2011).
[52] M. Claudon, D. Cosgrove, T. Albrecht, L. Bolondi, M. Bosio, F. Calliada, J.M. Correas, K. Darge, C. Dietrich, M. D'Onofrio, D.H. Evans, C. Filice, L. Greiner, K. Jager, N. Jong, E. Leen, R. Lencioni, D. Lindsell, A. Martegani, S. Meairs, C. Nolsoe, F. Piscaglia, P. Ricci, G. Seidel, B. Skjoldbye, L. Solbiati, L. Thorelius, F. Tranquart, H.P. Weskott, T. Whittingham, Guidelines and good clinical practice recommendations for contrast enhanced ultrasound (CEUS) - update 2008, Ultraschall Med. 29 (2008) 28–44.
[53] U.S. Department of Health and Human Services, Information for Manufacturers Seeking Marketing Clearance of Diagnostic Ultrasound Systems and Transducers (Food and Drug Administration), 2008.
[54] International Electrotechnical Commission, Ultrasonics - Hydrophones Part 2: Calibration for Ultrasonic Fields up to 40 MHz, Report No. 62127-2 ed1.0, IEC, Geneva, Switzerland, 2013.
[55] d. JN, M. Emmer, v. WA, M. Versluis, Ultrasonic characterization of ultrasound contrast agents, Med. Biol. Eng. Comput. 47 (2009) 861–873.
[56] G. Dimcevski, F.G. Erchinger, R. Havre, O.H. Gilja, Ultrasonography in diagnosing chronic pancreatitis: new aspects, World J. Gastroenterol. 19 (2013) 7247–7257.
[57] F. Erchinger, G. Dimcevski, T. Engjom, O.H. Gilja, Transabdominal ultrasound of the pancreas: basic and new aspects, Imaging in Medicine 3 (2011) 411–422.
[58] T. Bjanes, T. Kamceva, T. Eide, B. Riedel, J. Schjott, A. Svardal, Preanalytical stability of gemcitabine and its metabolite 2′, 2′-difluoro-2′-deoxyuridine in whole blood-assessed by liquid chromatography tandem mass spectrometry, J. Pharm. Sci. (2015).
[59] S.A. Sohaib, B. Turner, J.A. Hanson, M. Farquharson, R.T. Oliver, R.H. Reznek, CT assessment of tumour response to treatment: comparison of linear, cross-sectional and volumetric measures of tumour size, Br. J. Radiol. 73 (2000) 1178–1184.
[60] C.P. Nolsoe, T. Lorentzen, International guidelines for contrast-enhanced ultrasonography: ultrasound imaging in the new millennium, Ultrasonography 35 (2016) 89–103.
[61] R.L. Wahl, H. Jacene, Y. Kasamon, M.A. Lodge, From RECIST to PERCIST: evolving considerations for PET response criteria in solid tumors, J. Nucl. Med. 50 (Suppl 1) (2009) 122S–150S.
[62] J.L. Abbruzzese, R. Grunewald, E.A. Weeks, D. Gravel, T. Adams, B. Nowak, S. Mineishi, P. Tarassoff, W. Satterlee, M.N. Raber, A phase I clinical, plasma, and cellular pharmacology study of gemcitabine, J. Clin. Oncol. 9 (1991) 491–498.
[63] H. Inoue, Y. Arai, T. Kishida, M. Shin-Ya, R. Terauchi, S. Nakagawa, M. Saito, S. Tsuchida, A. Inoue, T. Shirai, H. Fujiwara, O. Mazda, T. Kubo, Sonoporation-mediated transduction of siRNA ameliorated experimental arthritis using 3 MHz pulsed ultrasound, Ultrasonics 54 (2014) 874–881.
[64] H. Dewitte, L.S. Van, C. Heirman, K. Thielemans, S.C. De Smedt, K. Breckpot, I. Lentacker, The potential of antigen and TriMix sonoporation using mRNA-loaded microbubbles for ultrasound-triggered cancer immunotherapy, J. Control. Release 194 (2014) 28–36.
[65] I. Skachkov, Y. Luan, A.F. van der Steen, d. JN, K. Kooiman, Targeted microbubble mediated sonoporation of endothelial cells in vivo, IEEE Trans. Ultrason. Ferroelectr. Freq. Control 61 (2014) 1661–1667.
[66] A.H. Ko, J. Hwang, A.P. Venook, J.L. Abbruzzese, E.K. Bergsland, M.A. Tempero, Serum CA19-9 response as a surrogate for clinical outcome in patients receiving fixed-dose rate gemcitabine for advanced pancreatic cancer, Br. J. Cancer 93 (2005) 195–199.
[67] A. Vincent, J. Herman, R. Schulick, R.H. Hruban, M. Goggins, Pancreatic cancer, Lancet 378 (2011) 607–620.
[68] N. Makrilia, K.N. Syrigos, M.W. Saif, Updates on treatment of gemcitabine-refractory pancreatic adenocarcinoma. Highlights from the "2011 ASCO annual meeting". Chicago, IL, USA; June 3-7, 2011, JOP 12 (2011) 351–354.
[69] P.F. Peddi, S. Lubner, R. McWilliams, B.R. Tan, J. Picus, S.M. Sorscher, R. Suresh, A.C. Lockhart, J. Wang, C. Menias, F. Gao, D. Linehan, A. Wang-Gillam, Multi-institutional experience with FOLFIRINOX in pancreatic adenocarcinoma, JOP 13 (2012) 497–501.
[70] A. Neesse, S. Krug, T.M. Gress, D.A. Tuveson, P. Michl, Emerging concepts in pancreatic cancer medicine: targeting the tumor stroma, Onco Targets Ther 7 (2013) 33–43.
[71] C. Bosetti, P. Bertuccio, M. Malvezzi, F. Levi, L. Chatenoud, E. Negri, V.C. La, Cancer mortality in Europe, 2005-2009, and an overview of trends since 1980, Ann. Oncol. 24 (2013) 2657–2671.
[72] A. Bouakaz, A. Zeghimi, A.A. Doinikov, Sonoporation: concept and mechanisms, Adv. Exp. Med. Biol. 880 (2016) 175–189.
[73] B. Helfield, X. Chen, S.C. Watkins, F.S. Villanueva, Biophysical insight into mechanisms of sonoporation, Proc. Natl. Acad. Sci. U. S. A. 113 (2016) 9983–9988.
[74] F. Yuan, M. Dellian, D. Fukumura, M. Leunig, D.A. Berk, V.P. Torchilin, R.K. Jain, Vascular permeability in a human tumor xenograft: molecular size dependence and cutoff size, Cancer Res. 55 (1995) 3752–3756.
[75] S. Kotopoulis, R. Haugsej, M. Mujic, A. Sulen, S.E. Gullaksen, E. McCormack, O.H. Gilja, M. Postema, B.T. Gjertsen, Evaluation of the effects of clinical diagnostic ultrasound in combination with ultrasound contrast agents on cell stress: Single cell analysis of intracellular phospho-signaling pathways in blood cancer cells and normal blood leukocytes. Ultrasonics Symposium (IUS), IEEE International (3–6 Sept. 2014).
[76] P. Reuter, J. Masomi, H. Kuntze, I. Fischer, K. Helling, C. Sommer, B. Alessandri, A. Heimann, T. Gerriets, J. Marx, O. Kempski, M. Nedelmann, Low-frequency therapeutic ultrasound with varied duty cycle: effects on the ischemic brain and the inner ear, Ultrasound Med. Biol. 36 (2010) 1188–1195.

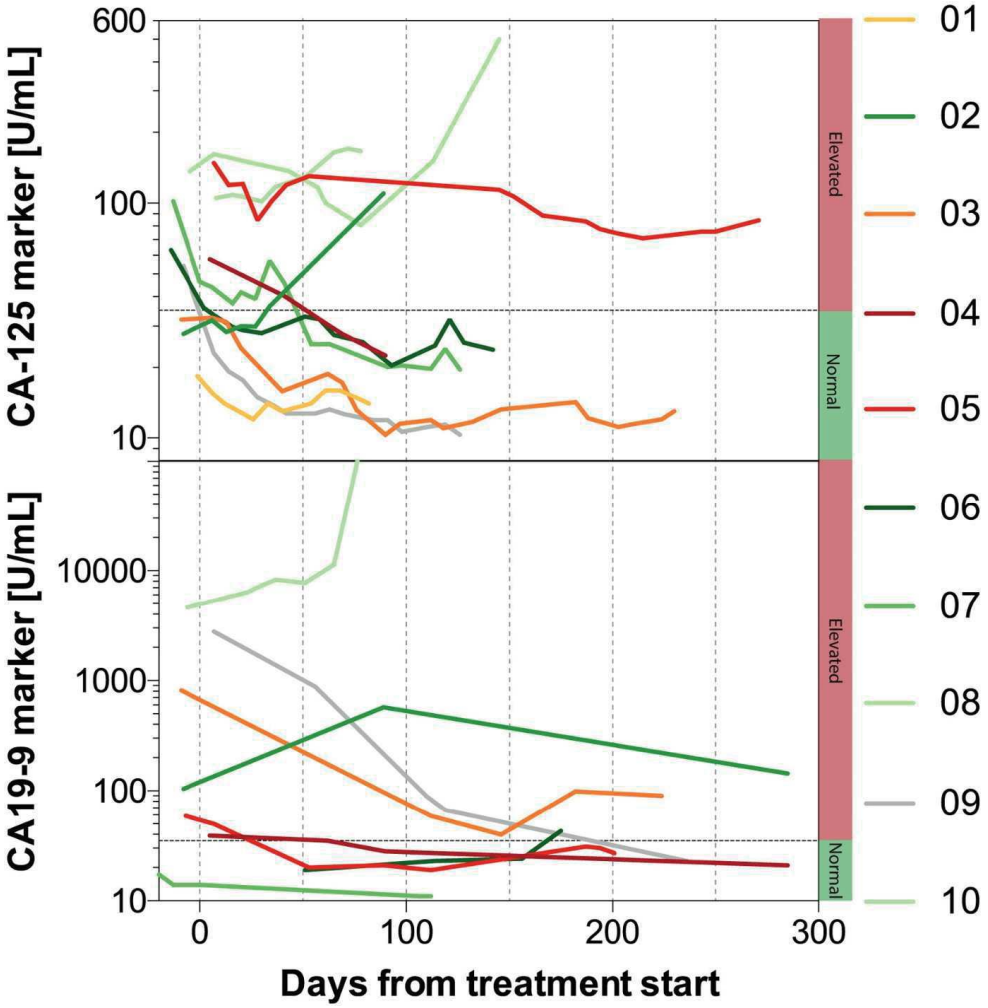

Supplemental Fig. 1. Cancer marker count as a function of treatment time. Green lines indicate patients with tumour size recession; red and grey lines indicate patients with increase in tumour size. A general decrease in tumour marker was observed for most patients. No correlation between tumour size and cancer maker change was observed.

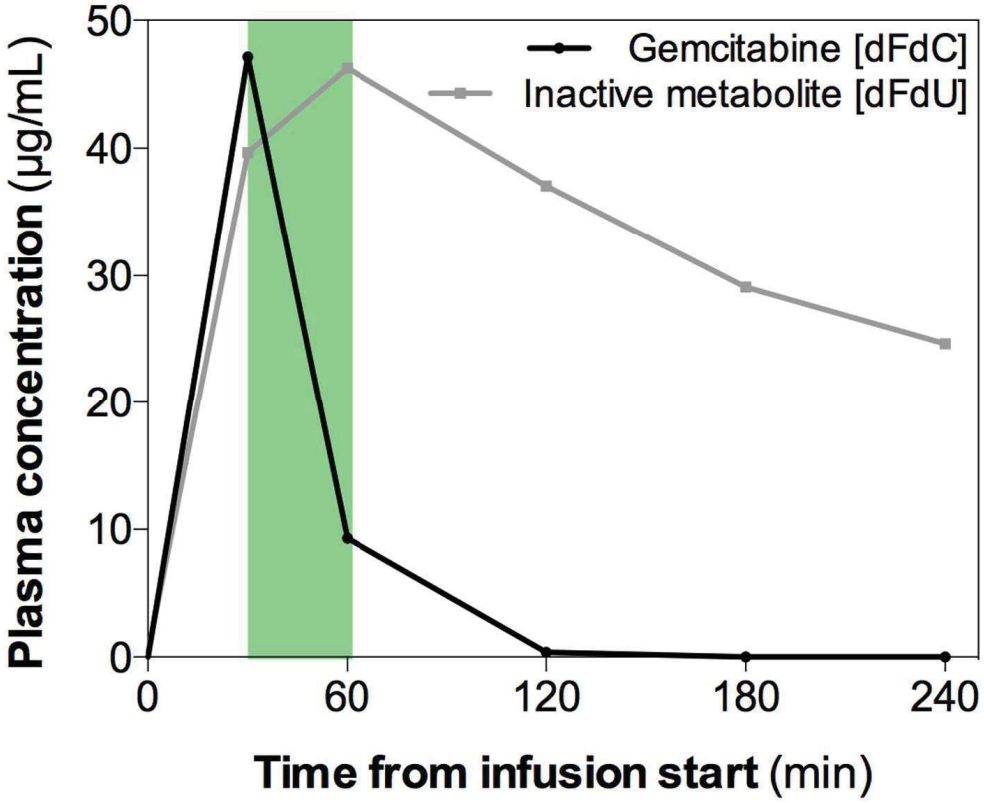

Supplemental Fig. 2. Representative concentration profile of gemcitabine (dFdC) and its inactive metabolite (dFdU) as a function of time in a patient treated with sonoporation. The green shaded area indicates the time of treatment with ultrasound and microbubbles. Plasma concentration of gemcitabine peaks at 30 min, where as its inactive metabolite peaks at 60 min, followed by a gradual decrease.

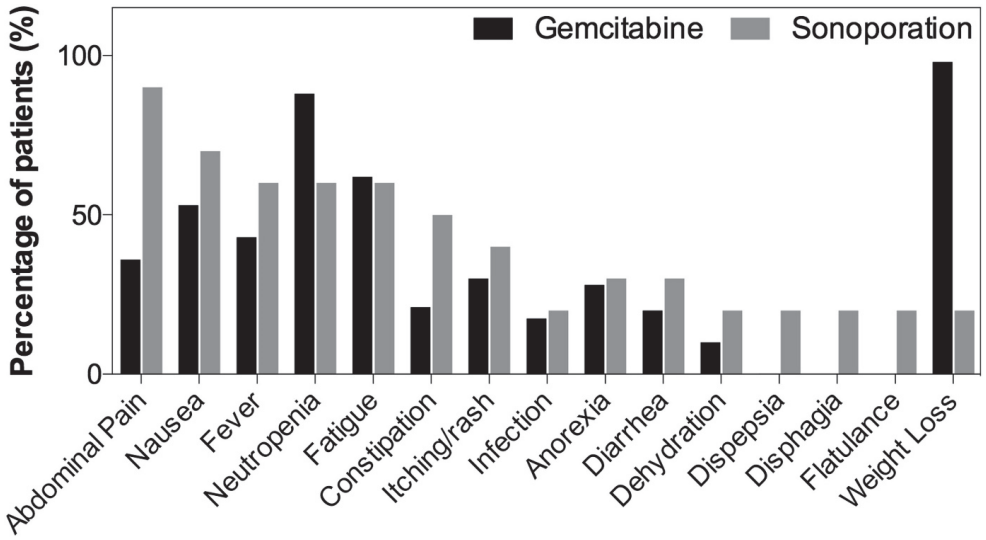

Supplemental Fig. 3. Percentage of patients experiencing adverse events with > 10% occurrence. A similar occurrence is observed when comparing our treated patients (sonoporation) to published data from gemcitabine treated patients (control group), except for abdominal pain and weight loss.

PAPER IV

Intracellular cytidine deaminase regulates gemcitabine metabolism in pancreatic cancer cell lines

Tormod K Bjånes[a,b], Lars Petter Jordheim[c], Jan Schjøtt[a,b], Tina Kamceva[a], Emeline Cros-Perrial[c], Anika Langer[b,d], Gorka Ruiz de Garibay[b,d], Spiros Kotopoulis[e,f,g], Emmet McCormack[b,d,*], Bettina Riedel[a,b,*]

Corresponding author: tormod.karlsen.bjanes@helse-bergen.no

[a]Section of Clinical Pharmacology, Department of Medical Biochemistry and Pharmacology, Haukeland University Hospital, Bergen, Norway
[b]Department of Clinical Science, Faculty of Medicine, University of Bergen, Bergen, Norway
[c]Univ Lyon, Université Claude Bernard Lyon 1, INSERM 1052, CNRS 5286, Centre Léon Bérard, Centre de Recherche en Cancérologie de Lyon, 69008 Lyon, France
[d]Centre for Cancer Biomarkers CCBIO, Department of Clinical Science, University of Bergen, Bergen, Norway
[e]Phoenix Solutions AS, Ullernchausseen 64, 0379 Oslo, Norway
[f]National Centre for Ultrasound in Gastroenterology, Haukeland University Hospital, Bergen, Norway
[g]Department of Clinical Medicine, University of Bergen, Bergen, Norway

*Joint senior authorship

Running title:

Cytidine deaminase and gemcitabine metabolism

Corresponding author:

Tormod Karlsen Bjånes

Haukeland University Hospital

Section of Clinical Pharmacology, Department of Medical Biochemistry and Pharmacology

Haukelandsveien 22

5021 Bergen

Norway

Email: tormod.karlsen.bjanes@helse-bergen.no

Number of:

- Pages: **29**
- Tables: **0**
- Figures: **3**
- Supplemental Tables: **2**
- Supplemental Figures: **3**
- References: **38**
- Words
    - Abstract: **231**
    - Introduction: **354**
    - Discussion: **1413**

(Keywords: cell models, drug toxicity, enzyme inhibitors, HPLC, mass spectrometry/MS, metabolomics, pharmacokinetics)

Abstract

Cytidine deaminase (CDA) is a determinant of *in vivo* gemcitabine elimination kinetics and cellular toxicity. The impact of CDA activity in pancreatic ductal adenocarcinoma (PDAC) cell lines has not been elucidated. We hypothesized that CDA regulates gemcitabine flux through its inactivation and activation pathways in PDAC cell lines.

Three PDAC cell lines (BxPC-3, MIA PaCa-2 and PANC-1) were incubated with 10 or 100 µM gemcitabine for 60 minutes or 24 hours, with or without tetrahydrouridine (THU), a CDA inhibitor. Extracellular inactive gemcitabine metabolite (dFdU) and intracellular active metabolite (dFdCTP) were quantified with liquid chromatography tandem mass spectrometry. Cellular expression of CDA was assessed with real-time PCR and Western blot.

Gemcitabine conversion to dFdU was extensive in BxPC-3 and low in MIA PaCa-2 and PANC-1, in accordance with their respective CDA expression levels. CDA inhibition was associated with low or undetectable dFdU in all three cell lines. After 24 hours gemcitabine incubation, dFdCTP was highest in MIA PaCa-2 and lowest in BxPC-3. CDA inhibition resulted in a profound dFdCTP increase in BxPC-3, but not in MIA PaCa-2 or PANC-1. dFdCTP concentrations were not higher after exposure to 100 vs. 10 µM gemcitabine when CDA-activities were low (MIA PaCa-2 and PANC-1) or inhibited (BxPC-3).

The results suggest a regulatory role of CDA for gemcitabine activation in PDAC cells, but within limits related to the capacity in the activation pathway in the cell lines.

Significance statement

The importance of cytidine deaminase (CDA) for cellular gemcitabine toxicity, linking a lower activity to higher toxicity, is well described. An underlying assumption is that CDA, by inactivating gemcitabine, limits the amount available for the intracellular activation pathway. Our study is the first to illustrate this regulatory role of CDA in pancreatic ductal adenocarcinoma cell lines by quantifying intracellular and extracellular gemcitabine metabolite concentrations.

Visual overview

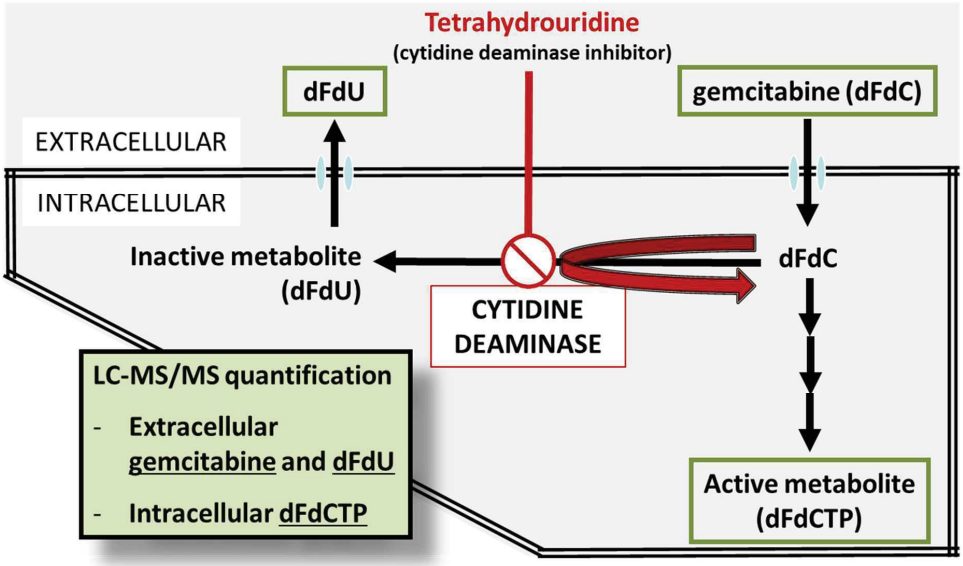

Introduction

Gemcitabine (2',2'-difluoro-2'-deoxycytidine, dFdC) is a nucleoside analogue used either alone or in combination with other cytostatic agents for treatment of inoperable pancreatic ductal adenocarcinoma (PDAC), and several other human cancers (Norwegian Medicines Agency, 2018). Following intracellular uptake, mainly by transmembrane equilibrative (hENT) and concentrative nucleoside transporter proteins (Wong et al., 2009), gemcitabine undergoes a stepwise phosphorylation process. Deoxycytidine kinase (dCK) catalyses the initial phosphorylation to gemcitabine monophosphate (dFdCMP), and is considered to be the rate limiting step in the activation pathway (Wong et al., 2009). The main active metabolite is gemcitabine triphosphate (dFdCTP), which inhibits DNA-replication. In tumor specimens from PDAC patients, high expression of hENT1 and dCK have been shown to favour the outcome of gemcitabine treatment (Marechal et al., 2012).

Cytidine deaminase (CDA) catalyses the inactivation of gemcitabine to 2',2'-difluoro-2'-deoxyuridine (dFdU) (Gusella et al., 2011; Simon et al., 2015; Cohen et al., 2018). CDA expression and activity in peripheral blood (Bowen et al., 2009) have been attributed both to lack of effect and increased toxicity of gemcitabine (Sugiyama et al., 2007; Ciccolini et al., 2010; Gusella et al., 2011). In PDAC tumor tissue, it has been found that CDA mRNA expression is higher compared to healthy tissues (Mameri et al., 2017). Bacteria and cells such as macrophages in the tumor microenvironment that express CDA might contribute to gemcitabine resistance (Vande Voorde et al., 2014; Weizman et al., 2014; Geller et al., 2017; Hessmann et al., 2018). However, the impact of intracellular CDA on gemcitabine metabolism in cancer cells is less studied (Morita et al., 2003; Vande Voorde et al., 2014).

Mameri and co-workers (Mameri et al., 2017) restored the expression of CDA in two *a priori* CDA-deficient cancer cell lines, and showed that survival of these cells was higher than that of their CDA-deficient counterparts following *in vitro* incubation with gemcitabine. Indeed, similar results have also been achieved by others, indicating a reciprocal relationship between intracellular CDA activity and cellular gemcitabine sensitivity (Morita et al., 2003;

Giovannetti et al., 2007; Yoshida et al., 2010; Peters et al., 2019). Thus, intracellular conversion of gemcitabine to dFdU is likely to be a mechanism contributing to gemcitabine resistance in this setting (Bardenheuer et al., 2005; Giovannetti et al., 2007; Ohmine et al., 2012; Vande Voorde et al., 2014; Mameri et al., 2017; Tibaldi et al., 2018).

In this study, we hypothesized that CDA plays a regulatory role in intracellular gemcitabine activation in PDAC cells. To test the hypothesis we assessed intracellular and extracellular concentrations of gemcitabine and metabolites after exposure to gemcitabine with and without the use of the CDA inhibitor tetrahydrouridine (THU). We also determined basal mRNA and protein expression profiles of CDA and other main proteins involved in the transport and metabolism of gemcitabine.

Materials and Methods

Chemicals, Reagents and Consumables

Unless otherwise stated, chemicals and reagents were purchased from Merck KGaA (Darmstadt, Germany) and were of analytical grade. Horse serum and sodium pyruvate were bought from Thermo Fisher Scientific (Oslo, Norway), culture flasks and cryotubes from VWR (Oslo, Norway), centrifuge tubes from Sarstedt (Oslo, Norway), and tetrahydrouridine (THU) from AH diagnostics (Oslo, Norway). All other reagents and equipment used for Liquid chromatography tandem mass spectrometry (LC-MS/MS) methods have been described previously (Bjanes et al., 2015; Kamceva et al., 2015).

Cell culture

Three human PDAC cell lines, BxPC-3, MIA PaCa-2 and PANC-1, generously provided by Prof. Anders Molven (University of Bergen), were cultured in 75 cm^2 flasks in a humidified atmosphere with 5 % CO_2 at 37 °C, and sub-cultured twice weekly. BxPC-3 cells were cultured in Roswell Park Memorial Institute 1640 medium (RPMI). MIA PaCa-2 and PANC-1 were cultured in Dulbecco's Modified Eagles Medium D5671 (DMEM). All media were supplemented with 10 % fetal bovine serum (FBS), 4 mM sodium pyruvate and 2 mM L-glutamine. The medium used for MIA PaCa-2 was additionally supplied with horse serum (2.5 %), as recommended by the manufacturer. No antibiotics were used. Mycoplasma tests performed on a regular basis were negative.

Gemcitabine incubation

Cell-free media (RPMI, DMEM, and DMEM with horse serum) were spiked with 10 or 100 µM gemcitabine. Resulting spiked medium samples were aliquoted and stored in 1.5 mL Eppendorf tubes at 4 °C, room temperature (RT) and 37 °C for up to seven days, and subsequently stored at -80°C until the entire batch was analysed concurrently. The concentration ratios of dFdU over the sum of gemcitabine and dFdU in each sample, dFdU/(gemcitabine+dFdU) (%), was used as an indicator of CDA activity.

PDAC cell lines (0.25 – 0.4 x 10^6 cells per well in 2 mL culture medium) were seeded in six-well plates 48 hours prior to gemcitabine incubation. Culture media was removed and replaced with freshly prepared drug-supplemented media at initiation of the experiments. The cells were incubated in quadruplicate for a) 24 hours with 10 or 100 µM gemcitabine, with or without 200 µM THU or b) 60 minutes with 10 or 100 µM gemcitabine with or without 200 µM THU. The two different durations of gemcitabine incubation were chosen based on a) that 24 hours is within a typical range applied in *in vitro* cytotoxicity experiments (Giovannetti et al., 2007; Yoshida et al., 2010; Mameri et al., 2017) and b) that 60 minutes *in vitro* incubation reflects a comparable exposure to *in vivo* gemcitabine treatment (Gusella et al., 2011). .

Following gemcitabine incubation, media was collected, transferred to cryotubes and stored at -80 °C until quantification of extracellular gemcitabine and dFdU. Wells were rinsed twice with PBS, and cells were subsequently trypsinized for five to eight minutes, harvested and gently re-suspended in cold culture medium. Manual cell counting was performed on a representative sample of the suspension. Cell suspensions were centrifuged for five minutes. Supernatant was discarded and the cell pellets were dissolved in cold 60 % methanol, transferred to cryotubes, vortexed for 20 seconds and snap frozen on liquid nitrogen. All samples were stored at -80 °C until quantification of intracellular dFdCTP.

Gemcitabine and -metabolite quantification

Quantification of gemcitabine and its metabolites was performed using an Agilent 1200 series HPLC-system (Agilent Technologies, Waldbronn, Germany) for chromatographic separation and an Agilent 6410 triple-quad mass spectrometer for mass detection. Gemcitabine and dFdU in culture media samples were quantified as described previously (Bjanes et al., 2015), optimized with lower limits of quantitation of 0.1 µM for both gemcitabine and dFdU. Gemcitabine triphosphate (dFdCTP) was analysed in cell lysates with a modified version of our previously published method (Kamceva et al., 2015). Modification consisted in shorter analysis time and with the mass spectrometer operating in positive ionization mode, since we were only interested in quantification of dFdCTP and not in the endogenous nucleosides that eluted later. dCTP was used as internal standard due to its similar structure and retention time with dFdCTP. Concentrations above the lower limit of quantitation of 0.05 µM were normalized to the cell count in each sample and expressed as *pmol per 10^6 cells* (abbreviated to *pmol/10^6* throughout the manuscript).

mRNA and protein expression

Extraction of mRNA was performed on cell pellets from each cell line, in quadruplicate, using the Qiagen column extraction kit. Two µg of mRNA was used for reverse transcription with M-MLV reverse transcriptase (InVitrogen). cDNA was diluted, and relative gene expression determined by PCR in a final volume of 6.67 µL with Takyon NoRox SYBR MasterMix blue dTTP (Eurogentec). Triplicate runs were performed on a Lightcycler (LC480, Roche Life Science). Relative quantification was performed by the ΔΔCT method using 28S mRNA expression as a housekeeping gene and mean CT values as reference. Primers used for each gene are given in Supplemental table 1A.

Total proteins were extracted using cold buffer (20 mM Tris-HCl pH 6.8, 1 mM $MgCl_2$, 2 mM EGTA, 0.5% NP40 and phosphatase inhibitor cocktails) with 60 minutes incubation on ice,

followed by centrifugation (15 minutes, 12 000 g, 4°C). Proteins were separated by SDS-PAGE and transferred onto PVDF membranes using the iBlot® system (Life Technologies). Membranes were incubated with specific antibodies, as shown in Supplemental table 1B. Protein expression was visualized using the Odyssey infrared system (LI-COR Biosciences). Protein bands were quantified using the Odyssey system, subtracting background noise from a similarly sized area just below the band, and presented as ratio of the expression of proteins of interest versus beta-actin expression.

Data processing and statistics

Quantitative data were analysed with SPSS Statistics 24.0 (IBM Inc., Armon, NY, USA) and GraphPad Prism 8 (San Diego, CA, USA) for Windows. Results were expressed as means ± standard deviations (SD) or as concentration ratios between analytes (%). A two-sided student's *t*-test was used to compare results in individual cell lines under different experimental conditions. One-way analysis of variance (ANOVA) with Bonferroni post hoc test was used to compare results in different cell lines. A *p*-value of less than 0.05 was considered significant.

Results

CDA activity in cell-free culture media

We investigated whether cell-free culture media had any CDA activity, which would be of importance in the subsequent interpretation of data from cell lines incubated with gemcitabine. We found CDA activity only in DMEM supplemented with horse serum, used for culturing MIA PaCa-2 cells. Within the maximum duration of our cell experiments (24 hours), the highest dFdU/(gemcitabine+dFdU) ratio at both gemcitabine concentrations was 6.3 % at 37 °C (Supplemental Figure 1). No CDA activity was found in either RPMI or DMEM media without horse serum.

Accumulation of inactive gemcitabine metabolite in culture media

To quantify inactivation of gemcitabine in PDAC cells, we measured extracellular dFdU concentrations after incubation with 10 and 100 µM gemcitabine for 60 minutes or 24 hours, with or without inhibition of CDA. After 24 hours incubation of BxPC-3, MIA PaCa-2 and PANC-1 with 100 µM gemcitabine, mean dFdU concentrations were 86.3, 23.5 and 7.3 µM, respectively (Figure 1A). After 60 minutes incubation with 100 µM gemcitabine, the corresponding dFdU concentrations were 17.7, 3.7 and 0.2 µM (Supplemental Figure 2A). The percentage conversion of gemcitabine to dFdU was similar when cells had been incubated with 10 µM gemcitabine, both after 60 minutes and 24 hours. After co-incubation with gemcitabine and THU, dFdU was low or undetectable in medium from all three cell lines both after 60 minutes and 24 hours.

Intracellular accumulation of active gemcitabine metabolite

After 24 hours incubation of BxPC-3, MIA PaCa-2 and PANC-1 with 10 µM gemcitabine, mean dFdCTP concentrations were 210, 1466 and 955 pmol/10^6, respectively (Figure 1B).

After 24 hours incubation with 100 µM gemcitabine, dFdCTP concentrations in BxPC-3 were significantly higher (851 pmol/10^6; $p<0.001$) than with 10 µM gemcitabine incubation. In MIA PaCa-2, dFdCTP concentrations were not significantly different between the two gemcitabine concentrations ($p = 0.12$), whereas in PANC-1 they were significantly lower at 100 µM gemcitabine (662 pmol/10^6; $p<0.05$). CDA-inhibition resulted in significantly higher dFdCTP concentrations in BxPC-3, with mean concentrations of 1370 ($p<0.01$) and 1368 pmol/10^6 ($p<0.05$) at 10 and 100 µM gemcitabine, respectively. In MIA PaCa-2 or PANC-1, dFdCTP concentrations were not significantly different with vs without CDA-inhibition.

After 60 minutes incubation with 10 µM gemcitabine, mean dFdCTP concentrations were 92, 80 and 110 pmol/10^6 in BxPC-3, MIA PaCa-2 and PANC-1, respectively. 60 minutes incubation with 100 µM gemcitabine did not result in significantly higher dFdCTP concentrations in any of the three cell line. Also, CDA-inhibition had no effect on dFdCTP concentrations at both gemcitabine concentrations under these experimental conditions (Supplemental Figure 2B).

Basal mRNA and protein expression

We assessed basal mRNA and protein expression of selected transporters and enzymes involved in gemcitabine uptake, metabolism and activity, in gemcitabine-untreated cell lines. Relative expression of mRNA and proteins are given in Figure 2A and Figure 2B, respectively. Original Western blots can be seen in Supplemental Figure 3. CDA showed highest mRNA and protein expression in BxPC-3. Lower CDA mRNA expression (Figure 2A) and zero protein expression (Figure 2B) was detected in both MIA PaCa-2 and PANC-1. The majority of the other transporters and enzymes revealed highest mRNA and protein expressions in PANC-1.

Discussion

Our overall finding was that intracellular cytidine deaminase plays a regulatory role for gemcitabine activation in PDAC cells, hence confirming our hypothesis.

Gemcitabine inactivation

Almost all gemcitabine added to the culture medium was converted to dFdU during 24 hours gemcitabine incubation of BxPC-3, highlighting the extensive CDA activity in this cell line. A comparable extent of gemcitabine conversion was reported by Bowen and co-workers (Bowen et al., 2009) in *ex vivo* whole blood from healthy volunteers; 50 % after five hours incubation and close to 100 % after 24 hours. In accordance with other publications (Funamizu et al., 2012a; Funamizu et al., 2012b), we also found that CDA displayed the highest mRNA (Figure 2A) and protein expression (Figure 2B) in BxPC-3, compared to MIA PaCa-2 and PANC-1.

Based on the pre-experimental stability assessments in cell-free culture media, all dFdU in BxPC-3 experiments was a result of cellular uptake, intracellular conversion and subsequent efflux into the culture medium. In MIA PaCa-2 and PANC-1, respectively, the extent of gemcitabine conversion to dFdU was 20–30% and <10 % of BxPC-3 (Figure 1A). This indicated that CDA-activities were lower in MIA PaCa-2 and PANC-1. Gemcitabine was also to some extent converted to dFdU in the medium used for culturing MIA PaCa-2 (Supplemental Figure 1). However, the conversion in cell-free medium only accounted for 20-30 % of the total amount found after 24 hours gemcitabine incubation of MIA PaCa-2 cells (Figure 1A). The finding of no detectable CDA protein expression (Figure 2B) in MIA PaCa-2 and PANC-1 did not fit with the appearance of dFdU following 24 hours gemcitabine incubation. These inconsistencies could preferably be explained by lack of sensitivity in the protein expression assay (Supplemental Figure 3), since both cell lines expressed CDA mRNA (Figure 2A). Moreover, it has been suggested that transcriptional, posttranscriptional

(Mameri et al., 2017) and posttranslational (Frese et al., 2012) modulations could blur the relationship between mRNA and protein expression and the observed CDA phenotype.

In all cell lines, a long-lasting and strong inhibition of gemcitabine inactivation was achieved with 200 µM THU even at the highest gemcitabine concentrations, and at both incubation durations. This is in line with previous studies in human blood performed by our own group (Bjanes et al., 2015) and other researchers (Bowen et al., 2009). dFdU could otherwise be assumed to be derived from the deamination of dFdCMP (Wong et al., 2009), but THU is not known to inhibit gemcitabine inactivating enzymes other than CDA (Heinemann and Plunkett, 1989). The fact that co-incubation of the cell lines with THU inhibited the formation of dFdU effectively underscores that direct gemcitabine deamination through CDA was the main source of dFdU in our experiments.

Gemcitabine activation

Without CDA-inhibition, BxPC-3 accumulated significantly less dFdCTP over 24 hours compared to the two other cell lines (Figure 1B). A probable explanation, in line with previous theories (Riva et al., 1992; Bardenheuer et al., 2005), was that the supply into the activation pathway was limited due to extensive conversion of gemcitabine to dFdU (Figure 1A). This notion was supported by the observation that dFdCTP concentrations in BxPC-3 were significantly higher when gemcitabine exposure was increased, either by increasing gemcitabine concentrations from 10 to 100 µM (Figure 1B, dashed line), or by inhibiting CDA (Figure 1B, solid line). No increase in dFdCTP concentrations was seen with increasing gemcitabine concentrations in MIA PaCa-2 or PANC-1, although baseline CDA-activities were low. The same was true in BxPC-3 when CDA was inhibited. These findings were consistent with saturation kinetics of dCK, as previously described by other authors (Grunewald et al., 1991; Wong et al., 2009).

Despite the distinct effects after 24 hours incubation in BxPC-3, CDA inhibition had no effect on dFdCTP concentrations in any of the three cell lines when incubated for 60 minutes (Supplemental Figure 2B). These findings could preferably be explained by sufficient concentrations of gemcitabine still available for the activation pathway in all three cell lines, but with dCK operating close to its saturation limit. This view is supported by the fact that the mean percentage gemcitabine remaining in the medium after 60 minutes vs. 24 hours incubation without THU, was 77 vs. <5% in BxPC-3, 92 vs. 66% in MIA PaCa-2 and >98 vs. 80% in PANC-1.

Overall perspective

Studies have highlighted the importance of CDA with respect to *in vivo* gemcitabine systemic pharmacokinetics (Sugiyama et al., 2007; Ciccolini et al., 2010; Gusella et al., 2011), and *in vitro* drug sensitivity (Yoshida et al., 2010; Funamizu et al., 2012b; Vande Voorde et al., 2014; Mameri et al., 2017), but the quantitative aspects of intracellular gemcitabine metabolism in PDAC cells has previously not been examined. We found that concentrations of both dFdU and dFdCTP after incubation with gemcitabine varied considerably between the PDAC cell lines, depending on CDA-activity. As all three cell lines in this study are frequently used in *in vitro* PDAC studies (Funamizu et al., 2010; Paproski et al., 2010; Funamizu et al., 2012a; Mariglia et al., 2018), the observed metabolic variability may be important to take into account when interpreting results from gemcitabine incubation experiments. Moreover, the quantitative contribution of intracellular CDA in gemcitabine metabolism provides a mechanistic explanation by which manipulating CDA-activity modifies cellular gemcitabine sensitivity, as demonstrated by Mameri and co-workers (Mameri et al., 2017) and Bardenheuer and co-workers (Bardenheuer et al., 2005).

By incubating the cell lines with gemcitabine with and without THU, we demonstrated that an extensive CDA-mediated gemcitabine conversion to dFdU in BxPC-3 was associated with less accumulation of the active metabolite dFdCTP. This was evident after 24 hours

incubation, but not after 60 minutes, indicating that a balanced substrate supply to dCK was an important factor for the accumulation of dFdCTP. In MIA PaCa-2 and PANC-1 no such effect of CDA-inhibition on the gemcitabine activation pathway was seen, which was consistent with their *a priori* low CDA activities. This supports the idea that CDA activity may be a predictor for gemcitabine toxicity by regulating intracellular gemcitabine metabolism (Bardenheuer et al., 2005; Tibaldi et al., 2018). The observation that MIA PaCa-2 cells produced both more dFdU and dFdCTP than PANC-1 cells following 24 hours gemcitabine incubation, could be explained by the higher expression of 5'-nucleotidases in PANC-1 (Figure 2B), in particular cN-IIIA. Indeed, this enzyme has been suggested to dephosphorylate dFdCMP and thus oppose the accumulation of dFdCTP (Li et al., 2008; Aksoy et al., 2009). To decipher the exact mechanisms of these differences and the involvement of each of the other proteins shown in Figure 2A-B, it would be necessary to develop additional tools (protein-deficient cells, specific inhibitors etc.) that are outside the scope of this work.

Direct quantification of gemcitabine and its metabolites (Figure 1A-B), combined with CDA-inhibition, provided insight into differential CDA-activities that could not be revealed by expression-analyses alone (Figure 2A-B). In a recent commentary by Peters and co-workers (Peters et al., 2019), phenotyping with cytidine or gemcitabine was also recommended over genotyping for pre-treatment assessment of *in vivo* CDA-activity in patients. Hodge and co-workers (Hodge et al., 2011a; Hodge et al., 2011b) also demonstrated the value of applying different drug concentrations and duration of incubations, combined with enzyme-inhibition, when studying cellular regulation of gemcitabine transport (Hodge et al., 2011b) and metabolic (Hodge et al., 2011a) pathways.

In our experiments, we measured the free dFdCTP concentrations, and did not have a measure of the total intracellular amount comprising both free and DNA-bound gemcitabine that might correlate better with cytotoxicity (Gandhi et al., 1991). The ratio between free and total dFdCTP is expected to change over time during and after gemcitabine incubation, and

cell lines might also behave differently based on intracellular enzyme expressions, illustrated by our own results in Figure 2A and Figure 2B. Based on *in silico* simulations, Battaglia and co-workers suggested that the rate of DNA-incorporation in general is a slow process compared to the production rate of dFdCTP (Battaglia and Parker, 2011). Hence, quantification of free dFdCTP could therefore be a better measure of cellular uptake and metabolism of gemcitabine following 60 minutes incubation, compared to 24 hours incubation. Incubation for 60 minutes with 10 – 100 µM gemcitabine *in vitro* might also more accurately represent the *in vivo* drug exposure during and after clinically applied 30-minutes gemcitabine infusions of 1000 mg/m^2, with a comparable concentration-time-product (AUC) of 41 ± 12 µM*h (Gusella et al., 2011). We calculated that 60 minutes or 24 hours *in vitro* incubation with 10 µM gemcitabine render AUCs of 10 or 240 µM*h, respectively.

In general, data from *in vitro* experiments should be interpreted with caution in terms of *in vivo* relevance. However, our findings that increased gemcitabine exposure does not necessarily lead to an increase in the intracellular active metabolite concentrations are in line with observations from *in vivo* studies, as illustrated by Hessmann and co-workers (Hessmann et al., 2018).

Conclusion

Our findings reveal quantitative aspects of gemcitabine intracellular metabolism in PDAC cell lines. The data support the notion that high CDA-activity limits intracellular dFdCTP accumulation. However, low CDA activity may not necessarily result in increased dFdCTP accumulation. Both CDA activity and the cellular ability to synthesize active metabolites should be taken into consideration in future studies of gemcitabine delivery to pancreatic cancer cells.

Acknowledgements

The authors would like to thank Elisa Thodesen Murvold and Philip Webber for valuable technical support, and Anders Molven for generously providing the PDAC cell lines.

Authorship contributions

Participated in research design: Bjånes, Jordheim, Schjøtt and Riedel

Conducted experiments: Bjånes, Kamceva and Cros-Perrial

Contributed new reagents or analytic tools: Bjånes, Jordheim, Schjøtt, McCormack

Performed data analysis: Bjånes, Jordheim, Schjøtt, Cros-Perrial, Langer, Garibay

Wrote or contributed to the writing of the manuscript: Bjånes, Jordheim, Schjøtt, Kamceva, Cros-Perrial, Langer, Garibay, Kotopoulis, McCormack, Riedel

References

Aksoy P, Zhu MJ, Kalari KR, Moon I, Pelleymounter LL, Eckloff BW, Wieben ED, Yee VC, Weinshilboum RM, and Wang L (2009) Cytosolic 5'-nucleotidase III (NT5C3): gene sequence variation and functional genomics. *Pharmacogenet Genomics* **19:**567-576.

Bardenheuer W, Lehmberg K, Rattmann I, Brueckner A, Schneider A, Sorg UR, Seeber S, Moritz T, and Flasshove M (2005) Resistance to cytarabine and gemcitabine and in vitro selection of transduced cells after retroviral expression of cytidine deaminase in human hematopoietic progenitor cells. *Leukemia* **19:**2281-2288.

Battaglia MA and Parker RS (2011) Pharmacokineticpharmacodynamic modelling of intracellular gemcitabine triphosphate accumulation: translating in vitro to in vivo. *IET Syst Biol* **5:**34.

Bjanes T, Kamceva T, Eide T, Riedel B, Schjott J, and Svardal A (2015) Preanalytical Stability of Gemcitabine and its Metabolite 2', 2'-Difluoro-2'-Deoxyuridine in Whole Blood-Assessed by Liquid Chromatography Tandem Mass Spectrometry. *J Pharm Sci* **104:**4427-4432.

Bowen C, Wang S, and Licea-Perez H (2009) Development of a sensitive and selective LC-MS/MS method for simultaneous determination of gemcitabine and 2,2-difluoro-2-deoxyuridine in human plasma. *J Chromatogr B Analyt Technol Biomed Life Sci* **877:**2123-2129.

Ciccolini J, Dahan L, Andre N, Evrard A, Duluc M, Blesius A, Yang C, Giacometti S, Brunet C, Raynal C, Ortiz A, Frances N, Iliadis A, Duffaud F, Seitz JF, and Mercier C (2010) Cytidine deaminase residual activity in serum is a predictive marker of early severe toxicities in adults after gemcitabine-based chemotherapies. *J Clin Oncol* **28:**160-165.

Cohen R, Preta LH, Joste V, Curis E, Huillard O, Jouinot A, Narjoz C, Thomas-Schoemann A, Bellesoeur A, Tiako Meyo M, Quilichini J, Desaulle D, Nicolis I, Cessot A, Vidal M, Goldwasser F, Alexandre J, and Blanchet B. Determinants of the interindividual

variability in serum cytidine deaminase activity of patients with solid tumours (2019). *Br J Clin Pharmacol* 85:1227-1238.

Frese KK, Neesse A, Cook N, Bapiro TE, Lolkema MP, Jodrell DI, and Tuveson DA (2012) nab-Paclitaxel potentiates gemcitabine activity by reducing cytidine deaminase levels in a mouse model of pancreatic cancer. *Cancer Discov* **2:**260-269.

Funamizu N, Kamata Y, Misawa T, Uwagawa T, Lacy CR, Yanaga K, and Manome Y (2012a) Hydroxyurea decreases gemcitabine resistance in pancreatic carcinoma cells with highly expressed ribonucleotide reductase. *Pancreas* **41:**107-113.

Funamizu N, Lacy CR, Fujita K, Furukawa K, Misawa T, Yanaga K, and Manome Y (2012b) Tetrahydrouridine inhibits cell proliferation through cell cycle regulation regardless of cytidine deaminase expression levels. *PloS one* **7:**e37424.

Funamizu N, Okamoto A, Kamata Y, Misawa T, Uwagawa T, Gocho T, Yanaga K, and Manome Y (2010) Is the resistance of gemcitabine for pancreatic cancer settled only by overexpression of deoxycytidine kinase? *Oncology reports* **23:**471-475.

Gandhi V, Huang P, Xu YZ, Heinemann V, and Plunkett W (1991) Metabolism and action of 2',2'-difluorodeoxycytidine: self-potentiation of cytotoxicity. *Adv Exp Med Biol* **309A:**125-130.

Geller LT, Barzily-Rokni M, Danino T, Jonas OH, Shental N, Nejman D, Gavert N, Zwang Y, Cooper ZA, Shee K, Thaiss CA, Reuben A, Livny J, Avraham R, Frederick DT, Ligorio M, Chatman K, Johnston SE, Mosher CM, Brandis A, Fuks G, Gurbatri C, Gopalakrishnan V, Kim M, Hurd MW, Katz M, Fleming J, Maitra A, Smith DA, Skalak M, Bu J, Michaud M, Trauger SA, Barshack I, Golan T, Sandbank J, Flaherty KT, Mandinova A, Garrett WS, Thayer SP, Ferrone CR, Huttenhower C, Bhatia SN, Gevers D, Wargo JA, Golub TR, and Straussman R (2017) Potential role of intratumor bacteria in mediating tumor resistance to the chemotherapeutic drug gemcitabine. *Science* **357:**1156-1160.

Giovannetti E, Mey V, Loni L, Nannizzi S, Barsanti G, Savarino G, Ricciardi S, Del Tacca M, and Danesi R (2007) Cytotoxic activity of gemcitabine and correlation with expression profile of drug-related genes in human lymphoid cells. *Pharmacol Res* **55:**343-349.

Grunewald R, Abbruzzese JL, Tarassoff P, and Plunkett W (1991) Saturation of 2',2'-difluorodeoxycytidine 5'-triphosphate accumulation by mononuclear cells during a phase I trial of gemcitabine. *Cancer Chemother Pharmacol* **27:**258-262.

Gusella M, Pasini F, Bolzonella C, Meneghetti S, Barile C, Bononi A, Toso S, Menon D, Crepaldi G, Modena Y, Stievano L, and Padrini R (2011) Equilibrative nucleoside transporter 1 genotype, cytidine deaminase activity and age predict gemcitabine plasma clearance in patients with solid tumours. *Br J Clin Pharmacol* **71:**437-444.

Heinemann V and Plunkett W (1989) Modulation of deoxynucleotide metabolism by the deoxycytidylate deaminase inhibitor 3,4,5,6-tetrahydrodeoxyuridine. *Biochem Pharmacol* **38:**4115-4121.

Hessmann E, Patzak MS, Klein L, Chen N, Kari V, Ramu I, Bapiro TE, Frese KK, Gopinathan A, Richards FM, Jodrell DI, Verbeke C, Li X, Heuchel R, Lohr JM, Johnsen SA, Gress TM, Ellenrieder V, and Neesse A (2018) Fibroblast drug scavenging increases intratumoural gemcitabine accumulation in murine pancreas cancer. *Gut* **67:**497-507.

Hodge LS, Taub ME, and Tracy TS (2011a) The deaminated metabolite of gemcitabine, 2',2'-difluorodeoxyuridine, modulates the rate of gemcitabine transport and intracellular phosphorylation via deoxycytidine kinase. *Drug Metab Dispos* **39:**2013-2016.

Hodge LS, Taub ME, and Tracy TS (2011b) Effect of its deaminated metabolite, 2',2'-difluorodeoxyuridine, on the transport and toxicity of gemcitabine in HeLa cells. *Biochem Pharmacol* **81:**950-956.

Kamceva T, Bjanes T, Svardal A, Riedel B, Schjott J, and Eide T (2015) Liquid chromatography/tandem mass spectrometry method for simultaneous quantification of eight endogenous nucleotides and the intracellular gemcitabine metabolite dFdCTP in human peripheral blood mononuclear cells. *J Chromatogr B Analyt Technol Biomed Life Sci* **1001:**212-220.

Li L, Fridley B, Kalari K, Jenkins G, Batzler A, Safgren S, Hildebrandt M, Ames M, Schaid D, and Wang L (2008) Gemcitabine and cytosine arabinoside cytotoxicity: association with lymphoblastoid cell expression. *Cancer Res* **68:**7050-7058.

Mameri H, Bieche I, Meseure D, Marangoni E, Buhagiar-Labarchede G, Nicolas A, Vacher S, Onclercq-Delic R, Rajapakse V, Varma S, Reinhold WC, Pommier Y, and Amor-Gueret M (2017) Cytidine Deaminase Deficiency Reveals New Therapeutic Opportunities against Cancer. *Clin Cancer Res* **23:**2116-2126.

Marechal R, Bachet JB, Mackey JR, Dalban C, Demetter P, Graham K, Couvelard A, Svrcek M, Bardier-Dupas A, Hammel P, Sauvanet A, Louvet C, Paye F, Rougier P, Penna C, Andre T, Dumontet C, Cass CE, Jordheim LP, Matera EL, Closset J, Salmon I, Deviere J, Emile JF, and Van Laethem JL (2012) Levels of gemcitabine transport and metabolism proteins predict survival times of patients treated with gemcitabine for pancreatic adenocarcinoma. *Gastroenterology* **143:**664-674 e661-666.

Mariglia J, Momin S, Coe IR, and Karshafian R (2018) Analysis of the cytotoxic effects of combined ultrasound, microbubble and nucleoside analog combinations on pancreatic cells in vitro. *Ultrasonics* **89:**110-117.

Morita T, Matsuzaki A, Kurokawa S, and Tokue A (2003) Forced expression of cytidine deaminase confers sensitivity to capecitabine. *Oncology* **65:**267-274.

Norwegian Medicines Agency (NOMA). Summary of product characteristics (SPC) Gemzar. Available from: https://www.legemiddelsok.no/. Last update November 15th 2018.

Ohmine K, Kawaguchi K, Ohtsuki S, Motoi F, Egawa S, Unno M, and Terasaki T (2012) Attenuation of phosphorylation by deoxycytidine kinase is key to acquired gemcitabine resistance in a pancreatic cancer cell line: targeted proteomic and metabolomic analyses in PK9 cells. *Pharm Res* **29:**2006-2016.

Paproski RJ, Young JD, and Cass CE (2010) Predicting gemcitabine transport and toxicity in human pancreatic cancer cell lines with the positron emission tomography tracer 3'-deoxy-3'-fluorothymidine. *Biochem Pharmacol* **79:**587-595.

Peters GJ, Giovannetti E, Honeywell RJ, and Ciccolini J (2019) Can cytidine deaminase be used as predictive biomarker for gemcitabine toxicity and response? *Br J Clin Pharmacol* **85:**1213-1214.

Riva C, Barra Y, Carcassonne Y, Cano JP, and Rustum Y (1992) Effect of tetrahydrouridine on metabolism and transport of 1-beta-D-arabinofuranosylcytosine in human cells. *Chemotherapy* **38:**358-366.

Simon N, Romano O, Michel P, Pincon C, Vasseur M, Lemahieu N, Barthelemy C, Hebbar M, Decaudin B, and Odou P (2015) Influence of infusion method on gemcitabine pharmacokinetics: a controlled randomized multicenter trial. *Cancer Chemother Pharmacol* **76:**865-871.

Sugiyama E, Kaniwa N, Kim SR, Kikura-Hanajiri R, Hasegawa R, Maekawa K, Saito Y, Ozawa S, Sawada J, Kamatani N, Furuse J, Ishii H, Yoshida T, Ueno H, Okusaka T, and Saijo N (2007) Pharmacokinetics of gemcitabine in Japanese cancer patients: the impact of a cytidine deaminase polymorphism. *J Clin Oncol* **25:**32-42.

Tibaldi C, Camerini A, Tiseo M, Mazzoni F, Barbieri F, Vittimberga I, Brighenti M, Boni L, Baldini E, Gilli A, Honeywell R, Chartoire M, Peters GJ, Giovannetti E, and Italian Oncological Group of Clinical R (2018) Cytidine deaminase enzymatic activity is a prognostic biomarker in gemcitabine/platinum-treated advanced non-small-cell lung cancer: a prospective validation study. *Br J Cancer* **119:**1326-1331.

Vande Voorde J, Sabuncuoglu S, Noppen S, Hofer A, Ranjbarian F, Fieuws S, Balzarini J, and Liekens S (2014) Nucleoside-catabolizing enzymes in mycoplasma-infected tumor cell cultures compromise the cytostatic activity of the anticancer drug gemcitabine. *The Journal of biological chemistry* **289:**13054-13065.

Weizman N, Krelin Y, Shabtay-Orbach A, Amit M, Binenbaum Y, Wong RJ, and Gil Z (2014) Macrophages mediate gemcitabine resistance of pancreatic adenocarcinoma by upregulating cytidine deaminase. *Oncogene* **33:**3812-3819.

Wong A, Soo RA, Yong WP, and Innocenti F (2009) Clinical pharmacology and pharmacogenetics of gemcitabine. *Drug Metab Rev* **41:**77-88.

Yoshida T, Endo Y, Obata T, Kosugi Y, Sakamoto K, and Sasaki T (2010) Influence of cytidine deaminase on antitumor activity of 2'-deoxycytidine analogs in vitro and in vivo. *Drug Metab Dispos* **38:**1814-1819.

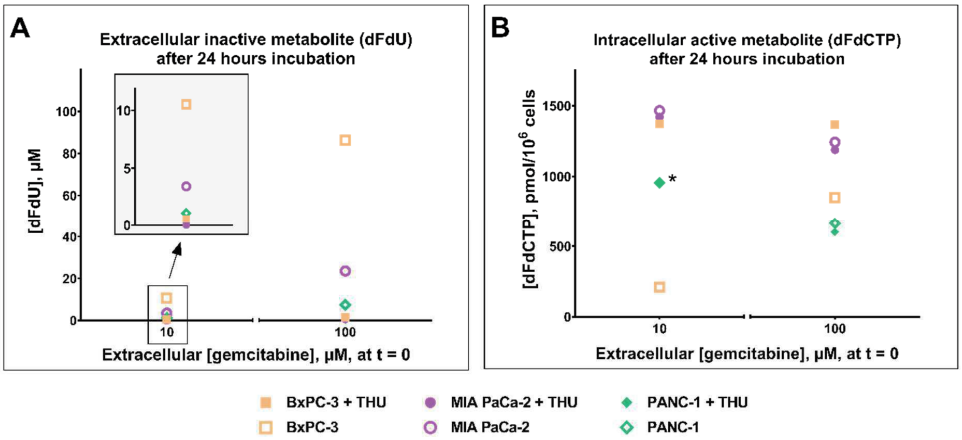

Figure 1. Concentrations of gemcitabine metabolites following 24 hours incubation with 10 or 100 µM gemcitabine ± 200 µM tetrahydrouridine (THU), a cytidine deaminase inhibitor. **A and B** show extracellular dFdU* (µM) and intracellular dFdCTP (pmol/10^6), respectively. **Insert** in Figure 1A: Data from 10 µM gemcitabine incubations in greater detail, with a differently scaled Y-axis. Data are displayed as means (n = 4 – 8). Error bars excluded from view for clarity. Original data (means and standard deviations) are shown in **Supplemental Table 2**. *dFdCTP concentrations in PANC-1 incubated with 10 µM gemcitabine with or without THU are overlapping, and therefore appear as a single symbol.

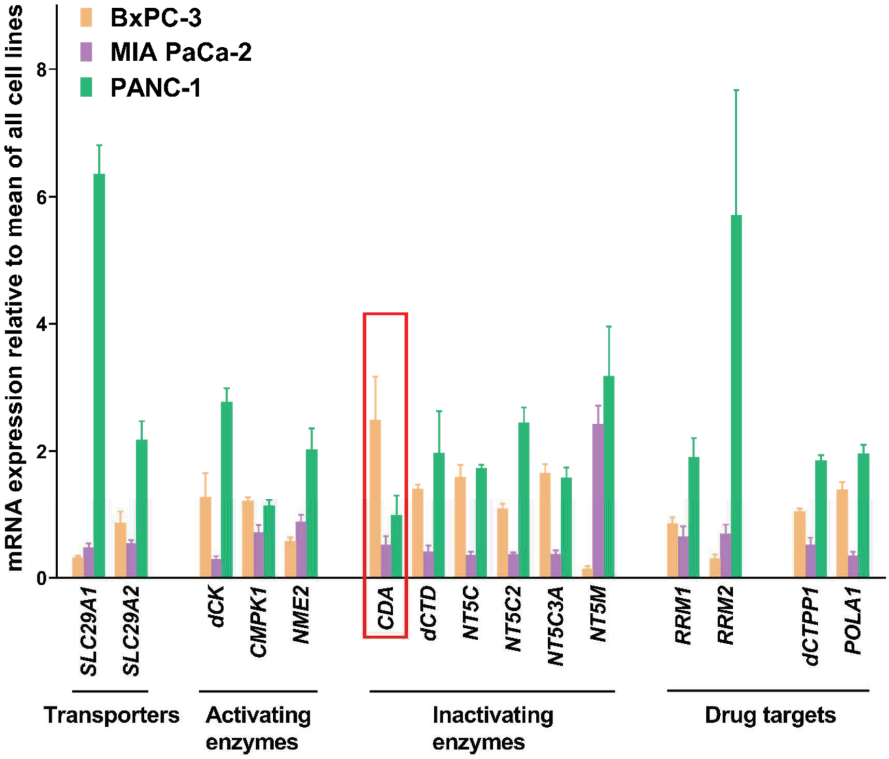

Figure 2A. Relative mRNA expression of selected proteins involved in the transport and metabolism of gemcitabine in BxPC-3, MIA PaCa-2 and PANC-1. Cytidine deaminase highlighted (red rectangle). Data are displayed as means of 4 independent samples studied in triplicate, and error bars are standard deviations.

SLC28A1*: Concentrative nucleoside transporter 1 (hCNT1); SLC29A1: Equlibrative nucleoside transporter 1 (hENT1); SLC29A2: Equlibrative nucleoside transporter 2 (hENT2); dCK: deoxycytidine kinase; CMPK1: uridine/cytosine monophosphate kinase; NME2: nucleoside diphosphate kinase (NdPK); CDA: Cytidine deaminase; dCTD: deoxycytidine monophosphate deaminase; NT5C: cytosolic 5'(3')-deoxyribonucleotidase (cdN); NT5C2: cytosolic 5'-nucleotidase II (cN-II); NT5C3: cytosolic 5'-nucleotidase III A (cN-IIIA); NT5M: mitochondrial 5'(3')-deoxyribonucleotidase (mdN); RRM1: Large subunit of ribonucleotide reductase; RRM2: Small subunit of ribonucleotide reductase; DCTPP1: deoxycytidine triphosphate pyrophosphatase 1; CTPS1*: cytidine triphosphate synthase 1; POLA1: deoxyribonucleic acid polymerase alpha

*mRNA expression of SLC28A1 not detectable.

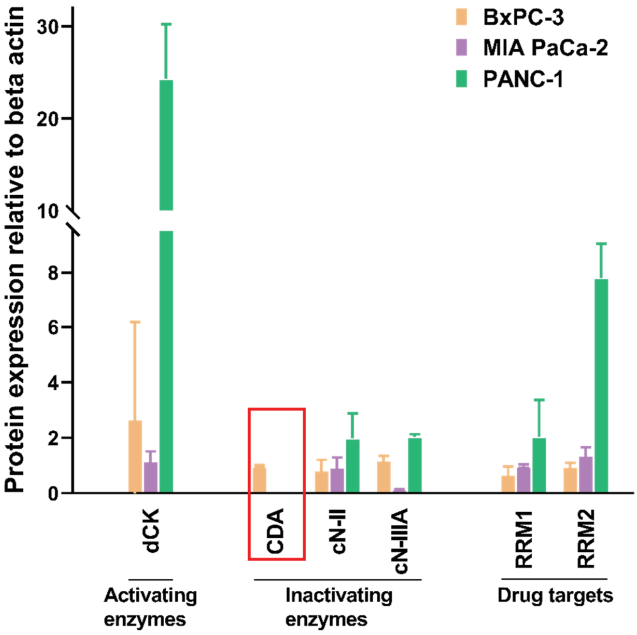

Figure 2B. Relative protein expression of selected proteins involved in the transport* and metabolism of gemcitabine in BxPC-3, MIA PaCa-2 and PANC-1. Cytidine deaminase highlighted (red rectangle). Data are displayed as means of 3 independent samples, and error bars are standard deviations. Raw data are available in Supplemental Figure 3.

dCK: deoxycytidine kinase; CDA: Cytidine deaminase; cN-II: cytosolic 5'-nucleotidase II (NT5C2); cN-IIIA: cytosolic 5'-nucleotidase III A (NT5C3); RRM1: Large subunit of ribonucleotide reductase; RRM2: Small subunit of ribonucleotide reductase

*Antibodies against transporter proteins (hCNT and hENT) not available

Supplemental table 1A. Primer sequences for RT-qPCR.

Gene	Forward primer (5'-3')	Reverse primer (5'-3')
RPS28	CGATCCATCATCCGCAATG	AGCCAAGCTCAGCGCAAC
SLC28A1	TCTGTGGATTTGCCAATTTCAG	CGGAGCACTATCTGGGAGAAGT
SLC29A1	GCTGGGTCTGACCGTCGTAT	CGTTACAGGGTGCATGATGG
SLC29A2	ATGAGAACGGGATTCCCAGTAG	GCTCTGATTCCGGCTCCTT
DCK	AAACCTGAACGATGGTCTTTTACC	CTTTGAGCTTGCCATTCAGAGA
CMPK1	GGGCATATTCTTTGCTTCCA	TGCATTTCAAGGTTCCACTG
NME2	ATGCAGTGCGGCCTGGTGGG	GACCCAGTCATGAGCACAAGAC
CDA	GAGCTGCAATCGTGTCTGG	CAGAGCAGCGGGAAACAG
DCTD	GTCGCCTTGTTCCCTTGTAA	TCTTGCTGCACTTCGGTATG
NT5C	GGACACGCAGGTCTTCATCTG	GCGGTACTTCTCACCCACACA
NT5C2	ACCTGCTGTATTACCCTTTCAGCTA	GCTCCACCGTTGATTCATGA
NT5C3A	AATCGGCGATGTACTAGAG	CATCTGCCATTCTTAAGTCTC
NT5M	CATCAGCATTTGGGAGTCAA	CGACACAATCTGCTCCAGAA
DCTPP1	AAATGGACATCAACCGGCGA	AGTCACAGGGAATGTCCGCA
CTPS1	GTGGCGAAATACACCGAGTT	TCCTCGAACACCAAATCCTC
POLA1	AGCTTGACCTGATTGCTGTC	ATGACGGGACAAAGACAAGG
RRM1	GCAGCTGAGAGAGGTGCTTT	CAGGATCCACACATCAGACA
RRM2	GAGTTCCTCACTGAGGCC	TTAGAAGTCAGCATCCAAG

RPS28; Ribosomal protein S 28; SLC28A1*: Concentrative nucleoside transporter 1 (hCNT1); SLC29A1: Equlibrative nucleoside transporter 1 (hENT1); SLC29A2: Equlibrative nucleoside transporter 2 (hENT2); dCK: deoxycytidine kinase; CMPK1: uridine/cytosine monophosphate kinase; NME2: nucleoside diphosphate kinase (NdPK); CDA: Cytidine deaminase; dCTD: deoxycytidine monophosphate deaminase; NT5C: cytosolic 5'(3')-deoxyribonucleotidase (cdN); NT5C2: cytosolic 5'-nucleotidase II (cN-II); NT5C3: cytosolic 5'-nucleotidase III A (cN-IIIA); NT5M: mitochondrial 5'(3')-deoxyribonucleotidase (mdN); RRM1: Large subunit of ribonucleotide reductase; RRM2: Small subunit of ribonucleotide reductase; DCTPP1: deoxycytidine triphosphate pyrophosphatase 1; CTPS1*: cytidine triphosphate synthase 1; POLA1: deoxyribonucleic acid polymerase alpha.

Supplemental table 1B. Antibodies used for Western blot.

Protein/target*	Clone / Reference	Dilution	Primary / Secondary	Host organism	Supplier
CDA	-/ab56053	1/500	Primary	Rabbit	Abcam
cN-II	3C1/H00022978-M02	1/500	Primary	Mouse	Abnova
cN-IIIA	-/ARP32185	1/1000	Primary	Rabbit	Aviva Systems Biology
dCK	-/ab96599	1/2000	Primary	Rabbit	Abcam
RRM1	-/sc11733	1/1000	Primary	Goat	Santa Cruz Biotechnology
RRM2	-/sc10846	1/1000	Primary	Goat	Santa Cruz Biotechnology
Beta-actin	AC-15/A5441	1/5000	Primary	Mouse	Sigma
Anti-murine	-/926-32210	1/5000	Secondary	Goat	LI-COR Bioscience
Anti-rabbit	-/926-68171	1/5000	Secondary	Goat	LI-COR Bioscience
Anti-goat	-/926-32214	1/5000	Secondary	Donkey	LI-COR Bioscience

CDA: Cytidine deaminase; cN-II: cytosolic 5'-nucleotidase II (NT5C2); cN-IIIA: cytosolic 5'-nucleotidase III A (NT5C3); dCK: deoxycytidine kinase; RRM1: Large subunit of ribonucleotide reductase; RRM2: Small subunit of ribonucleotide reductase

*Antibodies against transporter proteins (hCNT and hENT) not available

Supplemental table 2. Extracellular dFdU and intracellular dFdCTP concentrations following 24 hours gemcitabine (10 or 100 µM) incubation with or without 200 µM tetrahydrouridine. Data displayed in Figure 1A and 1B.

Cell line [Gemcitabine] ± 200 µM THU	Extracellular [dFdU], µM		Intracellular [dFdCTP], pmol/10^6	
	Mean	SD	Mean	SD
BxPC-3				
10 µM	10.5*	1.1	209.6	29.5
10 µM + THU	0.6*	0.05	1370.0	182.4
100 µM	86.3	4.1	850.5	127.1
100 µM + THU	1.5	0.02	1368.5	200.5
MIA PaCa-2				
10 µM	3.4*	0.8	1465.5	247.6
10 µM + THU	n.d.	n.d.	1420.4	95.7
100 µM	23.5*	7.1	1242.2*	197.0
100 µM + THU	0.8	0.2	1187.7*	203.6
PANC-1				
10 µM	1.1	0.0	954.7	224.7
10 µM + THU	0.2	0.0	950.9	66.8
100 µM	7.3	0.7	662.5	77.2
100 µM + THU	0.2	0.05	600.7	77.4

n = 4-8 per observation; * experiments with n=8

n.d.: not detectable

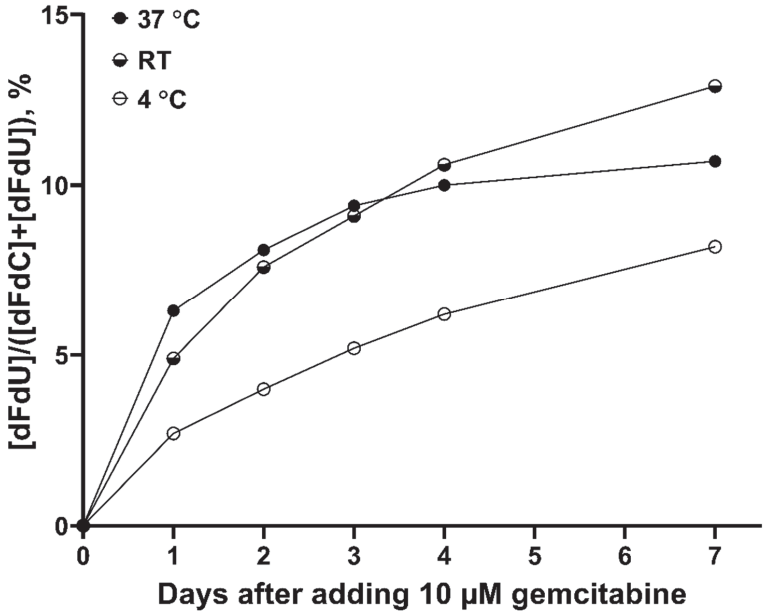

Supplemental Figure 1. Stability of 10 µM gemcitabine (dFdC) in Dulbecco's modified Eagles medium with horse serum at 4 °C, room temperature (RT) and 37 °C. dFdU concentrations relative to the sum of dFdC and dFdU concentrations ([dFdU]/([dFdC]+[dFdU]), %), was used as a measure of CDA-activity. No CDA activity was found in either of the two other culture media; RPMI and DMEM.

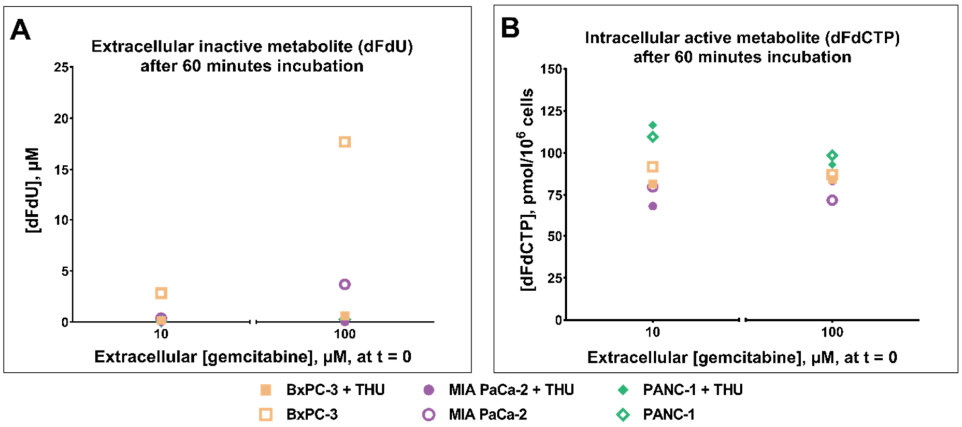

Supplemental Figure 2. Concentrations gemcitabine metabolites following 60 minutes incubation with 10 or 100 µM gemcitabine ± 200 µM tetrahydrouridine (THU), a cytidine deaminase inhibitor. **A and B** show extracellular dFdU* (µM) and intracellular dFdCTP (pmol/10^6), respectively. Data are displayed as means (n = 4 – 8). Error bars excluded from view for clarity.

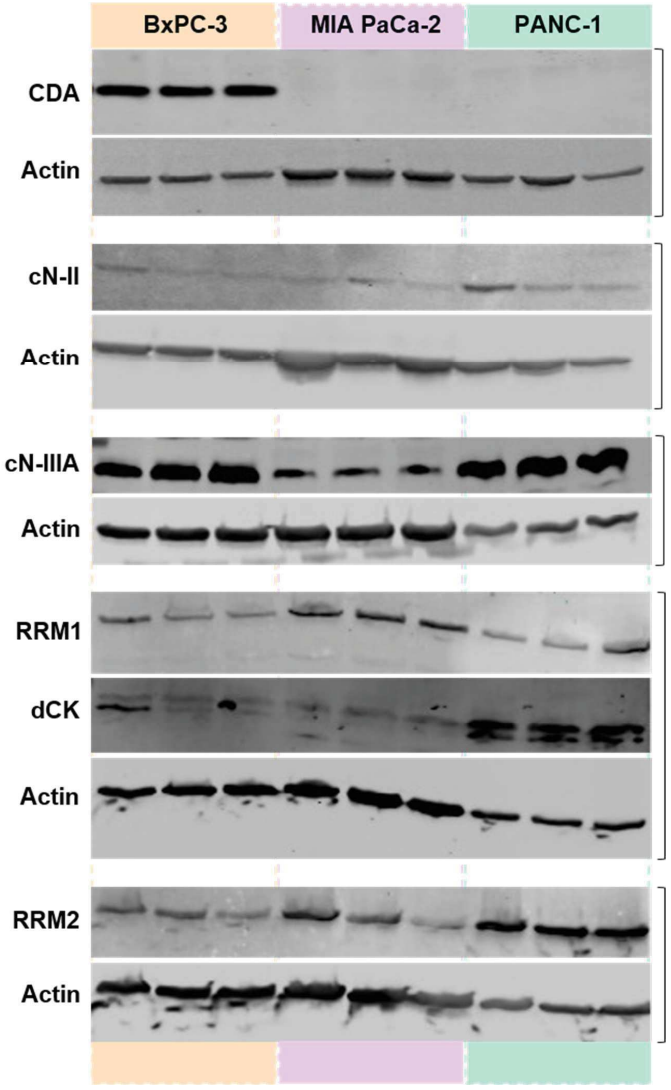

Supplemental Figure 3. Western blots of protein expression of selected proteins involved in the transport* and metabolism of gemcitabine in BxPC-3, MIA PaCa-2 and PANC-1. Brackets indicate the individual analytical runs, with each beta-actin control included.

CDA: Cytidine deaminase; cN-II: cytosolic 5'-nucleotidase II (NT5C2); cN-IIIA: cytosolic 5'-nucleotidase IIIA (NT5C3); dCK: deoxycytidine kinase; RRM1: Large subunit of ribonucleotide reductase; RRM2: Small subunit of ribonucleotide reductase

*Antibodies against transporter proteins (hCNT and hENT) not available

PAPER V

Ultrasound- and microbubble-assisted gemcitabine delivery to pancreatic cancer cells

Tormod Bjånes[a,b,*], Spiros Kotopoulis[c,d,e,*], Elisa Thodesen Murvold[f], Tina Kamceva[a], Bjørn Tore Gjertsen[b,g] , Odd Helge Gilja[d,e], Jan Schjøtt[a,b], Bettina Riedel[a,b,**] & Emmet McCormack[b,h,**]

[a]Department of Medical Biochemistry and Pharmacology, Haukeland University Hospital, Bergen, Norway
[b]Department of Clinical Science, Faculty of Medicine, University of Bergen, Bergen, Norway;
[c]Phoenix Solutions AS, Ullernchausseen 64, 0379 Oslo, Norway
[d]National Centre for Ultrasound in Gastroenterology, Haukeland University Hospital, Bergen, Norway
[e]Department of Clinical Medicine, University of Bergen, Bergen, Norway
[f]KinN Therapeutics AS, Bergen, Norway
[g]Department of Internal Medicine, Hematology Section, Haukeland University Hospital, Bergen, Norway
[h]Centre for Cancer Biomarkers CCBIO, Department of Clinical Science, University of Bergen, Bergen, Norway
[*] Joint first authorship
[**] Joint senior authorship

Corresponding author:
Tormod Karlsen Bjånes
E-mail: tormod.karlsen.bjanes@helse-bergen.no
Postal address: Haukeland University hospital, Department of Medical Biochemistry and Pharmacology, Postboks 1400, 5021 Bergen

Declarations of interest:
None

Keywords: gemcitabine, sonoporation, pancreatic cancer, PDAC, hENT, nucleoside transporters; in vitro

Highlights

- Treatment of pancreatic ductal adenocarcinoma (PDAC) is hampered by poor drug delivery

- We demonstrated that diagnostic intensity ultrasound and microbubbles (sonoporation) induced a moderate increase in gemcitabine uptake in PDAC cell lines

- Membrane transport proteins and gemcitabine metabolizing enzymes modified the effect of sonoporation on cellular drug uptake

Graphical abstract

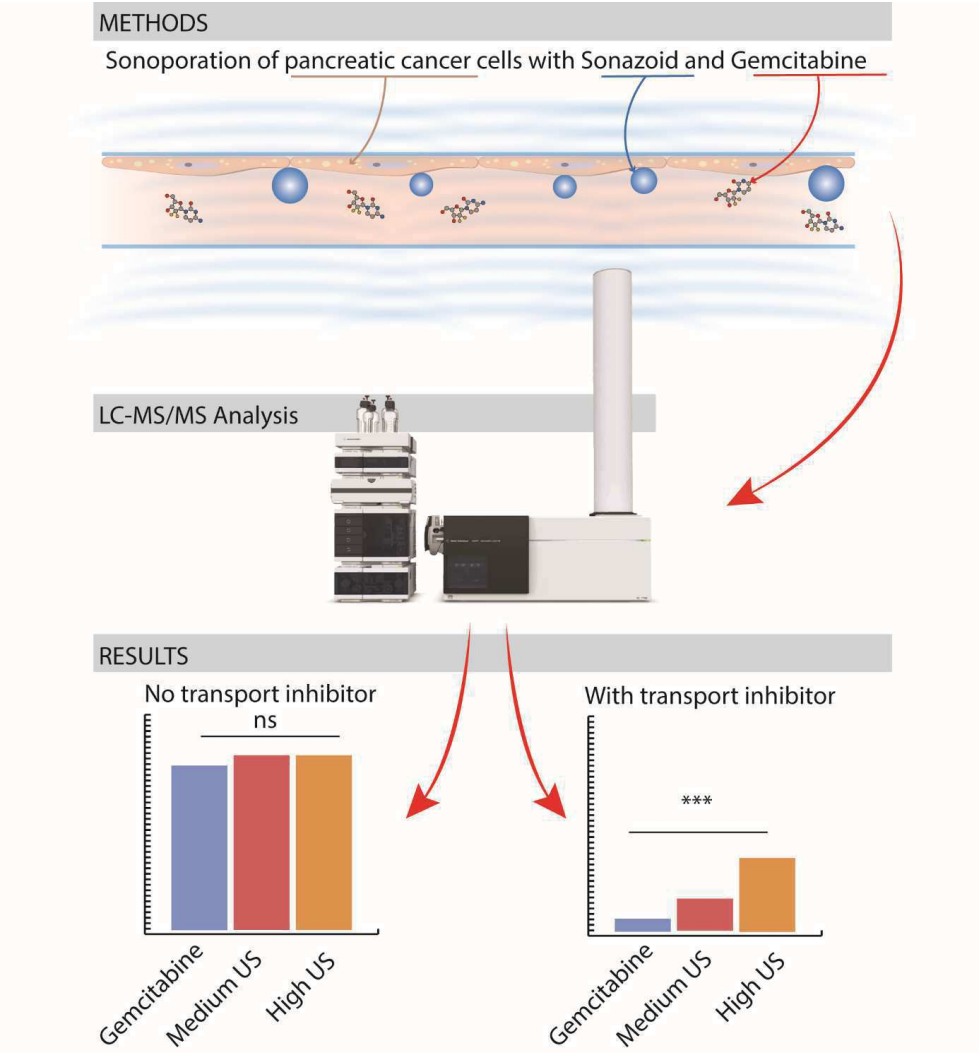

Abstract

Pancreatic ductal adenocarcinoma (PDAC) is a major cause of cancer deaths worldwide. Poor drug delivery to tumours is thought to limit chemotherapeutic treatment efficacy. Sonoporation combines ultrasound (US) and microbubbles to increase the permeability of cell membranes.

Methods: We assessed gemcitabine uptake combined with sonoporation *in vitro* in three PDAC cell lines (BxPC-3, MIA PaCa-2 and PANC-1). Cells were cultured in hypoxic bioreactors, and gemcitabine incubation and sonoporation was conducted in cells with operational and inhibited nucleoside membrane transporters. Intracellular active metabolite (dFdCTP), extracellular gemcitabine and inactive metabolite (dFdU) concentrations were measured with liquid chromatography tandem mass spectrometry.

Results & Discussion: Sonoporation with increasing US intensities resulted in decreasing extracellular gemcitabine concentrations in all three cell lines with inhibited membrane transporters. In cells with inhibited membrane transporters, without sonoporation, dFdCTP concentrations were reduced down to 10% of baseline. Sonoporation partially restored gemcitabine uptake in these cells, as indicated by a moderate increase in dFdCTP concentrations (up to 37% of baseline) in MIA PaCa-2 and PANC-1. In BxPC-3, gemcitabine was effectively inactivated to dFdU, which might represent a protective mechanism against dFdCTP accumulation in these cells. Intracellular dFdCTP concentrations did not change significantly following sonoporation in any of the cell lines with operational membrane transporters, indicating that the gemcitabine activation pathway may have been saturated with the drug.

Conclusion: Sonoporation allowed a moderate increase in gemcitabine transmembrane uptake in all three cell lines, but pre-existing nucleoside transporters were the major determinants of gemcitabine uptake and retention.

Introduction

Pancreatic ductal adenocarcinoma (PDAC) is one of the leading causes of cancer death worldwide [1, 2]. Late stage diagnosis precludes surgical excision in the majority of patients [3], and poor drug delivery into the tumour tissue may limit chemotherapeutic efficacy in patients with advanced disease [4-6].

Gemcitabine monotherapy is one of the three main chemotherapeutic drug regimens being used in the palliative setting of PDAC patients worldwide [7]. Following cellular uptake, primarily via the equilibrative nucleoside transporter 1 (hENT1), gemcitabine is either inactivated by cytidine deaminase (CDA) to 2',2'-difluoro-2'-deoxyuridine (dFdU) and effluxed, or phosphorylated through a series of nucleoside kinases to active metabolites. Deoxycytidine kinase (dCK), catalysing the initial phosphorylation of gemcitabine to gemcitabine monophosphate (dFdCMP), is a rate limiting step in the activation pathway [8]. The main active gemcitabine triphosphate (dFdCTP) metabolite exerts its activity by inhibiting DNA replication [8]. Expression of hENT1 [9, 10], CDA [11] and dCK [10] in tumour tissue have been associated with gemcitabine efficacy.

Paproski and co-workers showed that *in vitro* inhibition of hENT1 with dilazep reduced average gemcitabine uptake 24-fold and sensitivity 13-fold in both PDAC and non-PDAC cell lines. Restoration of nucleoside membrane transport by transfection with an active nucleoside influx pump re-established gemcitabine uptake and sensitivity [12]. This illustrated that hENT1 is of particular interest in studies of gemcitabine transport across cell membranes. Macrophages [13, 14], fibroblasts [2] and bacteria [15, 16] in the tumour microenvironment may also modulate gemcitabine efficacy. Moreover, limited drug delivery to PDAC tumours has been postulated to confer treatment failure [9].

The combination of microbubbles and ultrasound (US) may facilitate the formation of transient pores in biological membranes through a process commonly referred to as *sonoporation*, and thereby potentially allow increased tissue drug delivery and cellular uptake

[17]. In a phase 1 clinical trial, ten PDAC patients were treated with gemcitabine followed by repeated intravenous boluses of SonoVue® microbubbles and US focused at their primary tumours. The sonoporation treated patients experienced more tumour shrinkage, tolerated an increased number of treatment cycles, and survived longer than a historical control group treated with gemcitabine alone [18]. Similar results were achieved in a preclinical trial in mice with orthotopic PDAC xenografts [19]. It was postulated that the observed effects might partly be explained by increased gemcitabine delivery to PDAC tumour cells.

This hypothesis was not supported by Mariglia and co-workers [20], who found no increase in intracellular uptake and retention of a radiolabelled nucleoside analogue similar to gemcitabine, following *in vitro* sonoporation of a suspension of the PDAC cell line BxPC-3. The authors proposed that direct effects of sonoporation, rather than an increase of cellular gemcitabine delivery, could potentially explain an additive cytotoxicity which was observed at increasing US intensities, employing a frequency of 0.5 MHz and mechanical indices (MI) of 0.31 – 0.50 – 0.75, I_{SPPA} 1.61 – 4.32 – 9.36 W/cm^2 and I_{SPTA} 0.052 – 0.14 – 0.30 W/cm^2 [20].

Differences between cell lines regarding activities in hENT1 and enzymes involved in drug-metabolism, such as CDA, have not been taken into account in previous sonoporation studies of gemcitabine [18-20]. We therefore assessed *in vitro* uptake and metabolism of gemcitabine in three adherent PDAC cell lines, with and without inhibited hENTs and CDA, following incubation with therapeutically relevant drug concentrations, commercially available microbubbles and US intensities within a clinically translatable range. We hypothesized that the effect of sonoporation could depend on the activities of hENTs or gemcitabine metabolizing enzymes.

Materials and Methods

Chemicals and reagents

Chemicals and reagents were purchased from Merck KGaA (Darmstadt, Germany) unless otherwise stated, and were of analytical grade. Culture flasks and cryotubes were purchased from VWR (Oslo, Norway), centrifuge tubes from Sarstedt (Oslo, Norway) and Petaka® G3 LOT (Celartia, Columbus, OH, USA) hypoxic cell culture bioreactors (hereafter entitled "Petakas") from Tebu-Bio (Denmark). Horse serum and sodium pyruvate were obtained from Thermo Fisher Scientific (Oslo, Norway) and tetrahydrouridine (THU) from AH diagnostics (Oslo, Norway). Reagents and equipment used for liquid chromatography tandem mass spectrometric methods (LC-MS/MS) are described elsewhere [21, 22].

Cell culture

The PDAC cell lines, BxPC-3, MIA PaCa-2 and PANC-1, were kindly provided by Prof. Anders Molven (University of Bergen, Norway). BxPC-3 were cultured in Roswell Park Memorial Institute 1640 medium (RPMI) and MIA PaCa-2 and PANC-1 in Dulbecco's Modified Eagles Medium (DMEM) in a humidified atmosphere with 5 % CO_2 at 37 °C. Media were complemented with 4 mM sodium pyruvate, 2 mM L-glutamine and 10 % fetal bovine serum (FBS). Horse serum (2.5 %) was added to the medium used for MIA PaCa-2. No antibiotics were used. Mycoplasma-tests performed on a regular basis were negative.

Two or three days before experiments with gemcitabine, cells were harvested using 0.05 % trypsin-EDTA, counted and reseeded into Petakas (Figure 1A) at a density of 2.0 – 4.0 x 10^6 cells per 25 mL medium. Petakas were kept in a horizontal position for 24 hours to ensure even cell distribution over the surface, and then flipped to a vertical position with the air vent at the top, until the day of the experiments. At the day of experiments, the cell confluency was between 70 – 80 %. *A priori* evaluation of cell growth had been performed for each cell

line at four different seeding densities, and surface area coverage was quantified using MIPAR™ image analysis software [23] (Supplemental Figure 1).

Gemcitabine incubation and sonoporation

Three main series of sonoporation experiments were performed in all three cell lines: 1) 60 minutes incubation with 10 µM gemcitabine, 2) 20 minutes pre-incubation with 100 µM dilazep followed by 60 minutes incubation with 10 µM gemcitabine and 3) 60 minutes co-incubation with 10 µM gemcitabine and 200 µM tetrahydrouridine (THU), an inhibitor of cytidine deaminase (CDA).

In all experiments, we used one microbubble concentration and selected US intensities based on *a priori* optimization, using the cell-impermeable dye calcein as "model drug" (Supplemental Figure 2). Sonazoid® was prepared using the venting needle method. A total of 2 mL of saline (B.Braun AG, Melsungen, Germany) was slowly added to the vented vial and gently agitated for 30 seconds. Eighty µL Sonazoid® stock solution with 1.20 x 10^9 microbubbles per mL was added to 1 mL of the prepared gemcitabine solution, and injected into the Petakas. Air pockets were removed and the entire Petaka was exposed to US immediately thereafter. The Petakas (Figure 1A) were placed in the water bath of a custom-made US treatment system, with the cell monolayer on the upper surface to maximize cell-microbubble contact. The US treatment system (Figure 1B) was based on a previous design [24] and consisted of 128, 9×6 mm PZ26 elements firing upwards in groups of 16 elements at a time as a plane-wave into the Petaka. The US transducers were driven by a custom Open Ultrasound system (Lecoeur Electronique, Chuelles, France). The acoustic field had been calibrated in the fully assembled US chamber in three axes using a 200-µm needle hydrophone (Precision acoustics Ltd, Dorset, United Kingdom). The Petaka was placed at the acoustic focus. Ultrasound was applied for a total of 5 minutes at a frequency of 2.0 MHz. Two acoustic intensity levels were applied: ***Medium*** (MI 0.2, 80 cycles, duty cycle (DC) 1.8 %, I_{SPPA} 3 W/cm^2 and I_{SPTA} 50 mW/cm^2) and ***High*** (MI 0.378, 160 cycles, DC 3.6 %, I_{SPPA} 10

W/cm^2 and I_{SPTA} 358 mW/cm^2), in addition to ***Control*** (no US). After treatment, Petakas were returned to the incubator until completion of 60 minutes gemcitabine incubation time. Due to experimental time and resource constraints, a maximum of nine Petakas were used in each batch (see schematic timeline in Figure 1C).

At the end of experiments, 1 mL of medium was collected, transferred to cryotubes and kept at -80°C until quantification of extracellular gemcitabine and dFdU. The adherent cells were rinsed with phosphate buffered saline (PBS) and trypsinized for five to eight minutes and re-suspended in cold culture medium. Cells were counted and centrifuged at 1250 RPM for five minutes. Supernatants were discarded and cell pellets were either diluted and reseeded in 24-well plates for postexposure cell growth assays, or dissolved in cold 60 % methanol, transferred to cryovials, vortexed for 20 seconds, snap-frozen in liquid nitrogen and stored at -80 °C until quantification of intracellular dFdCTP.

Quantification of gemcitabine and its metabolites

Quantification of gemcitabine and its metabolites was performed using an Agilent 1200 series HPLC-system (Agilent Technologies, Waldbronn, Germany) for chromatographic separation and an Agilent 6410 triple-quad mass spectrometer for mass detection. Concentrations of gemcitabine and dFdU in culture media samples were measured according to our previously published method [21], with optimized lower limits of quantitation (LLOQ) of 0.1 µM for both analytes. Gemcitabine triphosphate (dFdCTP) was quantified in cell lysates with a slightly modified version of our previously published method [22]. Modification consisted of shorter analysis time and with the mass spectrometer operating in positive ionization mode, since we only quantified dFdCTP and not the endogenous nucleosides that eluted later. dCTP was used as internal standard due to its similar structure and retention time with dFdCTP. Concentrations above the LLOQ of 0.05 µM were normalized to the cell count in each sample and expressed as pmol per 10^6 cells (abbreviated to *pmol/10^6* throughout the manuscript).

Cell growth after incubation with gemcitabine ± sonoporation

Cell viability following exposure to 1) 60 min 10 µM gemcitabine alone, 2) sonoporation (High) alone, 3) 60 min 10 µM gemcitabine combined with sonoporation (High), and 4) Control (drug-free media, *i.e.* untreated cells), was assessed by monitoring cell growth for up to ten days. Each of the four experimental conditions was repeated once. BxPC-3 suspensions were diluted to 2500 cells/mL, MIA PaCa-2 and PANC-1 to 1000 cells/mL, and reseeded in triplicate into 24-well plates. Five daily snapshots from each well were captured using a Zeiss Vert.A1 microscope, Axiocam 105 colour camera and the Zeiss ZEN Pro 2012 blue edition software. Images (n=3600 in total) were analysed using MIPAR™ image analysis software [23]. Cell growth over time was expressed as percentage surface area coverage. Triplicate measurements from the repeated experiments (n=2) were combined into one graph for each cell line.

Statistical analyses

Quantitative data were processed using Microsoft Office Excel (2016) and GraphPad Prism 8 (San Diego, CA, USA). Variations of repeated measurements were expressed as mean±standard deviations (SD). Two-sided independent student's t-tests were used to compare means between measurements within each cell line. A one-tailed Pearson's correlation was used to describe linear relationships between US intensities and gemcitabine and – metabolite concentrations within each cell line. One-tailed was based on the assumption that increasing US intensities would have a one-directional effect on gemcitabine and - metabolite concentrations. Pearson's was based on the assumption that the measures of US intensities, MI and I_{SPTA}, represented continuous variables to be examined for a linear relationship to gemcitabine and - and metabolite concentrations. A p-value less than 0.05 was considered significant.

Results

Sonoporation and cellular gemcitabine uptake

Cell lines were incubated with gemcitabine and Sonazoid® microbubbles, and treated with US at medium and high intensities, and without US (control). Data from cells with operational membrane transporters are displayed in Figure 2A–I, with inhibited membrane transporters in Figure 2J–R, and from cells with inhibited cytidine deaminase in Figure 3.

Sonoporation of cells with operational membrane transporters

In BxPC-3, after 60 minutes incubation with 10 µM gemcitabine and with application of the highest US intensity, mean±SD extracellular gemcitabine concentrations were reduced from 9.0±0.4 µM (Control) to 8.2±0.4 µM (p=0.025) (Figure 2G). Extracellular dFdU (Figure 2D) and intracellular dFdCTP (Figure 2A) showed a trend towards higher concentrations, from 1.0±0.3 µM and 91.3±13.1 pmol/10^6 (Control) to 1.5±0.4 µM and 107.0±12.7 pmol/10^6 (High), respectively, but the observed changes were statistically not significant (p=0.07 and p=0.14 for dFdU and dFdCTP, respectively). A significant correlation was however observed between gemcitabine concentrations and MI (p=0.017, r^2=0.997), and dFdU concentrations and MI (p=0.035, r^2=0.988) in BxPC-3.

In addition, a significant correlation was observed between dFdCTP concentrations and MI (p=0.005, r^2=1.000) in MIA PaCa-2 (Figure 2B). In PANC-1, no correlations between concentrations of gemcitabine or -metabolites and US intensities were observed.

Inhibition of membrane transporters

Cells were incubated for 60 minutes with 10 µM gemcitabine, with or without 20 minutes pre-incubation with 100 µM dilazep [12]. Without US (Control), in BxPC-3, extracellular dFdU concentrations in BxPC-3 were reduced from 1.0 µM without dilazep (Figure 2D) to 0.1 µM with dilazep (Figure 2M). In MIA PaCa-2 and PANC-1, dFdU concentrations were already

low at baseline, and no further reductions could be quantified. In all three cell lines, intracellular dFdCTP concentrations were significantly reduced by dilazep: from 91.3 (Figure 2A) to 11.4 pmol/10^6 (Figure 2J) in BxPC-3, from 12.9 (Figure 2B) to 2.9 pmol/10^6 (Figure 2K) in MIA PaCa-2 and from 31.2 (Figure 2C) to 5.5 pmol/10^6 (Figure 2L) in PANC-1.

Sonoporation of cells with inhibited membrane transporters

Extracellular gemcitabine

In all three cell lines, following preincubation with dilazep, small but significant decreases in extracellular gemcitabine concentrations from approximately 9.5 µM without US to below 9.0 µM with increasing US intensity were noted (Figure 2P–R). Inverse correlations between gemcitabine concentrations and MI were observed for MIA PaCa-2 ($p=0.006$, $r^2=1.00$) (Figure 4Q) and PANC-1 ($p=0.006$, $r^2=1.00$) (Figure 4R).

Extracellular dFdU

In BxPC-3, extracellular dFdU concentrations increased from 0.1±0.04 (Control) to 0.2±0.03 µM at medium US intensity ($p=0.03$) and further to 0.4±0.09 µM at high intensity ($p=0.001$) (Figure 2M). This trend showed a correlation with the I_{SPTA} ($p=0.02$, $r^2=0.995$). No changes in dFdU concentrations were seen in MIA PaCa-2 (Figure 2N) or PANC-1 (Figure 2O).

Intracellular dFdCTP

Intracellular dFdCTP concentrations increased from 2.9±0.2 (Control) to 4.8±0.6 pmol/10^6 at high US intensity ($p=0.005$) in MIA PaCa-2 (Figure 2K) and from 5.5±2.6 to 11.7±2.4 pmol/10^6 ($p=0.036$) in PANC-1 (Figure 2L). In BxPC-3, an apparent small increase from 11.4±0.9 (Control) to 12.8±2.5 pmol/10^6 at high US intensity was statistically not significant ($p=0.367$) (Figure 2J). However, linear correlations between dFdCTP concentrations and MI were observed in BxPC-3 and MIA PaCa-2 ($p=0.0006$, $r^2=1.00$ and $p=0.0249$, $r^2=0.994$,

respectively), whereas in PANC-1 a correlation was seen between dFdCTP and I_{SPTA} ($p=0.0063$, $r^2=1.00$).

Sonoporation of cells with inhibited cytidine deaminase

Sixty minutes co-incubation with 10 µM gemcitabine and 200 µM THU resulted in dFdU concentrations <0.1 µM in all three cell lines (Figure 3D–F). Without US, no significant differences in extracellular gemcitabine (Figure 3G–I) or intracellular dFdCTP (Figure 3A–C) concentrations were seen with or without THU added. There was also no significant change in dFdCTP concentrations in any of the three cell lines co-incubated with gemcitabine and THU when US intensity was increased.

Cell growth after exposure to gemcitabine and/or sonoporation

Growth of the cell lines was followed for ten days after exposure to 10 µM gemcitabine, sonoporation (High), or both, and compared to untreated cells (Figure 4). In MIA PaCa-2 and PANC-1, no differences between treatment groups were seen. In BxPC-3, cells that had been incubated with gemcitabine, either alone or combined with sonoporation, showed a slower initial growth compared to untreated cells. When fitting the growth curves of BxPC-3 to a 4-point logistic curve, the groups treated with gemcitabine had significantly different points of inflection compared to untreated cells and those with sonoporation alone ($p<0.0001$), but the growth rate (Hill slope) was the same for all groups ($p=0.942$).

Discussion

To our knowledge, this is to date the most comprehensive *in vitro* study of gemcitabine cellular uptake combined with sonoporation, using diagnostic intensity US and microbubbles. Our data demonstrate that gemcitabine uptake and metabolite accumulation following sonoporation depend on the activities of membrane transporters and metabolizing enzymes within the cells.

Extracellular gemcitabine concentrations

In BxPC-3 with operational membrane transporters (Figure 2G), and in all three cell lines when membrane transporters had been inhibited prior to gemcitabine incubation (Figure 2P, Q and R), extracellular gemcitabine concentrations decreased with increasing US intensities. Decreasing gemcitabine concentrations indicated that sonoporation enhanced transmembrane gemcitabine transport, since cellular uptake was the only possible route of drug removal from the media in our experimental system.

Significance of membrane transporters

Our results indicated that sonoporation contributed only to a small proportion of cellular gemcitabine uptake compared to pre-existing nucleoside membrane transporters (hENT). When hENTs had been inhibited, dFdCTP concentrations were reduced to approximately 10–20 % (Figure 2J-L) of those in cells with operational membrane transporters (Figure 2A-C). This substantiated the idea of hENTs being the main determinants of gemcitabine uptake and ultimately of cellular accumulation of dFdCTP, which also is in accordance with previous studies [12, 25]. Sonoporation partially restored the supply of gemcitabine in transport-inhibited MIA PaCa-2 and PANC-1, reflected by increases in dFdCTP concentrations up to 4.8 and 11.7 pmol/10^6, respectively (Figure 2K and L). In both cell lines, these concentrations were 37.5 % of those achieved in cells with operational membrane transporters incubated

with gemcitabine, but without sonoporation (Figure 2B and C). In BxPC-3, however, where CDA is highly expressed [26], the increased gemcitabine uptake resulted in an increase in the inactive metabolite (dFdU) (Figure 2M) and no significant change in dFdCTP concentrations was noted (Figure 2J). Although there were no significant differences between the mean dFdCTP concentrations, the correlations may suggest that higher US intensities are warranted [27] in order to increase dFdCTP in cells with deficient membrane transporters.

Gemcitabine concentrations and enzyme saturation

When CDA was inhibited (Figure 3), conversion of gemcitabine to dFdU was abolished in all three cell lines. In BxPC-3, in which *a priori* CDA-activity was extensive, we had speculated whether the inhibition would allow more gemcitabine to be metabolized to dFdCTP. However, no increase in dFdCTP was noted, neither in BxPC-3, nor in the other cell lines. This might indicate that the activation pathway was already sufficiently supplied with gemcitabine, which is in line with dCK being a rate-limiting step in this pathway [28-30]. Indeed, the experiments with CDA inhibition were only performed in cells with operational membrane transporters which would allow continuous gemcitabine uptake from the medium, and therefore with limited additional effect of sonoporation. Whether a more pronounced effect of sonoporation could have been unmasked if cells were incubated with gemcitabine concentrations lower than 10 µM, further below a potential saturation of dCK [28-30], remains to be investigated.

Duration of incubation

Previous findings suggest that the sonoporation effect has a duration of up to and exceeding one hour [31-33], supports our choice of the drug incubation time of 60 minutes in our experiments. Also, shorter incubation times could have been relevant in order to detect more subtle changes in sonoporation-induced cellular gemcitabine uptake. It is likely that a major

proportion of gemcitabine transport across a permeabilized membrane would occur within seconds-to-minutes after initiation of drug incubation [34, 35]. Theoretically, if transport of gemcitabine through sonoporation-induced pores during this short time-scale were dominating, and hENT-mediated transport reached diffusion equilibrium later, early differences between cells with vs. without sonoporation would remain undetected. Drug-incubation and handling of Petakas was quite laborious and time consuming so that seconds-to-minutes experiments could not be performed. Also, since our final outcome measure was intracellular dFdCTP concentrations, a combined marker of cellular drug uptake and subsequent phosphorylation, 60 minutes gemcitabine incubation time was considered to be rational [35].

Cellular responses to sonoporation and gemcitabine

Growth curves over a 10-day period after exposure (Figure 4) indicated that BxPC-3 was more sensitive to gemcitabine than the other two cell lines. This agrees with the higher concentrations of dFdCTP in this cell line, compared to the other two cell lines (Figure 2A-C). Sonoporation, however, had no effect on cell growth over a 10-day period in any of the cell lines. We had shown in cells with operational membrane transporters, that sonoporation did not increase intracellular dFdCTP concentrations. This is in line with our observation that cell growth was not inhibited under these experimental conditions. However, cellular effects following a single 60-minutes treatment with gemcitabine and sonoporation with diagnostic intensity US might be more subtle than what can be observed with a growth assay. Mariglia and co-workers [20] used the MTT-assay 48 hours after sonoporation, and observed decreasing cell viability with increasing US intensities in suspended BxPC-3 cells. Definity® microbubbles used by Mariglia and co-workers are smaller and stiffer than the Sonazoid® microbubbles used in our study, but they also used higher MIs that are known to induce inertial cavitation. Furthermore, the Definity® microbubbles were driven at 0.5 MHz which is more than 20 times lower than their fundamental resonance frequency [36]. This suggests

that the microbubble behaviour may be significantly different between our study and the study by Mariglia and co-workers, making it difficult to directly compare them.

Implications, strengths and limitations

The majority of *in vitro* research on US and microbubble assisted drug delivery has been performed using fluorescence labelled dyes that have no routes of spontaneous cellular entry [27, 31, 37]. As such, they are ideal model drugs for mechanistic studies and for optimization of sonoporation settings. Methods for semiquantitative measurements of these compounds, such as flow cytometry, are readily available. However, cell impermeable compounds are unlikely to represent all relevant properties of therapeutically active drugs. Cellular drug uptake occurs via transmembrane transport proteins or via diffusion through the lipid bilayer, and might be counterbalanced by passive or active efflux [38-42]. As we have demonstrated, sonoporation-induced cellular uptake of gemcitabine was lower that the uptake mediated via nucleoside membrane transporters. This would not have been recognized by using cell impermeable model drugs alone. Their widespread application and the use of percentage "positive" cells in most studies, rather than quantitation of cellular drug concentrations, might even have contributed to exaggerated conclusions in terms of quantitative significance of sonoporation induced drug uptake.

Studying sonoporation and gemcitabine-uptake in PDAC cells cultured in hypoxic Petakas is of particular interest. It has been demonstrated that cellular responses to sonoporation depend on the condition of the cells [43, 44], which may be relevant for PDAC tumours when nutrient and oxygen supplies are limited [45]. Zhang and co-workers [46] showed that hypoxia induced perturbations in endogenous nucleotide pools, and they suggested that the efficacy and toxicity of nucleoside analogues such as gemcitabine would be modified accordingly. Moreover, US assisted drug delivery is not only a product of membrane pore formations; it has also been shown to interfere with the intracellular cytoskeleton [37], that

might theoretically regulate membrane transport proteins [47]. Most authors studying sonoporation, including Mariglia and co-workers [20], have reported results from cancer cell lines in suspension. In Petakas, the PDAC cells were treated while adherent. This may represent a more relevant condition compared to suspended cells in which the cytoskeleton might already have been rearranged prior to sonoporation [48].

Experiments were performed on plastic surfaces that do not mimic neither mechanical nor acoustic characteristics of tissue, which may increase acoustic aberration [49]. Furthermore, the static *in vitro* environment does not mimic the blood flow seen *in vivo*. A dynamic blood flow would drastically reduce the contact between bubbles and cells [50] and also affect how the cells grow [31]. The protein concentration in cell culture media are also low compared to blood, meaning the bubbles may have an increased stability as the proteins reduce the hydrophobicity of the lipids [51]. *In vivo*, the bubbles would not be directly in contact with the PDAC cells but initially with endothelial cells [50], hence the effect on the PDAC cells may be lower than *in vitro*. In addition, the pancreatic cancer microenvironment includes other cell types such as fibroblasts [2], macrophages [13, 14], and is typically displaying a desmoplastic reaction. Cells and surrounding tissue may be affected differently both by gemcitabine and sonoporation, and as a result the treatment outcome could theoretically also be influenced through effects on these cells/tissues.

Conclusions and future perspectives

Sonoporation with diagnostic intensity US and Sonazoid microbubbles allowed a moderate increase in gemcitabine transmembrane uptake in all three cell lines, but pre-existing nucleoside transporters were the major determinants of gemcitabine uptake and retention. Cell growth after a single 60 minutes treatment with sonoporation combined with gemcitabine was well preserved, which may reflect a general treatment resistance in these cell lines. Moreover, the data underscore that specific PDAC cell lines may respond differently to sonoporation due to different intracellular gemcitabine metabolism.

Future studies should include cells of multiple different origins, since a single response on a given cell line or drug may not represent a universally valid effect. Furthermore, sonoporation should be evaluated by using therapeutic drugs in more complex PDAC models that include multiple cell types and connective tissue components.

Authorship and contributions

Tormod Bjånes: Conceptualization, Data curation, Funding acquisition, Methodology; Writing – original draft, review&editing**: Spiros Kotopoulis**: Conceptualization, Data curation, Funding acquisition, Methodology, Software, Writing – original draft, review&editing; **Elisa Thodesen Murvold**: Methodology; **Tina Kamceva**: Methodology; **Bjørn Tore Gjertsen**: Conceptualization, Funding acquisition, Writing – review&editing; **Odd Helge Gilja**: Conceptualization, Funding acquisition, Writing – review&editing; **Jan Schjøtt**: Conceptualization, Funding acquisition, Supervision, Writing – review&editing; **Bettina Riedel**: Conceptualization, Funding aquisition, Project administration, Supervision, Writing – review&editing; **Emmet McCormack**: Conceptualization, Funding, Supervision, Writing – review&editing

Acknowledgements

This study was funded by the Western Health Board of Norway (Grant numbers 911779, 911182, 912035 and 912146), by the Norwegian Cancer Society (6833652, 182735) and by the Norwegian Research Council (SonoCURE grant no. 250317). This work was also supported in part by National Institutes of Health grant R01CA199646.
The authors would like to thank Lars Herfindal and Philip Webber for valuable advice and technical assistance in the project.

References

1. Bray, F., et al., *Global cancer statistics 2018: GLOBOCAN estimates of incidence and mortality worldwide for 36 cancers in 185 countries.* CA Cancer J Clin, 2018. **68**(6): p. 394-424.
2. Hessmann, E., et al., *Fibroblast drug scavenging increases intratumoural gemcitabine accumulation in murine pancreas cancer.* Gut, 2018. **67**(3): p. 497-507.
3. Malvezzi, M., et al., *European cancer mortality predictions for the year 2014.* Ann Oncol, 2014. **25**(8): p. 1650-6.
4. Uzunparmak, B. and I.H. Sahin, *Pancreatic cancer microenvironment: a current dilemma.* Clin Transl Med, 2019. **8**(1): p. 2.
5. Tod, J., et al., *Tumor-stromal interactions in pancreatic cancer.* Pancreatology, 2013. **13**(1): p. 1-7.
6. Koay, E.J., et al., *Transport properties of pancreatic cancer describe gemcitabine delivery and response.* J Clin Invest, 2014. **124**(4): p. 1525-36.
7. Health, T.N.D.o., *Nasjonalt handlingsprogram med retningslinjer for diagnostikk, behandling og oppfølging av pancreaskreft*. 2017.
8. Wong, A., et al., *Clinical pharmacology and pharmacogenetics of gemcitabine.* Drug Metab Rev, 2009. **41**(2): p. 77-88.
9. Farrell, J.J., et al., *Human equilibrative nucleoside transporter 1 levels predict response to gemcitabine in patients with pancreatic cancer.* Gastroenterology, 2009. **136**(1): p. 187-95.
10. Marechal, R., et al., *Levels of gemcitabine transport and metabolism proteins predict survival times of patients treated with gemcitabine for pancreatic adenocarcinoma.* Gastroenterology, 2012. **143**(3): p. 664-74 e1-6.
11. Serdjebi, C., G. Milano, and J. Ciccolini, *Role of cytidine deaminase in toxicity and efficacy of nucleosidic analogs.* Expert Opin Drug Metab Toxicol, 2015. **11**(5): p. 665-72.
12. Paproski, R.J., et al., *Human concentrative nucleoside transporter 3 transfection with ultrasound and microbubbles in nucleoside transport deficient HEK293 cells greatly increases gemcitabine uptake.* PLoS One, 2013. **8**(2): p. e56423.
13. Halbrook, C.J., et al., *Macrophage-Released Pyrimidines Inhibit Gemcitabine Therapy in Pancreatic Cancer.* Cell Metab, 2019. **29**(6): p. 1390-1399 e6.
14. Weizman, N., et al., *Macrophages mediate gemcitabine resistance of pancreatic adenocarcinoma by upregulating cytidine deaminase.* Oncogene, 2014. **33**(29): p. 3812-9.
15. Geller, L.T., et al., *Potential role of intratumor bacteria in mediating tumor resistance to the chemotherapeutic drug gemcitabine.* Science, 2017. **357**(6356): p. 1156-1160.
16. Vande Voorde, J., et al., *Nucleoside-catabolizing enzymes in mycoplasma-infected tumor cell cultures compromise the cytostatic activity of the anticancer drug gemcitabine.* J Biol Chem, 2014. **289**(19): p. 13054-65.
17. Postema, M. and O.H. Gilja, *Contrast-enhanced and targeted ultrasound.* World J Gastroenterol, 2011. **17**(1): p. 28-41.
18. Dimcevski, G., et al., *A human clinical trial using ultrasound and microbubbles to enhance gemcitabine treatment of inoperable pancreatic cancer.* J Control Release, 2016. **243**: p. 172-181.
19. Kotopoulis, S., et al., *Sonoporation-enhanced chemotherapy significantly reduces primary tumour burden in an orthotopic pancreatic cancer xenograft.* Mol Imaging Biol, 2014. **16**(1): p. 53-62.
20. Mariglia, J., et al., *Analysis of the cytotoxic effects of combined ultrasound, microbubble and nucleoside analog combinations on pancreatic cells in vitro.* Ultrasonics, 2018. **89**: p. 110-117.
21. Bjanes, T., et al., *Preanalytical Stability of Gemcitabine and its Metabolite 2', 2'-Difluoro-2'-Deoxyuridine in Whole Blood-Assessed by Liquid Chromatography Tandem Mass Spectrometry.* J Pharm Sci, 2015. **104**(12): p. 4427-32.

22. Kamceva, T., et al., *Liquid chromatography/tandem mass spectrometry method for simultaneous quantification of eight endogenous nucleotides and the intracellular gemcitabine metabolite dFdCTP in human peripheral blood mononuclear cells.* J Chromatogr B Analyt Technol Biomed Life Sci, 2015. **1001**: p. 212-20.
23. Sosa, J.M., et al., *Development and application of MIPAR™: a novel software package for two- and three-dimensional microstructural characterization.* Integrating Materials and Manufacturing Innovation, 2014. **3**(1): p. 123-140.
24. Yddal, T., et al., *Open-source, high-throughput ultrasound treatment chamber.* Biomed Tech (Berl), 2015. **60**(1): p. 77-87.
25. Hodge, L.S., M.E. Taub, and T.S. Tracy, *Effect of its deaminated metabolite, 2',2'-difluorodeoxyuridine, on the transport and toxicity of gemcitabine in HeLa cells.* Biochem Pharmacol, 2011. **81**(7): p. 950-6.
26. Funamizu, N., et al., *Hydroxyurea decreases gemcitabine resistance in pancreatic carcinoma cells with highly expressed ribonucleotide reductase.* Pancreas, 2012. **41**(1): p. 107-13.
27. De Cock, I., et al., *Ultrasound and microbubble mediated drug delivery: acoustic pressure as determinant for uptake via membrane pores or endocytosis.* J Control Release, 2015. **197**: p. 20-8.
28. Grunewald, R., et al., *Saturation of 2',2'-difluorodeoxycytidine 5'-triphosphate accumulation by mononuclear cells during a phase I trial of gemcitabine.* Cancer Chemother Pharmacol, 1991. **27**(4): p. 258-62.
29. Grunewald, R., et al., *Pharmacologically directed design of the dose rate and schedule of 2',2'-difluorodeoxycytidine (Gemcitabine) administration in leukemia.* Cancer Res, 1990. **50**(21): p. 6823-6.
30. Tham, L.S., et al., *Does saturable formation of gemcitabine triphosphate occur in patients?* Cancer Chemother Pharmacol, 2008. **63**(1): p. 55-64.
31. Bhutto, D.F., et al., *Effect of Molecular Weight on Sonoporation-Mediated Uptake in Human Cells.* Ultrasound Med Biol, 2018. **44**(12): p. 2662-2672.
32. Helfield, B., et al., *Biophysical insight into mechanisms of sonoporation.* Proc Natl Acad Sci U S A, 2016. **113**(36): p. 9983-8.
33. Haugse, R., et al., *Intracellular Signaling in Key Pathways Is Induced by Treatment with Ultrasound and Microbubbles in a Leukemia Cell Line, but Not in Healthy Peripheral Blood Mononuclear Cells.* Pharmaceutics, 2019. **11**(7).
34. Machrafi, H., *Nanomedicine by extended non-equilibrium thermodynamics: cell membrane diffusion and scaffold medication release.* Math Biosci Eng, 2019. **16**(4): p. 1949-1965.
35. Paproski, R.J., J.D. Young, and C.E. Cass, *Predicting gemcitabine transport and toxicity in human pancreatic cancer cell lines with the positron emission tomography tracer 3'-deoxy-3'-fluorothymidine.* Biochem Pharmacol, 2010. **79**(4): p. 587-95.
36. Shekhar, H., et al., *Effect of Temperature on the Size Distribution, Shell Properties, and Stability of Definity((R)).* Ultrasound Med Biol, 2018. **44**(2): p. 434-446.
37. Wang, M., et al., *Sonoporation-induced cell membrane permeabilization and cytoskeleton disassembly at varied acoustic and microbubble-cell parameters.* Sci Rep, 2018. **8**(1): p. 3885.
38. Paskeviciute, M. and V. Petrikaite, *Overcoming transporter-mediated multidrug resistance in cancer: failures and achievements of the last decades.* Drug Deliv Transl Res, 2019. **9**(1): p. 379-393.
39. Lammertink, B.H., et al., *Sonochemotherapy: from bench to bedside.* Front Pharmacol, 2015. **6**: p. 138.
40. Lee, S.C., et al., *Evaluation of transporters in drug development: Current status and contemporary issues.* Adv Drug Deliv Rev, 2017. **116**: p. 100-118.
41. Dobson, P.D. and D.B. Kell, *Carrier-mediated cellular uptake of pharmaceutical drugs: an exception or the rule?* Nature Reviews Drug Discovery, 2008. **7**: p. 205.
42. Dobson, P.D., et al., *Implications of the dominant role of transporters in drug uptake by cells.* Curr Top Med Chem, 2009. **9**(2): p. 163-81.

43. Fan, P., et al., *Cell-cycle-specific Cellular Responses to Sonoporation.* Theranostics, 2017. **7**(19): p. 4894-4908.
44. Pichardo, S., et al., *Influence of cell line and cell cycle phase on sonoporation transfection efficiency in cervical carcinoma cells under the same physical conditions.* IEEE Trans Ultrason Ferroelectr Freq Control, 2013. **60**(2): p. 432-5.
45. Cannon, A., et al., *Desmoplasia in pancreatic ductal adenocarcinoma: insight into pathological function and therapeutic potential.* Genes Cancer, 2018. **9**(3-4): p. 78-86.
46. Zhang, W., et al., *Analysis of deoxyribonucleotide pools in human cancer cell lines using a liquid chromatography coupled with tandem mass spectrometry technique.* Biochem Pharmacol, 2011. **82**(4): p. 411-7.
47. Mazzochi, C., D.J. Benos, and P.R. Smith, *Interaction of epithelial ion channels with the actin-based cytoskeleton.* Am J Physiol Renal Physiol, 2006. **291**(6): p. F1113-22.
48. Walther, C.G., R. Whitfield, and D.C. James, *Importance of Interaction between Integrin and Actin Cytoskeleton in Suspension Adaptation of CHO cells.* Appl Biochem Biotechnol, 2016. **178**(7): p. 1286-302.
49. Kinoshita, M. and K. Hynynen, *Key factors that affect sonoporation efficiency in in vitro settings: the importance of standing wave in sonoporation.* Biochem Biophys Res Commun, 2007. **359**(4): p. 860-5.
50. Mullick Chowdhury, S., T. Lee, and J.K. Willmann, *Ultrasound-guided drug delivery in cancer.* Ultrasonography, 2017. **36**(3): p. 171-184.
51. Jensen, M.O. and O.G. Mouritsen, *Lipids do influence protein function-the hydrophobic matching hypothesis revisited.* Biochim Biophys Acta, 2004. **1666**(1-2): p. 205-26.

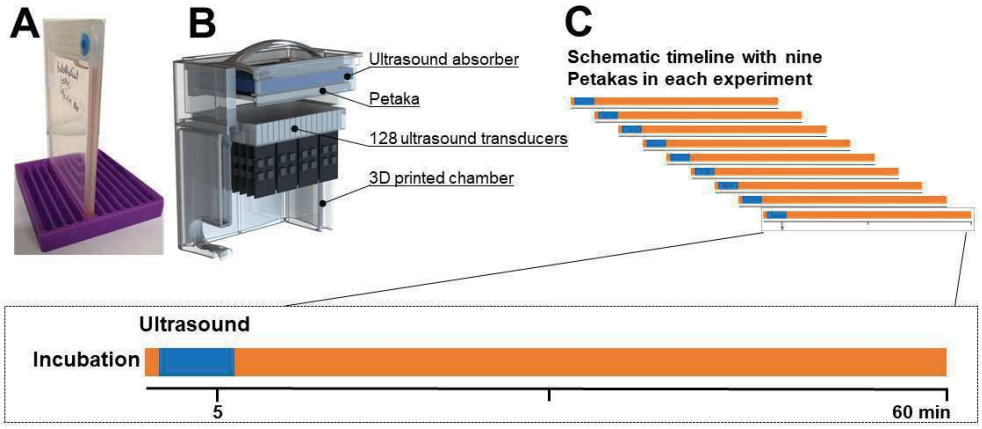

Figure 1. A) Petaka® G3 LOT hypoxic bioreactors, B) custom-made ultrasound treatment chamber and C) timeline of sonoporation experiments.

In each batch of experiments, up to nine Petakas (**A**) were sequentially incubated. (**C**). 1 mL culture medium with the appropriate gemcitabine concentrations and Sonazoid® microbubbles were injected through the injection port. Immediately following injection, the Petakas were transferred to the ultrasound treatment chamber (**B**), sonicated for five minutes (indicated by blue in the timelines) and returned to the incubator. Culture media and trypsinized cells were aspirated through the injection port after incubation with gemcitabine for 60 minutes (indicated by orange in the timelines).

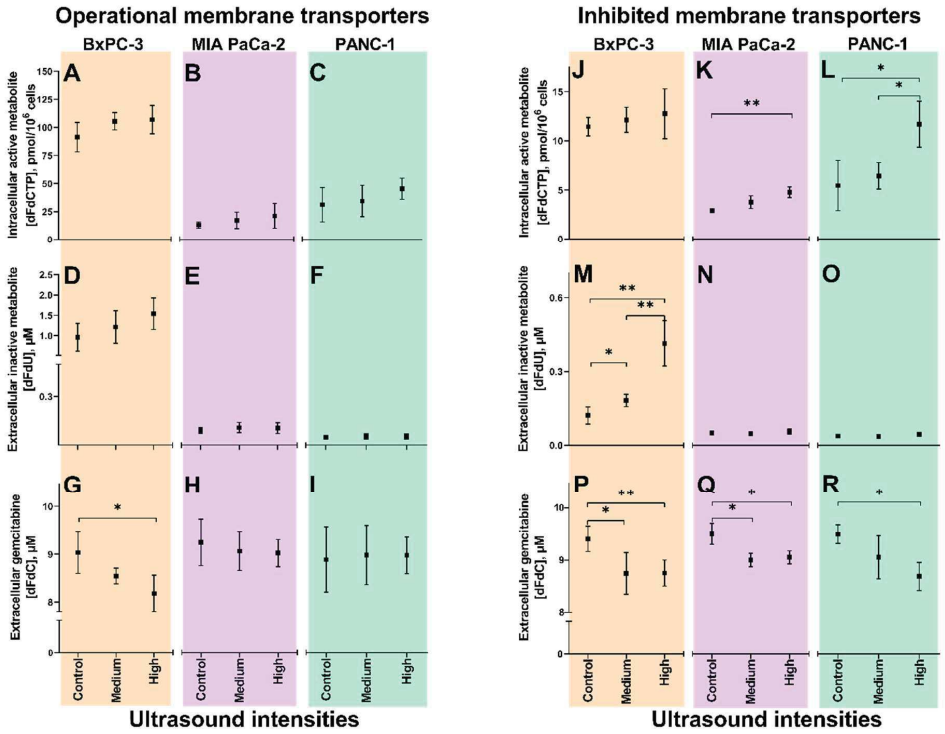

Figure 2.Gemcitabine uptake and metabolism following sonoporation of PDAC cell lines with operational (panels A-I) and inhibited (panels J-R) membrane transporters. Extracellular concentrations of gemcitabine (dFdC, panels G, H, I and P, Q, R), extracellular inactive metabolite (dFdU, panels D, E, F and M, N, O) and intracellular active metabolite (dFdCTP, panels A, B, C and J, K, L) in BxPC-3 (orange), MIA PaCa-2 (purple) and PANC-1 (green). Results displayed as mean±SD with 3 – 4 observations per datapoint. *p<0.05, **p<0.01 (Unpaired students t-tests). Notice the different scales on the Y-axes of extracellular dFdU and intracellular dFdCTP concentrations in experiments with operational vs. inhibited membrane transporters.

"Operational membrane transporters" (panels A – I): 60 minutes incubation with 10 µM gemcitabine, $3.84x10^6$ ppmL Sonazoid® microbubbles and 5 minutes ultrasound (US) at two acoustic intensities (Medium, High) and no US (Control).

"Inhibited membrane transporters" (panels J – R): 20 minutes pre-incubation with 100 µM dilazep followed by 60 minutes incubation with 10 µM gemcitabine, $3.84x10^6$ ppmL Sonazoid® microbubbles and 5 minutes US at two acoustic intensities (Medium, High) and no US (Control).

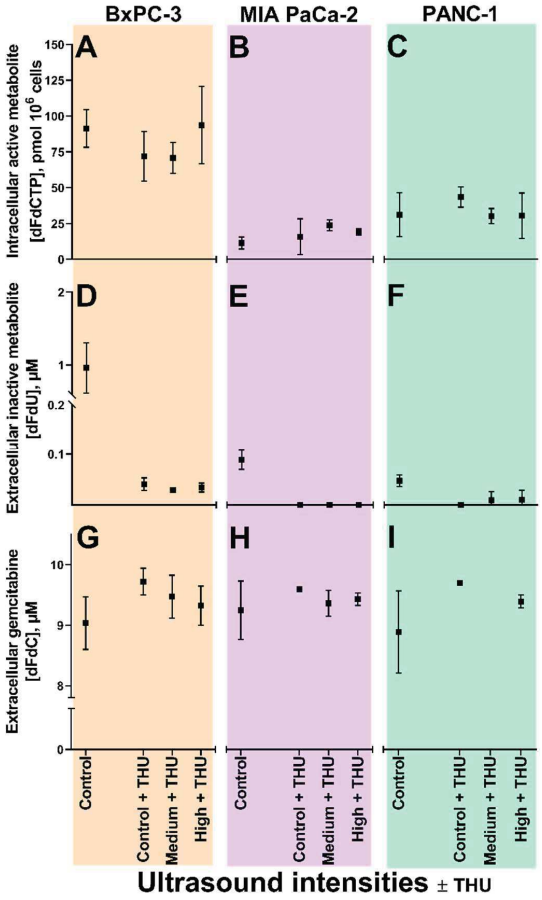

Figure 3. Gemcitabine uptake and metabolism following sonoporation of PDAC cell lines with inhibited cytidine deaminase.

Extracellular gemcitabine (dFdC, panels G, H, I), extracellular inactive gemcitabine metabolite (dFdU, panels D, E, F), and intracellular active gemcitabine metabolite (dFdCTP, panels A, B, C), in BxPC-3 (orange), MIA PaCa-2 (purple) and PANC-1 (green) cell lines following 60 minutes co-incubation with 10 µM gemcitabine ± 200 µM tetrahydrouridine, 3.84×10^6 ppmL Sonazoid® microbubbles and 5 minutes ultrasound (US at two acoustic intensities (Medium, High) and no US (Control) in Petakas. 60 minutes incubation with 10 µM gemcitabine without US included as control (leftmost data point in all panels).

Results displayed as mean±SD with 3 – 4 observations per data point.

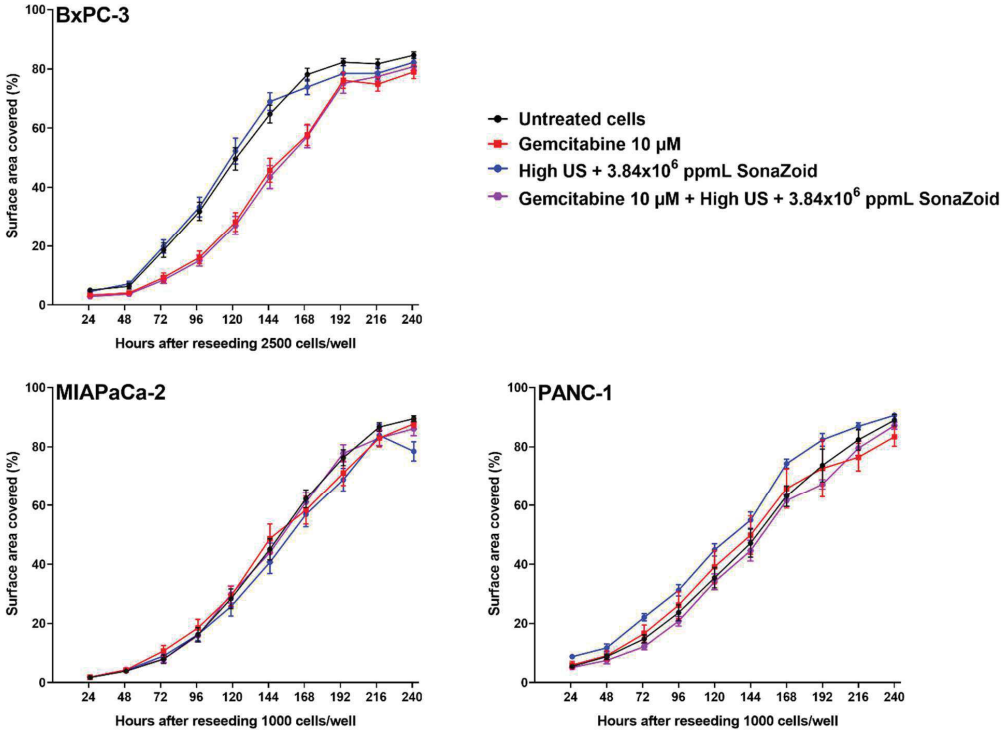

Figure 4. Growth of cell lines up to ten days after exposure to 10 µM gemcitabine over 60 minutes, sonoporation (High, 5 minutes) or both, compared to untreated cells (Control).

Each experiment was repeated once (n = 2). Cell growth was monitored after re-seeding the cells in 24 well-plates, and daily images were captured. Images were analyzed with MIPAR™ image analysis software, and cell growth over time was expressed as surface area coverage. All data from repeated experiments (n = 2) were combined and displayed as mean±SD

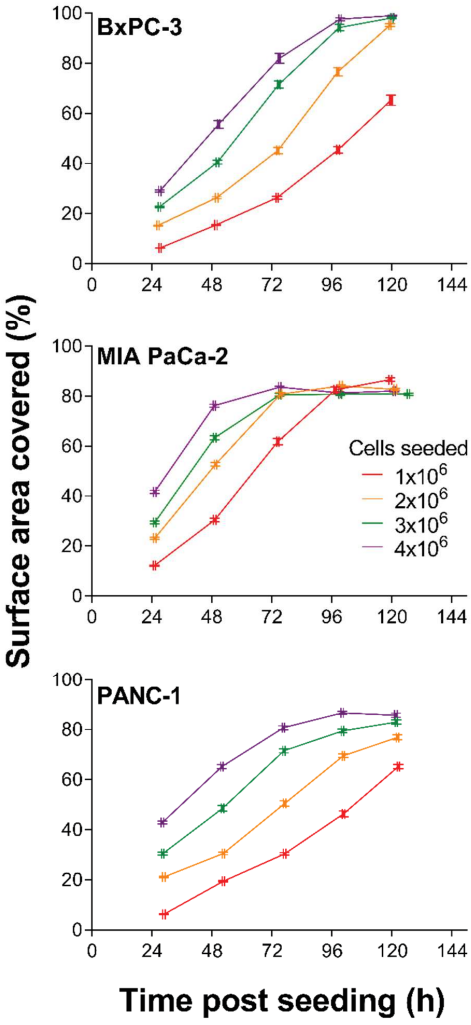

Supplemental Figure 1. Growth curves of BxPC-3, MIA PaCa-2 and PANC-1 seeded in Petakas at densities from 1.0 – 4.0 x 10^6 cells in 25 mL medium. 60 daily snapshots were captured across the surface of the Petakas. Images were analysed with MIPAR™ image analysis software and growth was expressed as surface area coverage (%) over time.

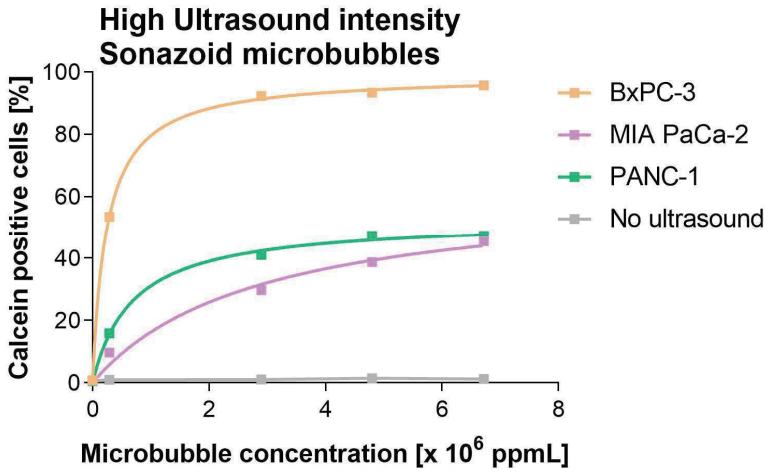

Supplemental Figure 2. Example of sonoporation-induced uptake of cell-impermeable calcein at High* ultrasound intensity and increasing concentrations of Sonazoid® microbubbles in all three cell lines. Increase in % positive cells was considered to be an indicator of increasing efficacy of cell membrane permeabilization.

*2.0 MHz, MI 0.378, 160 cycles, DC 3.6 %, I_{SPPA} 10 W/cm^2 and I_{SPTA} 358 mW/cm^2

Graphic design: Communication Division, UiB / Print: Skipnes Kommunikasjon AS

uib.no

ISBN: 9788230851043 (print)
9788230859261 (PDF)